

UNCLASSIFIED

AD 290 285

*Reproduced
by the*

**ARMED SERVICES TECHNICAL INFORMATION AGENCY
ARLINGTON HALL STATION
ARLINGTON 12, VIRGINIA**



UNCLASSIFIED

NOTICE: When government or other drawings, specifications or other data are used for any purpose other than in connection with a definitely related government procurement operation, the U. S. Government thereby incurs no responsibility, nor any obligation whatsoever; and the fact that the Government may have formulated, furnished, or in any way supplied the said drawings, specifications, or other data is not to be regarded by implication or otherwise as in any manner licensing the holder or any other person or corporation, or conveying any rights or permission to manufacture, use or sell any patented invention that may in any way be related thereto.

63-1-5

CATALOGED BY ASTIA
AS AD NO.

290285

290 285

ASTIA
RECEIVED
DEC 5 1962
ASTIA
©

HUGHES TOOL COMPANY · AIRCRAFT DIVISION
Culver City, California

Report 285-16 (62-16)

CONTRACT AF 33(600)-30271

HOT CYCLE ROTOR SYSTEM
WHIRL TESTS

March 1962

HUGHES TOOL COMPANY -- AIRCRAFT DIVISION
Culver City, California

For
Commander
Aeronautical Systems Division

Edited by:

K. B. Amer
Chief,
Helicopter Research Department

Approved by:

S. J. Chris
S. J. Chris
Project Engineer

J. L. Velazquez
J. L. Velazquez
Sr. Project Engineer

H. O. Nay
H. O. Nay
Manager,
Transport Helicopter Department



Hot Cycle Rotor During Whirl Test

ANALYSIS _____

MODEL _____

REPORT NO. _____

PAGE _____

PREPARED BY _____

CHECKED BY _____

TABLE OF CONTENTS

LIST OF FIGURES

LIST OF TABLES

1. SUMMARY

2. INTRODUCTION

3. TEST EQUIPMENT

3.1 General Test Setup and Test Rotor

3.2 Whirl Tower

3.3 Power Plant Installation

3.4 Power Plant Performance and Operational Characteristics

3.5 Van-to-Rotor Control System

3.6 Instrumentation

4. DESCRIPTION OF TESTS

4.1 General Discussion

4.2 Procedures

4.3 Log

5. TEST RESULTS AND ANALYSIS

5.1 Performance

5.2 Dynamics

5.3 Temperature and Leakage Surveys

5.4 Structural Effects

5.5 Sound Level Measurements

5.6 Post-Test Inspection

6. REFERENCES

APPENDICES

A. Whirl Tower Structural Analysis

B. Test Log Sheets

C. Method of Calculation; Area and Mass Weighted Parameters

D. Thermodynamic Calculation Procedure, Non-Rotating Components

E. Summary of Strain Gage and Thermocouple Locations

F. Nomenclature & Computer Program Formats

HUGHES TOOL COMPANY-AIRCRAFT DIVISION

ANALYSIS _____

MODEL _____

REPORT NO. _____

PAGE 11

PREPARED BY _____

CHECKED BY _____

LIST OF FIGURES

Frontispiece	Hot Cycle Rotor During Whirl Test
2. 1	Schematic - Hot Cycle System
2. 2	Blade Cross Section
3. 1-1	Test Site Installation
3. 1-2	Test Site Area
3. 1-3	Internal View of Control Van; Temperature, Pressure and Recording Instruments
3. 1-4	Perspective Sketch of Hot Cycle Rotor
3. 1-5	Hot Cycle Rotor Assembly
3. 3-1	Powerplant and Duct Installation
3. 3-2	Engine Rotated 180° for Calibration with Standard Nozzle
3. 3-3	Whirl Site Support Equipment
3. 5-1	Internal View of Control Van; Engine and Rotor Controls
3. 5-2	Control Installation - Cabin Flight
3. 6-1	Instrumentation Installation at Blade Aft Spar
3. 6-2	Instrumentation on Main Rotor Shaft
3. 6-3	Strain Gage B ridge Locations
3. 6-4	Thermocouple Locations
3. 6-5	Instrumentation Installation on Top of Rotor
3. 6-6	Instrumentation Installation on Top of Rotor
3. 6-7	Calibration of Lift Measuring Strain Gages
3. 6-8	Blade Hung Vertically for Bending Calibration and Frequency Measurements
3. 6-9	Slip Ring and Tachometer Drive Installation
3. 6-10	Oscillograph Installation
3. 6-11	Brown 48 - Point Temperature Recorder
3. 6-12	Multi-tube Manometer Bank and Single Point Temperature Recorder
3. 6-13	Turbine Discharge and Rotor Bearing Oil Temperature Recorders
5. 1-1	Hot Cycle Whirl Test Performance
5. 1-2	Nozzle Effective Velocity Coefficient
5. 1-3	Flow Function vs Nozzle Pressure Ratio
5. 1-4	Whirl Tower Station Designations for Power Calculation
5. 1-5	Velocity Profiles in Branch I
5. 1-6	Velocity Profiles in Branch II
5. 1-7	Average Velocity Profiles
5. 1-8	Graphical Integration of Average Velocity Profile in Branch I
5. 1-9	Graphical Integration of Average Velocity Profile in Branch II
5. 3-1	Measured Duct and Skin Temperatures; Inboard Segment
5. 3-2	Measured Duct and Skin Temperatures; Outboard Segment
5. 3-3	Flexure, Spar, and Cooling Air Temperature Distribution
5. 3-4	Transient Temperature, Predicted and Measured

HUGHES TOOL COMPANY-AIRCRAFT DIVISION

ANALYSIS _____

MODEL _____

REPORT NO. _____

 PAGE **iii**

PREPARED BY _____

CHECKED BY _____

- | | |
|---------|---|
| 5. 3-5 | Distribution of Temperature in the Hub |
| 5. 3-6 | Temperature of Rotor Components at Various Power Levels |
| 5. 3-7 | Temperature of Rotor Components at Various Power Levels |
| 5. 3-8 | Leakage Test, Typical Setup |
| 5. 4-1 | Pitch Arm Cyclic Load vs. Wind Speed |
| 5. 4-2 | Flapwise Cyclic Bending Moment vs Wind Speed, Inboard |
| 5. 4-3 | Flapwise Cyclic Bending Moment vs Wind Speed, Outboard |
| 5. 4-4 | Spar Cyclic Axial Load vs Wind Speed |
| 5. 5-1 | Engine Inlet Suppressor |
| 5. 5-2 | Engine Surplus Exhaust Suppressor |
| 5. 5-3 | Sound Pressure Levels |
| 5. 5-4 | Sound Pressure Level vs Frequency |
| 5. 5-5 | Sound Pressure Level vs Distance |
| 5. 5-6 | Noise Comparison for Take-Off Condition |
| 5. 6-1 | Rotor Removed from Tower for 18 Hour Inspection |
| 5. 6-2 | Rotor Disassembled for 35 Hour Inspection |
| 5. 6-3 | Rotor Disassembled for 35 Hour Inspection |
| 5. 6-4 | Hub Lower Shaft and Duct Outer Seal Rotating Surface After
18 Hours |
| 5. 6-5 | Hub Upper Radial Bearing and Seals Disassembled After
18 Hours |
| 5. 6-6 | Fabroid Flapping-Feathering Bearing, Showing Good
Condition After 35 Hours |
| 5. 6-7 | Hub Inner and Outer Seals |
| 5. 6-8 | Hub Upper Duct and Inner Seal Face, After 18 Hours |
| 5. 6-9 | Hub Lower Duct With Outer Seal Segmented Rings in
Position, After 18 Hours |
| 5. 6-10 | Close-Up of Articulate Duct Inboard Seal Segmented
Carbon Rings |
| D - 1 | Vertical Ducts Showing Location of Flow Measuring and
Hub Stations |
| D - 2 | Identification of Probe Locations at Flow Measuring and
Hub Stations |
| F. 3-1 | Input Format |
| F. 3-2 | Input Format - Listing of Input Data Cards |
| F. 3-3 | Printout |
| F. 3-4 | Program Listing |

HUGHES TOOL COMPANY-AIRCRAFT DIVISION

ANALYSIS _____

MODEL _____

REPORT NO. _____

PAGE iv

PREPARED BY _____

CHECKED BY _____

LIST OF TABLES

4. 3-1	Whirl Test Temperature Log
4. 3-2	Comparison of Whirl Test with Military Specifications
4. 3-3	Components Replaced with New Parts During Whirl Test
5. 1-1	Duct Losses From Engine to Hub Rotating Seal
5. 3-1	Rotor Component Temperatures
5. 3-2	Gas Leakage Measurements
5. 5-1	Sound Pressure Levels vs Frequency
E. 2-1	Tabulation of Strain Gage Installations
E. 2-2	Thermocouple Summary

ANALYSIS _____

MODEL _____

PREPARED BY _____

CHECKED BY _____

SECTION 1SUMMARY

This report has been prepared by Hughes Tool Company -- Aircraft Division to present the results of a 60 hour whirl test program conducted under Item 7a of USAF Contract AF 33(600)-30271 "Hot Cycle Pressure Jet Rotor System, "D/A Project Number 9-38-01-000, Subtask 616. It is submitted in fulfillment of Item 7c of the contract. The whirl test program was conducted primarily to establish the structural feasibility of the Hot Cycle Rotor System. Shown in the frontispiece is the 55 foot diameter Hot Cycle Rotor during whirl test.

The Hot Cycle Pressure Jet Rotor System is based on a principle wherein the exhaust gases from high pressure ratio turbojet engine(s) located in the fuselage are ducted through the rotor hub and blades and are exhausted through a nozzle at the blade tips. Forces thus produced drive the rotor.

The structural feasibility of the Hot Cycle Propulsion System has been more than demonstrated by 60 hours of whirl testing accomplished with no significant problems. The final 25 hours of the whirl test program have been conducted with no substitution or alteration of any components. The spectrum of test conditions agrees very closely with the conditions called for in the military specifications for rotor and engine preflight tests. No dynamic problems have evidenced themselves, in confirmation of the prediction of no resonances in the operating rotor speed range. The measured temperatures for all components have been within design limits. The measured loads have generally been within design limits. At the completion of the test the total leakage has been measured at a very small level (about 0.2%). A post-test inspection has revealed no basic mechanical or structural difficulties.

The two primary parameters required to predict Hot Cycle performance, duct friction coefficient and nozzle velocity coefficient, have been verified. The duct friction coefficient has been shown to be less than the conservative value of 0.004 used for performance predictions. The nozzle velocity coefficient has been shown to be 0.98; thus showing greater efficiency than the conservative value of 0.955 used for performance predictions. As a result, the maximum measured thrust of over 20,000 pounds compares very well with predicted thrust.

HUGHES TOOL COMPANY-AIRCRAFT DIVISION

285-16

ANALYSIS _____

MODEL _____

REPORT NO.

(62-16) PAGE 1-2

PREPARED BY _____

CHECKED BY _____

Based on this favorable performance comparison, it is estimated that the T-64 gas generators, which will ultimately power the present hot cycle rotor and which has a much higher pressure ratio than the J-57 used for the whirl test, will produce a maximum thrust of about 28,000 pounds.

ANALYSIS _____

PREPARED BY _____

CHECKED BY _____

SECTION 2INTRODUCTION

The helicopter industry is continuously striving to advance the rotary wing state of the art in order to improve the efficiency of the helicopter. One area in which a great deal of effort has been expended is that of the propulsion system. The gear boxes and drive shafting normally used to transmit engine power to the rotor have been a major source of cost, weight, and maintenance. While significant advances have been made, a major improvement is still required. The Hot Cycle Propulsion System promises such a major advance.

Figure 2.1 illustrates schematically the Hot Cycle Rotor System in which a turbine gas generator mounted in the fuselage exhausts through ducts to the rotor tips where the jets propel the rotor. In this way, the power of the engine drives the rotor without requiring mechanical components such as the power turbine, gear boxes, shafting etc. of the conventional propulsion system. As a result, there is a substantial saving in weight and complexity.

Although the Hot Cycle Rotor System has long been recognized as a potential means of accomplishing substantial improvements in rotor propulsion systems, several developments were required for its realization; these are:

1. Small high pressure ratio turbojets to minimize the volume of flow through the blade ducts.
2. High temperature duct material to contain the full turbojet temperature with acceptable weight.
3. Unique blade structure design to eliminate fatigue in hot parts, to provide for thermal expansion, and to be dynamically suitable.
4. Demonstration of structural feasibility by means of actual whirl test of a full scale rotor system.

The T64 engine gas generator has fulfilled the first requirement. This engine has completed its Preliminary Flight Rating Test and is currently undergoing a Flight Qualification Test. Thus, unlike other novel propulsion systems which have been proposed, no special engine development program is required.

ANALYSIS _____

PREPARED BY _____

CHECKED BY _____

The material Rene' 41 has fulfilled the second requirement. This material is suitable for operation up to temperatures of over 1200°F.

The blade structure to satisfy the third requirement is illustrated in Figure 2.2, and was developed under the present contract. The hot gases pass through the two central ducts which are attached to the skin by closely placed ribs. The skin-duct structure is divided into spanwise segments by chordwise flexures which makes this structure flexible in a spanwise direction and also causes the axial and bending loads to be carried in the two spars. This eliminates the fatigue loading from the hot parts while the spars, which carry the fatigue loads, are kept cool by the insulating air chamber and by a flow of ambient air which is pumped spanwise by centrifugal force. This flexibility also permits relative thermal expansion of the hot parts. Another important factor is that the dynamic characteristics in bending are determined entirely by the two spars. This permits tuning the blade by varying the spar dimensions so as to obtain the optimum natural frequencies.

This report presents the results of the final portion of the contracted work program -- the Whirl Test Program. As spelled out in the Contract, a total of 60 hours of whirl testing were to be conducted. The first 25 hours were specified to prove the structural feasibility of the concept. Maneuver and transient conditions were investigated in the following 10 hours. The last 25 hours consisted of an endurance-type test with no changes or modifications of components.

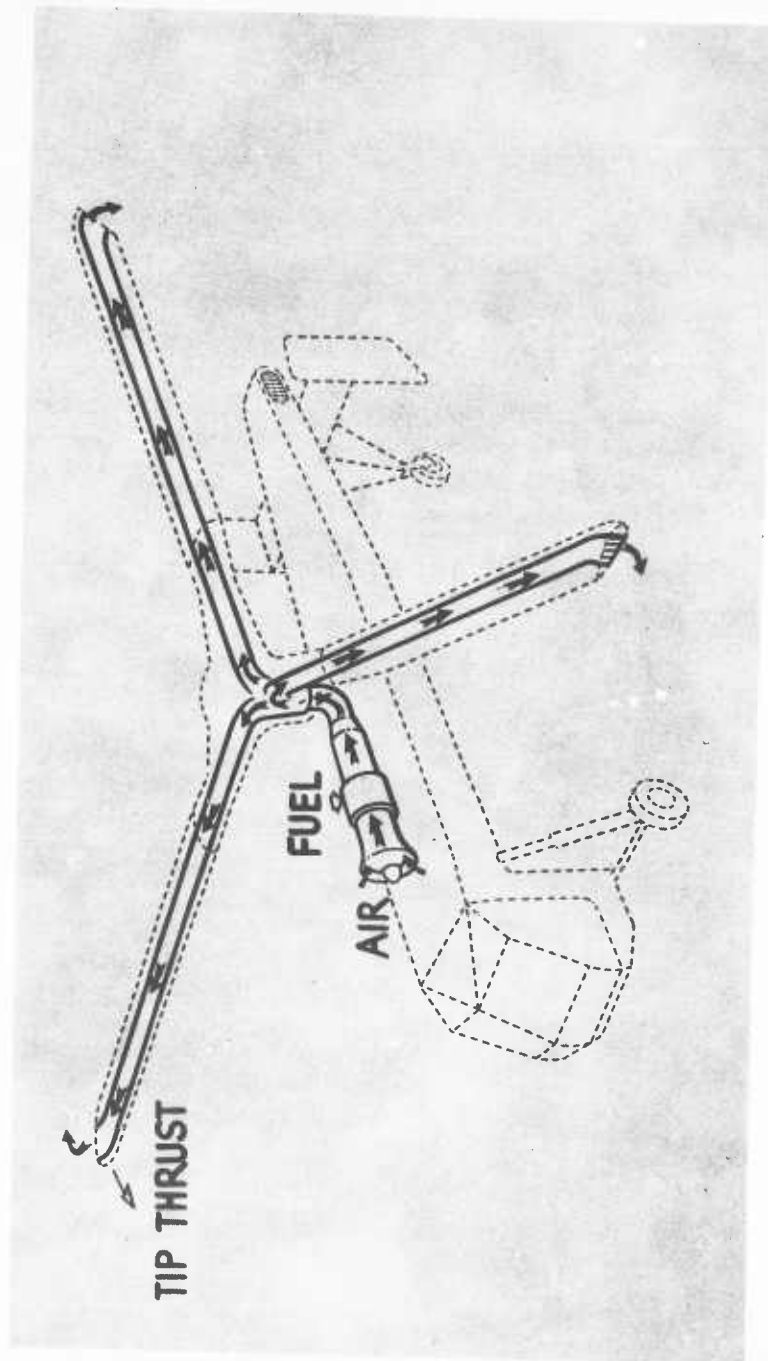


Figure 2.1 Schematic - Hot Cycle System

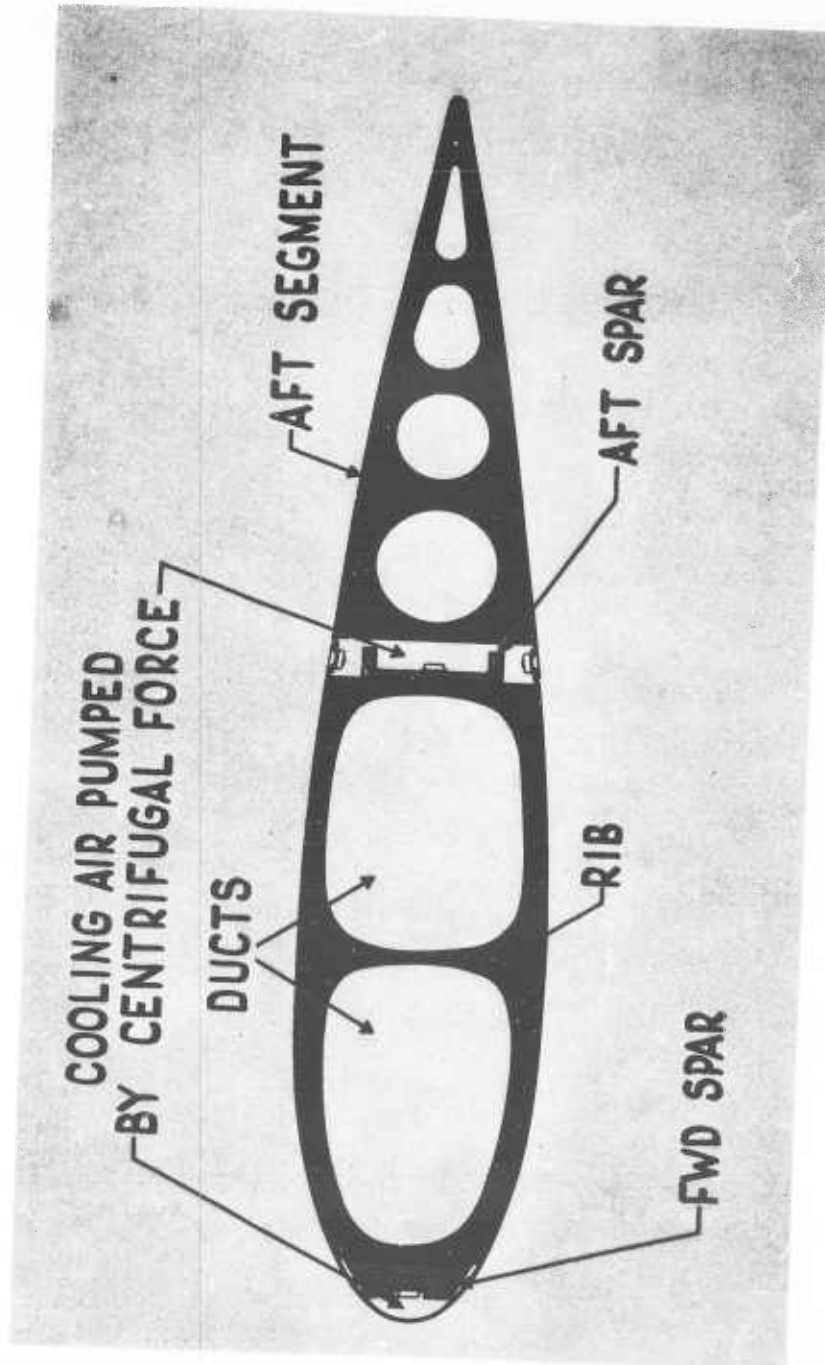


Figure 2.2 Blade Cross Section

ANALYSIS _____

PREPARED BY _____

CHECKED BY _____

SECTION 3TEST EQUIPMENT3.1 GENERAL TEST SETUP AND TEST ROTOR3.1.1 General Arrangement of Test Site

The Hot Cycle Rotor Test Site is located in an open area, adjoining the HTC-AD runway, approximately 800 feet from the nearest building or public road. See Figure 3.1-1 and 3.1-2. Two major installations on the site are the tower, complete with rotor, and the control van.

The tower is approximately thirty feet high, is built of large diameter steel tubes and is secured at its base to a reinforced concrete pad. A hydraulically operated permanent work platform long enough to service an entire blade, is attached to the whirl tower.

A Pratt & Whitney J-57 engine is located at the base of the tower with the exhaust directed toward the landing strip. Intake and exhaust suppressors are used to minimize the engine intake and the excess output noises of the engine. (See Section 5.5) Accessories such as engine starter, power generator, fuel trailer, lubrication oil pump, and air compressor are grouped around the tower as close to their point of application as practicable, as shown in Figure 3.1-2.

The control van is located seventy-two feet south of the tower in such a manner as to give a clear view of the tower and surrounding area. Housed within the van are rotor controls, engine controls, and instrumentation equipment. An interior view of the van showing the power plant engineers station and the instrumentation is given on Figure 3.1-3.

Because of the experimental nature of the program, considerable attention was given to the provision of barriers and safety equipment to protect test personnel in case of rotor or test equipment failure.

3.1.2 Test Rotor

Figures 3.1-4 and 3.1-5 show a schematic and photograph of the Hot Cycle Rotor Structure as fabricated for this test.

The blade design incorporates two machined titanium alloy spars that comprise the only continuous member running from the blade root to the tip. The spars are separated fifteen inches chordwise by eighteen identical sheet-metal segments 12.50 inches long, made up of two ducts contained

ANALYSIS _____

PREPARED BY _____

CHECKED BY _____

within nine ribs and an outer cover. The segments are bolted to the spars and are jointed together by bellows-type flexible couplings riveted to the outer cover. The ducts and skins of adjacent segments are slip-jointed. In this arrangement the spars are the only members that react normal blade bending loads and centrifugal loads. Torsional and chordwise shear loads are carried by the assembly of segments. For convenience, the blades were color coded blue (instrumented blade), red and yellow.

The rotor blade retention and hub structure consists of a free-floating hub supporting three coning blades by means of converging tension straps and a monoball-type bearing. The free-floating hub transfers the loads to the mast and then through two bearing systems to the supporting trusses. This hub must also provide clearance for the ducts which transfer gases used in propulsion from below the hub to the three blades. The over-all hub structure provides support for the control system.

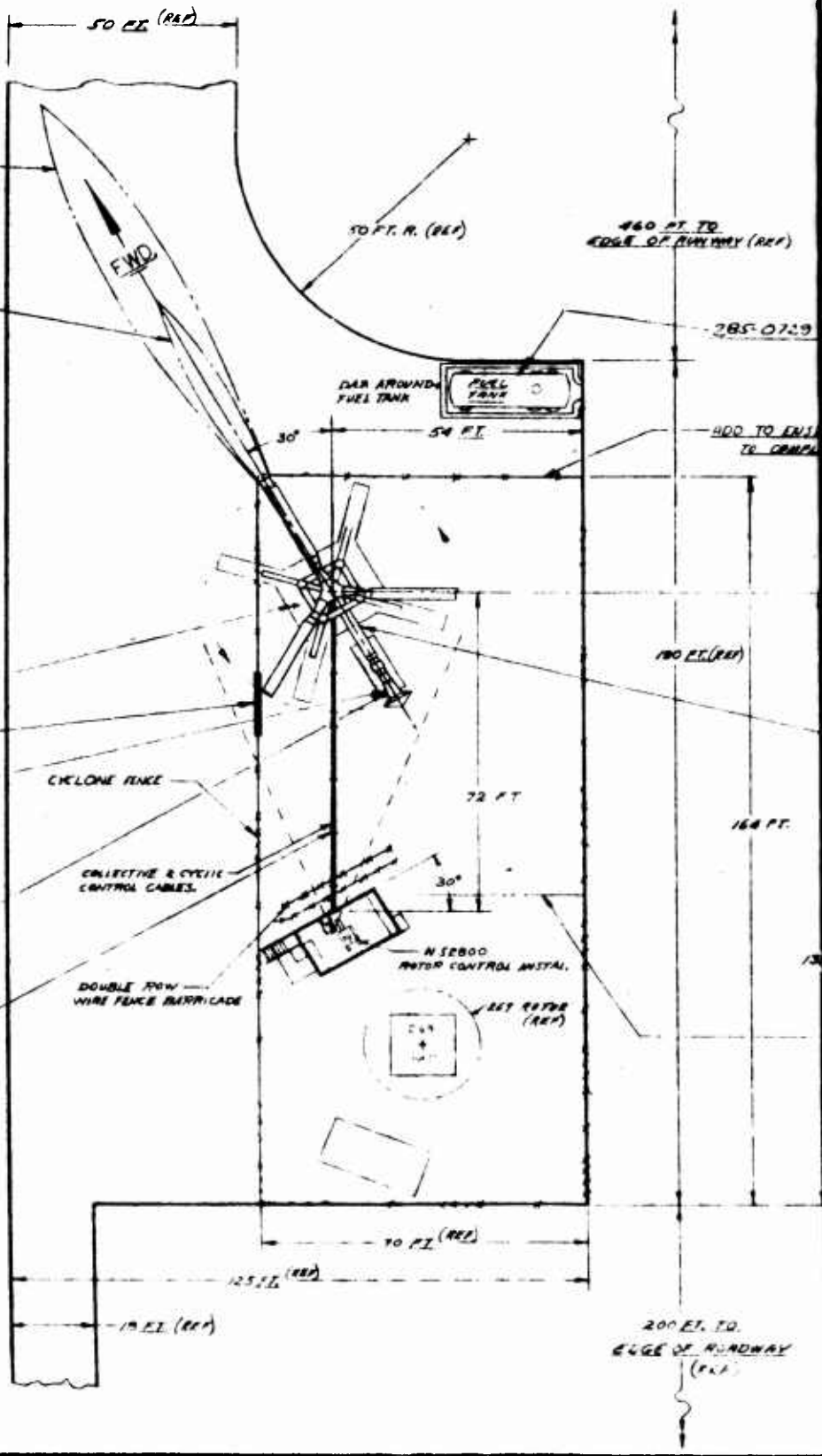
The control system is intended to be as conventional and troublefree as possible. The various components were located so as to keep them small in size, relatively cool and readily accessible.

A complete discussion of the design and fabrication of the rotor is contained in References 3.1-1, 3.1-2, and 3.1-3.

1

FULL POWER
VEL. = 70 FT @ SEC.
TEMP. = 120° - 100° F.

100% RATING
VEL. = 70 FT @ SEC.
TEMP. = 125° F.



285-0721 PRO

14 FT GATE MIN.

285-0725 BENCHPLANT INSTAL.
285-0723 ENGINE SUPPORT STAND.
285-0724 THROTTLE CONTROL

CYCLONE FENCE

COLLECTIVE & CYCLIC CONTROL CABLES

285-0729 FUEL LINES (REF)

DOUBLE ROW WIRE FENCE BARRICADE

285-0762 BENCH (REF)

N 5800 MOTOR CONTROL INSTAL.

285-0728 (REF)

125 FT (REF)

10 FT (REF)

200 FT. TO EDGE OF ROADWAY (REF)

10 FT. R. (REF)

460 FT. TO EDGE OF RAMPWAY (REF)

285-0729

400 TO ENDS TO COMPA

100 FT (REF)

164 FT.

72 FT

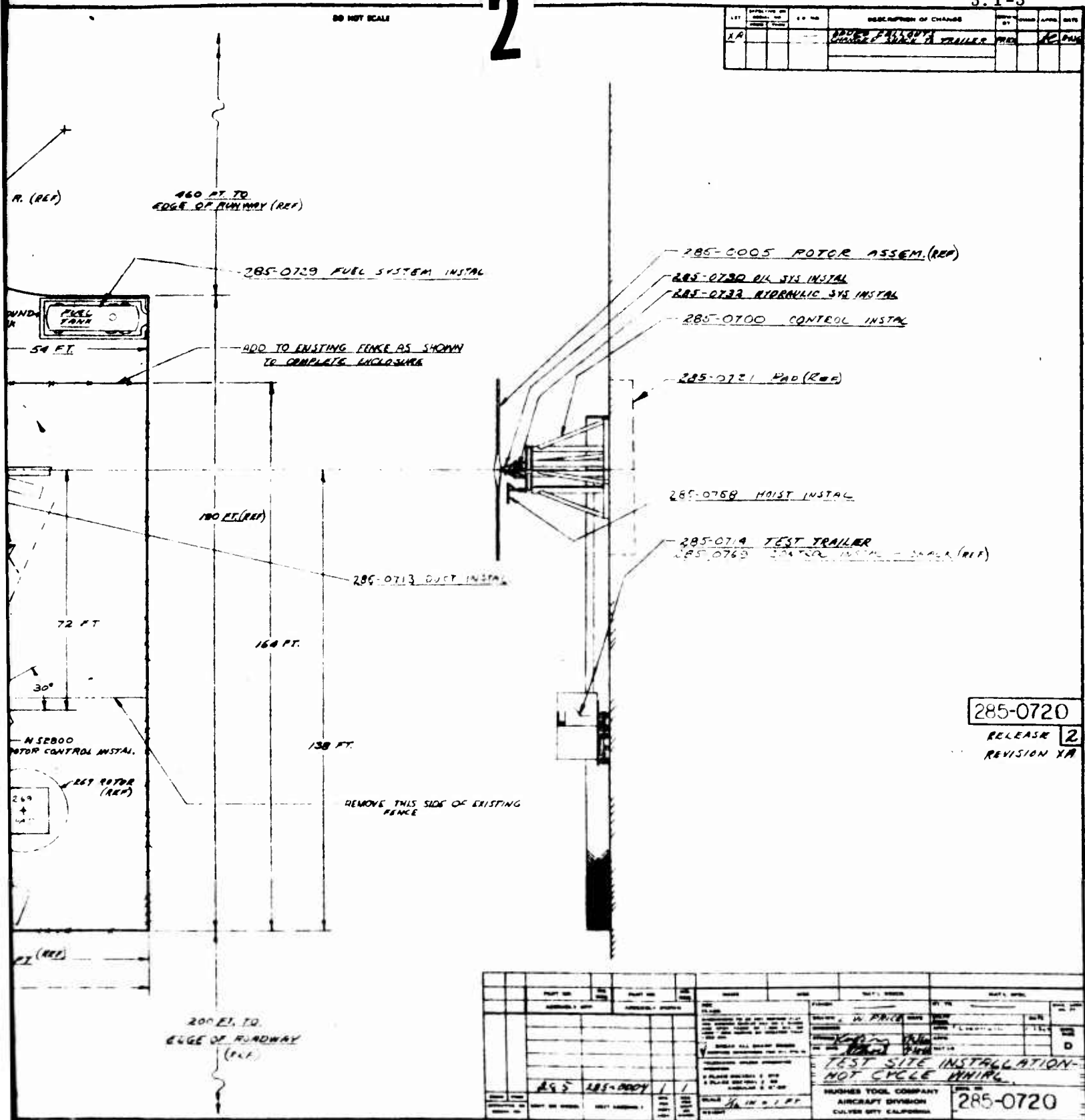
30°

50 FT (REF)

2

DO NOT SCALE

REV	DESCRIPTION OF CHANGE	BY	DATE
1A	ADDED FUEL SYSTEM TRAILER	MEG	12/19/62



285-0720
RELEASE 2
REVISION 1A

REV	DESCRIPTION OF CHANGE	BY	DATE
1	ADDED FUEL SYSTEM TRAILER	MEG	12/19/62

TEST SITE INSTALLATION - NOT CYCLE DRINK

HUGHES TOOL COMPANY
AIRCRAFT DIVISION
CULVER CITY CALIFORNIA

285-0720



Figure 3.1-2 Test Site Area

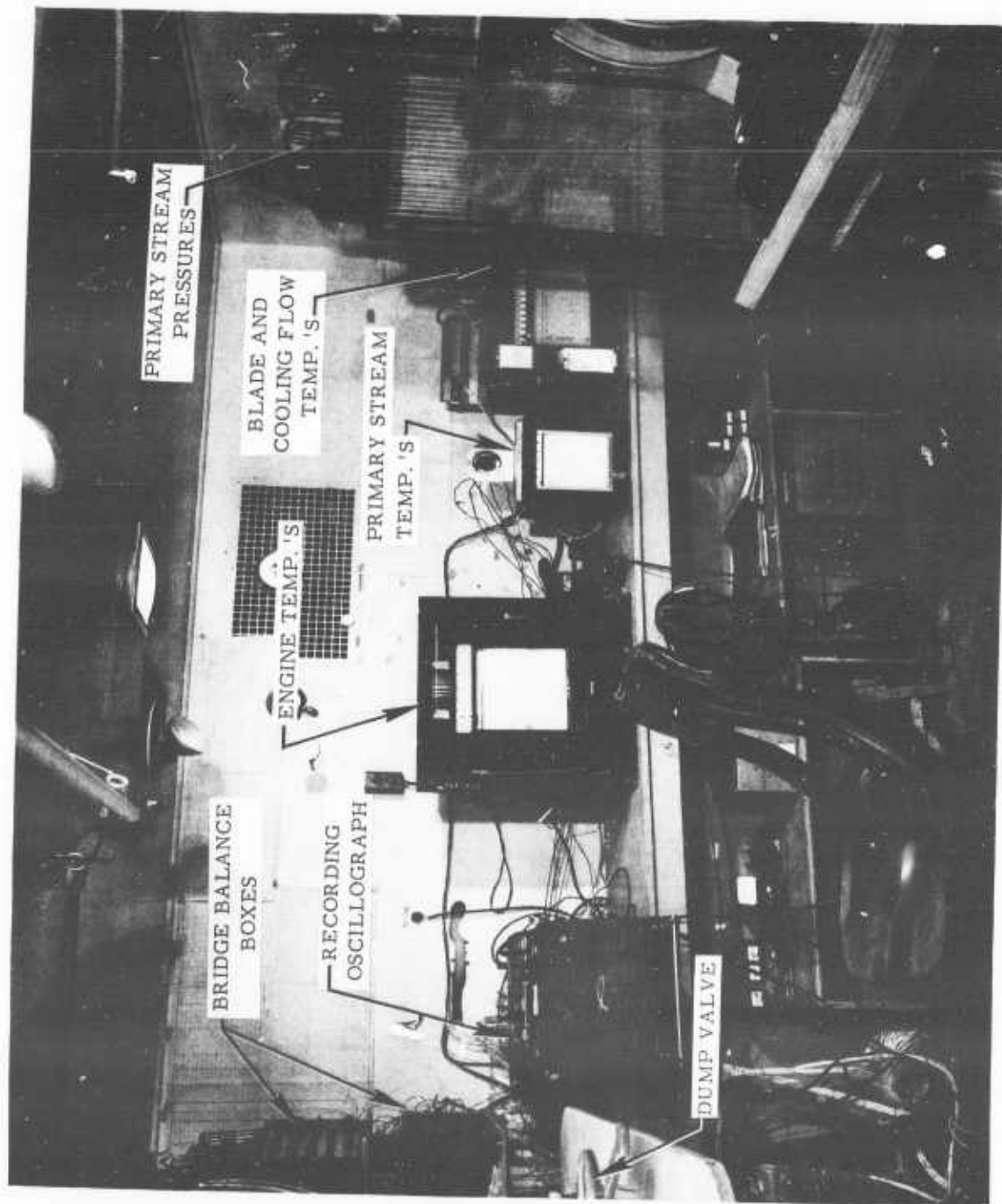


Figure 3.1-3 Internal View of Control Van; Temperature, Pressure and Strain Recording Instruments

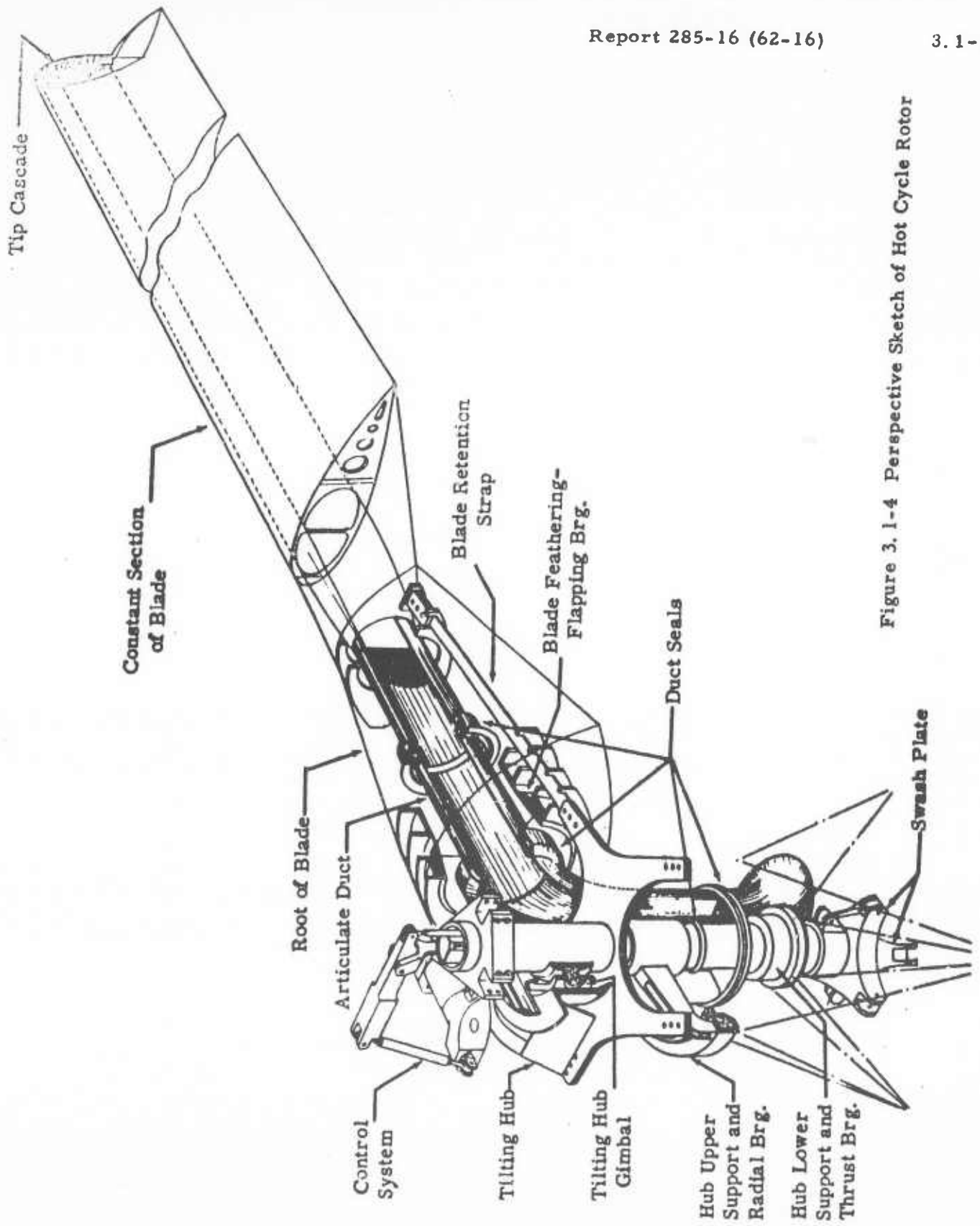


Figure 3.1-4 Perspective Sketch of Hot Cycle Rotor

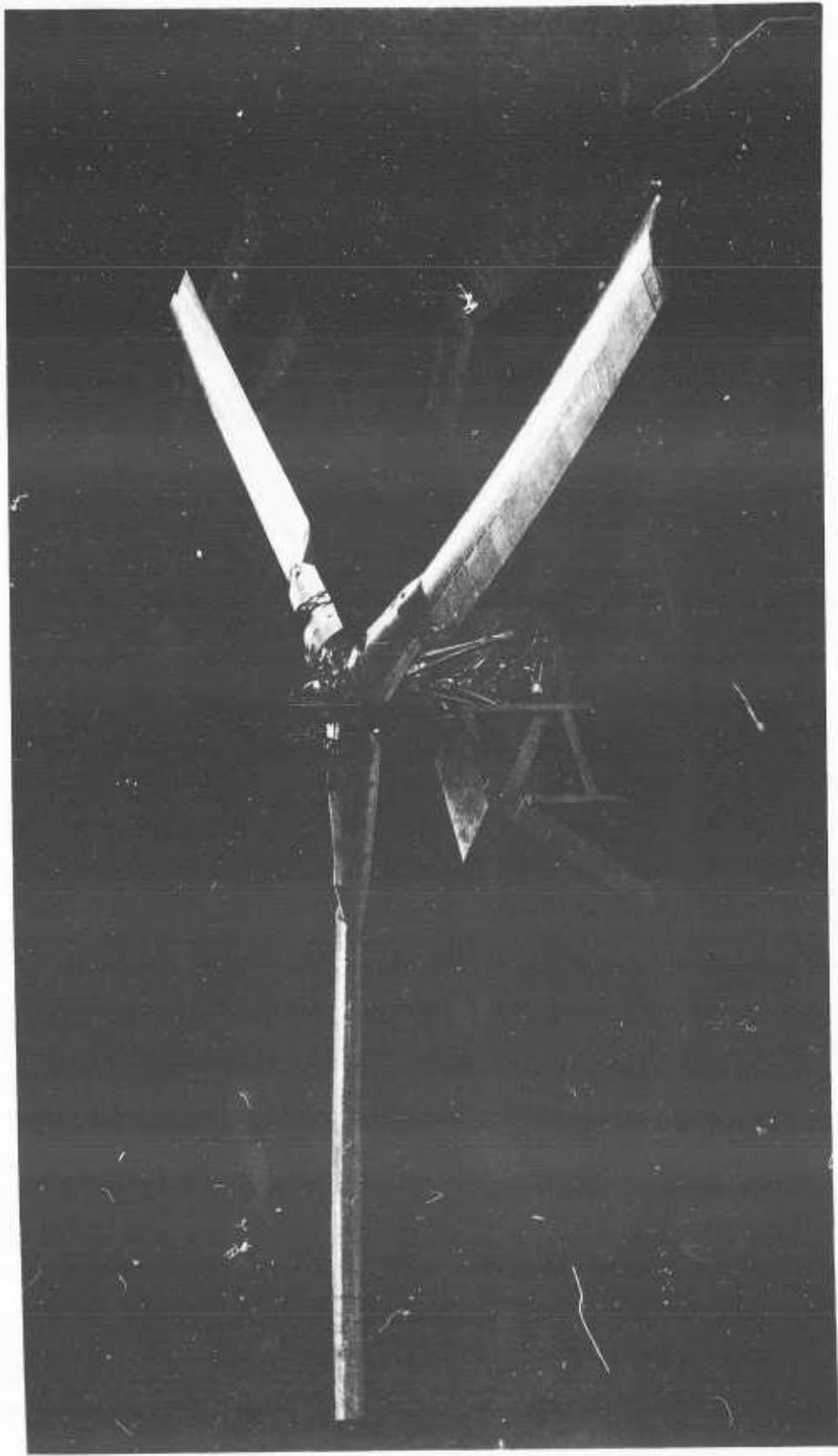


Figure 3.1-5 Hot Cycle Rotor Assembly

ANALYSIS _____

MODEL _____

REPORT NO. _____

PREPARED BY _____

CHECKED BY _____

3.2 WHIRL TOWER

The support tower is composed of three main structural components; the upper rotor mounting truss (285-0523), the center structure (285-0703) and the lower support structure (285-0701) which attaches to the reinforced concrete base. These may be seen in the photographs of the Frontispiece and Figure 3.1-2. The upper mounting truss is a welded steel tube structure which provides support for the main rotor shaft bearings. Side loads are applied at the upper bearing and side and thrust load are taken at the lower bearing. The truss base is attached to the 285-0703 structure assembly with four 5/8 and eight 3/8 high strength bolts (180-200 KSI). The 285-0703 structure assembly acts as a spacer for transferring rotor imposed loads from the mounting truss to the main tower (285-0701). In addition it houses and supports the control system actuating cylinders. It is a welded structure composed of 5.0 inch heavy steel tubes. The lower and main tower structure (285-0701) is a welded structure consisting of large I-beams and steel tubes. The base of the tower is attached to a 2 foot thick reinforced concrete pad by 68 one-inch bolts. In general the tower is designed from rigidity considerations and is not critical for imposed loads.

The whirl test duct system is composed of two parts; the vertical ducts for carrying the hot gas to the rotor system and the horizontal ducts for exhaust overflow. Valves are located in each path to provide adjustment for operating requirements. Potential rust and subsequent spalling of the vertical ducts (test stand items only) represented a source of potential damage to the hub and blade ducts and seals. For this reason, the vertical ducts are made from corrosion resistant steel. The duct system is supported from the tower at appropriate points. Bellows are provided in the duct system to allow for differential expansion.

Structural analysis of the tower and ducting is contained in the Appendix A.

ANALYSIS _____

PREPARED BY _____

CHECKED BY _____

Engine throttle control was initially maintained from the mobile control van by a hydraulic servomechanism actuated by the twist grip on the collective pitch stick. This was later changed by the addition of a separate throttle control lever operating in series with the stick grip. Emergency throttle cut-off was instantly available through the use of a hydraulic accumulator which discharges high pressure fluid into the throttle servo when electrically actuated.

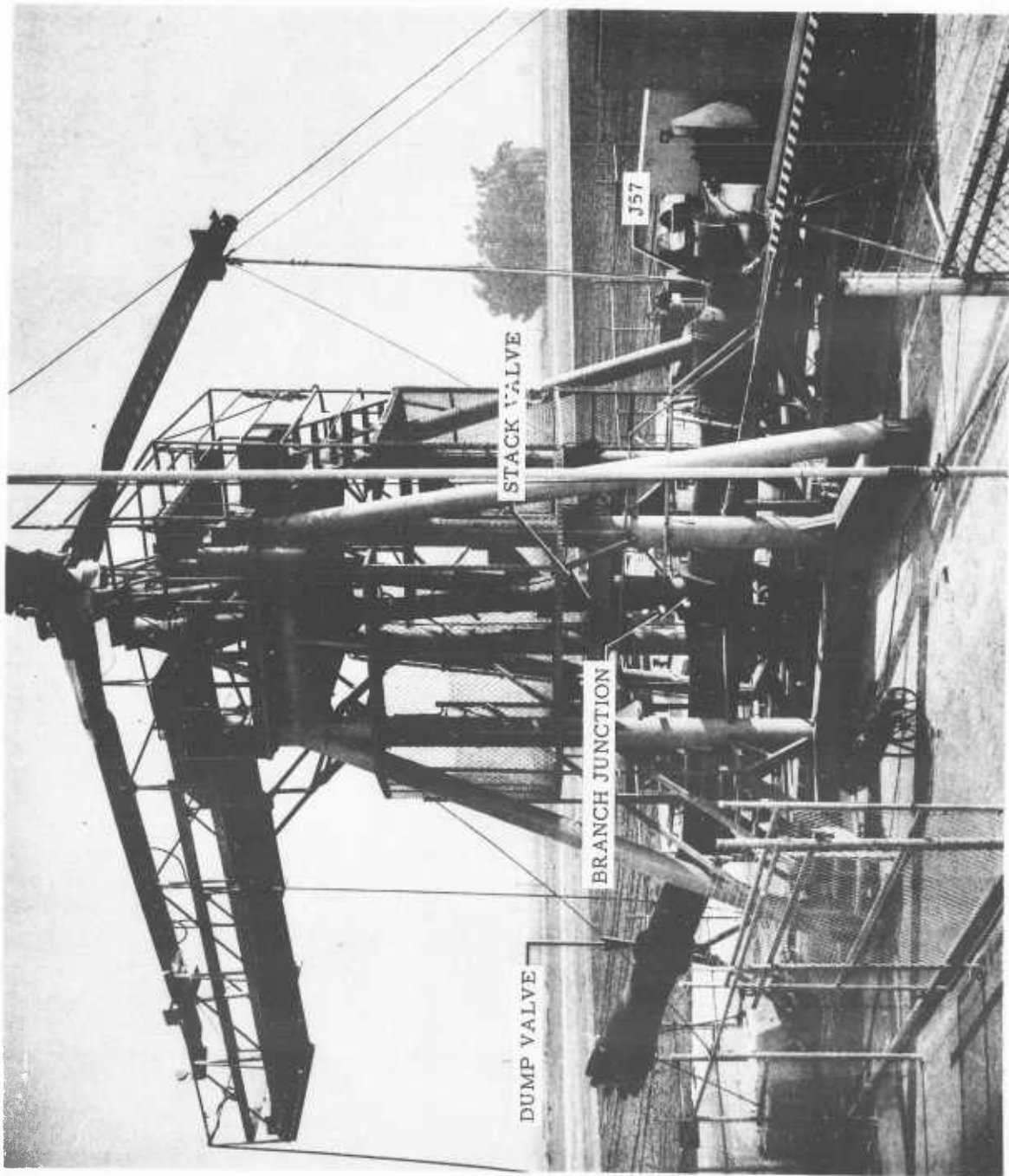


Figure 3. 3-1 Powerplant and Duct Installation

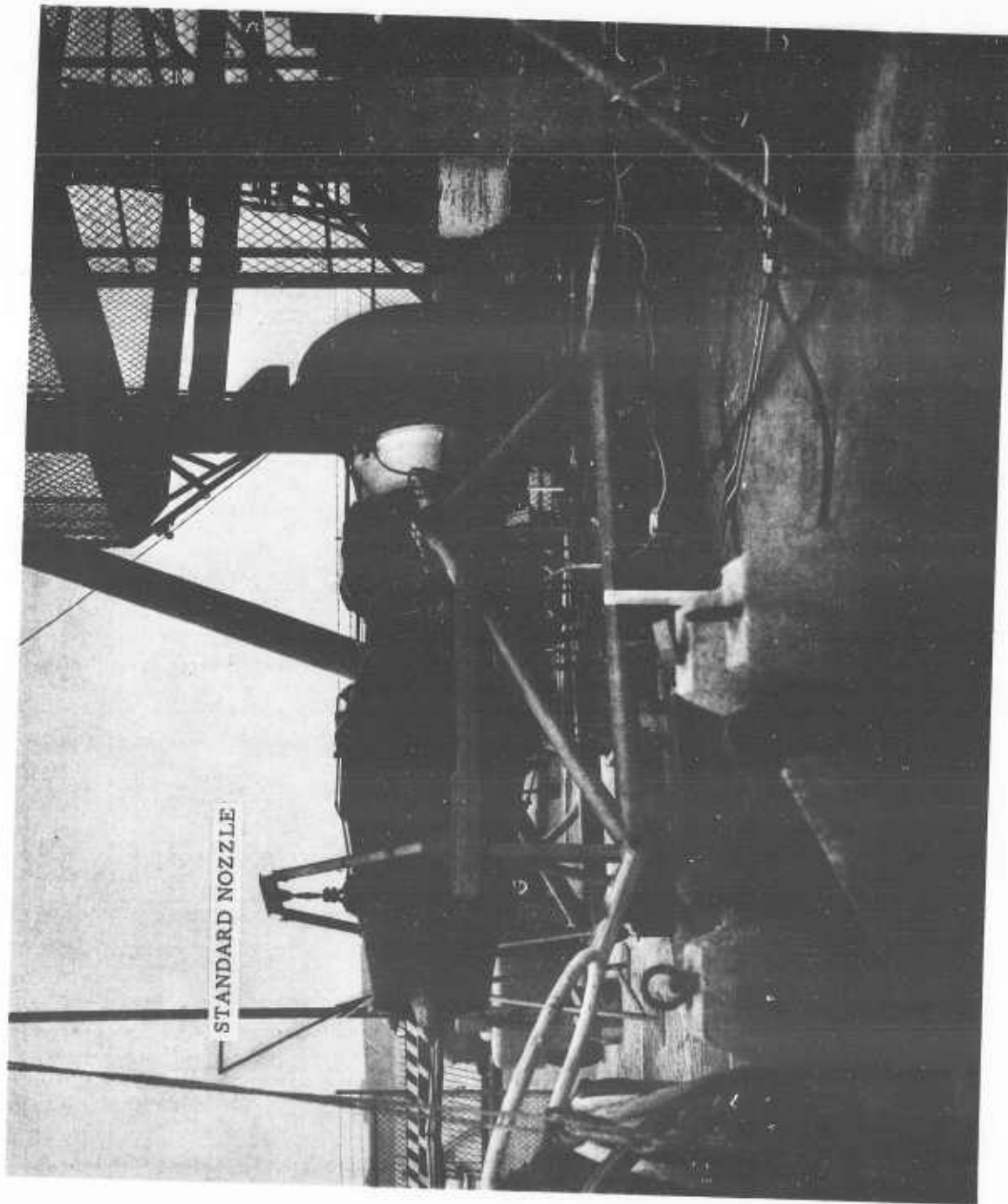


Figure 3.3-2 Engine Rotated 180° for Calibration with Standard Nozzle

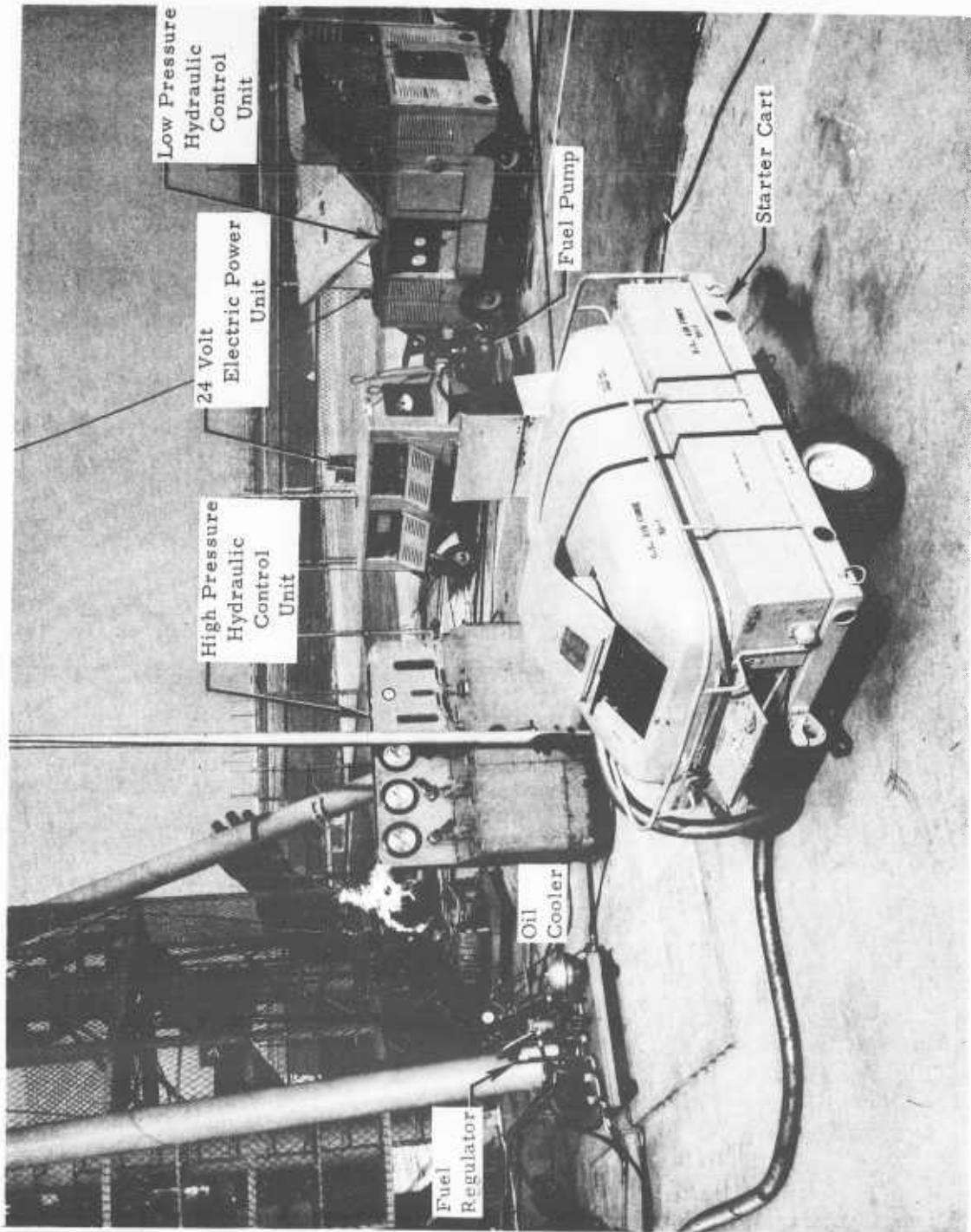


Figure 3. 3-3 Whirl Site Support Equipment

ANALYSIS

PREPARED BY

CHECKED BY

3.4 POWER PLANT PERFORMANCE AND OPERATIONAL CHARACTERISTICS

During most of the operation of the whirl test installation, the engine is operated in complete accordance with the recommendations of the applicable technical orders and operating instructions for the J-57 (References 3.3-1 and 3.4-1). When operated in this manner, however the engine is incapable of exhaust gas temperatures equivalent to the maximum rated temperature of the T-64 gas generator: i. e., J-57 - 1148°F, T-64 - 1180°F to 1225°F. Further, the 1148°F is the maximum observed sea level value thereby indicating a probable lower value for the particular engine used. (It should be noted that Reference 3.4-1 shows 30 minute temperatures of 1200°F at 55,000 feet altitude and two minute acceleration limit values of 1220°F for the J-57.)

A method of operation of the J-57 was established and coordinated with Pratt & Whitney Aircraft to achieve the necessary elevated temperatures without distress to the engine. The operating procedure is as follows:

- a. Trim and calibrate the engine with the standard exhaust nozzle prior to connection to the test rig ducting. This trim setting remains unchanged throughout the test operation of the engine.
- b. For all operation simulating T-64 power settings of maximum continuous or below, the operation of the J-57 is maintained on the operating line (P_{T_7} vs. N_2)* established during the standard calibration run.
- c. Military rated power of the T-64 is simulated by reducing the effective exhaust nozzle area of the J-57 through manipulation of the exhaust dump valve. This procedure allows an ample increase in T_{T_7} * although the increase in P_{T_7} is only slight, i. e., the T-64 simulated exhaust temperatures are reached without exceeding the J-57's P_{T_7} limitation.

The T-64's exhaust pressure values are not simulated exactly. This latter deviation is of little consequence as sufficient exhaust pressure is generated to choke the rotor tip nozzles, thereby permitting accurate extrapolation to T-64 conditions. However, meeting the T-64's exhaust temperature is important to demonstrate the mechanical integrity of the rotor blade and seals at prototype temperature. The calibration is discussed completely in Reference 3.4-2.

* See Nomenclature in Appendix F.

ANALYSIS _____

PREPARED BY _____

CHECKED BY _____

Although operation of the J-57 in this manner decreases the surge margin, no difficulty was incurred during steady state or transient runs.

During operation at maximum N_2 , it was found that as the exhaust dump valve position was moved to regulate the system's pressure, several peaks in P_{T7} were observed subsequent to installation of inlet and exhaust noise suppressors. The first peak was at $N_1 = 97$ to 100%, second at $N_1 = 92$ to 94%, and the third at $N_1 = 88$ to 90%. These peaks were generally 1 to 1.5 psi above the general level of P_{T7} and always below values corresponding to the engine pressure ratio limit of the J-57. In order to achieve maximum power from the engine near a T_{T7} of 1200°F, it was necessary to operate at an N_2 of approximately 89%. This generally resulted in a T_{T7} operation at 1220 to 1240°F depending on ambient conditions and is comparable to the 1225°F take off rating of the advanced T-64. These peaks were slightly shifted depending on the particular inlet and exhaust noise suppressors in use at the time.

ANALYSIS _____

PREPARED BY _____

CHECKED BY _____

3.5 TEST SITE ROTOR CONTROLS

All of the whirl tower control items were originally designed for and successfully used on the Hughes developed U. S. Air Force XH-17 Helicopter under contract AF 33(038)-8907. They are considerably oversize, but for economy were adapted to the requirements of this program.

The whirl tower rotor controls are actuated by conventional cyclic and collective pitch sticks in the control van, shown in Figure 3.5-1. Stick motions are transmitted through a mixing linkage, shown in Figure 3.5-2, to the three quadrants that drive cables running 75 feet horizontally to the rotor tower. Relative locations of the tower, van, and run of control cables were shown previously in Figures 3.1-1 and 3.1-2.

On the tower the cables control three servo-cylinders connected to the rotor swashplate. The cylinders were designed for 3000 psi. hydraulic pressure, but were operated in this test at 625 psi. .

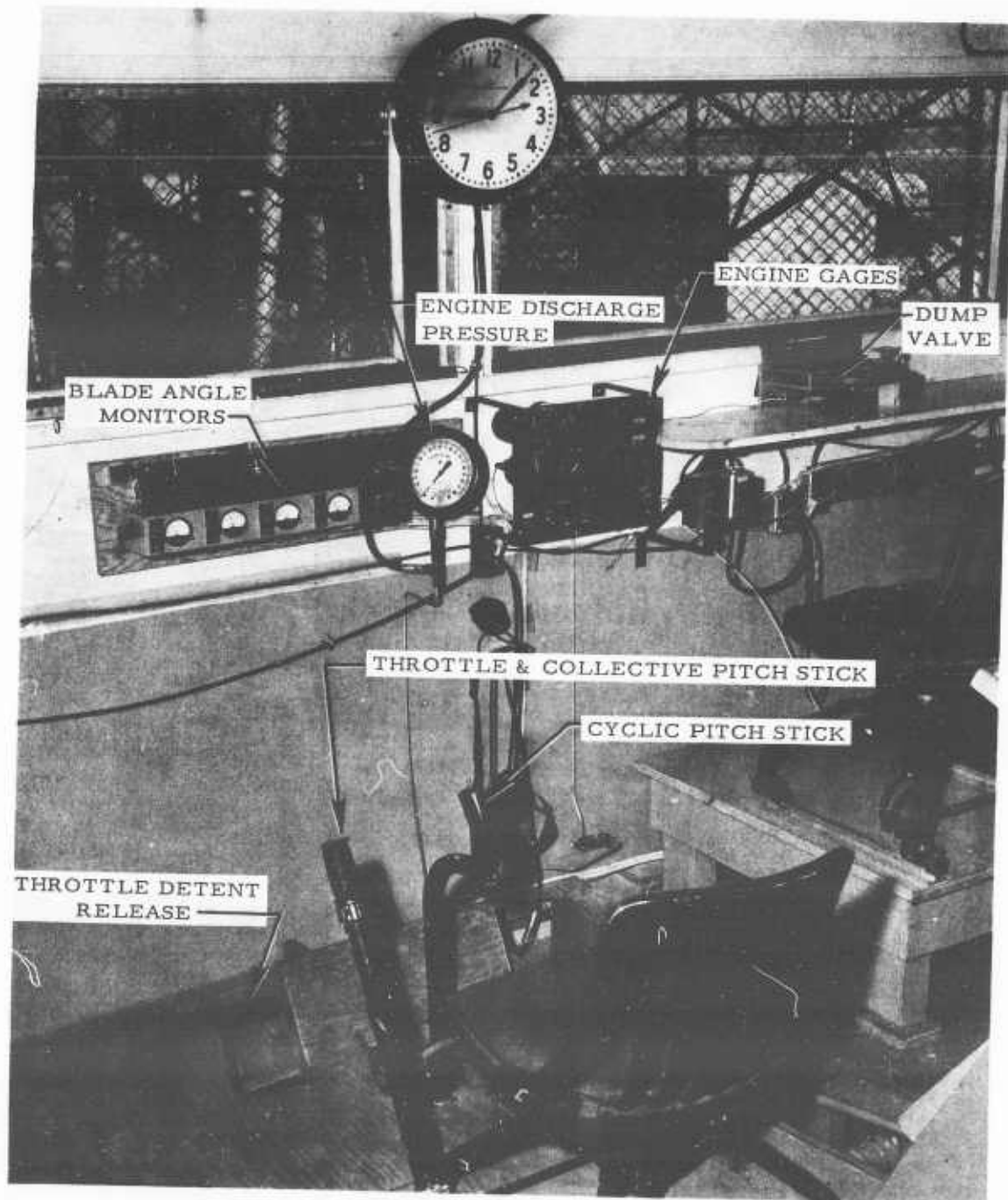


Figure 3.5-1 Internal View of Control Van; Engine and Rotor Controls

1

WHEEL END SPRING TUBE
AN 300-18 NUT (TENSILE TORQUE 180,000 IN-LB)
AN 300-18 WASHER
AN 300-18-2 COTTER

WHEEL END SUPPORT FITTING
AN 300-18-2A TAPER PIN
AN 300-18-2A RETAINER END
AN 300-18-2A CHECK BOLT
AN 300-18-2A WASHER
AN 300-18-2A NUT

WHEEL CONTROL FITTING
AN 300-18-2A TAPER PIN
AN 300-18-2A WASHER
AN 300-18-2A NUT

WHEEL TORQUE TUBE

WHEEL CONTROL ROD ASSEMBLY
AN 114-12 BOLT
AN 114-12 NUT
AN 300-18 WASHER
AN 300-18-2 COTTER PIN

WHEEL FITTING ASSEMBLY
AN 114-12 BOLT
AN 300-18 WASHER
AN 300-18-2A NUT

SEE SHEET 2 FOR ASSEMBLY DETAILS

WHEEL BRACKET ASSEMBLY
WHEEL LONG CONTROL FITTING
WHEEL TENSION ASSEMBLY
AN 300-18-2A BEARING
AN 300-18-2A BEARING
WHEEL RET-131 RETAINER
WHEEL RET-131 RETAINER
AN 114-12 BOLT (TIGHTEN THIS NUT
AN 300-18-2A NUT (TIGHTEN TIGHT ONLY)
AN 300-18 WASHER
AN 300-18-2 COTTER
AN 300-18 BOLT (TENSILE TORQUE 180,000 IN-LB)
AN 300-18 WASHER
AN 300-18 NUT
AN 300-18-2 COTTER
AN 300-18-2A SPRING

WHEEL CONTROL ROD WASH END
AN 114-12 BOLT
AN 114-12 NUT
AN 300-18 WASHER
AN 300-18-2 COTTER

WHEEL TORQUE TUBE END

WHEEL FITTING WASH END
AN 114-12 BOLT
AN 300-18 WASHER
AN 300-18-2A NUT

WHEEL SUPPORT FITTING
AN 300-18-2A TAPER PIN
AN 300-18-2A WASHER
AN 300-18-2A NUT

WHEEL BRACKET ASSEMBLY
AN 114-12 BOLT
AN 114-12 NUT
AN 300-18 WASHER
AN 300-18-2 COTTER

WHEEL CONTROL FITTING
AN 300-18-2A TAPER PIN
AN 300-18-2A WASHER
AN 300-18-2A NUT

WHEEL END SUPPORT FITTING
AN 300-18-2A BEARING
AN 300-18-2A RETAINER END
AN 300-18-2A CHECK BOLT
AN 300-18-2A BOLT
AN 300-18-2A WASHER
AN 300-18-2A NUT
WHEEL END SPRING TUBE

WHEEL CONTROL FITTING
AN 300-18-2A TAPER PIN
AN 300-18-2A WASHER
AN 300-18-2A NUT

WHEEL END SPRING ASSEMBLY
AN 300-18 NUT
AN 300-18 WASHER
AN 300-18-2A BEARING
AN 300-18-2A CHECK BOLT
AN 300-18-2A BOLT
AN 300-18-2A WASHER
AN 300-18-2A NUT
AN 300-18-2A COTTER
AN 300-18-2A BOLT
AN 300-18-2A WASHER
AN 300-18-2A NUT

PLAN VIEW

FORWARD

WHEEL SUPPORT - DRILL & REAM
1. PLACE THE SPRING EQUIPMENT
AN 114-12 BOLT
AN 300-18-2A NUT
AN 300-18 WASHER

SEE SHEET 2 FOR
DETAIL OF THIS

AN 114-12 BOLT
AN 300-18-2A NUT
AN 300-18-2A COTTER
AN 300-18 WASHER

WHEEL END SPRING ASSEMBLY
AN 300-18 NUT
AN 300-18 WASHER
AN 300-18-2A BEARING
AN 300-18-2A CHECK BOLT
AN 300-18-2A BOLT
AN 300-18-2A WASHER
AN 300-18-2A NUT
AN 300-18-2A COTTER
AN 300-18-2A BOLT
AN 300-18-2A WASHER
AN 300-18-2A NUT

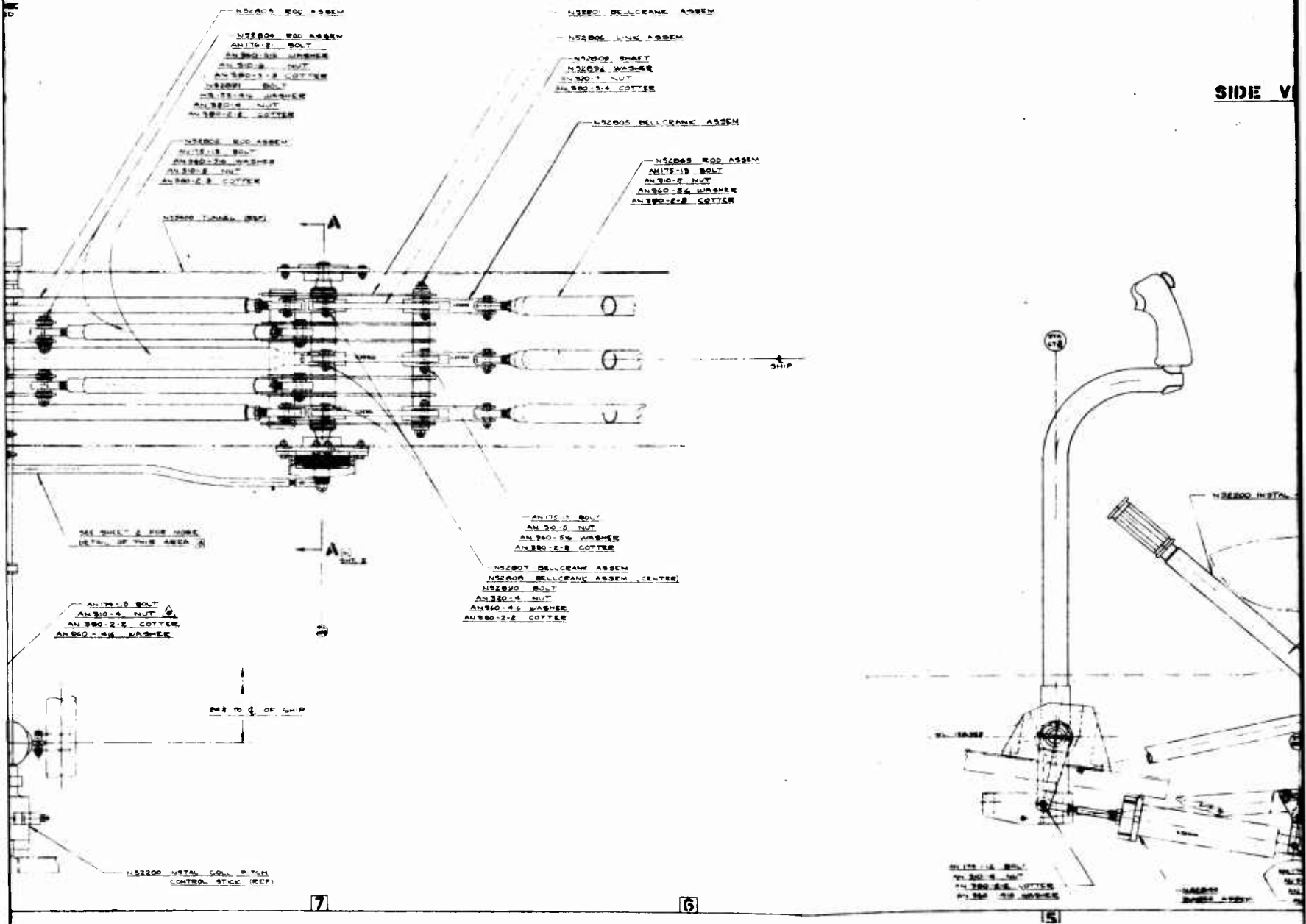
5

6

2

VIEW

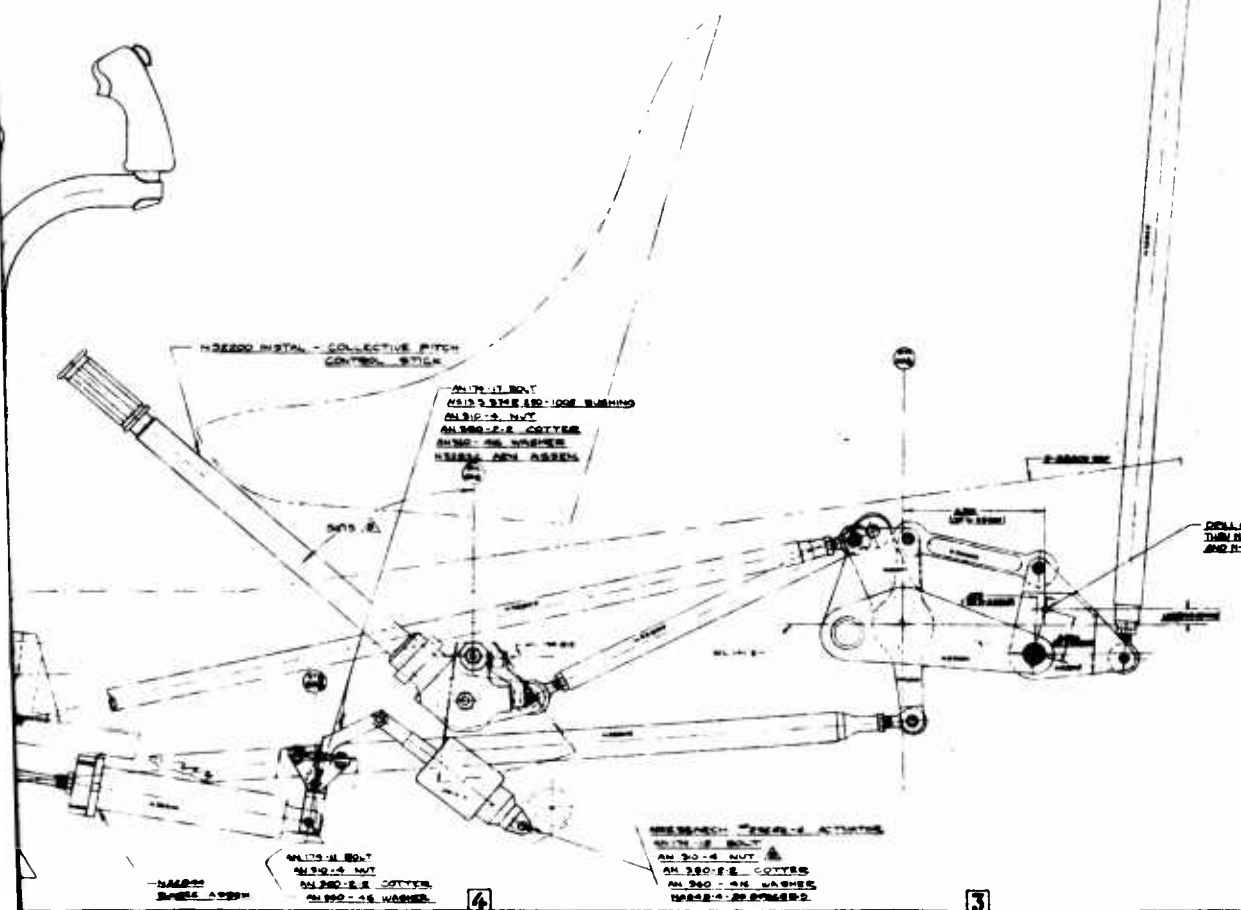
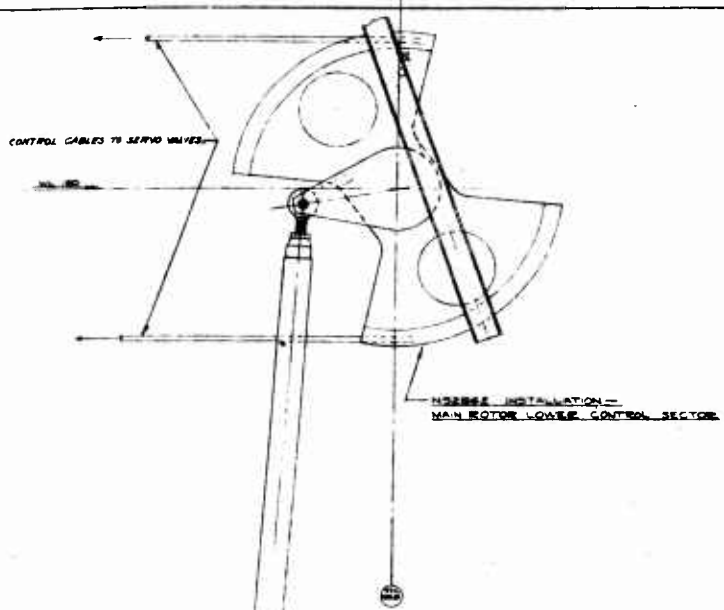
SIDE V



3

SIDE VIEW

←
FORWARD



NOTES:

1. DIMENSIONS SHOWN FOR ASSEMBLY FITTINGS, ETC. ARE TO BE HELD PITCH STICKS IN VERTICAL - 90° - POS.
 2. ALL 20200 TAPER PINS MUST BE INSURE THAT THE SMALL END OF THE TAPER NOT EXTEND MORE THAN 1/8" ABOVE OR NOT LESS THAN FLUSH WITH SURFACE. TOBUE NUT FINGER TIGHT ONLY.
- ⚠ ADJUST FRICTION BRACK TO GIVE MINIMUM OF DISCONNECTIVE PITCH STICK HANDLE. H-22222 DISCONNECTIVE AT TIME OF ADJUSTMENT.
 - ⚠ COLLECTIVE PITCH STICK TUBE IN POSITION INSURE PIN IS IN PLACE.

20200 TAPER PIN
20200 TAPER PIN
20200 TAPER PIN
20200 TAPER PIN

4

20200 TAPER PIN
20200 TAPER PIN
20200 TAPER PIN
20200 TAPER PIN

3

2

ANALYSIS _____

MODEL _____

REPORT NO. _____

PREPARED BY _____

CHECKED BY _____

3. 6 INSTRUMENTATION

3. 6. 1 Strain Gage Installation

The high temperatures at which the Hot Cycle Rotor Blade operates present numerous difficulties in attachment and operation of the strain gages. The strain gages chosen, Baldwin¹ ABD-13 and Tatnall² C6-142-350B, are designed for use at 350°F and higher. The gages are considered fatigue resistant and stable at the temperatures indicated. The ABD-13 gages and some of the C6-142-350B gages were bonded to the various components with Baldwin EPY 400 Cement, capable of service at 600°F with proper cure, with very good results. The remainder of the C6-142-350B gages were bonded to the components using Tatnall GA-50 cement. All strain gages were cured at 350°F except those on aluminum components.

In addition, the problems of bridge configuration had to be considered. Most bridge locations are such that a temperature gradient could exist across the bridge. Such a condition causes an apparent strain when the normal bridge configurations are used. As a result it was necessary to use an eight gage bridge, as in the case of the spars where there are four strain gages on the top, and four strain gages on the bottom of the spar. Each four gages are wired in such a fashion as to be completely temperature compensated. The two four gage bridges were then wired in parallel to give the desired sensitivity, either to bending moments or to axial loads.

All strain gage installations were waterproofed and potted by using Dow-Corning³ RTV 601 silastic rubber compound. The RTV 601 maintains its properties at elevated temperatures and showed fair resistance to abrasion. It was satisfactory in all respects. A typical strain gage installation on the aft spar of the blue blade, the only strain gaged blade, is shown in Figure 3. 6-1. The strain gaged rotor shaft is shown in Figure 3. 6-2. The strain gage wiring on the spars and other fatigue loaded parts was attached with RTV 601 which proved to be highly satisfactory throughout the test.

1 Baldwin-Lima-Hamilton Corporation, Waltham 54, Massachusetts

2 Budd Company, Instruments Division, Phoenixville, Pennsylvania

3 Dow-Corning Corporation, Midland, Michigan

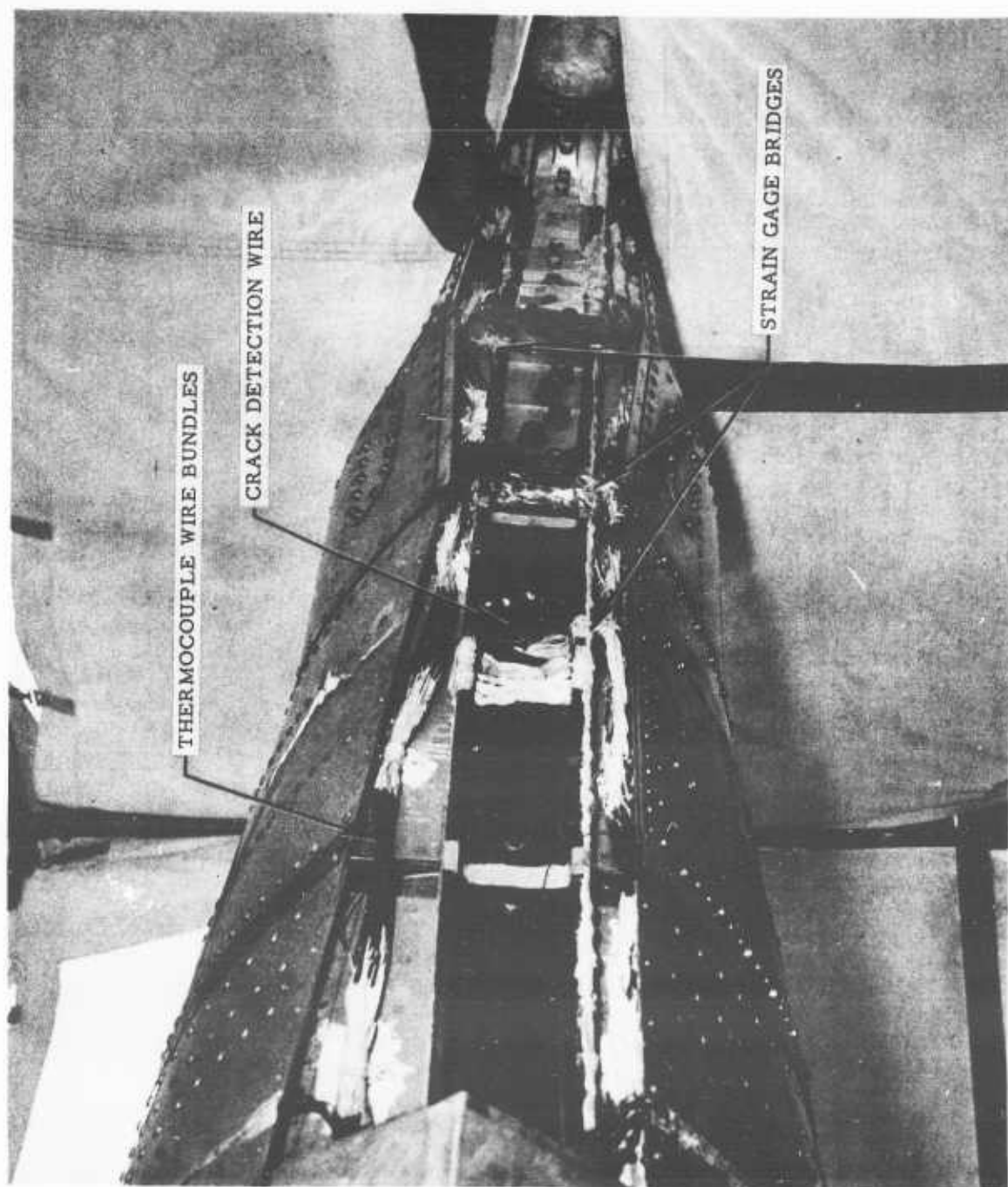


Figure 3.6-1 Instrumentation Installation at Blade Aft Spar

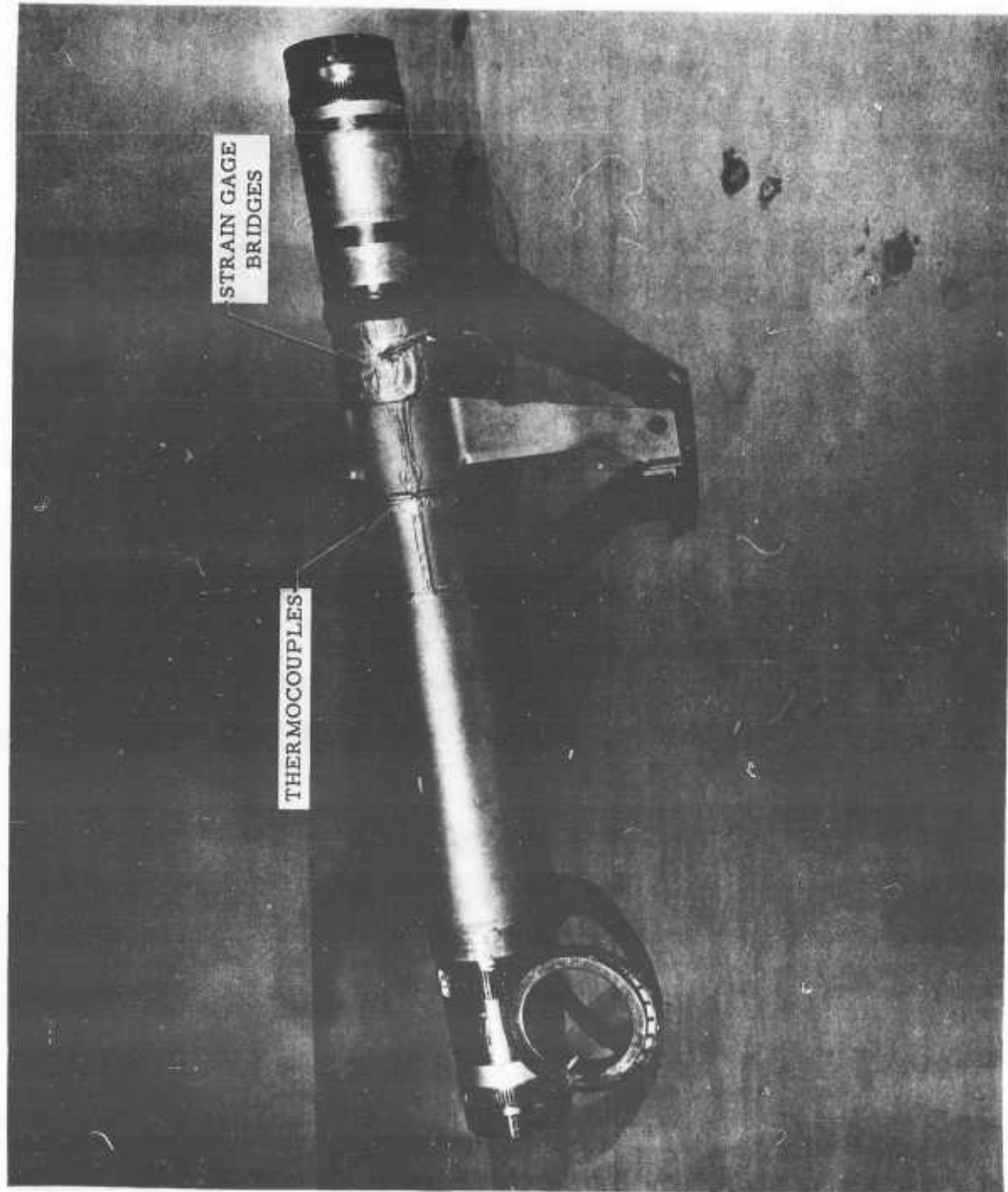


Figure 3.6-2 Instrumentation on Main Rotor Shaft

ANALYSIS _____
 PREPARED BY _____
 CHECKED BY _____

Strain gage bridges located on the structural components of the blade and hub are shown on Figures 3.6-3. Information pertaining to all of the individual strain gage bridges used is given in Table E.2-1, Appendix E.

3.6.2 Thermocouple Installation

Chrome-alumel thermocouples were used throughout on the whirl test rotor. The thermocouple wires, which were 30 gage wire (AWG), were double insulated with fiberglass. The particular type wire used was Thermoelectric Company¹ GG 30CT.

The thermocouples used on the duct walls, flexures, blade skins, and other areas which were not fatigue loaded, were attached by spot welding the ends of the wire to the part directly. These spot welds formed the junction at which the temperature was measured.

The installation of thermocouples on fatigue loaded parts such as the spars, rotor shaft, and hub gimbal lugs presented the same difficulty in attachment as encountered with the strain gages, i. e., high temperature bonding problems. The thermocouple was formed by fusing the two wires into a bead with a submerged mercury arc. This thermocouple was then installed using EPY-400² cement with a fiberglass retainer pad. These installations were then cured at temperatures in excess of 350°F.

All thermocouple lead wires on the blades were tied into bundles and attached to the blade structure with either spot welded sheet metal retaining clips or screw-on clamps. At least 3 clips were used for each standard blade segment. Slack was allowed at the flexure to prevent breaking of the wire due to blade deflection. To prevent centrifugal force from causing the wire bundles to slip and break, RTV 601 was used to anchor the thermocouple lead wires in the retention clips. This installation can be seen in Figure 3.6-1. The location of the individual thermocouples is shown in Figure 3.6-4 and listed in Table E.2-2, Appendix E.

3.6.3 Miscellaneous Instrumentation Installation

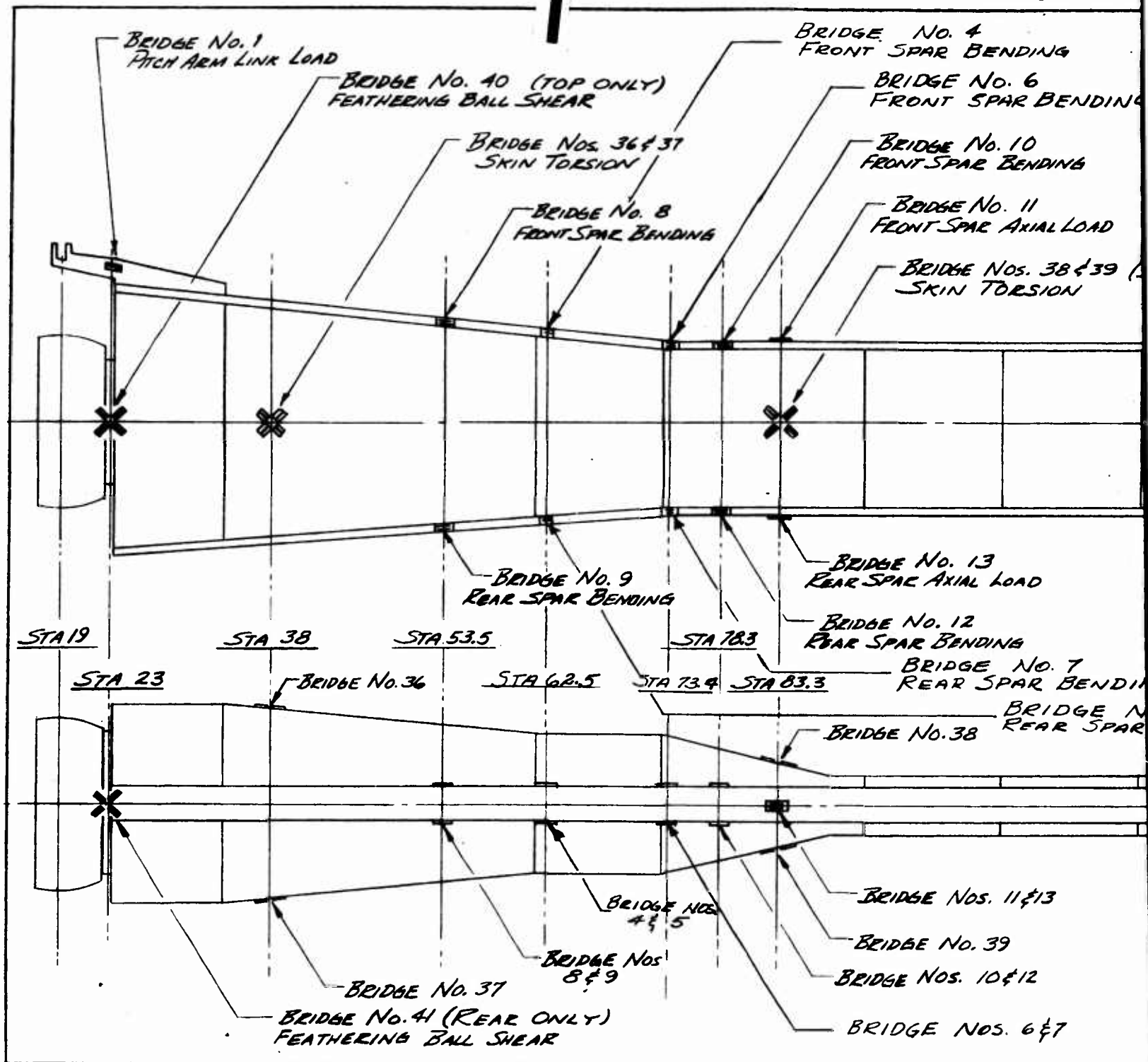
3.6.3.1 Crack Detection Wire

A crack detection wire was installed on all spars as a precautionary measure. 40 gage heavy Formvar copper wire was cemented to the spars with G. A. -50 cement between stations 55 and 90. The cement

1 Thermoelectric Company, Saddle Brook, New Jersey

2 Baldwin-Lima-Hamilton Corporation, Waltham 54, Massachusetts

1



2

STRAIN GAGE LOCATIONS
HOT CYCLE WHIRL TEST BLADE

ENDING
6
R BENDING

10
BENDING

11
AXIAL LOAD

15. 38 & 39 (STA 83.5)
TENSION

LOAD

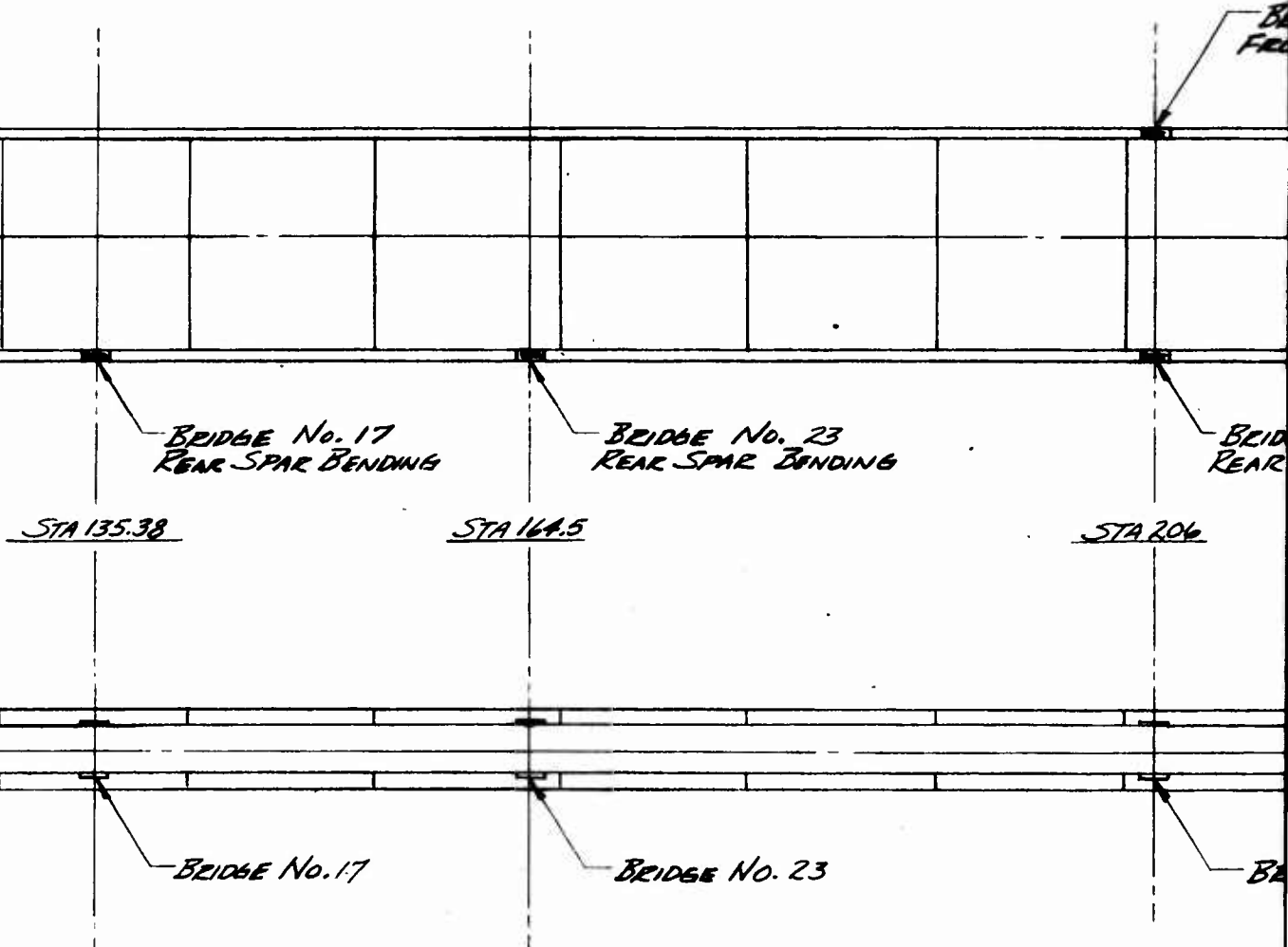
16
NO. 7
PAR BENDING
BRIDGE No. 5
REAR SPAR BENDING

11 & 13

19

12

5. 6 & 7



3

BRIDGE No. 34
180° GIMBAL LUG BEND

BRIDGE No. 24
FRONT SPAR BENDING

BRIDGE No.
AXIAL LOA

BRIDGE No. 25
REAR SPAR BENDING

BRIDGE No. 29
REAR SPAR BENDING

STA 206

STA 270

BRIDGE No.
IN-PLANE BE

BRIDGE No.
AXIAL L

BRIDGE
90°

BRIDGE Nos. 24 & 25

BRIDGE No. 29

STRA
HOT

4

285-1007

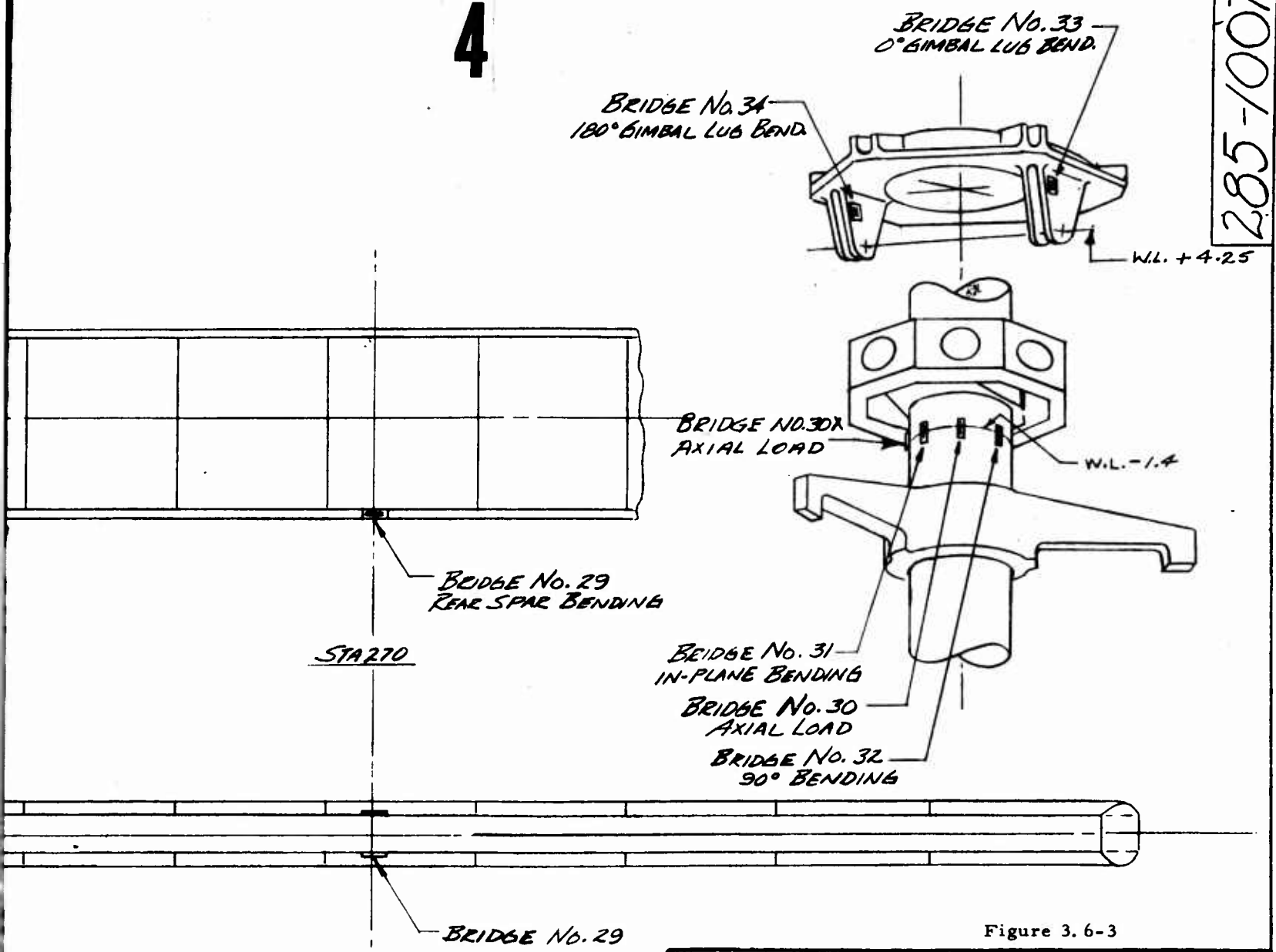


Figure 3.6-3

STRAIN GAGE BRIDGE
LOCATIONS
HOT CYCLE WHIRL TEST
ROTOR

285-1007

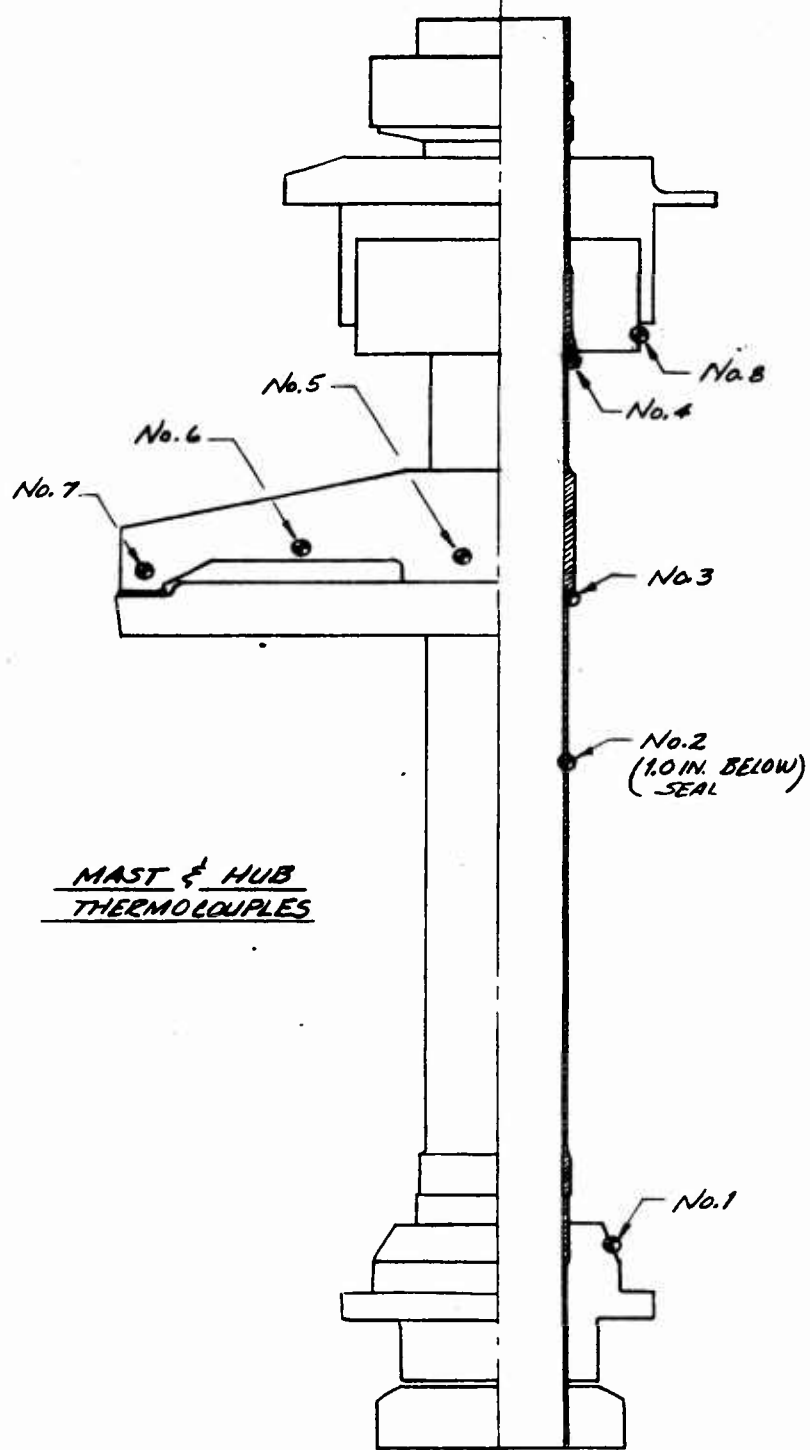
REV D.W.N. 3-15-62 L.L.E. 4-3-61

1

FLEXURE INSTRUMENT

CODE: BC-2-3 = BLUE BLADE
RC-2-3 = RED BLADE
YC-2-3 = YELLOW BLADE

INSTR. FLEXURES:
BLUE BLADE - Nos. 1, 2, 3
RED BLADE - Nos. 4, 5, 6
YELLOW BLADE - Nos. 7, 8



NOTES:

1. ALL THERMOCOUPLES CHROMEL ALUMINUM
2. REF DWGS: 2B5-0937, -0949, -0950, -0951
3. INSTRUMENTATION INB'D OF STA 91 ON BLADE
4. THE COUNTERPART OF BCD- OTHER BLADES IS: RED RCD
5. THE COUNTERPART OF BCD- OTHER BLADES IS: RED RCD
6. THE COUNTERPART OF BCD- OTHER BLADES IS: COOLING

INSTRUMENTATION

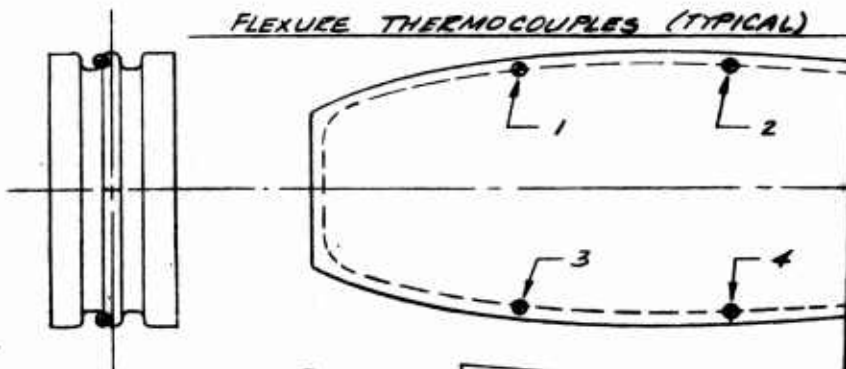
2-3 = BLUE BLADE, FLEX. 2 FROM ROOT, TC No. 3
 2-3 = RED BLADE, ETC.
 2-3 = YELLOW BLADE, ETC.

EXURES:

BLUE BLADE - Nos. 2, 4, 6, 8, 10, 12, 14, 16 & 18
 RED BLADE - Nos. 2 & 18
 YELLOW BLADE - Nos. 2 & 18

2

FLEXURE THERMOCOUPLES (TYPICAL)



CHROMEL ALUMEL
 -0949, -0950, -0951, -1002
 PART OF STA 91 ON BLUE BLADE ONLY
 PART OF BCD-1 ON THE
 IS: RED RCDF, YELLOW YCDF
 PART OF BCD-2 ON THE
 IS: RED RCDR, YELLOW YCDR
 PART OF BCD-5 ON THE
 IS: COOLING AIR, STA 78

DUCT GIMBAL RING

BBJ-1
 ON INNER SURF
 OF TUBE

BHD-1
 OUTER FWD SURF OF INB'D
 ART. DUCT SEAL AT TOP ONLY

HUB DUCT

DUCT GIMBAL RING

STA 21.9

BR-1
 ON INNER SURF
 OF FLEXURE
 STA 57 COOLING AIR

STA 19

STA 24.25

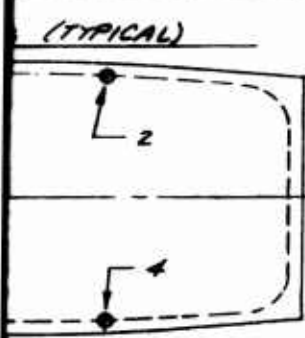
STA 33.25

STA 45

STA 57 COOLING AIR

C

3



BS-1-7, BS-18-7

BS-1-8, BS-18-8

BS-1-1

BS-1

BS-4

BFS-1
BRS-1

BS-1-10, BS-18-10

BS-1-9, BS-18-9

BFS-2

SECTIONS C-C & D-D
SKIN THERMOCOUPLES

FLEXURE
No. 1

SEG. No 1

SEG. No 2

SEG. No 3

SEG. No 4

SEG. No 5

STA 83.3

INNER SURF
FLEXURE
FAST COOLING
AIR

BR-2
INNER SURF.
OF RIB

BR-3
INNER SURF.
OF RIB

C23, C24
C15, C16
BCD-5

C21, C22

BRS-2

BRS-2, BFS-2



STA 45

STA 63

STA 73

STA 91

STA 103.5

STA 116

STA 128.5

STA 141

STA 153

COOLING
AIR

C16, C24

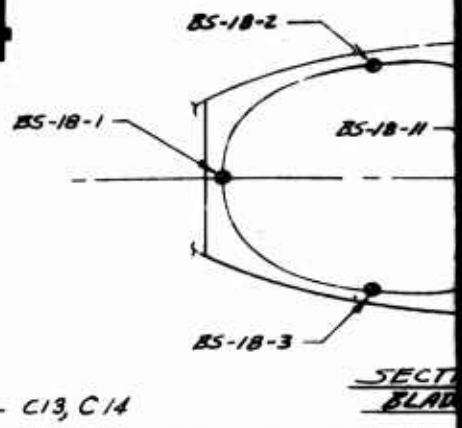
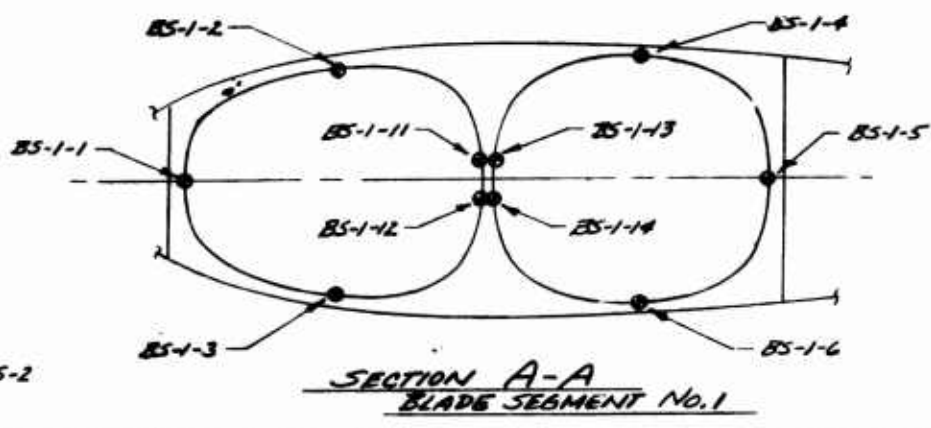
BRS-1
BFS-1

STA 83.3

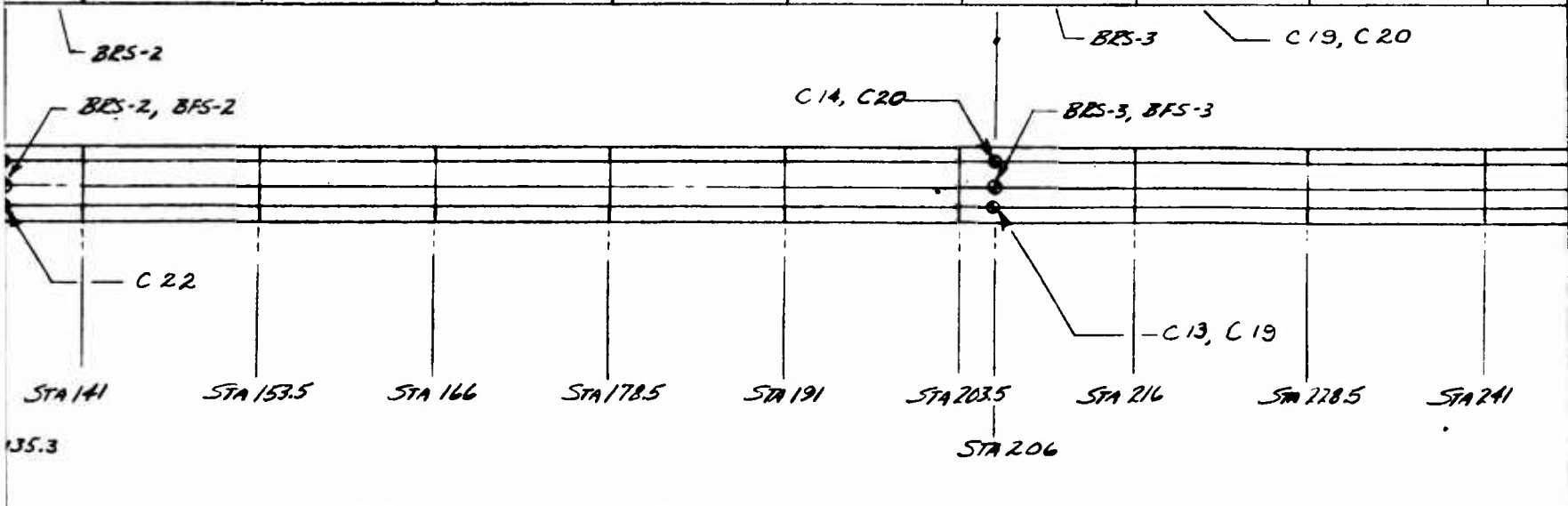
BCD-5

STA 135.3

4



SEG. No. 4	SEG. No. 5	SEG. No. 6	SEG. No. 7	SEG. No. 8	SEG. No. 9	SEG. No. 10	SEG. No. 11	SEG. No. 12	SEG. No. 13



35.3

5

THERMOCOUPLE LOCATIONS
HOT CYCLE WHIRL TEST BLADES

285-1008

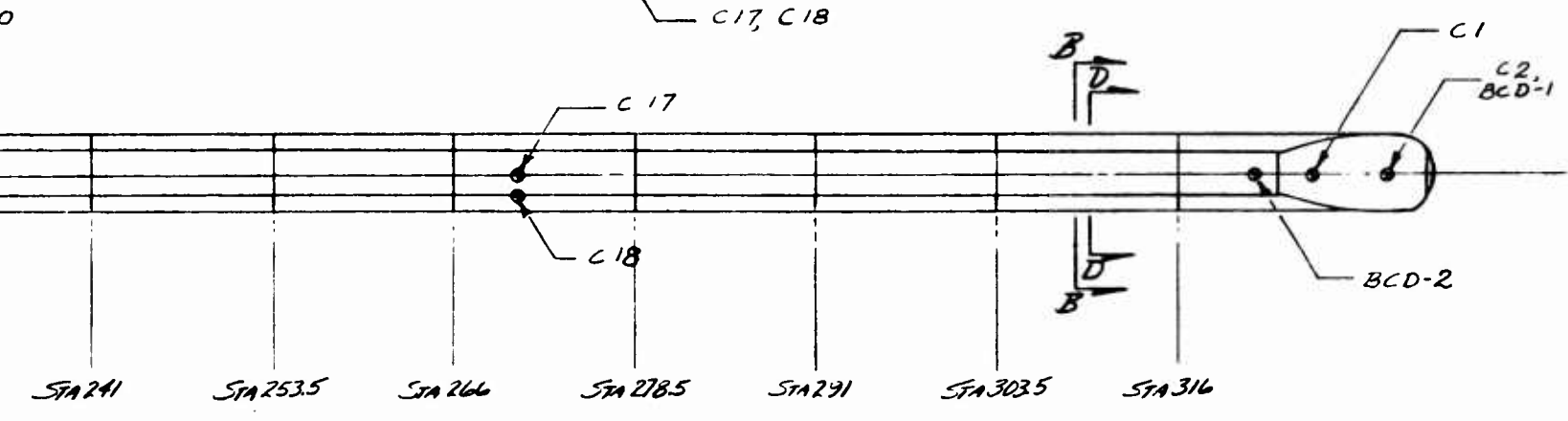
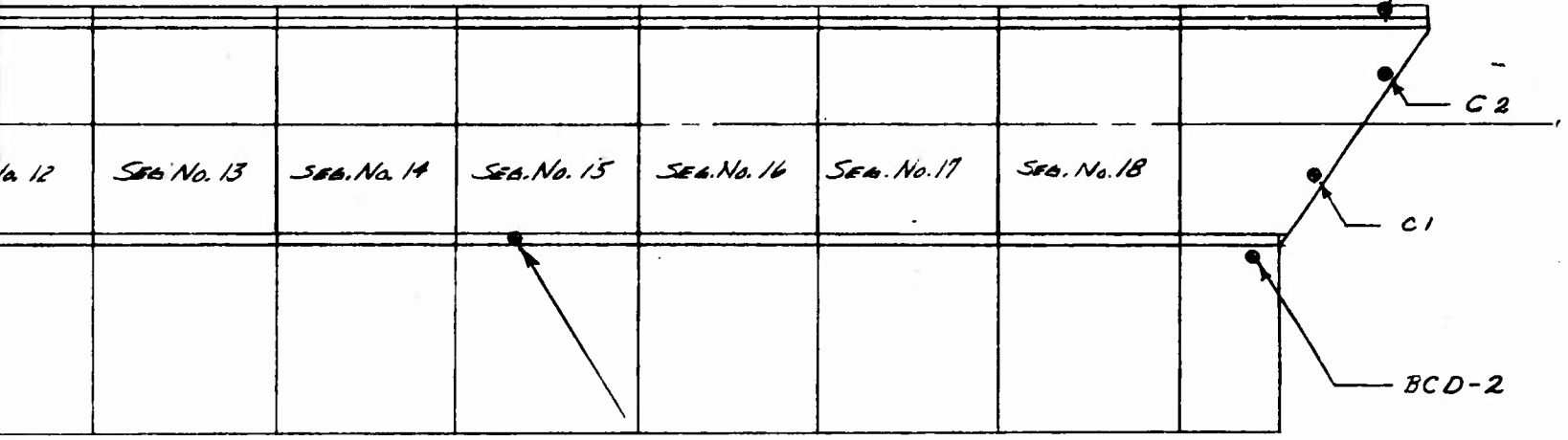
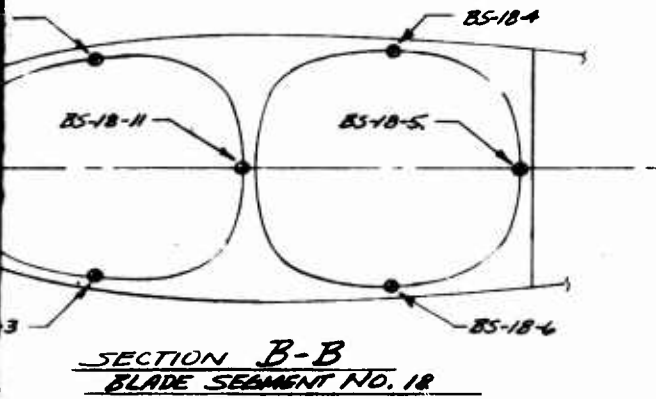


Figure 3.6-4

REV D.W.N. 3-15-62 LLE 5-3-61

ANALYSIS _____

PREPARED BY _____

CHECKED BY _____

was cured at 350°F. All spars were hooked up in a series circuit so that a crack in any spar would break the wire and extinguish a light bulb mounted on top of the hub. The light bulb and batteries are shown in Figure 3.6-5. The crack detection wire on the aft spar of the blue blade can be seen in Figure 3.6-1.

3.6.3.2 Hub Tilt Stop Position Indicator

A hub tilt stop indicating system was used to determine when the 2° tilt stops were disengaged. This system consisted of three microswitches hooked in series with a light and battery. When all three microswitches were closed, indicating every 2° tilt stop was disengaged, a red light mounted on the skirt of the hub was actuated.

3.6.3.3 Hub Tilt Indicator

The motion of the hub was measured by using the 285-0956 hub tilt pickup. The pickup consisted of a strain gaged cantilever beam with a ball on one end and a teflon covered fitting attached to the hub structure. The surface upon which the beam rubbed was cylindrical about the feathering axis of the yellow blade so that the pickup registered hub tilt about one axis only. This installation can be seen in Figure 3.6-5.

3.6.3.4 Blade Coning Indicator

Blade coning and flapping was measured using the 285-0947 flap angle pickup. The pickup consisted of a strain gaged beam connected to a spring loaded beam whose outboard end rested on a teflon pad mounted on the blade. This installation can be seen on 285-0947. It was necessary to use the spring loaded beam to cut down the deflection of the strain gaged member. The teflon pad was a cylindrical surface whose center was the feathering axis of the blade. Thus the pickup was unaffected by a change in pitch of the blade. This installation is shown in Figure 3.6-6.

3.6.3.5 Strap Windup Indicator

The amount of strap windup is directly related to the movement of the 285-0303 torque tube assembly with respect to the hub. The pickup was a strain gaged member attached to the hub at one end with the other end connected to the torque tube assembly by a link, as shown on 285-0947. The installation is shown in Figure 3.6-6.

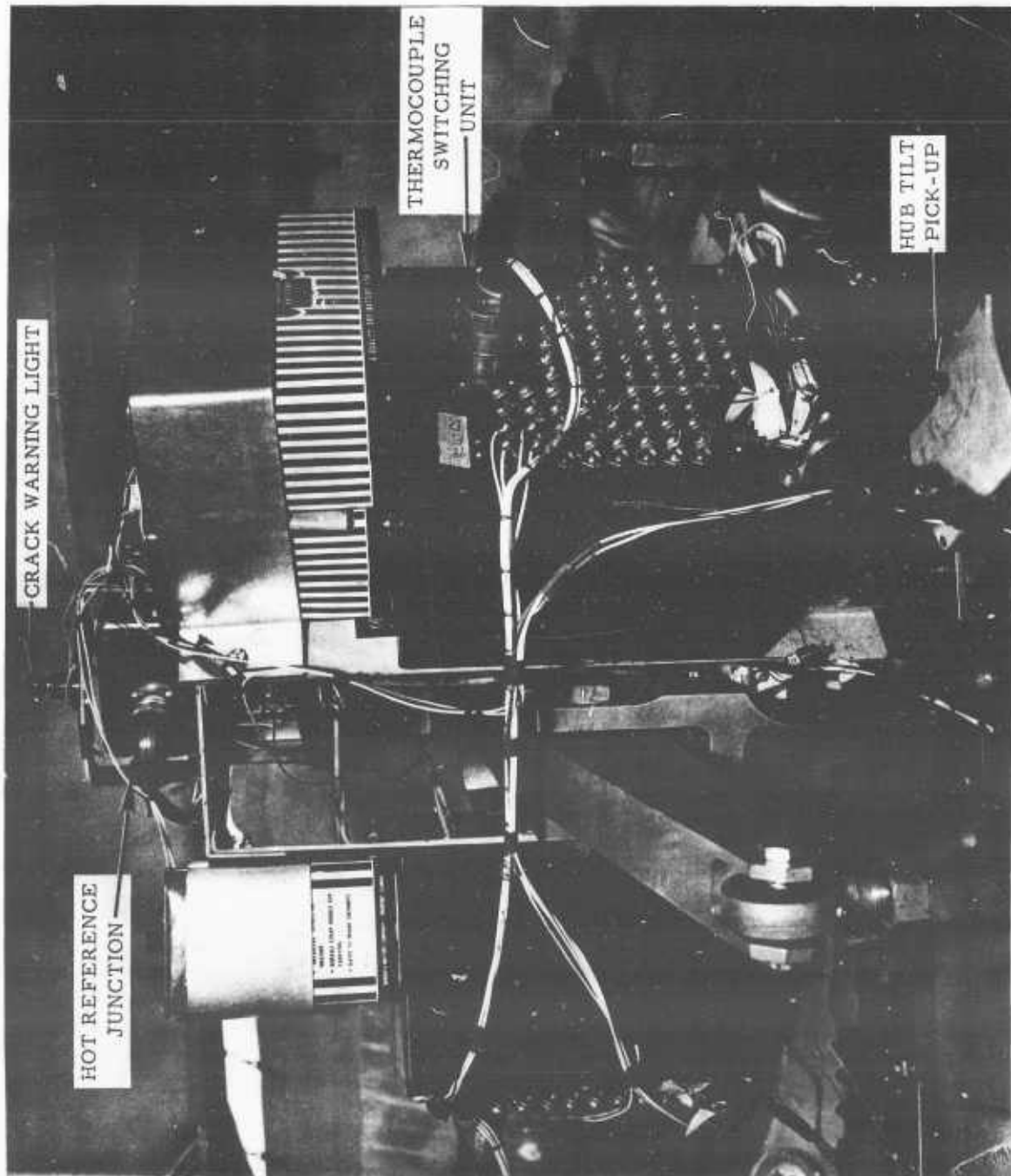


Figure 3. 6-5 Instrumentation Installation on Top of Rotor

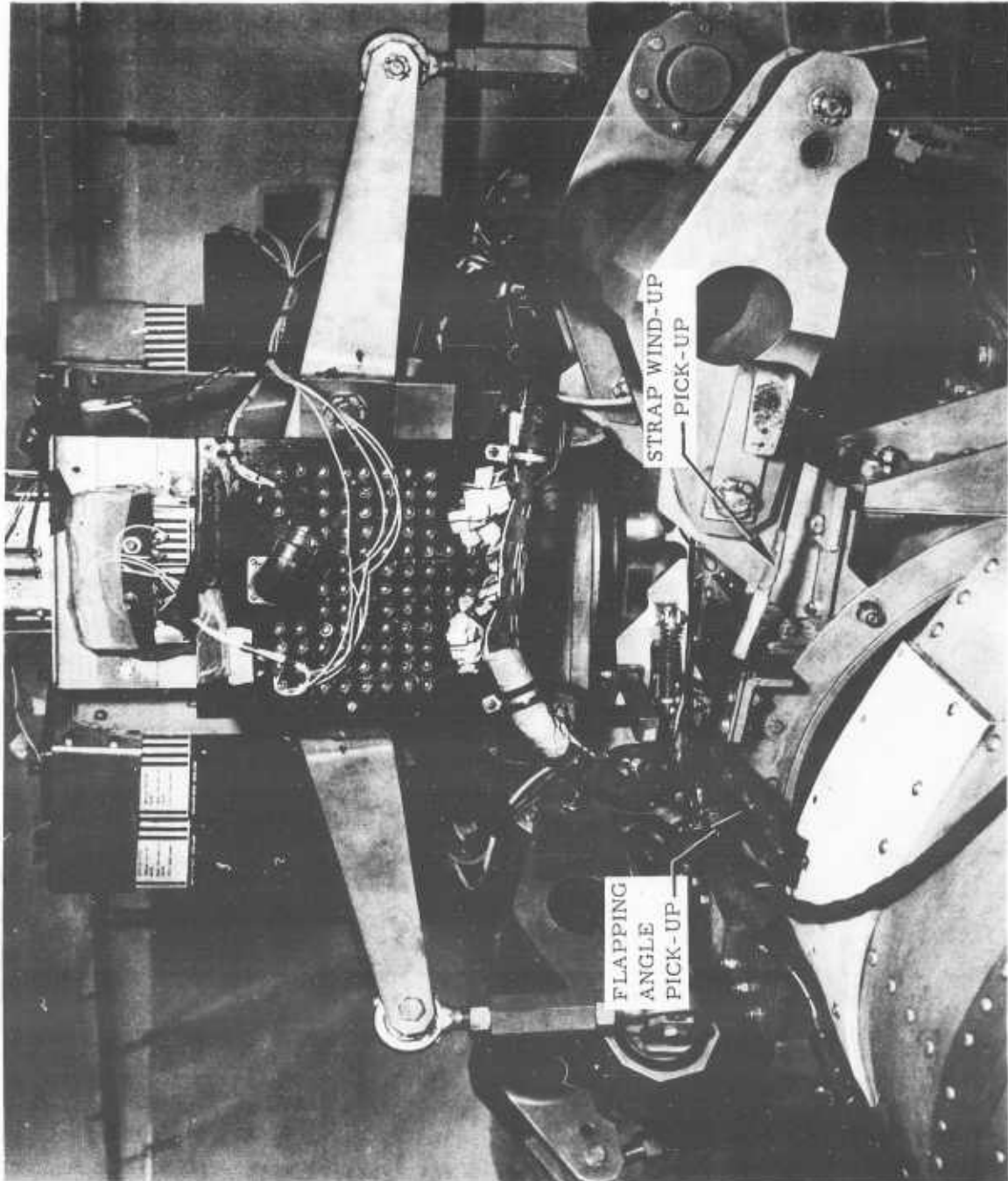


Figure 3.6-6 Instrumentation Installation on Top of Rotor

ANALYSIS _____

MODEL _____

REPORT NO. _____

PREPARED BY _____

CHECKED BY _____

3.6.3.6 Azimuth and RPM Indicator

An azimuth indicator and rpm indicator were installed for recording this information on the oscillograph records. A magnet was attached to the shaft directly underneath the blue blade. A coil was placed on the stationary structure in such a fashion that when the blue blade was pointing forward it caused a blip on the oscillograph record. In addition, a tachometer generator was attached to the rotor shaft and connected to a tachometer indicator mounted on the instrument panel in front of the pilot.

3.6.3.7 Vibration Pickup

Two accelerometers were placed on the rotor to measure the vibration and check for resonant frequencies. One accelerometer sensitive to horizontal accelerations was mounted on the upper truss 285-0523-1 directly beneath the upper bearing at W.L. -19.0. The other accelerometer, oriented so as to be sensitive to vertical accelerations, was attached to the stationary swashplate 285-0313 at W.L. -57.0.

3.6.3.8 Control Movement Sensors

The movements of the control sticks and the hydraulic control cylinders were monitored by using 3 turn variable potentiometers. The potentiometers were equipped with spring loaded sheaves around which was wrapped the braided wire cable attached to the particular item. One potentiometer was attached to each one of the control hydraulic cylinders. The cyclic pitch control had two potentiometers attached to it. One responded to fore and aft movement of the stick, the other to lateral movements. One potentiometer was also attached to the collective pitch control stick.

3.6.3.9 Oil Temperature Sensors

A thermocouple was installed in the oil return line from the thrust bearing to detect any significant temperature increase. The output of this thermocouple was monitored by a Brown Strip Chart recorder placed in front of the pilot. In addition a thermoswitch set at 225°F was placed in the oil return line from the upper bearing. When this switch closed it flashed a warning light on the panel in front of the pilot.

ANALYSIS _____

PREPARED BY _____

CHECKED BY _____

3.6.4 Pressure Instrumentation

For whirl tests, primary stream pressure instrumentation was provided at three stations; two stations each being parallel branch pairs. These locations are referred to as turbine discharge, flow measuring, and hub stations. The former two stations also include total temperature thermocouples for engine monitoring and flow determination.

The turbine discharge averaging total pressure rake is engine supplied while the flow measuring and hub station rakes are HTC-AD designed and fabricated. Details of these latter two rakes are provided by HTC-AD Drawing 285-1015.

3.6.5 Calibration Procedure

3.6.5.1 Strain Gage Installations

a. Rotor Shaft Axial Bridges

The rotor shaft axial load and lower pylon bridges were calibrated at the same time on the whirl test stand. This was accomplished by hooking a crane to the 285-0765 hoist fitting which was attached to the 285-0306 control support assembly, using a hydraulic cylinder and a 100,000 pound load ring. The load ring was calibrated in the lab before being used. The load ring was strain gaged and the output read on a Baldwin Lima-Hamilton Type 20 strain indicator. The load was applied as follows; 0, 4000, 8000, 12000, 16000, 18000 and 24000 pounds. The output of the pylon strain gage bridge and shaft strain gage bridges were recorded by an oscillograph. The calibration hook up is shown in Figure 3.6-7. The calibration procedures demonstrated that the rotor shaft bending bridges were not sensitive to axial loads. The pylon gages were monitored during the pressure testing so that a correction could be applied to values obtained during the runs.

b. Rotor Shaft Bending Bridges

The rotor shaft bending bridges were calibrated by two methods. During the assembly of the rotor the rotor shaft bending bridges

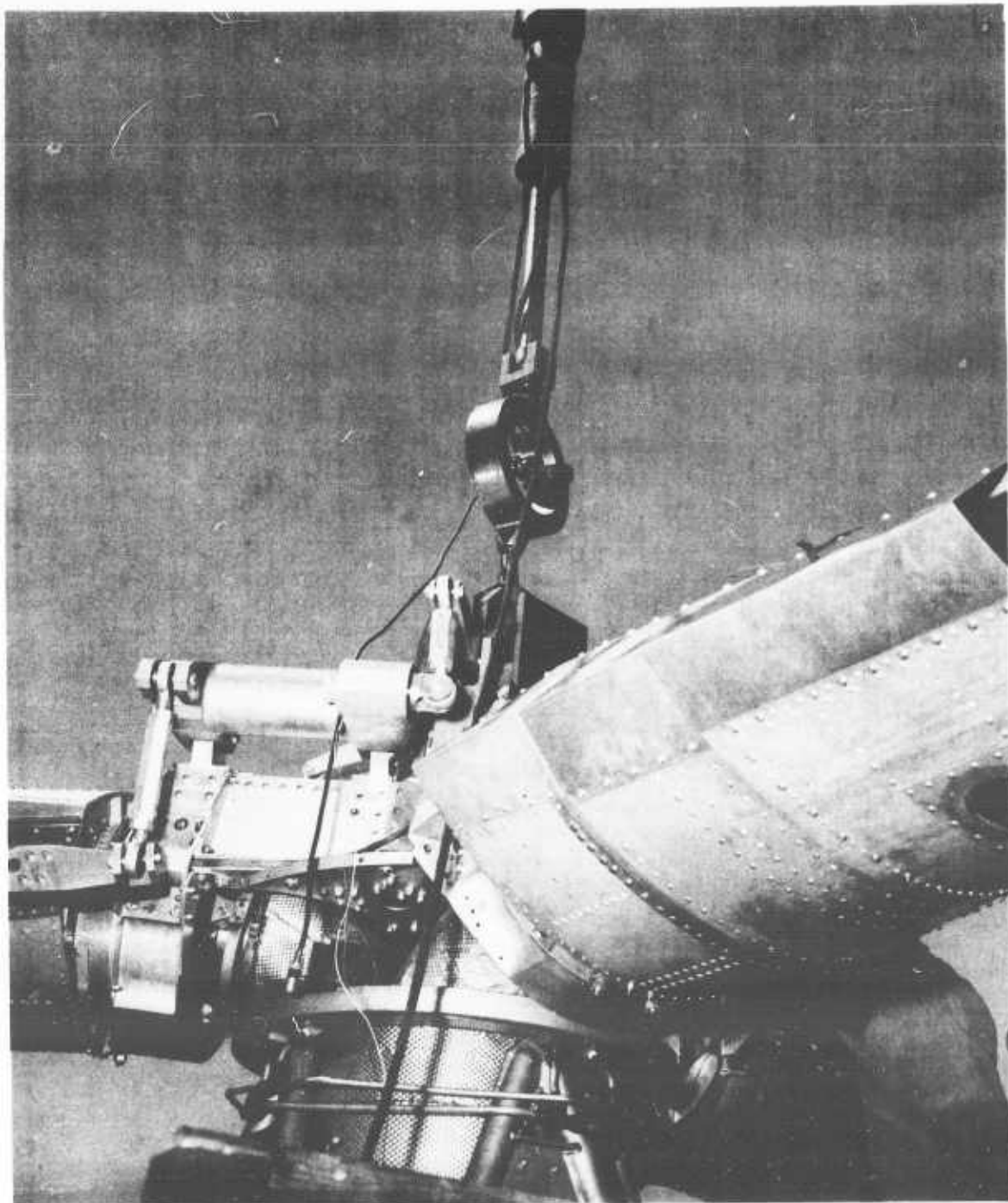


Figure 3.6-7 Calibration of Lift Measuring Strain Gages
(Note load ring and hydraulic cylinder attached
between hub shaft and crane.)

ANALYSIS _____

PREPARED BY _____

CHECKED BY _____

were calibrated by attaching a cable to the top of the rotor shaft and applying a load through a hydraulic cylinder and load ring. The load was applied in 200 pound increments up to 1000 pounds and the output recorded using a Type "L" Baldwin strain indicator.

The hub gimbal lugs bridges were also calibrated during assembly in the shop by pulling on the hub with a cable and hydraulic cylinder connected to a load ring. The load was applied in 200 pound increments up to a maximum of 1000 pounds. A cable was also attached to the hub and to the pylon base to prevent rotation of the hub due to eccentric loading. The output of the gages was recorded on a Baldwin Type "L" strain indicator.

After the rotor was installed on the whirl tower following the 35 hour inspection the rotor shaft bending gages in line with the blue blade and the hub gimbal lug gages were calibrated by attaching the 285-0923-3 tip loading fixture to the blue blade and pulling on it with a hydraulic cylinder and load ring attached to a crane. The load was applied in increments of 500 pounds up to a maximum load of 2000 pounds. The blade was supported at the tip by the crane so that it was level and props were placed beneath the hub on the side opposite the blue blade to prevent rotation due to the eccentricity of the blade retention straps and hub trunnion. The calibration of the bending bridge oriented at 90° to the blue blade was accomplished by pulling on the tip of the yellow blade in a similar manner.

c. Flapwise Bending Bridge Calibration

The flapwise bending bridges were calibrated in the shop during the assembly of the rotor with the blade hanging in the 285-0921 blade support fixture which was attached to a gantry crane as shown in 285-0925. The installation is shown in Figure 3.6-8. Shims were inserted between the droop stop rollers and the support fixture so that the blade was prevented from swinging. A flapwise load was then applied at the tip through a load ring and load cell. The 285-0944 loading fixture was attached to the blade at Station 312.6. The load was applied in 20 pound increments up to a maximum of 100 pounds. The output of the strain gages were recorded by an oscillograph.

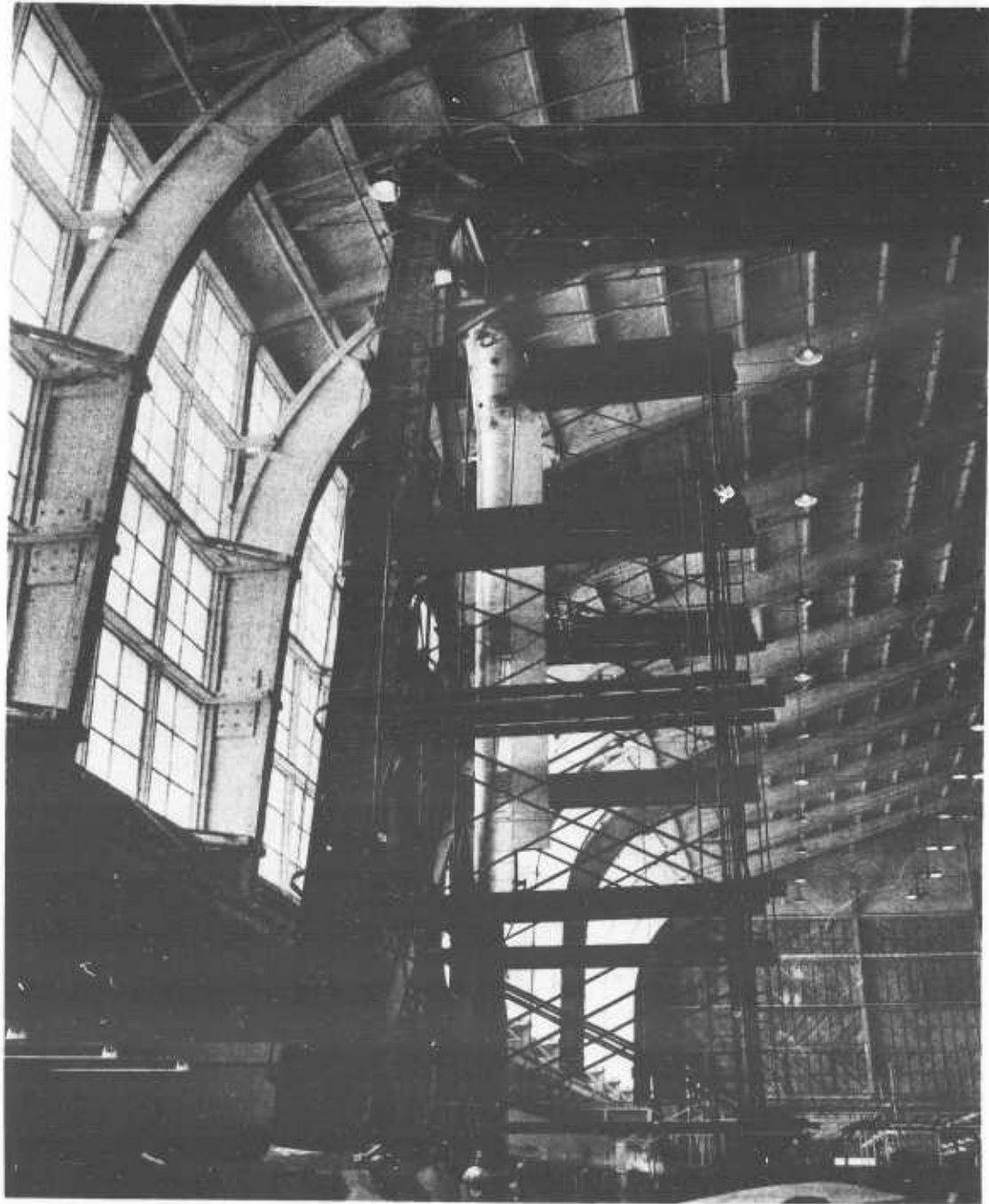


Figure 3.6-8 Blade Hung Vertically for Bending Calibration and Frequency Measurements

ANALYSIS _____

PREPARED BY _____

CHECKED BY _____

After the inspection which followed 35 hours of whirl testing, the flapwise bending gages were calibrated with the rotor installed on the whirl tower. For this calibration the blade was raised so that it was clear of the droop stop and supported on the 285-0939 blade support between Stations 63 and 73. Dead weight was added in 20 pound increments up to a maximum of 100 pounds at Station 314.4. The outputs of the strain gages were recorded by an oscillograph.

d. Chordwise Bending Bridges

The chordwise bending gages were calibrated with the blade supported as shown in Figure 3.6-8 and described in 3.6.5.1, above. The 285-0923-3 tip loading fixture was attached to the blade, and to this fixture a cable carried the load of a hydraulic cylinder. This cylinder was placed in series with a 10,000 pound load ring and a 10,000 pound load cell which were attached to an I-beam anchored to the floor by lead weights. The 285-0923-7 chordwise load fixture was attached to the blade at Station 320.9. The gages were calibrated by applying an axial load to prevent the blade retention straps from buckling, and then applying chordwise loads in increments. The tip loading fixture was designed so that the axial loads were applied along the feathering axis of the blade. The axial loads with the chordwise load increments were as follows;

7000 pounds; 0, 30, 60, 90, 120, 150 pounds
6000 pounds; 0, 20, 40, 60, 80, 100 pounds
5000 pounds; 0, 20, 40, 60, 80, 100 pounds
4000 pounds; 0, 20, 40, 60, 80, 100 pounds

Dimensional scales were attached to the blade at the tip and near the root, and the deflection of the blade was measured by means of a transit. The output of the strain gages were recorded by using an oscillograph.

e. Blade Torsion and Pitcharm Bridges

The blade torsion and pitch arm strain gage bridges were calibrated with the blade supported as described previously in 3.6.5.1, c. In addition, the 285-0923-5 blade torsion fitting was attached to the end of the blade. The 285-0935 torsion test load jig was hooked to the fitting at the tip of the blade in such a fashion that the torsion was applied without causing

ANALYSIS _____

PREPARED BY _____

CHECKED BY _____

translation of the blade tip. A recently calibrated load cell connected the pitch arm assembly to the blade support fixture. The torque applied to the blade by a hydraulic cylinder was measured by both a load ring and a load cell attached in series with a cable which wrapped around the blade torsion fitting. Torque was applied (in both directions) in 1000 inch-pound increments up to a maximum of 10,000 inch-pounds. Blade torsional deflection and the pitch calibration were accomplished at the same time since the load cell attached to the pitch arm assembly measured directly the reaction force at the pitch arm. An oscillograph was used to record the output of the strain gages.

f. Feathering Ball Horizontal Shear Bridge

The strain gage bridge which measures horizontal shear at the feathering ball was calibrated by attaching a cable, load ring, hydraulic cylinder, and load cell in series to the pitch arm and pulling horizontally. The load was applied in 200 pound increments up to a total of 1000 pounds. The output of the load cell as well as that of the horizontal shear bridge was recorded using an oscillograph.

g. Feathering Ball Vertical Shear Bridge

The vertical shear strain gage bridge at the feathering ball was calibrated by applying a load at the attachment for the 285-0133 droop stop installation. The blade was supported at the tip so that the droop stop was clear. The load was applied in 200 pound increments to a maximum of 1000 pounds. The load was applied by using a hydraulic cylinder, load cell, and load ring in series. The output of the load cell and the vertical shear bridges was recorded by an oscillograph.

h. Swashplate Drag Link Bridge

The 285-0332 drag link assembly was reworked to act as a load cell in measuring the stationary swashplate drag loads. The assembly was calibrated in a baldwin static test machine using a Baldwin Type "L" strain indicator. The load was applied in 200 pound increments to a maximum load of 2000 pounds.

ANALYSIS _____

PREPARED BY _____

CHECKED BY _____

i. Control Force Bridges

The 285-0326-3 rod ends were reworked so that they could be used as transducers in measuring the control forces. The rod ends were calibrated in a Baldwin test machine using a Baldwin-Lima-Hamilton Type 20 strain indicator. The load was applied in 500 pound increments to a maximum of 5000 pounds.

j. Horizontal Force Bridges

The hub support upper structural truss strain gage bridges were calibrated in the fore and aft direction at the same time the hub gimbal lugs and rotor shaft in-plane gages were calibrated as described in 3.6.5.1, b. The lateral direction calibration was accomplished by rotating a blade to a position 90° to the fore and aft direction and pulling on the tip with the crane. The blade was held horizontal for this calibration. The load was applied in 500 pound increments to a maximum of 2000 pounds by using a hydraulic cylinder and load ring.

k. Flapping Angle Measuring Bridge

The 285-0948 flapping angle pickup was calibrated by attaching the crane to the tip of the blade and raising it in 2° increments to a maximum of 10° as measured by a precision clinometer on the pitch control arm. Shims were used to hold the hub level and to prevent rotation of the hub about the trunnion. A small outboard load was maintained to prevent damage to the feathering ball during the calibration. The output of the pick-up was recorded by using an oscillograph.

l. Hub Tilt Measuring Bridge

The calibration of the 285-0956 hub tilt pick-up was accomplished by pulling down on the yellow blade with 2° hub tilt stops disengaged. Two clinometers were used, one a precision clinometer, to measure the hub tilt, and the other one to make sure that the hub was level in the direction normal to the yellow blade. The hub was tilted in 2° increments until the full travel, 9.6° , was reached. The calibration was performed in both directions, first by pulling down on the yellow blade and then by pulling down on the red blade. An oscillograph was used to record the output of the pick-up.

ANALYSIS _____

PREPARED BY _____

CHECKED BY _____

m. Strap Wind-up Measuring Bridge

The strap wind-up pickup, 285-0948, was calibrated by installing a template at the 3/4 radius point on the blade. The blade was then moved in 2° increments until maximum travel was reached. The angles were measured by using a precision clinometer attached to the template. The output of the strap wind-up pickup was recorded by an oscillograph.

n. Duct Torsion Bridge

The 285-0178 articulated duct gimbal ring was strain gaged to measure the duct torsion loads. This assembly was supported in the 285-0943 test jig and dead weight loads applied at the end of an arm to give 200 inch pound torque increments up to a maximum of 1000 inch pounds. The output of the gages was monitored by a Baldwin Type "L" strain indicator. The torque was applied in both directions during the calibration.

3.6.5.2 Thermocouple Calibrations

The thermocouple wire used was calibrated by the manufacturer and guaranteed to be within standard tolerances. The various recorders used were calibrated according to the manufacturer's directions several times throughout the whirl test program.

3.6.5.3 Miscellaneous Calibrations

a. Control Cylinder Movement Sensors

The variable potentiometers attached to the hydraulic control cylinders were calibrated by moving the collective control stick the amount which caused the control cylinders to move exactly one inch. Since these potentiometers are linear, it was unnecessary to calibrate to full travel.

b. Control Stick Movement Sensors

The variable potentiometers attached to the collective pitch and cyclic pitch control sticks were calibrated by moving the control sticks through their respective full ranges in 2° increments as measured by a precision clinometer attached to the template at the 3/4 radius point of the blade. The output of the potentiometers was recorded by using an oscillograph.

ANALYSIS _____

PREPARED BY _____

CHECKED BY _____

3.6.6 Recording Instrumentation

3.6.6.1 Strain Gage Instrumentation

a. Strain Gage Wiring

The inboard ends of the strain gage wiring were equipped with a Winchester M4P plug which fitted into a Winchester M4S socket contained on one of three boxes attached to the 285-0306 upper control support assembly. From the three boxes the wires ran to the 285-0310-17 conduit assembly which was supported by spokes in the center of the rotor shaft. The wire ran to a 44 channel slip ring assembly mounted on the lower end of the rotor shaft as shown on 285-0500. The slip ring had coin silver rings and silver graphite brushes. The 44 channel slip ring as installed is shown in Figure 3.6-9. From the slip ring the wires ran to a junction box at the end of the main instrumentation cable. Cannon XL-3 plugs were used in this box. The instrumentation cable ended at the bridge balance boxes in the control van. All strain gage circuits were powered by a parallel power connection at the upper junction box. Thus each bridge required only two wires through the slip ring assembly. This made a total of 21 channels available for strain gage bridges through the slip ring.

b. Strain Gage Bridge Balance Box

Two bridge balance boxes were used to condition the signal for recording by the oscillograph. One, a 20 channel box was built by American Helicopter Corporation while the other, a 15 channel box, was made by HTC-AD. Both bridge balance boxes had individual balance control, and attenuation for each channel. In addition, an internal electrical calibration device was contained in each unit. The balance boxes are shown in Figure 3.6-10.

c. Strain Gage Recording Instrumentation

A CEC¹ 5-119P3-50 model recording oscillograph was used to record the output of the various transducers. The oscillograph, shown in Figure 3.6-10, had provision for 50 channels and a mirror galvanometer compatible with the transducer involved was used in each channel. The magazine was a CEC 5-036C

¹ Consolidated Electrodynamics Corporation, Pasadena, California

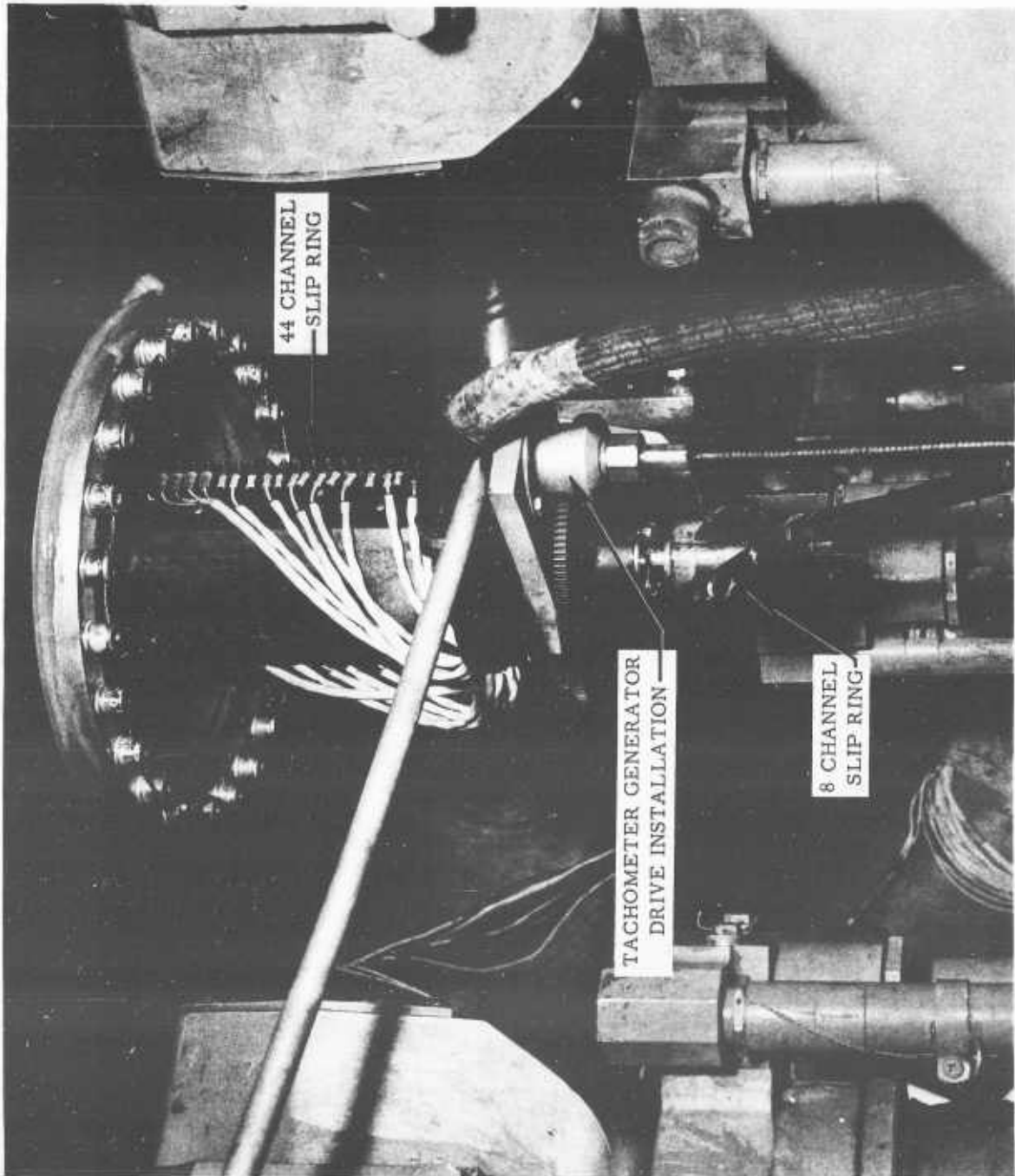


Figure 3.6-9 Slip Ring and Tachometer Drive Installations

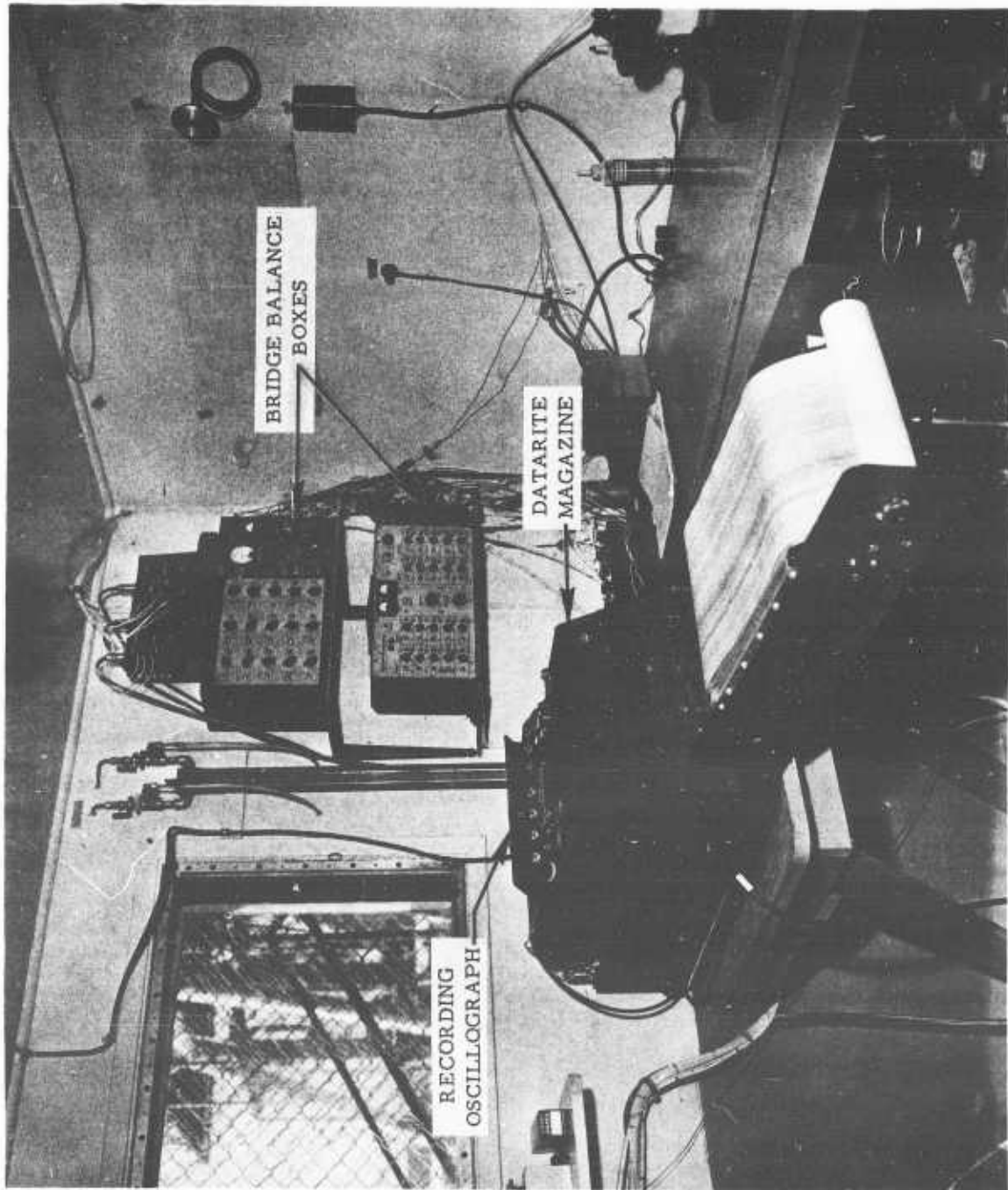


Figure 3.6-10 Oscillograph Installation

ANALYSIS _____

MODEL _____

RECORD NO. _____

(62-16) PAGE 3.6-22

PREPARED BY _____

CHECKED BY _____

Datarite equipped with CEC 5-046 take up reel. The Datarite Magazine processed the record as it was taken, and so provided instant read-out of the test data. Kodak type 33 paper was used throughout the test and proved to be very satisfactory.

3.6.6.2 Thermocouple Instrumentation

a. Thermocouple Switches and Hot Reference Junction

The chromel-alumel thermocouple lead wire was run to the Minneapolis-Honeywell 918W2P aircraft type, 48 point switching unit which had compensated terminals. From the thermocouple switching units the thermocouple lead wires went to a Pace model FRJ-33-3 hot reference junction. The hot reference junction was used so that no error would be introduced by junction of dissimilar metals at the slip ring, plugs, etc.. The 48 point switching unit together with the hot reference junction is shown in Figure 3.6-5.

b. Thermocouple Slip Ring Installation

The thermocouple signal copper leads, together with six other wires necessary for the operation of the hot reference junction and switching units ran through the 285-0310-17 conduit assembly to an eight channel slip ring attached to the bottom of the 44 channel slip ring as shown on 285-0500. The eight channel slip ring can be seen in Figure 3.6-9.

c. Temperature Recorders

Temperatures from the rotor were recorded by a 12 point Brown recorder with a 0 to 1200°F capability. This combination of the 12 point recorder and the three 48 point switching units made it possible to read a total of 144 thermocouples. The Brown recorder and recorder control switches are shown in Figure 3.6-11.

Temperatures at the 285-1015 duct pressure rake installation were recorded on a Leeds and Northrup Speedomax H single point strip chart recorder. The recorder had a range of 0 to 1200°F. A manually operated thermocouple selector switch was provided to monitor the thermocouples. The recorder is shown in Figure 3.6-12.

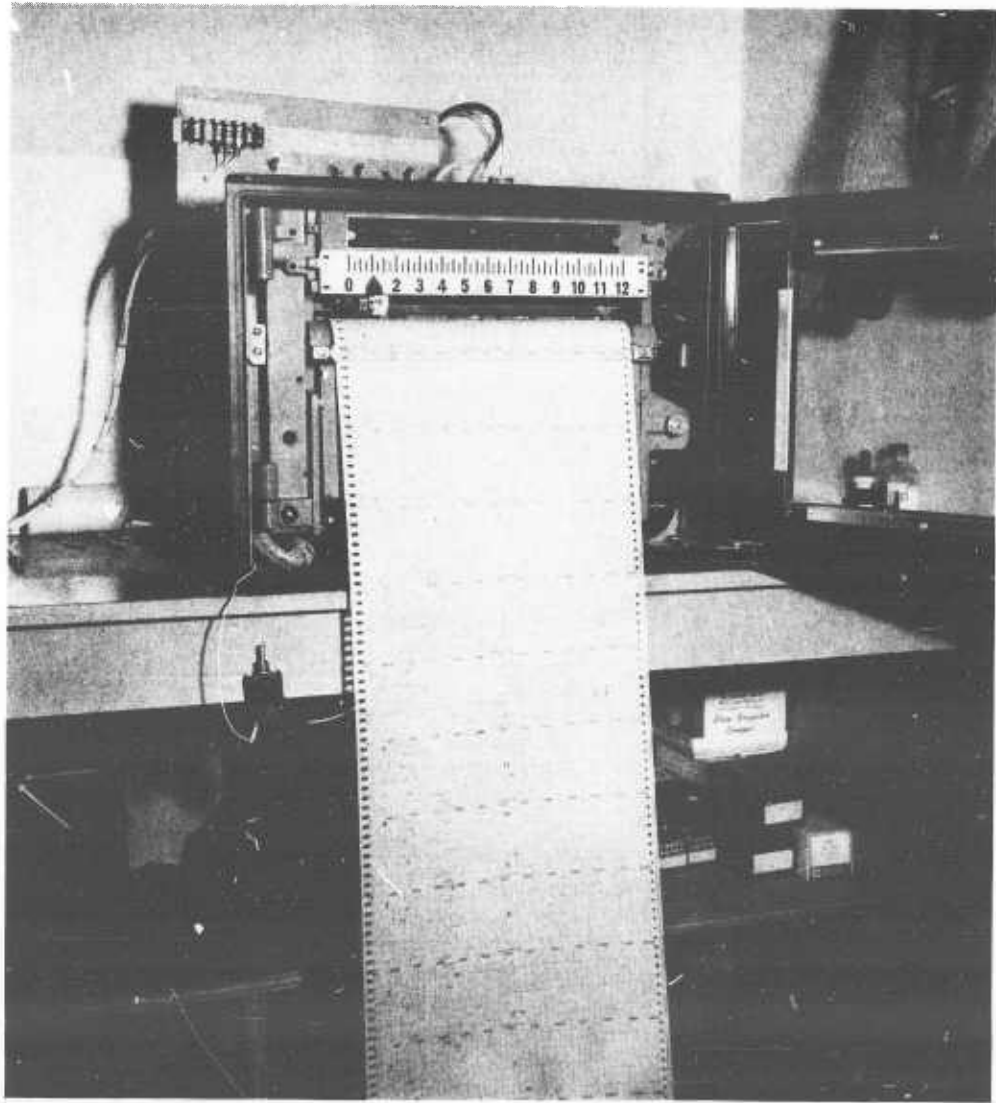


Figure 3.6-11 Brown 48-Point Temperature Recorder



Figure 3.6-12 Multi-tube Manometer Bank and Single-Point Temperature Recorder

ANALYSIS _____

PREPARED BY _____

CHECKED BY _____

Turbine discharge temperature of the J-57 engine was recorded on a Leeds and Northrup Speedomax H single point strip chart recorder with a 0-1000°C temperature range. The recorder is shown in Figure 3.6-13.

Thrust bearing oil return temperature was monitored by a -0.5 to +10.5 millivolt Brown strip chart recorder. The recorder had a scale that was calibrated to read in degrees Fahrenheit. The recorder was connected to a Thermoelectric Company protected type chromel-alumel thermocouple inserted in the oil return line. The recorder is shown in Figure 3.6-13.

3.6.6.3 Manometers

Primary stream pressure distributions were measured with an HTC-AD fabricated 50 tube manometer. The fluid employed therein was TBE manometer fluid with a usable column height of approximately 48 inches. The reservoir pressure was monitored with a single tube, well type mercury manometer (Meriam) and although control of the engine was accomplished by continuous monitoring with a 30 psig maximum Helicoid Pressure Gage, another mercury manometer was used for accurate measurement of the turbine discharge pressure. Figure 3.6-16 is a photograph of these manometer instruments within the control van.

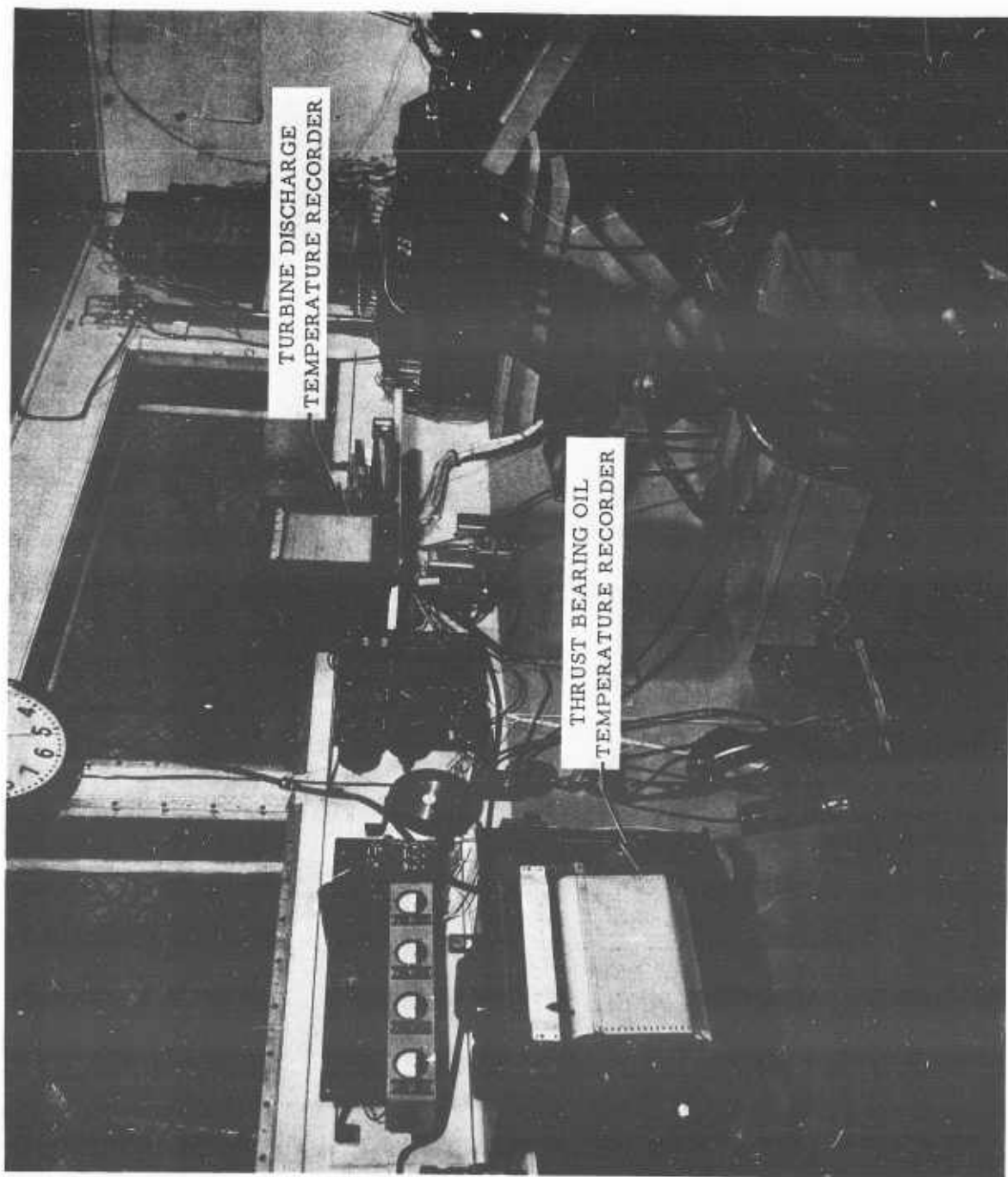


Figure 3.6-13 Engine Turbine Discharge and Rotor Bearing Oil Temperature Recorders

ANALYSIS _____

PREPARED BY _____

CHECKED BY _____

SECTION 4DESCRIPTION OF TESTS4.1 GENERAL

This section discusses the procedure used during the whirl test program and summarizes the test conditions. In general, the whirl test program was conducted in accordance with Report No. 285-8-3SR "Proposed Whirl Tower Program," dated November 1961 (Reference 4.1-1).

ANALYSIS

MODEL

REPORT NO.

PREPARED BY S. J. Chris 3/13/62

CHECKED BY

4.2 PROCEDURES

Following is an outline of the procedures for operation of the equipment described and shown previously in Section 3. The procedures were refined in the early tests and this outline was utilized thereafter in the conduction of the whirl tests.

4.2.1 Ground Equipment

- a. Start hydraulic unit for engine oil cooler pumps.
- b. Start hydraulic unit for rotor control power units.
- c. Start auxiliary starter compressor.

4.2.2 Engine Starting Procedure

Pilot

- a. Place Collective Pitch control at 2° or 4° as required for particular test.
- b. Place Cyclic Pitch control in neutral.
- c. Start rotor bearing lubricating oil system, vacuum pump first.
- d. Power lever to "fuel cut-off".
- e. At 12 to 15% N_2 move power lever to idle (fuel flow will move to 1000 PPH). Allow engine to accelerate to idle speed (approximately 60 to 70 rotor rpm).

Power Plant Eng.

- a. 28 V inverter switch to "on".
- b. Butterfly valve closed.
- c. Exhaust dump valve full open.
- d. Fuel shutoff valve - open.
- e. Oil cooling hydraulic system - on.
- f. Fuel boost pump - on.
- g. Energize starter (record time)
- h. At 8 to 10% N_2^* - energize ignition.

* N_2 = high pressure compressor rpm

ANALYSIS

PREPARED BY S. J. Chris 3/13/62

CHECKED BY

- i. Record time to reach idle rpm.
- j. De-energize ignition when lite-off is evident.
- k. De-energize starter at 25 to 30% N₂ rpm.

4.2.3 Test Procedure

Pilot

- a. Increase power to produce 170 rpm to disengage centrifugally operated 2° rotor hub tilt stops. (watch for signal light)
- b. Adjust cyclic pitch control to level swash plate.
- c. Proceed with test maneuvers.

- d. Following tests, return to 170 rpm.
- e. Bring engine to idle.

4.2.4 Engine Shutdown Procedure

Pilot

- a. Power lever to idle for 5 minutes to stabilize engine temperatures.

Power Plant Eng.

- a. When oscillograph has been calibrated, open butterfly to rotor.
- b. Adjust exhaust dump valve to bring engine operation on line.

- c. Adjust exhaust dump valve as necessary to maintain on-line engine operation. For max temp tests adjust dump valve to reduce exhaust area and thus produce temp desired (off-line operation)

- d. Close butterfly to rotor.

Power Plant Eng.

HUGHES TOOL COMPANY-AIRCRAFT DIVISION

ANALYSIS

MODEL

REPORT NO

PAGE 4.2-3

PREPARED BY S. J. Chris 3/13/62

CHECKED BY

- b. Power lever to 75% N₂ to scavenge oil system for 30 seconds.
- c. Power lever - off.

- a. Fuel boost pump - off (when engine has stopped.)
- b. Fuel shutoff valve - closed.
- c. Oil cooling hydraulic system - off.

- d. After rotor has coasted to stop, shut off rotor bearing lubricating oil system, pressure pump first.

- d. Instrumentation and master electrical switch - off.

4.2.5 Unsatisfactory Engine Start

Note:

- a. If fuel flow exceeds 1000 pph - discontinue the start.
- b. If exhaust gas temperature exceeds 610°C (1130°F), even momentarily, discontinue start.

Pilot

Power Plant Eng.

- a. Power lever - off.

- a. Ignition switch - off.
- b. Starter switch - off.
- c. Fuel boost pump switch - off (when engine has stopped rotating)

Note: Purge engine exhaust system as follows

- b. Power lever - cutoff.

- d. Ignition switch - off.
- e. Fuel boost pump - on.
- f. Fuel shutoff valve - open.
- g. Engine start switch - on.
- h. Maintain cranking for 10 to 20 seconds.
- i. Engine start switch - off.
- j. Fuel boost pump - off (when engine has stopped)

HUGHES TOOL COMPANY-AIRCRAFT DIVISION

ANALYSIS

MODEL

REPORT NO

PAGE 4.2-4

PREPARED BY S. J. Chris 3/13/62

CHECKED BY _____

k. Fuel shutoff valve - closed.

4.2.6 Emergency Shutdown Procedure

4.2.6.1 Controlled Emergency

Pilot

Power Plant Eng.

a. Engine power lever to idle.

a. Open exhaust dump valve.
b. Close butterfly valve.

b. Collective pitch control to 4-2°.

c. Cyclic pitch control to approximately level hub position.

c. If possible comply with normal shutdown procedures above.

4.2.6.2 Uncontrolled Emergency

Pilot

Power Plant Eng.

a. Place power lever in cutoff
b. Dump collective pitch.
c. Cyclic pitch control to approximately level hub position if emergency allows.

OR Use emergency engine shutoff switch.

ANALYSIS

PREPARED BY

CHECKED BY

4.3 TEST LOG

A detailed log of the tests is presented in Appendix B. Table 4.3-1 summarizes the hours spent at various temperature levels. The hours at each of the temperatures are further broken down to show the portion of time during the final 25 hours of running during which there were no change of components. Also shown in Table 4.3-1 are the exhaust temperatures of both the standard and an advanced version of the T-64 gas generator (ST129). It can be seen that a total of 5.5 hours were run at temperatures of 1200° to 1275°F which is equivalent to the Take Off rating (five-minute rating) of the T-64 (ST129). A total of 14.8 hours were run at engine discharge temperatures of 1100° to 1200° which is equivalent to the Take Off rating of the standard T-64 and to the Military Power rating of both the standard and ST129 versions of the T-64. Table 4.3-2 compares the hours run at Take Off and Military temperature levels with the hours of running required by Military specifications. Inasmuch as the Hot Cycle rotor is both a rotor and a portion of an engine, both rotor and engine 50 hour specifications are presented. It can be seen that the hours at the Take Off temperature level are approximately twice those called for in the specifications and the hours at the Military temperature level are three to five times the values in the Military specifications. Also shown in Table 4.3-2 is a comparison of the number of power transients performed during the whirl test program with those called for in the Military specifications. It can be seen that the number of transients performed is approximately equal to the average of the two specifications.

Table 4.3-3 lists all components replaced with new parts during the 60 hour whirl test program. The time at which the part was replaced and the total hours in service are tabulated, as well as the reason for the replacement. Note that there were no changes in components whatsoever during the final 25 hours of whirl testing.

ANALYSIS _____

PREPARED BY _____

CHECKED BY _____

TABLE 4.3-1

HOT CYCLE ROTOR WHIRL TEST

TEMPERATURE LOG

T _T °F 7 Engine Discharge	Equivalent T-64 Engine Rating	Time at Temperature		
		0-35 Hours Whirl Test	35-60 Hours Whirl Test (No Change of Components)	Total
1200-1275	Take-off, ST129: 1225	3.2	2.3	5.5
1100-1200	Military, ST129: 1180 Take-off, Std: 1180 Military, Std: 1150	6.9	7.9	14.8
900-110	NRP, Std. and ST129: 1100 75% NRP, Std. and ST129: 1010	5.8	2.6	8.4
900		19.1	12.2	31.3
TOTALS		35.0	25.0	60.0

ANALYSIS _____

PREPARED BY _____

CHECKED BY _____

TABLE 4. 3-2COMPARISON OF WHIRL TEST WITH
MILITARY SPECIFICATIONS

Power Condition	Hot Cycle Whirl Test	MIL T 8679 50 Hour Rotor Ground Endurance	MIL E 8597 Engine PFRT
Take Off, hours	5.5	2.5	2.7
Military, hours	14.8	2.5	4.0
Number of Transients	37.0	30.0	48.0

TABLE 4.3-3

COMPONENTS REPLACED WITH NEW PARTS DURING WHIRL TEST

HTC-AD Dwg. No. and Description	Time - Rotor Hours		Reason
	Installed	Replaced In Service	
285-0179-11 Sheet metal cyl. section of inboard artic. duct, 3 blades	0	1 1	Damage resulting from binding of artic. duct outboard seal.
285-0178-5 Flexure assy's of artic. duct inboard gimbal, 3 blades	0 1	1 1 35 34	" " " " " " Conservative precaution. No sign of damage.
285-0162 Lip seal, artic. duct outboard, 3 blades	0	7 7	Replaced by 285-0217. Improved design to prevent binding.
285-0217 Lip seal, artic. duct outboard, 3 blades	7	18 11	Conservative precaution. Moderate wear. Small crack in one leaf of one seal.
285-0161 Seal cyl., artic. duct outboard, 3 blades	18	35 17	Conservative precaution. Moderate wear.
285-0161 Seal cyl., artic. duct outboard, 3 blades	0	35 35	Flame plate spalling due to effect of heat cycles on uneven coating on out-of-round base part.
285-0126 Blade feathering bearing ball, 1 blade	0	35 35	Chrome plate on alum. casting blistered
285-0155 Blade feathering fabric bearing, 2 blades	0	35 35	Teflon fabric scored in handling, 1 blade. Loose bond to metal at corners of fabric segments, 1 blade.

TABLE 4.3-3 (Continued)

COMPONENTS REPLACED WITH NEW PARTS DURING WHIRL TEST

HTC-AD Dwg. No. and Description	Time - Rotor Hours		Reason
	Installed	Replaced In Service	
285-0121 Armalon anti-fret shims on blade strap, 3 blades	0	35	35 Handling damage.
285-0198 Armalon anti-fret shims on spars, 3 blades	0	35	35 Handling damage.
285-0160 Carbon seal segments, artic. duct inboard, 1 blade	0	35	35 Handling damage.
285-0590 Caron-faced unit, hub inner seal	0	35	35 Carbon softened and eroded.
285-0514 Hub gimbal bearings	0	35	35 Slight fretting.
285-0303 One large Timken bearing, control torque tube	0	35	35 Small amount of rust
285-0307 Rod end bearings, central control rods	0	35	35 To stay within estimated service life. No evidence of damage.
285-0313 Two Fafnir bearing, swashplate	0	35	35 Rust and some roughness.

ANALYSIS _____

PREPARED BY _____

CHECKED BY _____

SECTION 5

TEST RESULTS AND ANALYSIS

This section of the report presents test results and analysis in the areas of performance, dynamics, thermal considerations (temperature and leakage measurements) structure, sound, and post-test inspection.

5.1 PERFORMANCE5.1.1 Summary

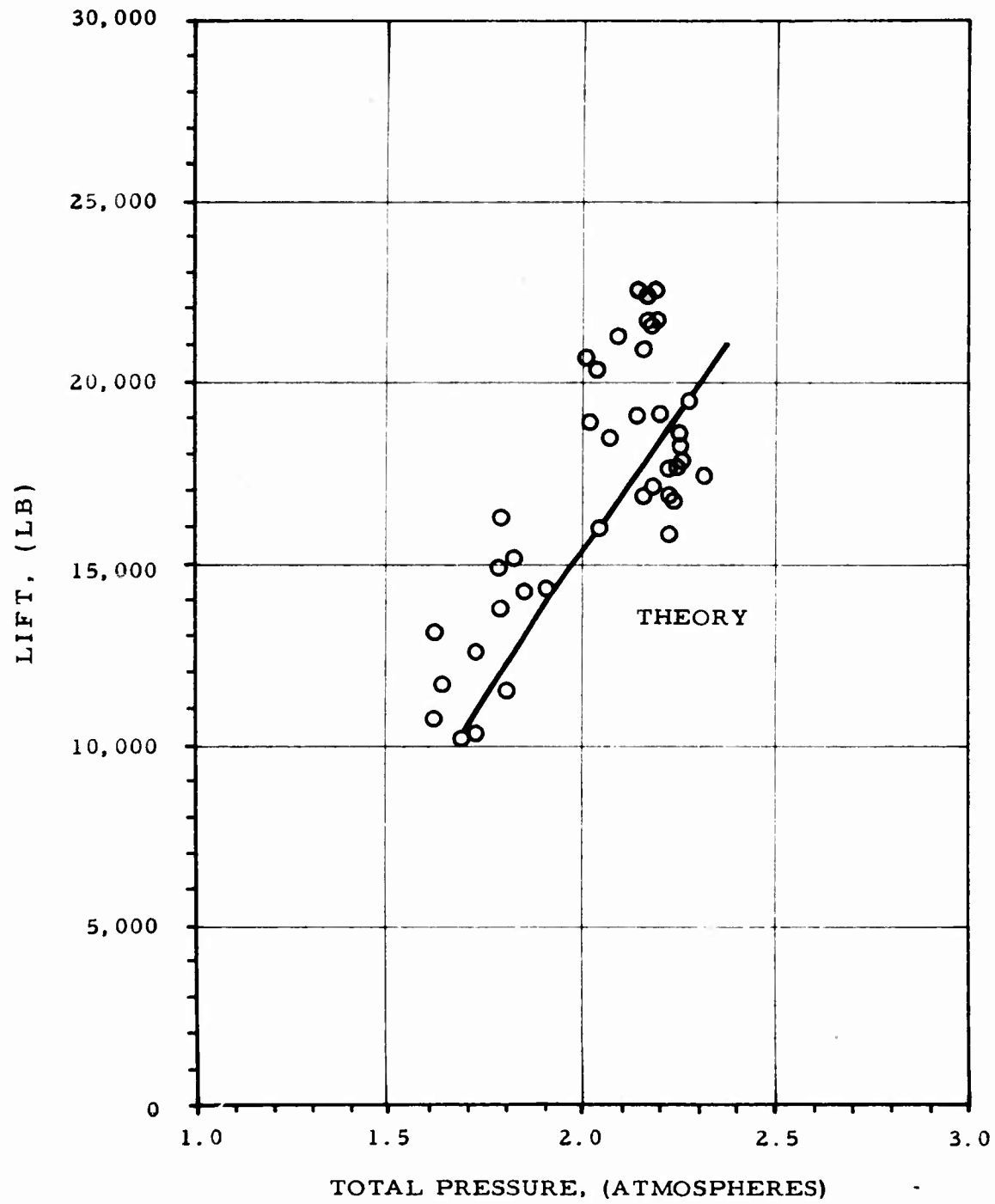
Section 5.1 presents the results of performance measurements made during the 60 hours whirl test program. It is shown that the two key parameters affecting the conversion of engine gas power to rotor power (duct friction coefficient and nozzle velocity coefficient) are both better than originally estimated. It is shown that the duct friction coefficient (and hence the pressure loss) for the test rotor is actually less than the value of .004 used for performance estimates. It is also shown that the nozzle velocity coefficient, which is a measure of efficiency of the tip nozzle in converting pressure energy to jet velocity is about 2-1/2% better than the value of .955 used for performance estimates.

As an over-all check of the performance of the test rotor and propulsion system, Figure 5.1-1 presents a comparison of measured and predicted rotor thrust. It can be seen that the agreement is very good. In this figure, the values of thrust are plotted against total pressure at the rotating seal. In this section, the procedures required to calculate rotor thrust from measurements of total pressure and other data are described. Figure 5.1-1 also shows a maximum value of measured thrust of about 22,000 pounds. For the higher pressure ratio available from the T 64 gas generators (≈ 2.8 atmospheres) the maximum thrust will be about 28,000 pounds.

5.1.2 Discussion

A performance analysis of the Hot Cycle Whirl Test System requires a study of the internal thermodynamics of the gas generator and ducting coupled with the external aerodynamics of the rotor blades. For simplicity, the performance of the J 57-P-19W gas generator, ducts, and blades are presented separately. Once introduced sequentially, however, the various analyses are assembled into an IBM-7090 computer program to permit a comparison of aerothermal predictions with strain gauge measurements of rotor thrust on the main rotor shaft and support pylons. This comparison, then permits a

FIGURE 5.1-1

HOT CYCLE WHIRL TEST PERFORMANCE

ANALYSIS _____

PREPARED BY _____

CHECKED BY _____

direct check on the over-all efficiency of the system. Also, through pressure and temperature measurements at several stations along the system, the thermodynamic performance can be studied in increments thereby permitting isolation of any possible problem areas.

Nomenclature for this work is given in Appendix F.

5.1.3 Internal Thermodynamic Performance

This section presents the pressure and temperature losses from the engine to the rotating seal (hub) station. Duct losses between the rotating seal station and nozzle inlet station are covered in Sections 5.1.5.2 and 5.1.7.1. These sections also present data on the tip nozzle coefficients.

5.1.3.1 Pressure and Temperature Losses

Pressures, temperatures, and flow rates are provided by Table 5.1-1. The station locations are identified by Figure D-1 in Appendix D. From Table 5.1-1 column 5, it can be seen that generally, the duct loss in temperature between the engine and the rotating seal station is of the order of 80-100°F for high power runs. These values were fairly constant despite the fact that the blanket of insulation (fiberglass backed with aluminum foil) around the vertical ducts was saturated with rain water on occasion.

The total pressure loss parameter given by column 8 has a range from 0.071 to 0.098 showing a total pressure loss between the engine and the rotating seal station from 7.1 to 9.8% of engine discharge pressure. The variation of pressure loss is mostly due to changing the position of the exhaust dump valve for off-line operation and these losses agree well with the predicted values for the whirl test installation.

TABLE 5.1-1

DUCT LOSSES FROM ENGINE TO ROTATING SEAL (HUB) STATION

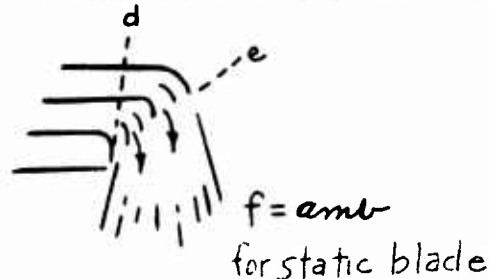
Run	1	2	3	4	5	6	7	8	9	10
P_{T_7}	T_{T_7}	$P_{T_{Hub}}$	$T_{T_{Hub}}$	$T_{T_7} - T_{T_{Hub}}$	P_{T_7}/P_{amb}	W_{Hub}	$P_{T_7} - P_{T_{Hub}}$	T_{amb}	P_{amb}	
No.	psia	$^{\circ}F$	$^{\circ}F$	$^{\circ}F$	--	Lb/Sec	$\frac{P_{T_7}}{P_{T_7}}$	$^{\circ}F$	psia	
20	23.97	707	21.65	686	21	1.623	0.097	56	14.77	
21	26.43	788	23.92	762	26	1.790	0.095	56	14.77	
22	29.58	878	26.65	831	47	2.003	0.098	56	14.77	
34	36.91	1275	34.08	1186	89	2.492	0.077	50	14.81	
1	35.43	1102	32.56	1006	96	2.397	0.081	49	14.78	
10*	35.10	1166	32.48	1071	95	2.387	0.075	66	14.70	
11*	35.30	1239	32.80	1152	87	2.401	0.071	66	14.70	
50*	34.68	1076	31.73	980	96	2.362	0.085	62	14.69	
36	36.37	1275	33.56	1186	89	2.455	0.077	55	14.82	
35	35.05	1230	32.44	1141	89	2.366	0.074	54	14.82	
1	36.33	1115	32.90	1017	98	2.452	0.095	49	14.81	

*Test runs of October and November, 1961. All other run numbers correspond to test series of February 27-28, 1962.

5.1.3.2 Nozzle Coefficients

The effective velocity coefficient defined in Reference 5.1-1 is:

$$C_{vf} = \frac{v_{eff}}{(v_f)_{is}}$$



where, v_{eff} = jet velocity for full expansion to ambient pressure based on nozzle inlet (Sta. d) conditions = $\frac{F_g}{w/g}$

$$(v_f)_{is} = \text{jet velocity for full isentropic expansion to ambient pressure based on nozzle inlet conditions} = \left\{ \frac{2g T_{Td} \gamma R}{\gamma - 1} \left[1 - \left(\frac{P_f}{P_{Td}} \right)^{\frac{\gamma - 1}{\gamma}} \right] \right\}^{\frac{1}{2}}$$

- A = flow area
- p = density
- F^g = gross thrust
- P^g = static pressure
- w = nozzle flow rate

This coefficient was measured on the tip nozzle as a function of nozzle pressure ratio with the blade non-rotating. From this test, it was seen that the effective velocity coefficient is approximately 0.98 in the choked region ($P_{Td}/P_f \geq 1.86$) which is 2.5% better than the 0.955 value used in earlier performance predictions. Further, due to the discharge of the nozzles into a vortex wake region at the tip of the loaded rotor, the local back pressure on the nozzle is considerably below atmospheric ambient pressure. This causes early choking of the nozzle for engine discharge pressures corresponding to P_{Td}/P_{amb} considerably below 1.86. Or, for a loaded rotating blade,

$$P_{Td}/P_f > P_{Td}/P_{amb}$$

This is pointed out to show that when considering the operation of the nozzle only, the coefficients may be defined in terms of the local back pressure P_f but for the overall performance of the ship, P_{amb} is the logical reference since it is the only measurable value.

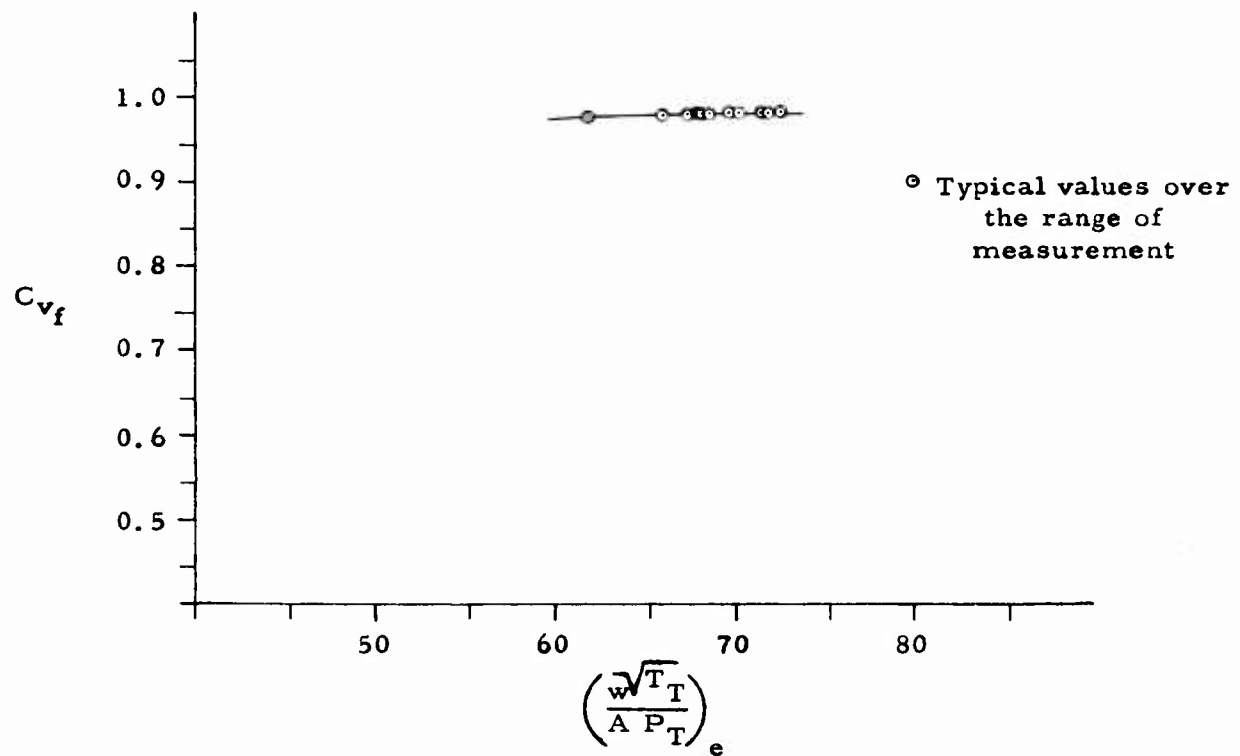
It was found that a rotational speed of 170 rpm (design normal = 240 rpm) at approximately 6° collective pitch was suitable to cause choked flow. For a wide range of engine power, rpm, and collective pitch, Figure 5.1-2 shows the effective velocity coefficient as a function of the nozzle exit flow parameter and shows an almost constant coefficient of approximate 0.98 throughout the performance range of interest. This is substantiated by Figure 5.1-3 which shows the actual and ideal flow vs nozzle pressure ratio (P_{Td}/P_{amw}) utilizing nozzle coefficients corresponding to choked flow. The lower curve shows the flow function values corresponding to $(P_{Td}/P_f) = (P_{Td}/P_{amw})$ which is incorrect when applied to the rotating system as explained above.

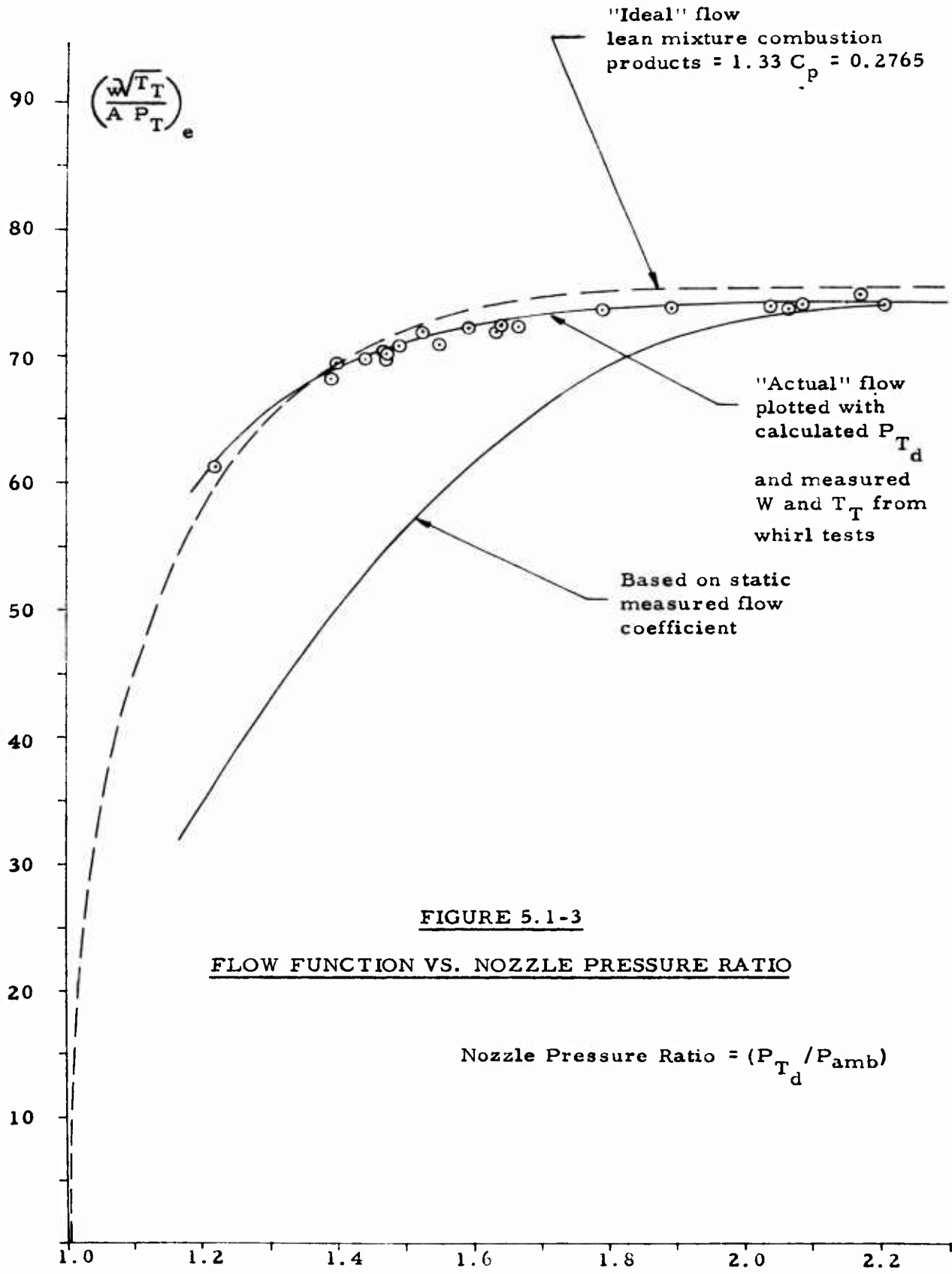
5.1.3.3 Refinements of Weight Flow Measurement (See Fig. 5.1-4 for Branch Location)

A correct determination of the mass flow through the rotor is a requisite for accuracy in any subsequent performance calculation. Therefore, when in the early phase of the test program, discrepancies were discovered in the mass flow measurement, an effort was made to determine their origin. As the test data accumulated, it became apparent that in spite of symmetry of the test rig, the flow in the duct system was not symmetrical. In addition, the velocity distribution across the diameter of the duct was distinctly different from the Nikuradse profile used tentatively in previous computations. Eventually, these irregular conditions existing in the system were linked with the rotation of flow generated by the engine since the exhaust gas leaving the turbine disc at an angle contains considerable rotational energy. In a smooth and vaneless duct, the rotation is not immediately converted or dissipated. It moves along with the flow and substantially changes the velocity pattern from a classical distribution. From a large number of test runs taken over the entire range of rotor operation during October 27 through November 1, 1961, this

FIGURE 5.1-2

EFFECTIVE VELOCITY COEFFICIENT VS. FLOW FUNCTION





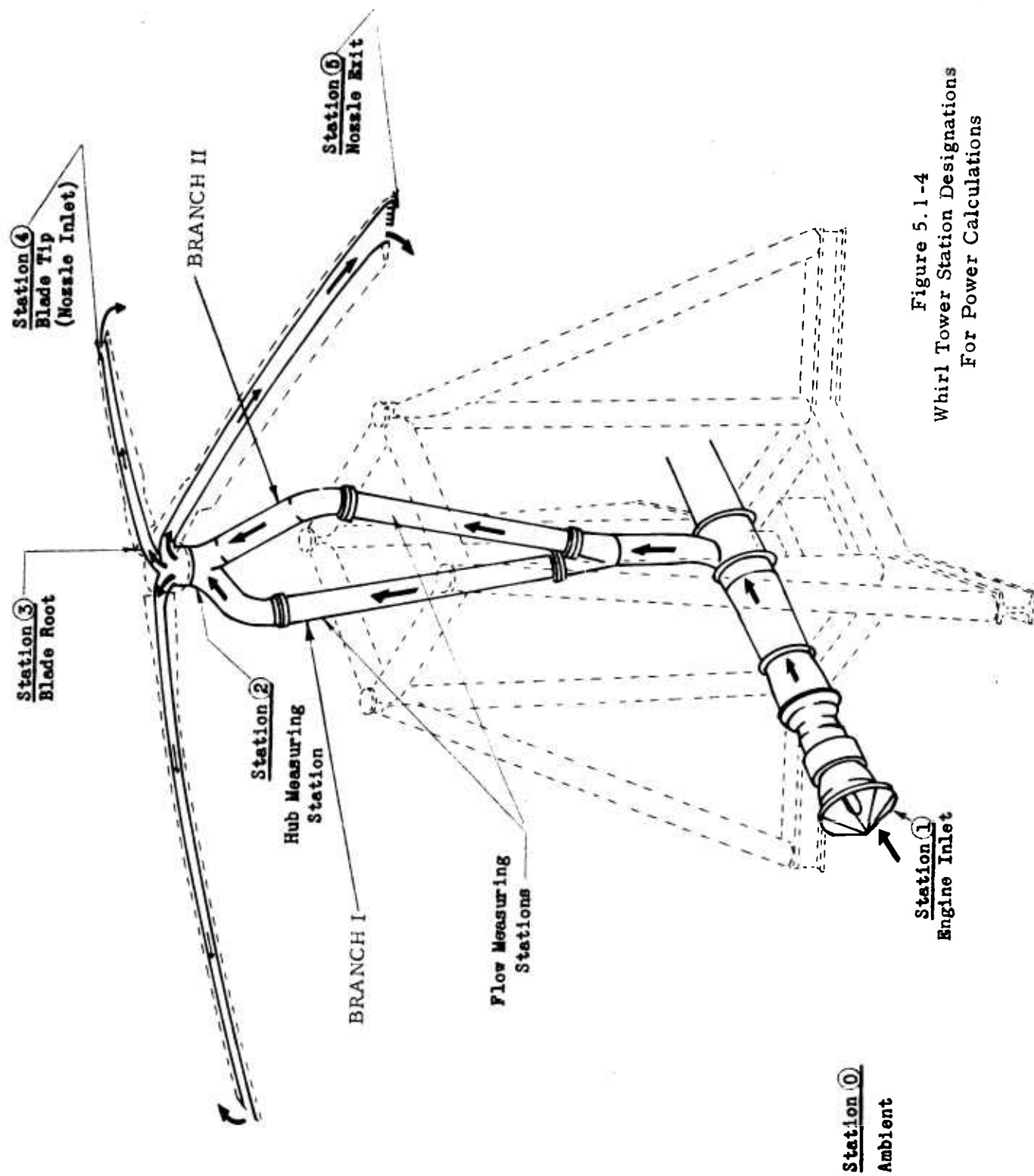


Figure 5.1-4
Whirl Tower Station Designations
For Power Calculations

HUGHES TOOL COMPANY-AIRCRAFT DIVISION

ANALYSIS _____

MODEL _____

REPORT NO. _____

PAGE 5.1-10

PREPARED BY _____

CHECKED BY _____

pattern was found to be fairly stable.

The test data from the flow measuring stations showed that the velocity profiles from the Branch I station plotted as $\frac{v}{v_c}$ vs $\frac{r}{r_p}$ are almost flat in the center over about half of the duct diameter. The curves seem to be pivoted on the center and inclined at various angles from the inboard to the outboard side of the test rig. For the purpose of analysis all curves were transformed into the equivalent symmetrical profiles by plotting their mean ordinates. Or,

$$\frac{v}{v_c} \text{ mean} = 1/2 \left[\frac{v}{v_c} \text{ left} + \frac{v}{v_c} \text{ right} \right],$$

where r = radial distance from center line

r_p = pipe radius

v = local velocity

v_c = centerline velocity

left and right = corresponding radial positions either side of center line.

It must be noted that the area weighted velocity computed for the original profile remains unchanged after such a transformation. Applied graphically, this method allows a fast and direct comparison of the large number of test data. It was thus disclosed that when reduced to the symmetrical form, all velocity profiles nearly coincided. Later this significant observation led to a further simplification of the method used in evaluating the weight flow in the system. Additionally, in computing the average velocity, an assumption was made that the transformed profiles also represented the duct sections other than those in the plane of probes. With this assumption, which incidentally is believed to represent the actual flow, a constant could be found showing how the average velocity at the flow measuring station of Branch I is related to the velocity measured in the duct center. Similarly, another constant relationship $\left(\frac{v}{v_c}\right)_{\text{average}}$ was determined for the flow at the Branch II

station. Although the velocity distribution in Branch II was markedly different, the same rules as described above were applicable. When the data from 50 test runs were analyzed, over 90% of the transformed profiles were found to be within $\pm 1\%$ from their mean value. This narrow spread most likely reflects the error of measurement. Outside of that band, the remaining 10% of the runs did not have a deviation exceeding 3% of the mean value.

In Branch I, low rotation tends to produce the steepest velocity profile.

HUGHES TOOL COMPANY-AIRCRAFT DIVISION

ANALYSIS _____

MODEL _____

REPORT NO. _____

PAGE 5. 1-11

PREPARED BY _____

CHECKED BY _____

On the other hand high rotation tends to produce flatter profiles. The range from steep to flat is very small, namely an average velocity equal to $.93 v_c$ to $.95 v_c$. In Branch II, rotation seems to act in the opposite direction, with effects less visible. The average velocities of the runs analyzed is represented by 935 and 927 as used for the Z_1 and Z_2 values in the computer program (see Appendix D). The interesting fact is that although the average values for Branches I and II may deviate up to $.95 v_c$ and $.91 v_c$ respectively, their mean value remains the same throughout all runs (around $.93 v_c$). The implication of this relationship is very convenient.

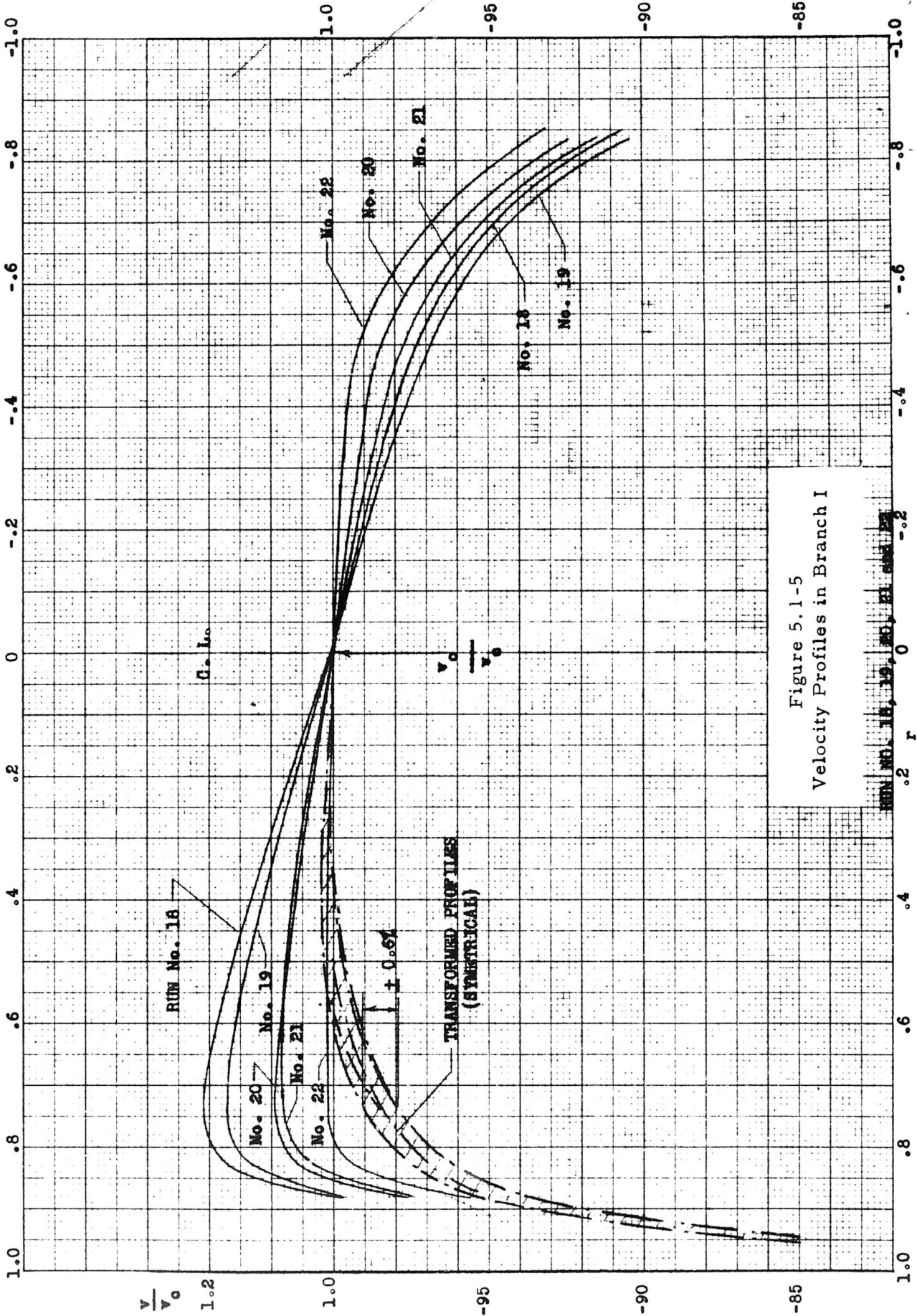
Figures 5.1-5 and 5.1-6 show the typical velocity profiles in Branch I and Branch II respectively. A series of five tests was selected for the purpose of illustrating conditions existing in both ducts. The test runs, taken at a constant pitch of 9° , cover the range of rpm from 170 to 240. The difference in velocity distribution between Branch I and II is obvious. The spread of the "equivalent" profiles in the two branches is respectively less than $+ .6\%$ and less than $+ .2\%$. It is seen that the similarity of the "equivalent" profiles persists in spite of the varying power and the apparent scatter of actual velocity profiles.

Figure 5.1-7 shows the accumulated results from the 50 tests with both branches being included. The cross hatched areas around the two "average" profiles include also the most deviated profiles. The heavy line contours represent the majority of 90% of the test runs. Included for comparison are two analytically defined Nikuradse contours. These are drawn for the extreme Reynolds numbers that may occur in the duct. The more pronounced fullness of the actual profiles can be expected as the result of wall cooling of the hot gases which is the present case. The difference between Branch I and Branch II profiles is attributed mainly to rotation.

Figures 5.1-8 and 5.1-9 show a further step in computing the average velocity. The curves on Figure 5.1-8 are directly derived from the Branch I average contour (heavy line) shown in Figure 5.1-7. Figure 5.1-9 similarly corresponds to Branch II of Figure 5.1-7. The area under the upper curves is equal to the result of the integral defining the area weighted total velocity. The area under the lower curve equals the integral used in computing the mass weighted total pressure (see Appendix C).

5.1.4 J 57 Performance

Various aspects of the J 57 engine performance and operational characteristics are presented in Section 3.4 and Reference 3.4-2. To determine the engine air injection rate, an enthalpy balance across the engine is made as follows:



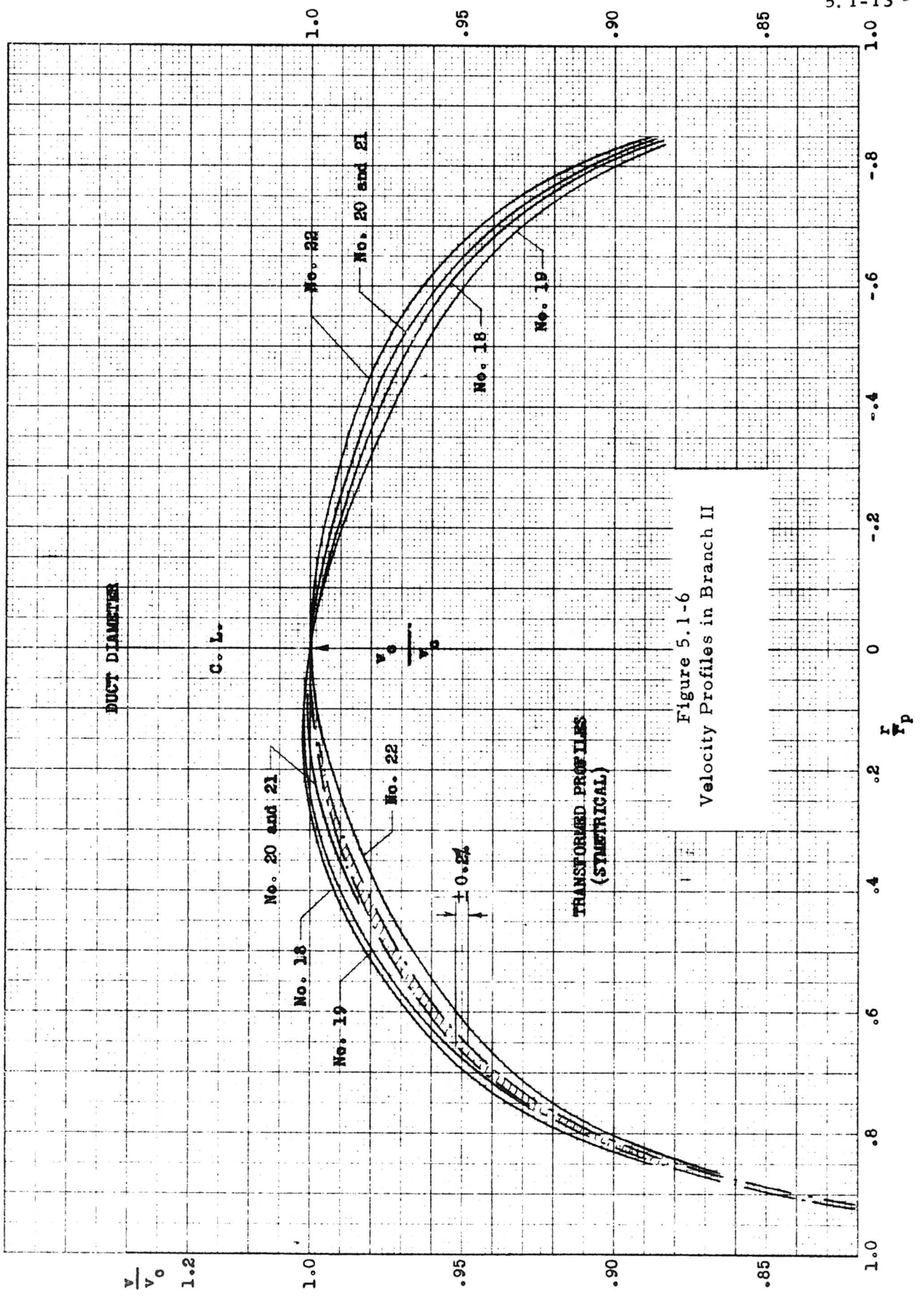


Figure 5.1-6
 Velocity Profiles in Branch II

DUCT DIAMETER

C. L.

$\frac{v_0}{v_b}$

TRANSFORMED PROFILES
 (SYMMETRICAL)

$\pm 0.2\%$

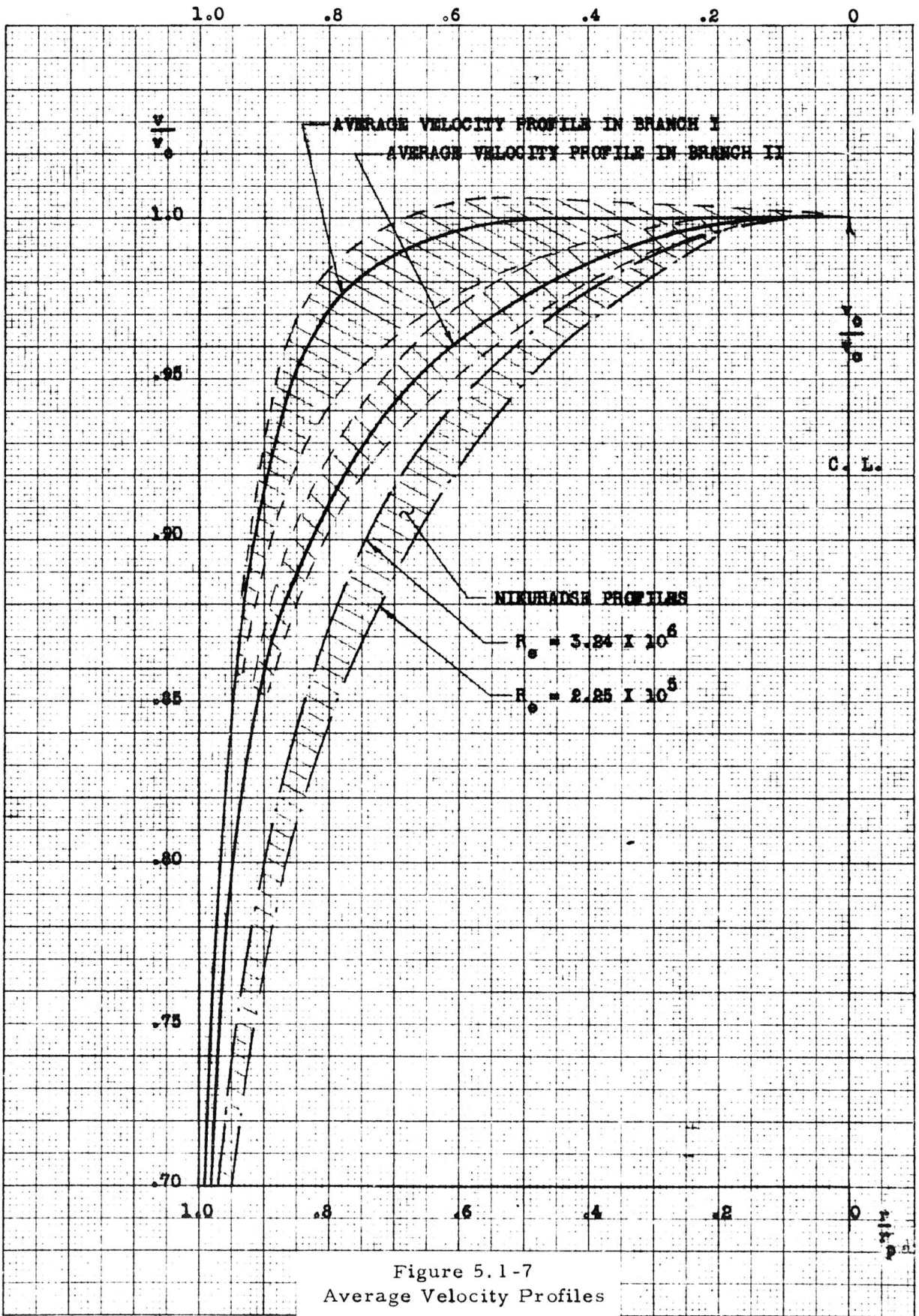
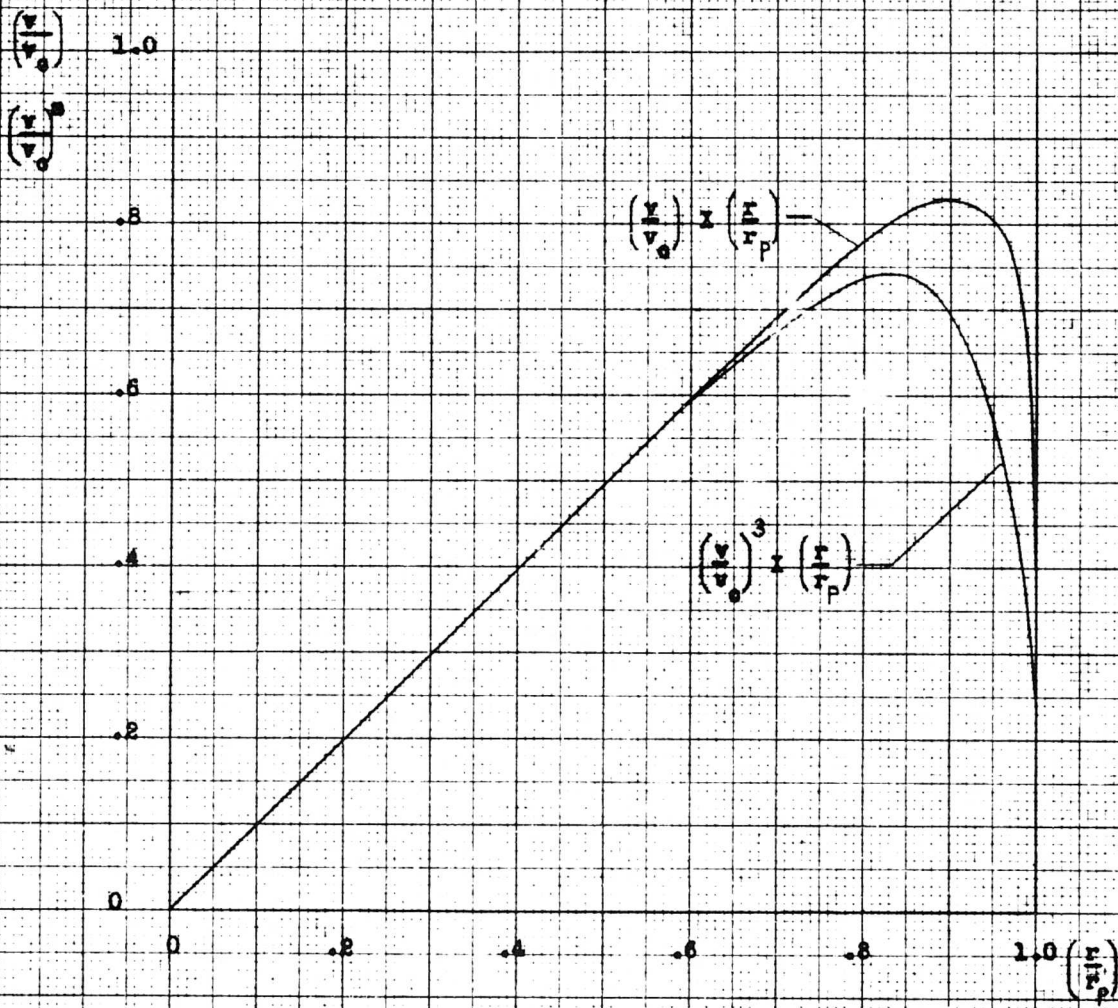


Figure 5.1-7
Average Velocity Profiles

10 A 10 TO THE 1/2 INCH 359-11
KEUFFEL & ESSER CO. BUFFALO, N.Y.

AREA UNDER UPPER CURVE = $\int_0^1 \left(\frac{v}{v_0}\right) \left(\frac{r}{r_p}\right) d\left(\frac{r}{r_p}\right)$

AREA UNDER LOWER CURVE = $\int_0^1 \left(\frac{v}{v_0}\right)^3 \left(\frac{r}{r_p}\right) d\left(\frac{r}{r_p}\right)$



AREA WEIGHTED AVERAGE VELOCITY = $2 \int_0^1 v dv = .952 v_0$

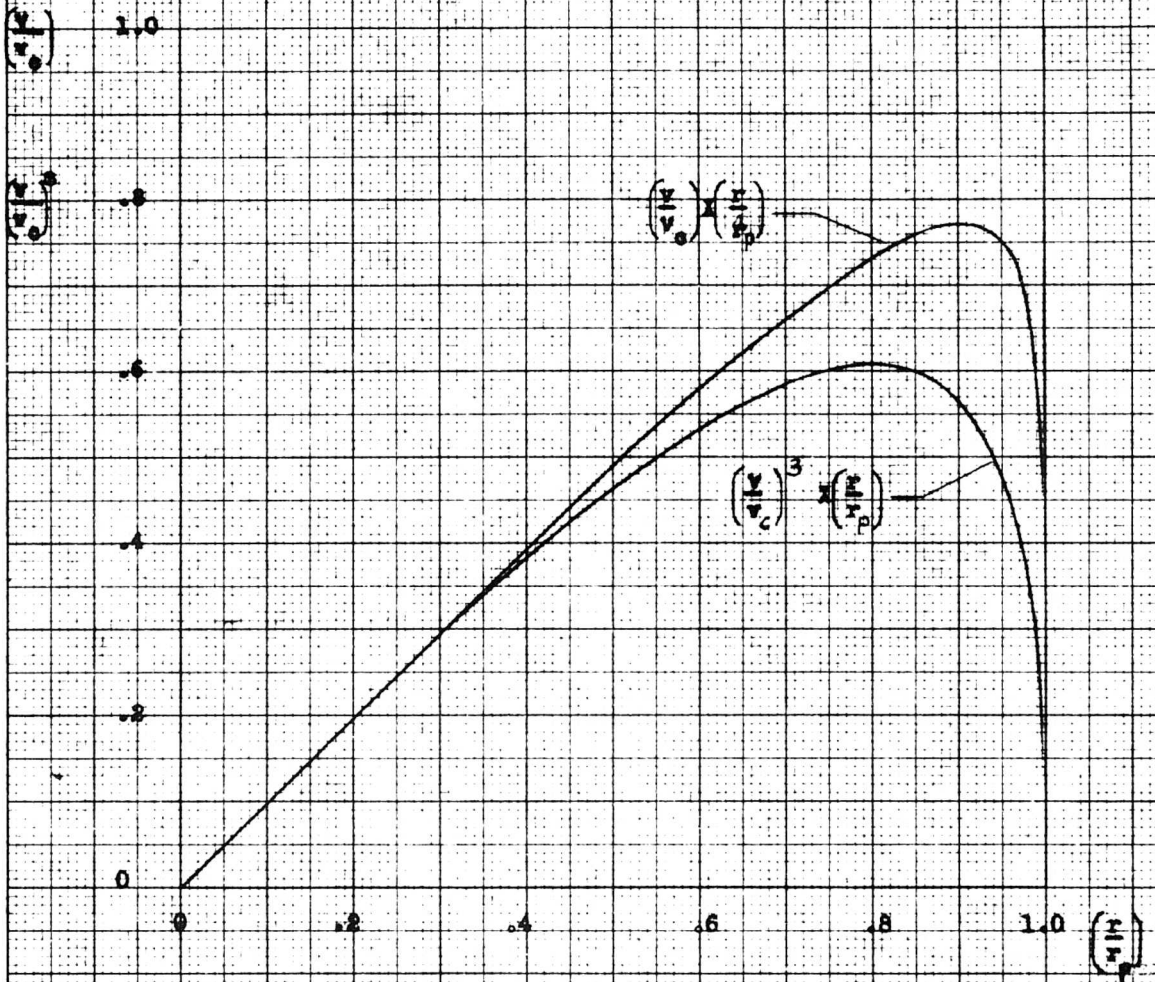
1/2 MASS WEIGHTED AVERAGE TOT. PRESSURE = $1/2 \int_0^1 \frac{v^3}{.478} = .463 P_{T_0}$

Figure 5.1-8
Graphical Integration of Average Velocity
Profile in Branch I from Figure 5.1-7

110T 1/2 IN. 355 KEUFFEL & ESSER CO. MADE IN U.S.A.

$$\text{AREA UNDER UPPER CURVE} = \int_0^1 \left(\frac{v}{v_c}\right) \left(\frac{r}{r_p}\right) d\left(\frac{r}{r_p}\right)$$

$$\text{AREA UNDER LOWER CURVE} = \int_0^1 \left(\frac{v}{v_c}\right)^3 \left(\frac{r}{r_p}\right) d\left(\frac{r}{r_p}\right)$$



$$\text{AREA WEIGHTED AVERAGE VELOCITY} = 2 \times 0.455 v_c = 0.91 v_c$$

$$1/2 \text{ MASS WEIGHTED AVERAGE TOT. PRESSURE} = 1/2 \times \frac{0.89}{0.455} P_c = 0.97 P_c$$

Figure 5.1-9
Graphical Integration of Average Velocity Profile in Branch II from Figure 5.1-7

ANALYSIS _____ MODEL _____ REPORT NO. _____
 PREPARED BY _____
 CHECKED BY _____

$$W_{a_2} h_{T_2} + \eta_B W_f Q_f = h_{T_7} W_7$$

- Where
- W_{a_2} compressor inlet air flow rate
 - h_{T_2} total enthalpy of incoming air
 - η_B combustion efficiency (≈ 0.96)
 - Q_f lower heating value of JP-4 fuel ($\approx 18,400$ BTU/LB)
 - W_f fuel flow rate
 - h_{T_7} total enthalpy at turbine exhaust (400% theoretical air)
 - W_7 turbine exhaust gas flow rate. = $W_{a_2} + W_f$

Thus, the engine air ingestion rate is

$$W_{a_2} = \frac{(\eta_B Q_f - h_{T_7})}{h_{T_7} - h_{T_2}} W_f$$

This equation is employed in the Non-Rotating Component equations of Appendix D.

The h_{T_2} values for air are taken from Reference 5. 1-4 and are linearized over the ambient temperature range for use in the computer program. Also, the h_{T_7} values are taken from the same reference for 400% theoretical air and is linearized over three temperature ranges for use. The values of specific heat at constant pressure and volume as well as gas constant is computed by the method of Reference 5. 1-5.

5. 1. 5 Rotor Power

To determine the rotor power through aerothermal analysis, the system is separated into two components (rotating and non-rotating) and the corresponding analyses are programmed for the IBM 7090 in subroutine form. For convenience the nomenclature and the input and output formats are given in Appendix F.

5.1.5.1 Non-Rotating Components

The non-rotating components include the J 57 gas generator and ducts required to deliver the hot gas to the rotor hub. Due to the length of the calculation, the details are given in Appendix D.

5.1.5.2 Rotating Components

The rotor power available is computed from the gas conditions of mass flow, temperature, and pressure existing at the tips of the rotating blades. These conditions differ from those at the rotor hub because of friction and centrifugal force acting on the gas. The gas conditions at the rotor hub are assumed equal to those discharging from the non-rotating ducting, described in Section 5.1.5.1. The calculation procedure for computing the changes of gas conditions in going from hub to blade tip is described in Reference 5.1-3. Reference 5.1-3 is based on one dimensional, compressible flow relations developed in Reference 5.1-6 and extended to the rotating helicopter blade case in Reference 5.1-7. Because the treatment of References 5.1-3, -6, and -7 is one dimensional, it was necessary to anticipate a simplification of what is really a complicated three-dimensional flow by computing the output gas conditions on a mass and/or area weighted basis. The gas conditions derived in Appendix D and computed in Steps 38, 100a and 100b are then used directly in this section. The equations that are used to convert gas conditions at the rotor hub to rotor power at the blade tips are as follows:

(1) Blade Root Pressure Ratio

$$P_{T_3} = P_0 \times r_2 \times \left(\frac{r_3}{r_2} \right)$$

Where $r_2 = \bar{P}_{T \text{ Hub}} / P_0$

(2) Blade Duct Inlet Number

(Substitute values of W , T_{T_3} , and P_{T_3} , and iterate to 0.1%

to find M_3)

$$\left(\frac{W \sqrt{T_T}}{A P_T} \right)_3 = \frac{M_3 \sqrt{\frac{\gamma g}{R}}}{\left(1 + \frac{\gamma-1}{2} M_3^2 \right) \frac{\gamma+1}{2(\gamma-1)}}$$

ANALYSIS _____
 PREPARED BY _____
 CHECKED BY _____

MODEL _____

- (3) Change in Mach Number Through Blade Duct
 The blade is arbitrarily broken into 100 equal steps
 for analysis purposes.

$$\therefore \frac{\Delta r}{R} = .01$$

Steps are then numbered $n = 0, 1, 2, 3, \dots, 99$.

$$M = M_3 \quad (n = 0)$$

$$\Delta M = \frac{2f \gamma R}{D} \left(\frac{\Delta r}{R} \right) \frac{M^3 \left(1 + \frac{\gamma-1}{2} M^2 \right)}{(1 - M^2)}$$

$$- \frac{V_T^2 M \left(1 + \frac{\gamma-1}{2} M^2 \right)^2}{g (C_p - C_v) J T_{T_3} (1 - M^2)} \left(\frac{2n+1}{2} \right) \left(\frac{\Delta r}{R} \right)^2$$

$$M_{n=1} = M_3 + \Delta M_{n=0}$$

$$M_{n=2} = M_{n=1} + \Delta M_{n=1}$$

$$M_4 = M_{TIP} = M_{n=99} + \Delta M_{n=99}$$

- (4) Pressure Ratio Produced by the Rotation Blade
 (Constant duct area, constant total temperature)

$$\frac{\text{Total pressure at tip}}{\text{Total pressure at root}} = \left(\frac{r_4}{r_3} \right)$$

$$= \frac{M_3}{M_4} \left(\frac{1 + \frac{\gamma-1}{2} M_4^2}{1 + \frac{\gamma-1}{2} M_3^2} \right)^{\frac{\gamma+1}{2(\gamma-1)}}$$

ANALYSIS _____

MODEL _____

REPORT NO. _____

PREPARED BY _____

CHECKED BY _____

(5) Gas Conditions at Blade Tip

$$\text{Mass Flow} \quad W_{g4} = W_g$$

$$\text{Temperature} \quad T_{T4} = T_{T3} = T_{T2}$$

$$\text{Pressure Ratio} \quad r_4 = r_2 \times \left(\frac{r_3}{r_2}\right) \times \left(\frac{r_4}{r_3}\right)$$

(6) Jet Velocity

$$V_j = C_{ve} \sqrt{2 g J C_p T_{T4} \left[1 - \left(\frac{1}{r_4}\right)^{\frac{k-1}{\gamma}}\right]}$$

(7) Rotor Power Available

$$\text{RHP} = \frac{W_g (V_j - V_T) V_T}{g \times 550}$$

It should be noted that computation of rotor power available depends on the value of several coefficients which are functions of the particular Hot Cycle hardware. These coefficients include f , the blade duct friction coefficient, C_{ve} , the nozzle velocity coefficient, and r_3/r_2 , the ratio of total pressure at the blade root to that at the rotor hub. These coefficients are established by tests such as References 5.1-1 or 5.1-8, or are given reasonable values based on tests of similar components. Reference 5.1-1 permits determination of C_w , the nozzle flow coefficient, as well as C_{ve} , the velocity coefficient. However, it was necessary to assume a value for f , the duct friction coefficient. By using the flow function, Equation 2, it is possible to make a cross-check on the assumed value of f . This is accomplished by recognizing that if there are no leaks, all of the mass flow that leaves the rotor hub must pass through the blade nozzles, which have total area A_N . With the assumption of fixed gas temperature from the hub to the blade tip (which was found to be quite reasonable during whirl tests), the total pressure at the nozzle is therefore fixed. Since the pressure ratio at the hub, $r_2 = P_{T \text{ hub}}/P_0$ is known, and the pressure ratio from the hub to the blade root, r_3/r_2 is also available, the blade pressure ratio $(r_4/r_3)_N$ that will satisfy the flow function at the nozzle is therefore determined.

ANALYSIS _____
 PREPARED BY _____
 CHECKED BY _____

Since r_4/r_3 is a function of f , in Equations (3) and (4), the accuracy of the assumed value of f can be established by comparing the values of r_4/r_3 from Equation (4) with $(r_4/r_3)_N$ from Equation (15). The procedure used to compute $(r_4/r_3)_N$ is as follows; (An iterative procedure is required to establish nozzle pressure ratio.):

- (8) Critical Nozzle Pressure Ratio

$$r_{4 \text{ CRIT}} = \left(1 + \frac{\gamma-1}{2}\right) \frac{\gamma}{\gamma-1}$$

- (9) Initial Assumed Value of Nozzle Pressure Ratio

$$r_{4a} = (r_4)_{\text{assumed}} = 1.15 r_2$$

- (10) Nozzle Mach Number for Assumed Nozzle Pressure Ratio

If $r_{4a} > r_{4 \text{ crit.}}$, $M_5 = 1.000$, otherwise, use following equation:

$$M_5 = \sqrt{\frac{(r_{4a}) \frac{\gamma-1}{\gamma} - 1}{\frac{\gamma-1}{2}}}$$

- (11) Flow Function at Nozzle Mach Number

$$\left(\frac{W \sqrt{T_T}}{A P_T}\right)_5 = X = \frac{M_5 \sqrt{\frac{\gamma g}{R}}}{\left(1 + \frac{\gamma-1}{2} M_5^2\right) \frac{\gamma+1}{2(\gamma-1)}}$$

- (12) Nozzle Flow Coefficient C_W

Find C_W for assumed value of r_{4a} , or assume value $\cong .98$

ANALYSIS _____
 PREPARED BY _____
 CHECKED BY _____

MODEL _____

(13) Computed Nozzle Pressure Ratio

$$r_{4 \text{ comp.}} = \frac{W_g \sqrt{T_T}}{C_w A_n P_o X}$$

(14) Iterated Value of Nozzle Pressure Ratio

If $r_{4 \text{ comp}} < r_{4a}$, reduce r_{4a} by .01 and repeat 10, 11, 12, and 13 until $r_{4 \text{ comp}} \geq r_{4a}$. This last value of $r_{4a} = r_{4 \text{ comp.}}$

(15) Blade Pressure Ratio Based on Flow Through Nozzle $(r_{4/r_3})_N$

$$(r_{4/r_3})_N = \frac{r_{4 \text{ comp.}}}{r_2 \times \left(\frac{r_3}{r_4}\right)}$$

The value of $(r_{4/r_3})_N$ can be compared to r_{4/r_3} of Equation (4) to evaluate the assumed value of duct friction coefficient f .

5. 1. 6 Rotor Thrust Calculation

The computed thrust of the rotor in hovering is determined from the rotor power available and the rotor geometry using standard NACA methods presented in Reference 5. 1-9. The approach is to make the power available equal to the power required; the power required is the sum of the induced power and the profile power. The geometry of the whirl test tower introduces some ground effect; its influence on induced power is determined from the empirical data presented in Figure 5-13 of Reference 5. 1-9. The profile power coefficient presented in Reference 5. 1-9 was obtained for a 12% thick blade. As the Hot Cycle blades are 18% thick, the profile power has been increased by 17% to allow for the increased drag of the thicker section. The blades are twisted -8° ; therefore the correction to the over-all power coefficient presented on page 85 of Reference 5. 1-9 is used. Applying the above factors, the equation for power as a function of thrust - Equation 36 of Reference 5. 1-9 becomes:

$$C_P = C_1 \left[\frac{C_T^{3/2}}{\sqrt{2} B} \left(\frac{T_\infty}{T}\right)^{3/2} + 1.17 \left(\frac{g d_e}{8} + \frac{2}{3} \frac{g l}{a} \frac{C_T}{B^2} + \frac{\sqrt{2}}{g a^2} \left(\frac{C_T}{B^2}\right)^2 \right) \right]$$

This equation is iterated for various values of thrust until the power required is equal to the power available from Section 5. 1. 5.

ANALYSIS

PREPARED BY

CHECKED BY

5. 1. 7 Rotor Thrust Measurement

The best evidence of the performance of the hot cycle rotor is a direct comparison of measured and computed rotor thrust as a function of engine power. Data were obtained during the 60 hour endurance test and reduced according to the procedures discussed in Section 5. 1. 5. 1 and 5. 1. 5. 2 on Non-Rotating and Rotating Ducting, and Section 5. 1. 6 on Rotor Thrust. Excellent agreement was obtained for the over-all performance conversion of measured engine output to measured rotor thrust.

5. 1. 7. 1 Rotating Duct Thermodynamics

Computed rotor thrust and measured rotor thrust are both direct functions of rotor power. Rotor power in turn is critically dependent on the actual hardware duct friction coefficient, f , and nozzle velocity coefficient, C_{V_e} . These two factors are the biggest unknowns in the rotating system. In the initial design stages, assumed values of $f = 0.004$ and $C_{V_e} = 0.955$ were chosen. All performance predictions in application studies such as Reference 5. 1-10 and in the whirl tower performance estimate, Reference 5. 1-3 were based on these values of f and C_{V_e} .

The velocity coefficient C_{V_e} was measured during the tether tests discussed in Reference 5. 1-1. It is shown in that report that, at maximum nozzle pressure ratios, the measured velocity coefficient of the tip cascade is equal to 0.98 at pressure ratios corresponding to those available from the T-64 gas generator (2.6 - 2.9). This measured value is approximately 2.5% higher than the assumed value of 0.955.

The duct friction coefficient of $f = 0.004$ was shown to be conservative by comparison of nozzle pressure ratio derived in two different ways. A reference value of r_4 was computed by starting from the hub pressure ratio r_2 , multiplying it by the assumed value of

$$\left(\frac{r_3}{r_2} \right)$$

and multiplying again by the blade pressure ratio

$$\left(\frac{r_4}{r_3} \right)$$

which is a function of the assumed duct friction coefficient, $f = 0.004$ (Equations (1) through (5) of 5. 1. 5. 2). A second value of nozzle pressure ratio, r_{4N} was

ANALYSIS _____

PREPARED BY _____

CHECKED BY _____

computed using the nozzle flow function equation and making the assumption that all of the mass flow that passed through the hub measuring station also passed through the tip nozzle. No evidence whatsoever was found of any appreciable leaks, so it is felt reasonable to assume all the gas went out the tip nozzle. When this second value of tip nozzle pressure ratio was computed (r_{4N} , from Equations (8) through (15) of Section 5.1.5.2), it was found that r_{4N} was 5 to 6% higher than the reference value based on computations

using $f = 0.004$. The tip nozzle pressure ratio computed for the nozzle, r_{4N} , is the actual pressure ratio required to push the measured mass flow through the nozzle. If any lower pressure is available the mass flow will not go through the nozzle. Since it was established that the measured flow did go through the tip nozzles, the reference pressure ratio based on the duct friction coefficient was too low. Since a low computed nozzle pressure is caused by a high duct friction coefficient, a reduction of duct friction coefficient will permit the nozzle pressure based on f to rise to the value permitted by the nozzle equation, r_{4N} . Therefore, the duct friction must be somewhat lower than the assumed value of 0.004. Consequently, performance computations based on $f = 0.004$ are conservative, and higher rotor powers will be computed when the lower and more accurate value of f is established.

5.1.7.2 Rotor Aerodynamics

Figure 5.1-1 shows that measured rotor thrust agrees very well with the computer rotor thrust as a function of rotating seal pressure ratio, up to the maximum value available from the J-57 turbojet used during the whirl tests. The calculated curve of Figure 5.1-1 includes an allowance for the power required to centrifugally pump the spar cooling air on the test rotor. The mean value of maximum measured lift was approximately 20,000 pounds, at a seal pressure ratio of 2.2 atmosphere. It should be noted that extrapolation of the J-57 data (which agrees very well with theory) indicates that the rotor will produce over 28,000 pounds of lift at a 2.82 pressure ratio which is available from the ST129 model of the T-64 gas generator.

ANALYSIS _____

PREPARED BY _____

CHECKED BY _____

5.2 ROTOR DYNAMICS

A free floating hub configuration was selected for the Hot Cycle Rotor to avoid the need for lead-lag hinges. No dynamic or flutter problems were evidenced during the entire whirl test program. During the early phases of the program, while building up to higher values of rpm and collective pitch, the cyclic and collective controls were pulsed to establish proximity to resonance of flutter conditions. At no time were such conditions in evidence.

Reference 5.2-1 discusses the calculated dynamic characteristics of the Hot Cycle rotor and concludes that there are no resonant conditions in the operating rotor speed range. The absence of any dynamic problems during the whirl test program substantiates the prediction of Reference 5.2-1.

ANALYSIS

PREPARED BY

CHECKED BY

5.3 TEMPERATURE AND LEAKAGE SURVEYS

5.3.1 Comparison of Design With Measured Temperatures

5.3.1.1 Summary

Table 5.3-1 compares measured and estimated component temperatures corresponding to gas temperature as measured at the flow measuring stations. No correction is made to account for the difference in ambient conditions. The analysis of all data leads to the following conclusions:

- a. The temperatures of the duct and flexures are as predicted.
- b. All remaining components operate at temperatures considerably lower than predicted. Spars, outer skin, and hub temperatures compared with the estimates are more than 40% or 50% cooler. These low thermocouple readings are confirmed by indications of temperature sensitive tape checked at corresponding locations.

5.3.1.2 Discussion

This section contains a brief study of temperature distribution prevailing in the hot cycle rotor under maximum operating conditions. The objective was to provide:

- a. A comprehensive presentation of data from the whirl test program.
- b. A check of all component temperatures earlier predicted in Reference 5.3-1.

Several figures are prepared to enable a quick review of thermal conditions in the whirling rotor. Where applicable, the "predicted" reference temperature is included for a direct comparison with the measured temperatures. An interpolation equation is given below for reducing estimates to correspond to the actual test component temperatures.

$$T = 100 + \frac{(T_{1200} - 100)(T_{\text{gas}} - 100)}{1100}$$

This equation was applied when correcting data tabulated in the summary. It appears that corrections are small and in many cases the basic prediction from Reference 5.3-1 can be used either as a reference or as an indication of the highest possible temperature. The estimates were based on 1200° gas temperature and 100°F day at sea level. One exception was the duct temperature used in the analysis of flexures, which was 1050°F. In this case corrections were used in reverse to predict the average temperature of flexures when the duct temperature increased to 1200°F.

ANALYSIS _____

PREPARED BY _____

CHECKED BY _____

TABLE 5.3-1

COMPONENT TEMPERATURES

COMPONENT	Predicted at 1200°F Gas Temp.	Corrected for 1176°F Gas Temp.	Measured	Estimated Absolute Error*	Actual Error	Component Temp. % of Estimated
Duct 3/8" from chord line BS-1-13	1177	1153	1105	-50, +30	+48	4.2% Cooler
Duct top, BS-18-4 Blade Radial Station	1105	1083	1070	-50, +30	+13	1.2% Cooler
Outer Skin on the Rib, BS-18-7	465	457	272	-60, +100	+185	41% Cooler
Rear Spar BRS-3	430	423	240	-60, +100	+183	42% Cooler
Flexure BC ₂ Aver.	645	633	640	- 0, +200	- 7	1% Hotter

*ERROR = Measured - Predicted

ANALYSIS _____

PREPARED BY _____

CHECKED BY _____

5. 3. 1. 3 Temperature Survey

Data from the following tests were selected to include two representative maximum temperature steady state runs, a fast acceleration transient, and a high temperature transient.

- (1) Test Run No. 66, Dec. 1, 1961, turbine discharge temperature $T_{T_7} = 1255^{\circ}\text{F}$, turbine discharge pressure $P_{T_7} = 21.1$ psig, gas temperature at flow measuring stations 1176°F , ambient temperature 64°F , 235 RPM at 8.5° collective pitch.
- (2) Test Run No. 11, October 27, 1961, $T_{T_7} = 1237^{\circ}\text{F}$, $P_{T_7} = 20.6$ psig, gas temperature at flow measuring stations 1152°F , ambient temperature 65°F , 240 RPM at 9° collective pitch. (Data from Run No. 11 are used only on Figure 5. 3-5 for the record of the hub mast temperatures).
- (3) Transient test on December 11, 1961, Run No. 19, gas temperature at flow measuring stations 720°F to 1175°F .
- (4) Transient test on Dec. 13, 1961, $T_{T_7} = 1220^{\circ}\text{F}$, $P_{T_7} = 21.1$ psig, 240 RPM at 8° collective. Gas temperature at flow measuring station not recorded due to thermocouple failure.

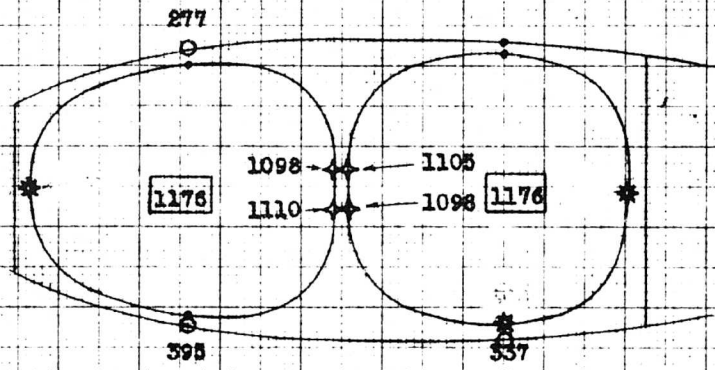
Figure 5. 3-1 shows duct and outer skin temperatures measured at the inboard segment (No. 1) during Run No. 66.

Figure 5. 3-2 shows similar data taken at the outboard Section No. 18 during the same runs. It can be seen that both the duct wall temperature and the temperature of the outer skin are lower than estimated.

Figure 5. 3-3 shows the temperature distribution in the flexures, spar and cooling air. This is the most complete set of data that covers any specific area of the rotor. The plot makes a good picture of temperature distribution along the blade.

For the flexure temperature distribution the test results of Figure 5. 3-3 positively confirm all predictions. These data are based on 35 active thermocouples. The figure also shows the spread of temperatures that may be expected to exist within any flexure.

- OUTER SKIN
- ◇ DUCT WALL
- * → INACTIVE
- - - PREDICTED
- GAS TEMP



SEGMENT 1 (INBOARD)
LOCATION OF THERMOCOUPLES

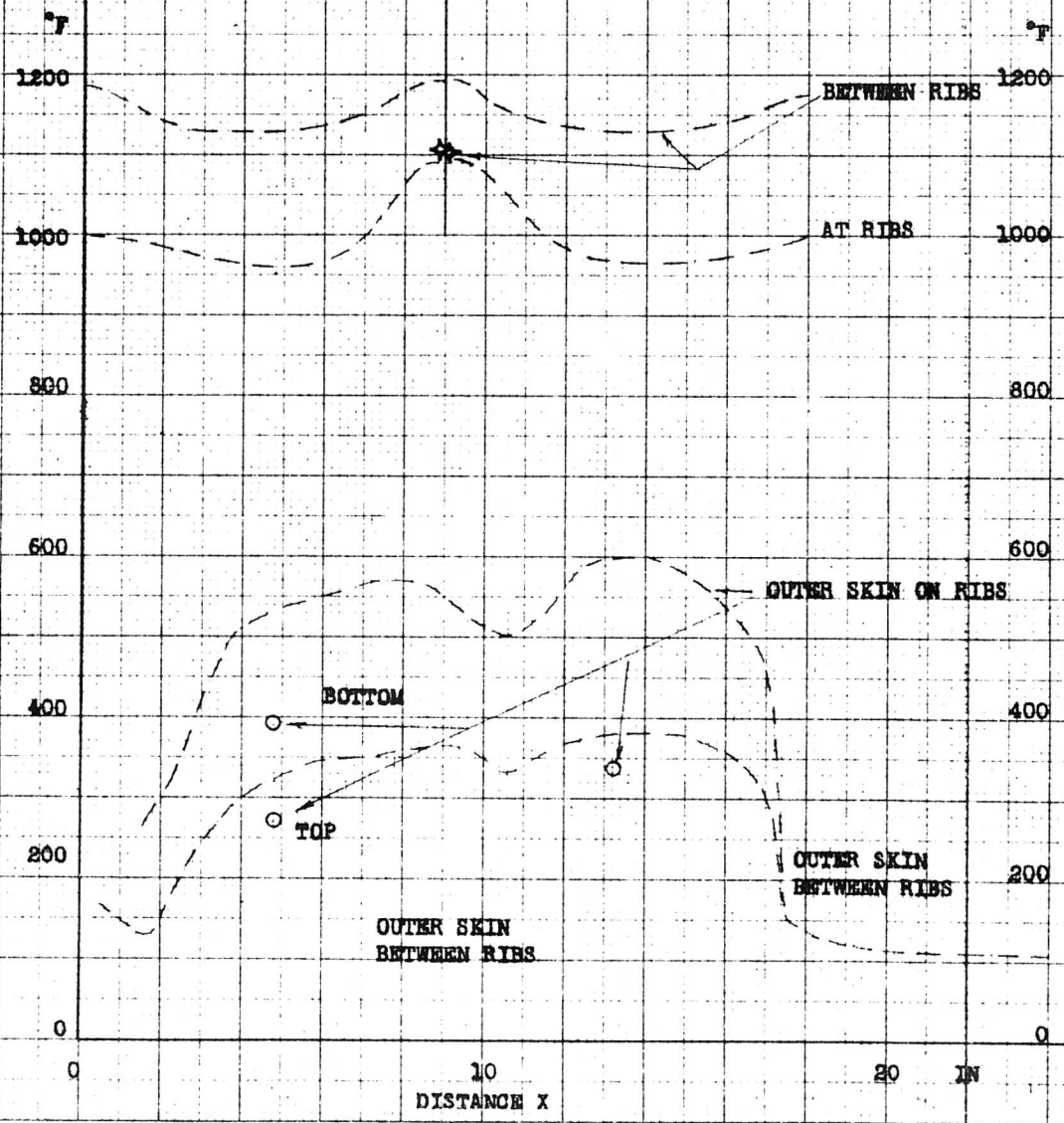
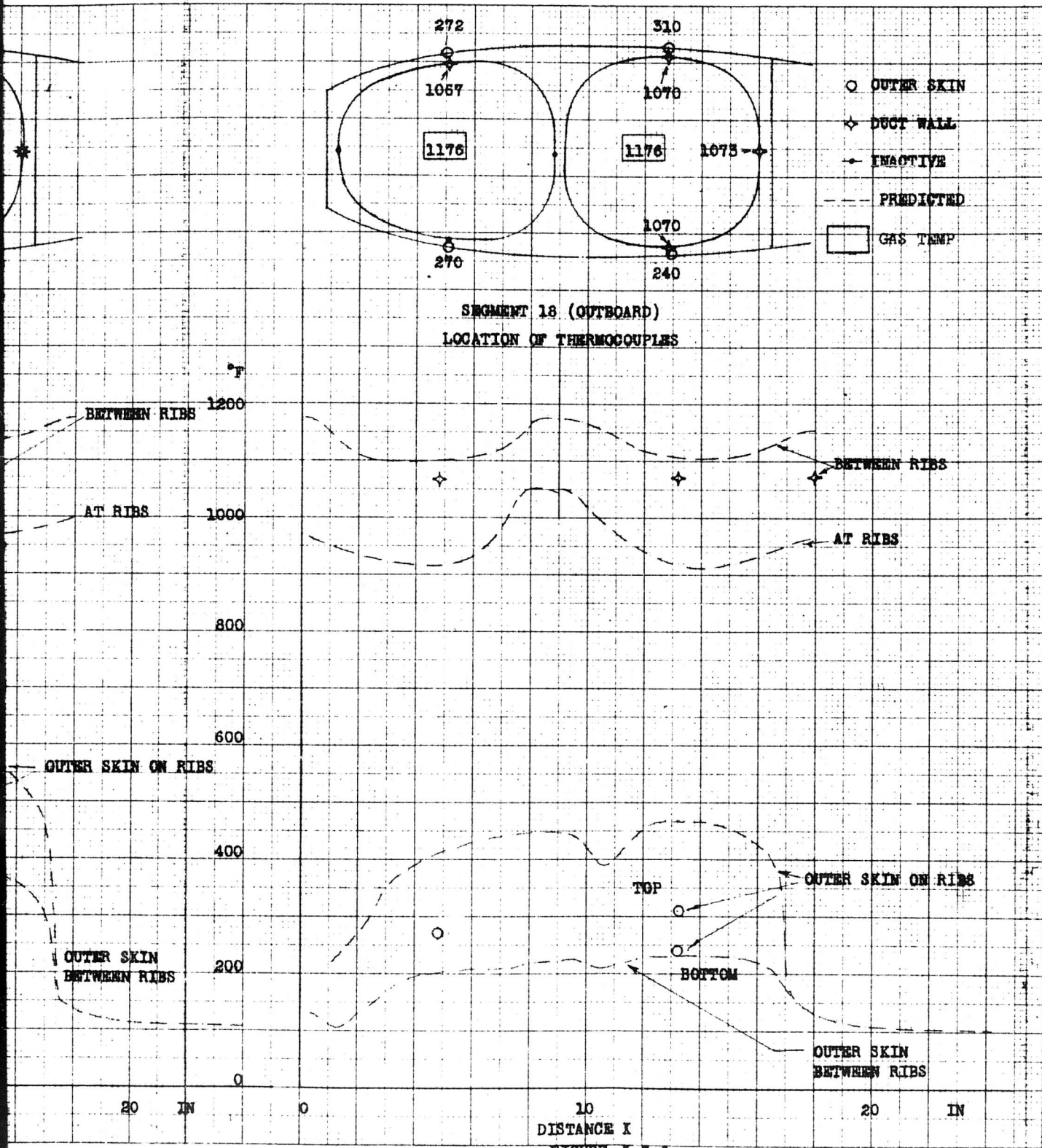


FIGURE 5.3-1
DUCT AND OUTER SKIN TEMPERATURES (INBOARD SEGMENT)
RUN NO. 66

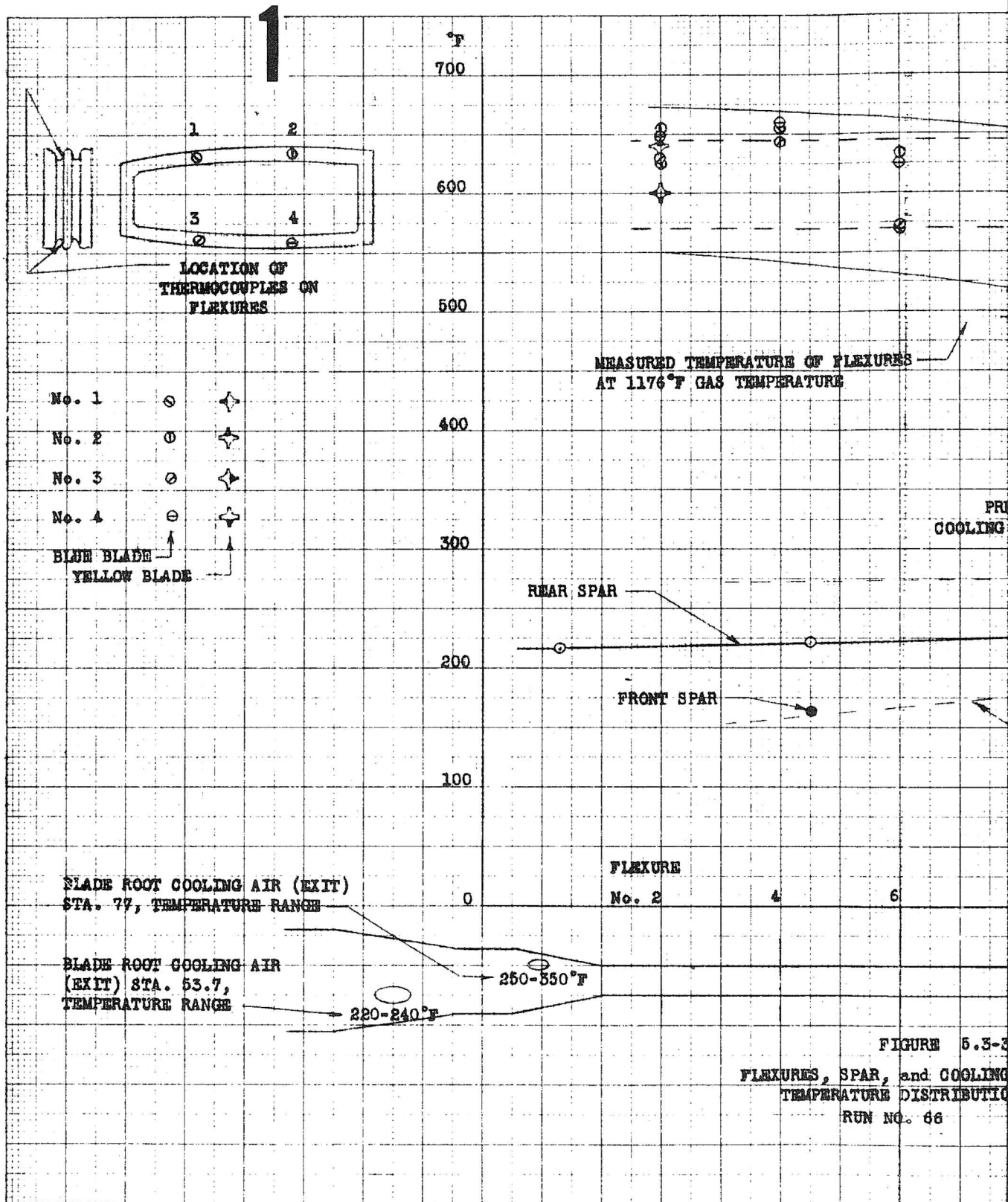
KE 10 X 10 TO THE 1/2 INCH 359-111G
 KEUFFEL & ESSER CO. MADE IN U.S.A.



SEGMENT)

DUCT AND OUTER SKIN TEMPERATURES (OUTBOARD SEGMENT)
RUN NO. 66

FIGURE 5.3-2



2

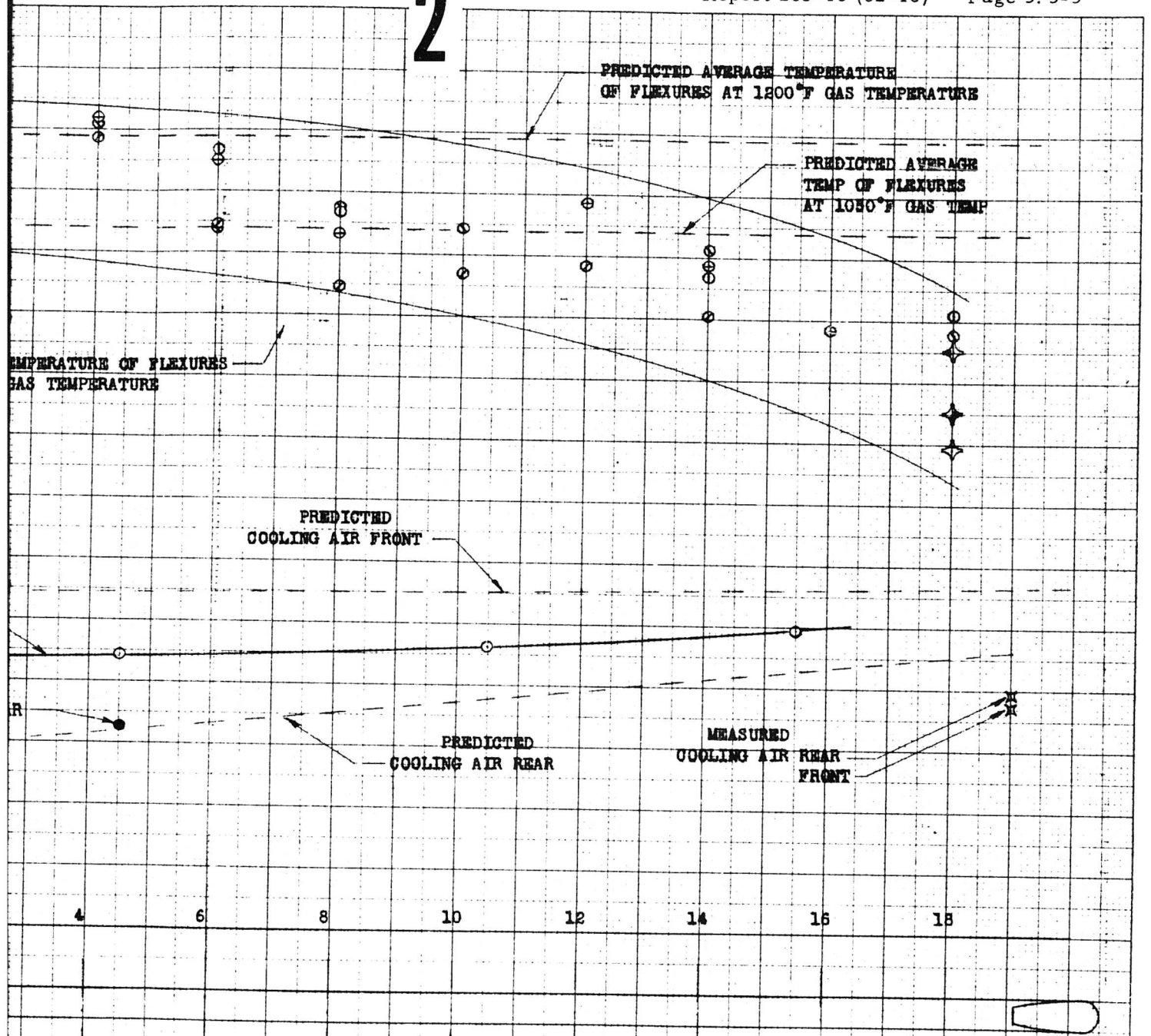


FIGURE 5.3-3

FLEXURES, SPAR, and COOLING AIR
TEMPERATURE DISTRIBUTION

RUN NO. 66

1-11-61 JWR

ANALYSIS _____

PREPARED BY _____

CHECKED BY _____

The rear spar temperature is included on the same figure. This is also a very well instrumented component covered with 8 active thermocouples. At sections where thermocouples were close together the average values were used in the plot. The front spar is covered only with a single active thermocouple. This thermocouple consistently indicated that the front spar is always cooler than the rear spar. Similarly the front spar cooling air has lower temperature than air in the rear cooling duct. When compared with the estimates, it is evident that both spars actually operate at lower temperatures than predicted.

Figure 5.3-3 also shows the temperatures of the blade root cooling air as measured at Station 53.4 and Station 77 on all three blades.

Figure 5.3-4 shows a plot of transient temperatures during acceleration runs. The curves are directly transcribed from the Leeds Northrup recorder equipped with the selector switch for this purpose. It is interesting to note that the outer skin temperatures change little between idling and the maximum power. The differential temperature between the duct and the skin is largest at steady state. Transient runs did not disclose the existence of any critical thermal conditions in the blade.

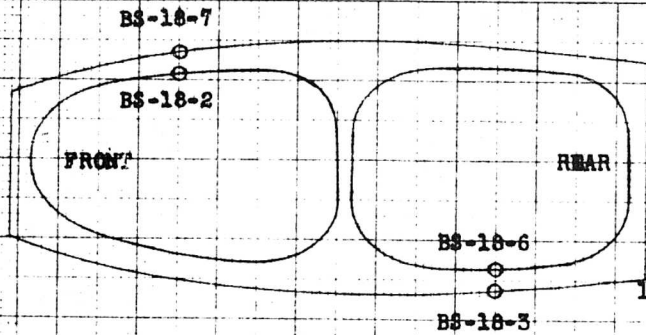
Figure 3.3-5 shows temperatures prevailing in the hub of the rotor. Two hot runs are presented. Run No. 66 with gas temperature 1176°F and Run No. 11 with gas temperature 1152°F. It can be seen that the hub assembly temperatures are considerably lower than predicted. Since the hub assembly was not a subject of Reference 5.3-1, the predicted values were taken from Reference 5.3-2. As higher readings from Run No. 66 cannot be explained entirely by the small difference in gas temperature, they evidently indicate some minor leakage in the hub.

Figure 5.3-6 and 5.3-7 show the relation between the temperature of pertinent rotor components and the turbine discharge temperature T_{T_7} . It is interesting to note that most of the component temperatures are almost directly proportional to T_{T_7} . The data of Figures 5.3-6 and 5.3-7 represent 13 test runs taken at various rotor rpm and engine temperature levels. The hottest run of this series was run No. 11 earlier described in Section 5.3.1.3.

5.3.2 Leakage Results

A typical test setup used for the measurement of gas leakage in the various components of the rotor system is shown on Figure 5.3-8.

The component under test, having its inlets and outlets sealed, is



SEGMENT NO. 18

LOCATION OF THERMOCOUPLES
BETWEEN RIBS

NOTE:

READINGS OF DUCT WALL
TEMPERATURE BS-18-2 and BS-18-6
WERE ALMOST IDENTICAL

READINGS OF OUTER SKIN TEMPERATURE
BS-18-7 and BS-18-9 WERE
WITHIN $\pm 5\%$ FROM THEIR AVERAGE
VALUE.

HEAVY LINES REPRESENT PLOT OF AVERAGE
TEMPERATURE OF DUCT WALL OR
OUTER SKIN.

TRANSIENT TEMPERATURES:

Test on Dec. 13-1961 at
1230° Eng. Disch. Temp.

Test on Dec. 11-1961 at
1170° Eng. Disch. Temp.

Predicted at 1200° Duct Gas. Temp.

STEADY STATE:

Test Run No. 6 on Dec. 1-1961 at
highest recorded gas temp. (1176°F)
(spar thermocouples not at
No. 18 segment)

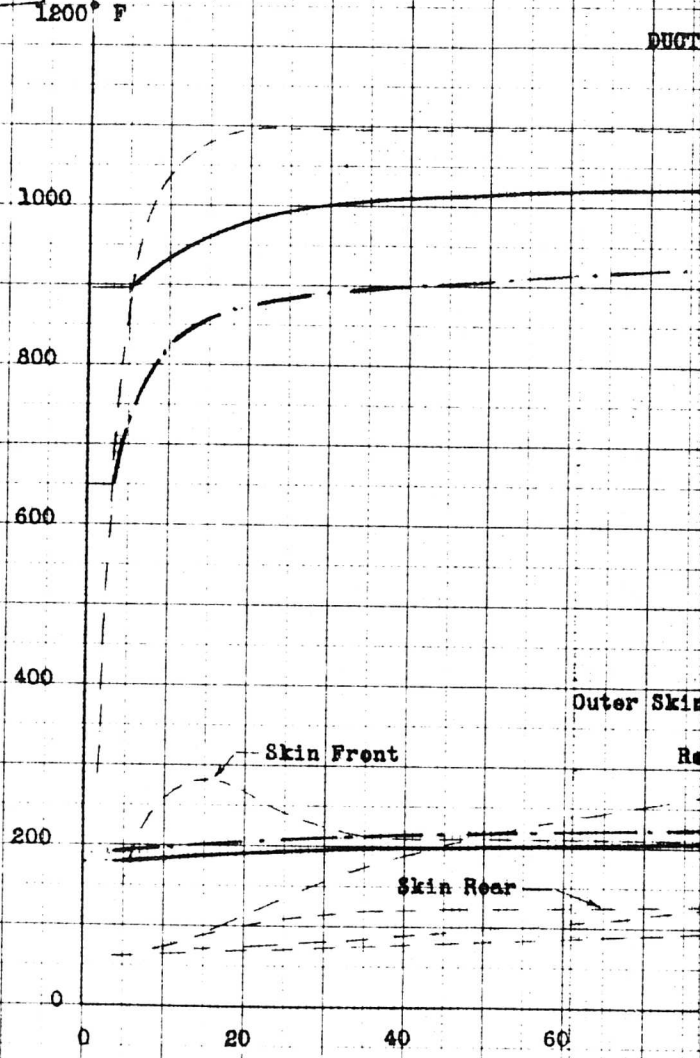


FIGURE 5.3-4
TRANSIENT TEMPERATURE
PREDICTED AND MEASURED

2

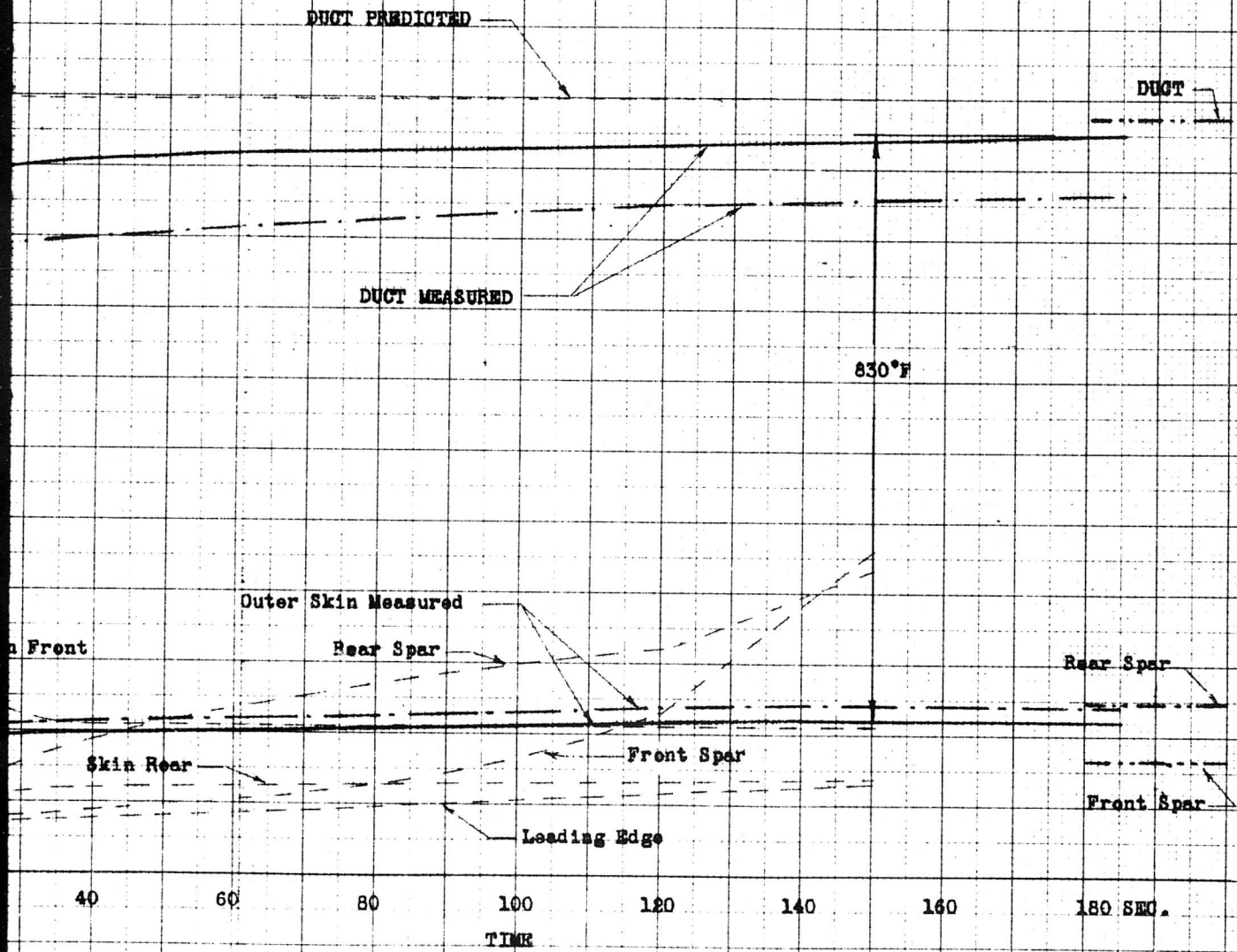


FIGURE 5.3-4
TRANSIENT TEMPERATURE
PREDICTED AND MEASURED

NOTE:
 TEMPERATURE INDICATED BY UPPER NUMBER
 AT EACH THERMOCOUPLE REPRESENTS MEASUREMENTS
 FROM RUN NO. 11 (Oct. 27-61) AT 1152°F GAS TEMPERATURE
 THOSE TEMPERATURES ARE CONSIDERED REPRESENTATIVE
 FOR "HOT" RUNS.
 INTERMEDIATE NO. IS RECORDED ON (Dec. 1-61)
 RUN NO. 6, (66), AT 1176°F GAS TEMPERATURE
 HIGH DIFFERENCE BETWEEN TWO READINGS INDICATES
 LEAKAGE IN THE HUB.
 THERMOCOUPLES No. 3, 4 and 8 WERE INACTIVE.

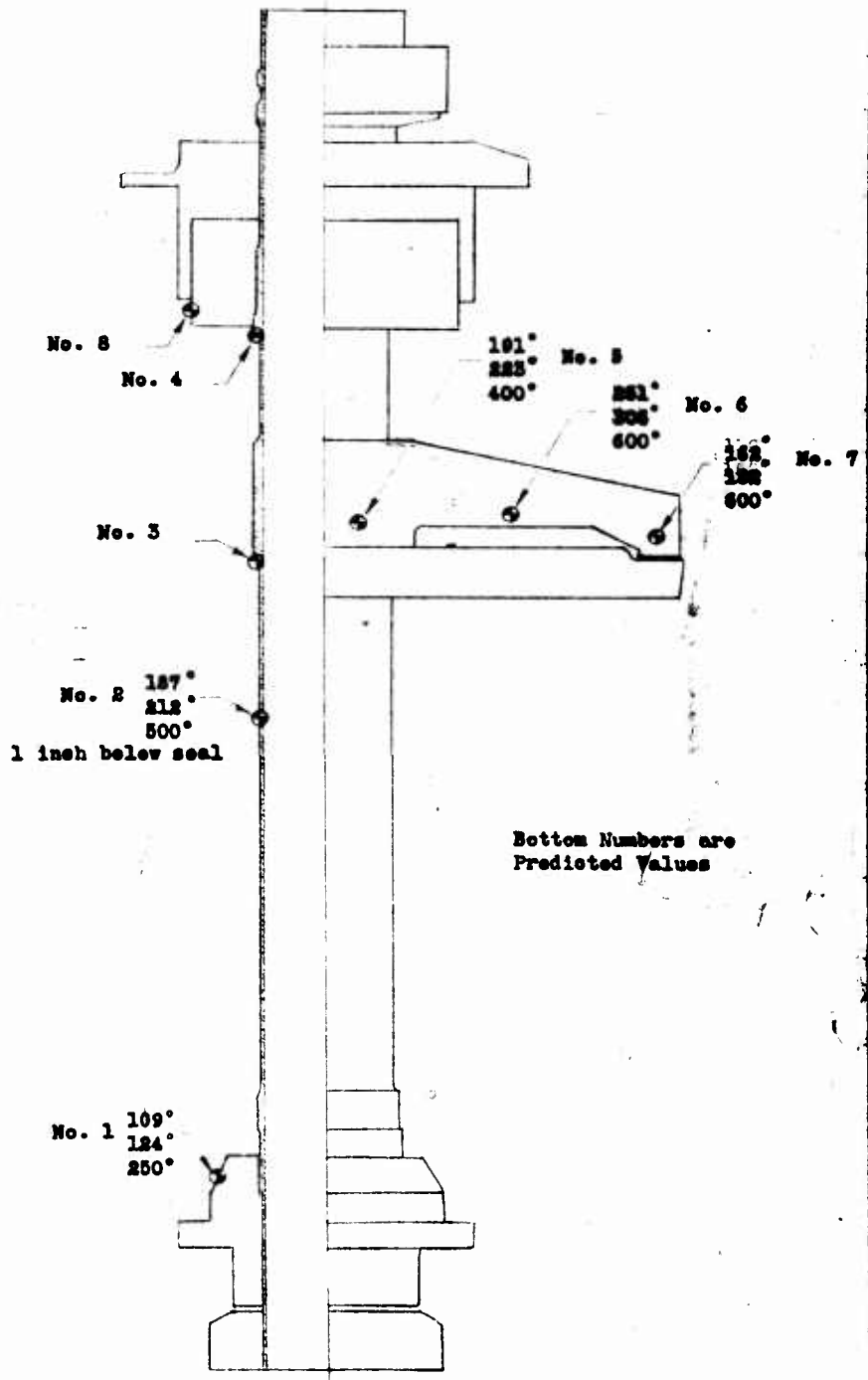


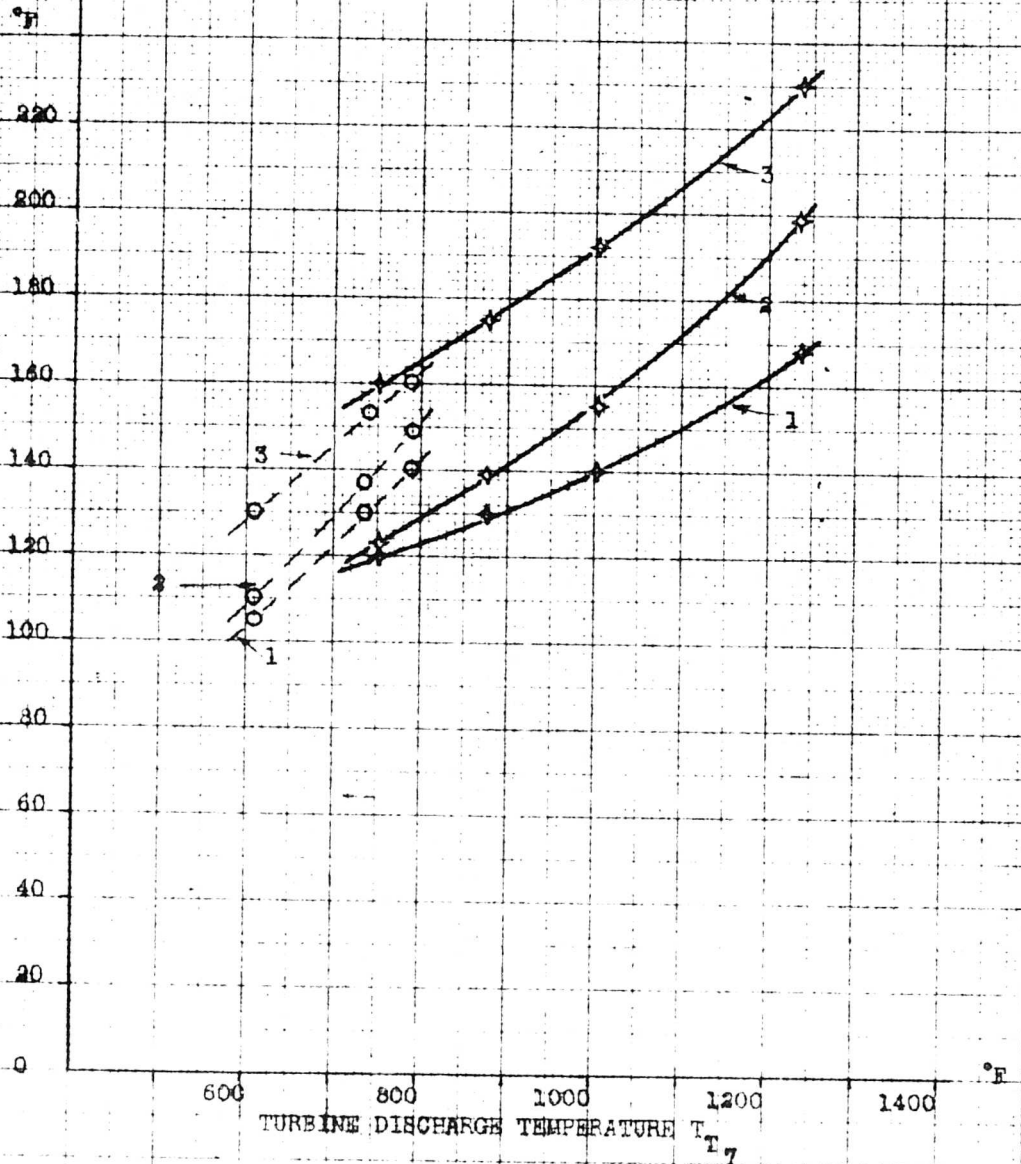
FIGURE 5.3-5
 DISTRIBUTION OF TEMPERATURE
 IN THE HUB

11-30-61 MKG

Location of Thermocouples:

- 1 Front spar, center web outside at station 135
- 2 Rear spar, center web outside at station 135
- 3 Rear spar top flange at station 270
(This is the highest recorded temperature of a spar at any section.)

—◆— 240 RPM
 - - ○ - - 170 RPM



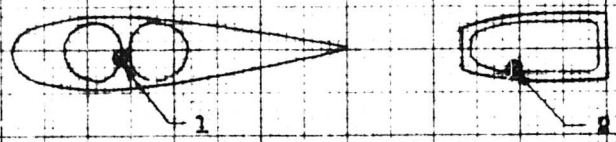
HOT CYCLE HELICOPTER

Fig. 5.3-6

TEMPERATURE OF ROTOR COMPONENTS AT VARIOUS POWER LEVEL

359-11
 10X 10 TO THE MINOR
 NEW YORK, N.Y.

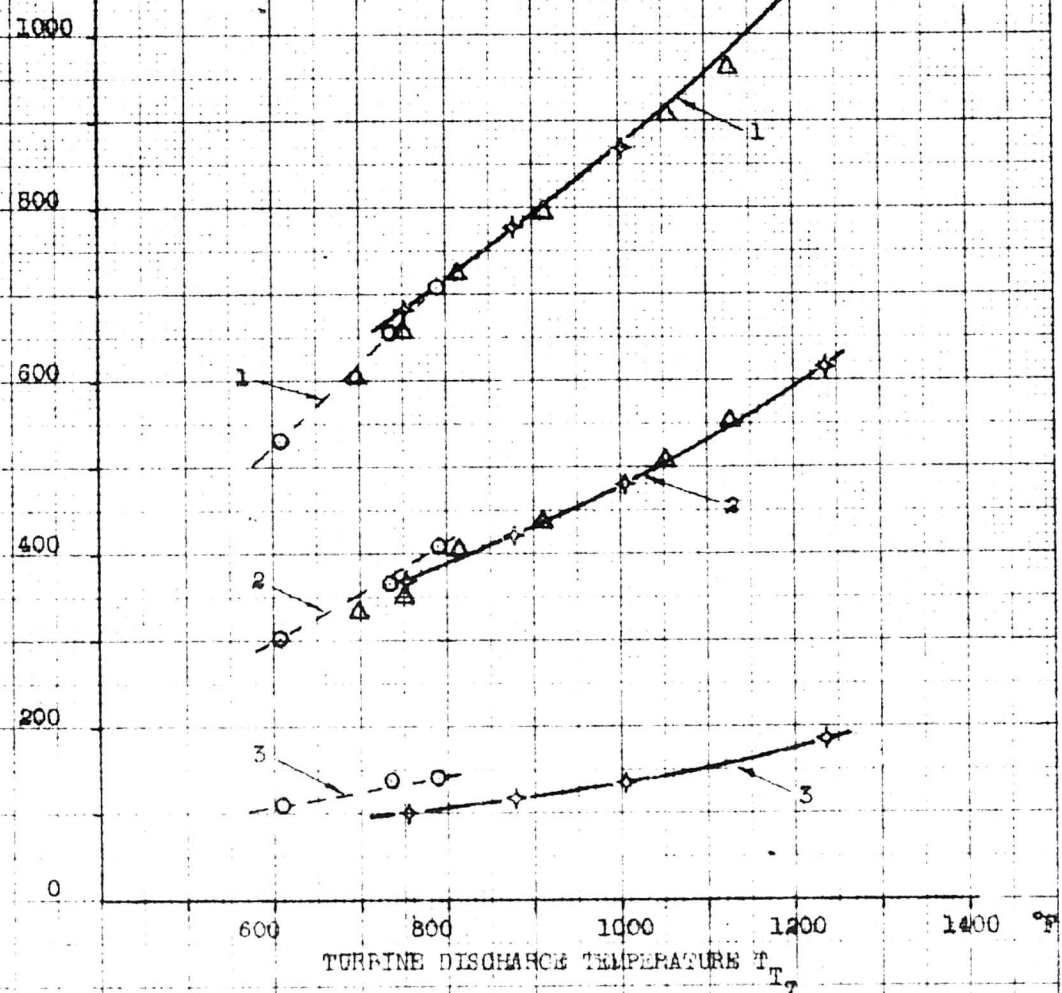
11-30-61 JTR



Location of Thermocouples:

- 1 duct wall as indicated above at station 95
- 2 flexure as indicated above at station 105
- 3 hub mast 10 in. below seal.

* ———— ◆ ———— 240 RPM
 △ 220 RPM
 - - - ○ - - - 170 RPM



10 X 10 TO THE 1/4 INCH 359-11
 REUTEL 6-1960

HOT CYCLE HELICOPTER

Fig. 5.3-7

TEMPERATURE OF ROTOR COMPONENTS
AT VARIOUS POWER LEVEL

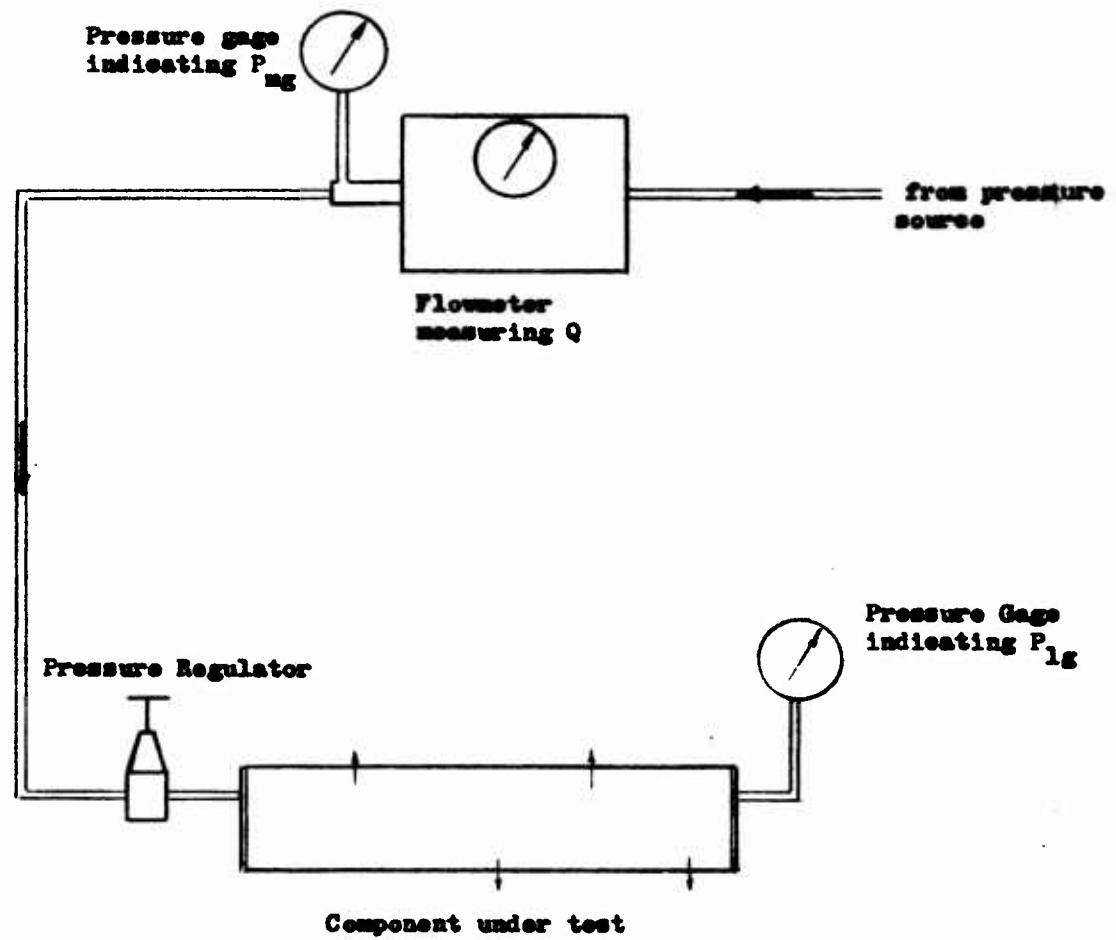


Figure 5.3-8
Leakage Test
Typical Test Setup

ANALYSIS _____

MODEL _____

PREPARED BY _____

CHECKED BY _____

connected to the pressure source through a flow meter. One of the two pressure gages required for the test is coupled directly to the meter, while the other measures pressure maintained in the tested duct. The measurement of air flow (cfm) and the indications of the two pressure gages (psig) are used to estimate the rate of leakage under typical high power whirl conditions.

The flow rate through the meter W_m equals the rate of leakage in the component W_l ; the ratio of the corrected leakage W_w representing the whirl conditions to the measured leakage can be expressed in terms of a fundamental equation.

$$W_m = W_l = \frac{Q}{60} \rho_m \text{ (lb/sec)}$$

$$\begin{aligned} \frac{W_w}{W_l} &= \frac{K A \rho_w Y \sqrt{2g (P_{wa} - P_{am}) / \rho_w}}{K A \rho_l Y \sqrt{2g (P_{la} - P_{am}) / \rho_l}} = \quad (1) \\ &= \frac{\rho_w}{\rho_l} \sqrt{\frac{P_{wg} \rho_l}{P_{lg} \rho_w}} = \sqrt{\frac{P_{wg} P_{wa}}{P_{lg} P_{la}}} \end{aligned}$$

Where

- Q = flow meter readout (cfm)
- ρ = specific weight (lb/ft³)
- W = air flow (leakage) lb/sec
- Subscripts single or combined
- m flow meter
- l test condition
- w whirl condition
- g gage pressure
- a absolute pressure
- am ambient pressure

Equation (1) determines the correction necessary to convert the rate of measured leakage at a duct test pressure P_{lg} , to that which will occur at whirl pressure P_{wg} .

$$W_w = W_l \sqrt{\frac{P_{wg} P_{wa}}{P_{lg} P_{la}}}$$

ANALYSIS _____

MODEL _____

REPORT NO. _____

PREPARED BY _____

CHECKED BY _____

In addition, due to the elevated whirl temperature, the density of escaping gas is considerably lower than the density of ambient air used for testing. The ratio of densities at different temperatures (other parameters being constant) is

$$\frac{\rho_w}{\rho_1} = \frac{T_1}{T_w}$$

on the other hand, the effect of temperature on the gas escape velocity acts in the opposite direction. The ratio of the escape velocities is

$$\frac{v_w}{v_1} = \frac{T_w}{T_1}$$

The combined effect of the above relations results in

$$\frac{W_w}{W_1} = \sqrt{\frac{T_1}{T_w}} \quad (2)$$

The correction factor due to the combined differences of pressure and temperature that exist between the test and the whirl conditions is:

$$\frac{W_w}{W_1} = \sqrt{\frac{P_{wg} \times P_{wa} \times T_1}{P_{lg} \times P_{la} \times T_w}} \quad (3)$$

The rate of leakage measured at the test pressure of 23.6 psig and standard ambient conditions at sea level is converted to the anticipated leakage at the 21 psig blade pressure and 1190°F gas temperature as follows:

$$\begin{aligned} W_w &= \frac{Q}{60} P_m \sqrt{\frac{P_{wg} \times P_{wa} \times T_1}{P_{lg} \times P_{la} \times T_w}} \\ &= \frac{Q P_{ma} 144}{60 \times 53.35 \times 530} \sqrt{\frac{P_{wg} \times P_{wa} \times T_1}{P_{lg} \times P_{la} \times T_w}} \quad (4) \end{aligned}$$

This equation was used to prepare Table 5.3-2.

ANALYSIS _____

PREPARED BY _____

CHECKED BY _____

and for the test pressure $P_1 = 20$ psig,

$$W_w = \frac{5.00}{10^5} Q P_{mg} \quad (5)$$

Equations (4) and (5) were used to prepare Table 5.3-2.

285-16
(62-16)

TABLE 5. 3-2

LEAKAGE MEASUREMENTS

Assembly Under Test	Hours Whirl Time Before Test	P1 Psig Duct Test Pressure	Q cfm Meter Flow Rate	W _w #/sec Corrected Leakage	Leakage % of Component Flow	Remarks
Blue Blade	0	23.6	Less than 1 cfm	0.00393	0.027	
Red Blade	0	23.6	"	0.00393	0.027	
Yellow Blade	0	23.6	"	0.00393	0.027	
Hub Ass'y	0	23.6	"	0.00393	0.009	
Blue Blade	18	23.6	0.9	0.00355	0.024	
Red Blade	18	23.6	1.5	0.00592	0.038	
Yellow Blade	18	23.6	2.8	0.01105	0.072	
Total 3 Blades	18	23.6	5.2		0.044	
Rotor System*	18	23.6	17.0	0.0672	0.146	
Rotor System	18	20	17.0	0.0767	0.168	On the tower.
Rotor System	35	Negligible	20.0	-	High Leak due to defective seal	On the tower
Blue Blade	35	23.6	1.5	0.00593	0.0388	
Red Blade	35	23.6	2.7	0.0109	0.0698	
Yellow Blade	35	23.6	2.7	0.0107	0.0698	
Hub Ass'y	35	23.6	4.5	0.0178	0.0387	As rec'd from tower
Hub Ass'y	35	23.6	1.8	0.00712	0.0154	After rapping to seat seals
Hub Ass'y	35	23.6	0.6	0.00237	0.00515	Reassembled after teardown
Rotor Ass'y	35	20	17	0.0767	0.168	Reassembled after teardown
Blue Blade	60	23.6	2.0	0.00792	0.0517	
Red Blade	60	23.6	4.0	0.0158	0.103	
Yellow Blade	60	23.6	3.2	0.0131	0.0855	
Hub Ass'y	60	23.6	13.2	0.0523	0.114	

* Note: Rotor System includes the hub plus the three blades

ANALYSIS _____

PREPARED BY _____

CHECKED BY _____

5.4 STRUCTURAL EFFECTS

5.4.1 Comparison of Design With Measured Mechanical Strains

Typical Strain Gage data obtained during the whirl test are presented in Figures 5.4-1 through 5.4-4. These are discussed below.

5.4.1.1 Blade Pitch Arm Loads

Pitch Arm cyclic load versus wind speed is presented in Figure 5.4-1. All of the measured cyclic pitch arm loads fall well below the design limit. (Reference 5.4-1)

5.4.1.2 Rear Spar Flapwise Bending Moments at Station 53.5 Inches

Blade cyclic flapwise bending moments versus wind speed are plotted for blade station 53.5 inches in Figure 5.4-2. The moments plotted are the maximum cyclic moments that occurred during typical operating conditions. The measured cyclic bending moments are below the design allowable limit, (Reference 5.4-1) with the exception of one point. A few cycles at this amplitude occurred and probably resulted from wind gusts.

5.4.1.3 Rear Spar Flapwise Bending Moments at Station 73.4 Inches

Blade cyclic flapwise bending moments versus wind speed are plotted for blade station 73.4 inches in Figure 5.4-3. The moments plotted are the maximum cyclic moments that occurred during typical operating conditions. The measured cyclic bending moments are below the design allowable limit, (Reference 5.4-1) with the exception of one point. This point occurred during large wind gusts with the wind varying from 19 to 25 MPH.

5.4.1.4 Front and Rear Spar Cyclic Axial Load (Cyclic Chordwise Bending)

Plotted in Figure 5.4-4 are the measured cyclic axial loads in the rear spar at station 103 inches, and front spar at station 83.3 inches, versus wind speed. The loads plotted are the maximum cyclic loads that occurred during typical operating conditions. Three points for the rear spar and nine points for the front spar fell above the endurance limit, (Reference 5.4-1). It is believed that the spar cyclic axial loads (cyclic chordwise bending) were aggravated by gusty wind conditions. It is estimated that the small number of cycles above the endurance limit, used up a very small percentage of the service life of the blade.

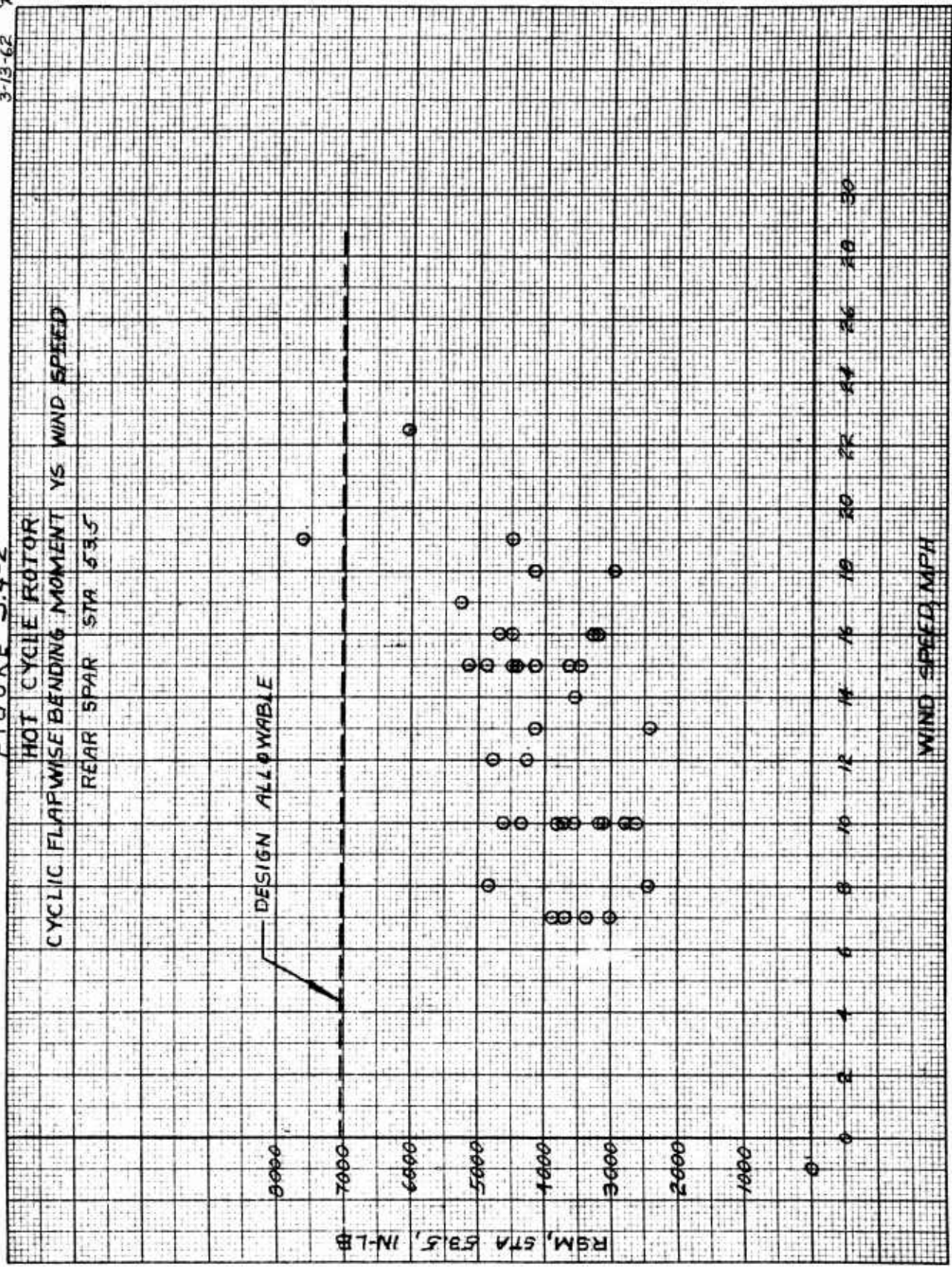
10 X 10 TO THE 1/2 INCH 359-11
 KEUFFEL & ESSER CO. PLACING

FIGURE 5.4-1
 HOT CYCLE ROTOR
 CYCLIC PITCH ARM LOAD VS WIND SPEED



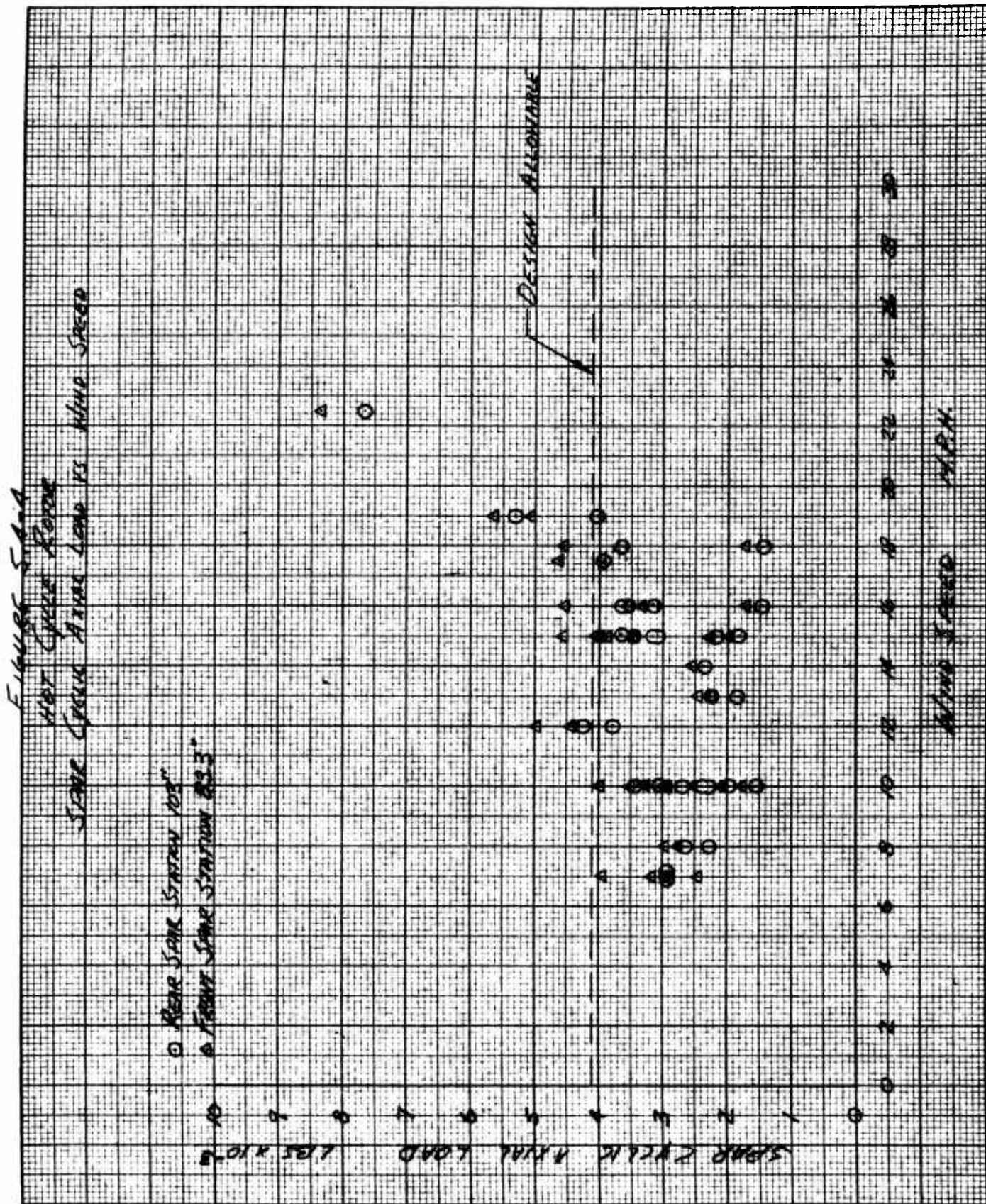
FIGURE 5.4-2

3-13-62
 CA



NO. 1 TO 1, INC.
KEUFFEL & ESSER CO.
MADE IN U.S.A.

359

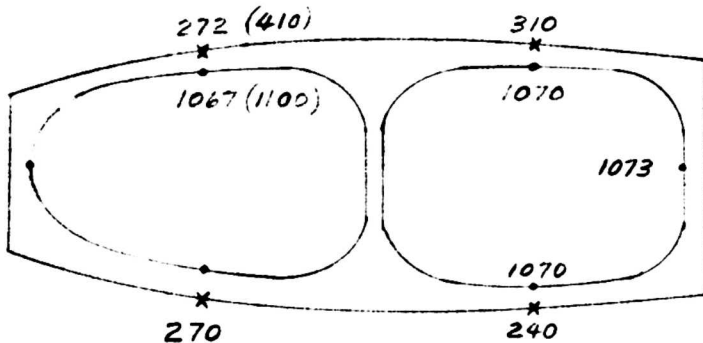


5.4.2 THERMAL EFFECTS ON STRUCTURE

A COMPARISON OF DESIGN WITH MEASURED TEMPERATURES FOR THE HOT CYCLE ROTOR IS PRESENTED IN SECTION 5.3.1. THE RESULTS, FOR THE MOST PART, SHOW THAT PREDICTED VALUES USED IN DESIGN WERE REASONABLY ACCURATE FOR CRITICAL COMPONENTS.

THE ANALYSIS WHICH FOLLOWS SINGLES OUT SEVERAL COMPONENTS AND ANALYZES THE THERMAL EFFECTS OF THE MEASURED TEMPERATURES. FROM AN OVERALL STANDPOINT, INSPECTION OF THE ROTOR SUBSEQUENT TO COMPLETION OF THE WHIRL TESTS SHOWED NO DELETERIOUS EFFECTS OF TEMPERATURE ON THE STRUCTURE.

5.4.2.1 BLADE SEGMENT RIBS



x SKIN TEMP. (°F) AT RIB (MEASURED)

• DUCT WALL TEMP. (°F) BETWEEN RIBS (MEASURED)

() VALUES IN PARENTHESES ARE DESIGN VALUES

NOTE: TEMPERATURE COMPARISON SHOWN IS FOR SEGMENT 18. THERMOCOUPLES COULD NOT BE LOCATED ON THE DUCT WALL AT THE RIB BECAUSE OF FABRICATION RESTRICTIONS.

ANALYSIS HOT CYCLE
 PREPARED BY C.R. SMITH
 CHECKED BY _____

BLADE SEGMENT RIBS (CONT'D)

THERMAL STRESSES AS CALCULATED IN REF. 5.4-1 ARE BASED ON TEMPERATURES AT THE RIB. IF IT IS ASSUMED THAT MEASURED VS. DESIGN TEMPERATURES OF THE DUCT AT THE RIB ARE DIFFERENT BY THE SAME INCREMENT AS THE TEMPERATURES BETWEEN RIBS THE FOLLOWING MAY BE SURMISED:

$$\Delta T (\text{DUCT BETWEEN RIBS}) = 1100 - 1067 = 33^\circ\text{F}$$

FROM PREDICTED CURVE T (AT RIB) = 915°F
 (REF. SECTION 5.3.1)

$$T_{\text{CORRECTED}} (\text{AT RIB}) = 915 - 33 = 882^\circ\text{F}$$

$$\text{THEN: } \Delta T' (\text{DUCT TO SKIN}) = 882 - 272 = 610^\circ\text{F}$$

$$\Delta T' (\text{DESIGN}) = 1050 - 500 = 550^\circ\text{F} (\text{REF. 5.2-1, PG. 5.2.4.12})$$

THEREFORE THE THE THERMAL STRESSES BASED ON MEASURED TEMPERATURES ARE HIGHER THAN DESIGN BY THE RATIO:

$$R = \frac{610}{550} = 1.11 \text{ OR } 11\% \text{ HIGHER.}$$

ALTHOUGH THE ABOVE ANALYSIS INDICATES THE POSSIBILITY OF HIGHER THERMAL STRESSES POST TEST INSPECTIONS OF THE DUCT WALLS SHOWED NO EVIDENCE OF PERMANENT SET.

5.4.2.2 BLADE SPARS

MEASURED TEMPERATURES OF THE SPARS WERE WELL BELOW PREDICTED TEMPERATURES. AT THESE LOW TEMPERATURES THE EFFECT ON THE MATERIAL PROPERTIES OF TITANIUM IS NEGLIGIBLE.

	<u>DESIGN TEMPERATURE</u>	<u>MAX MEASURED TEMPERATURE</u>
FRONT SPAR	460°F	170°F
REAR SPAR	435°F	230°F

HUGHES TOOL COMPANY-AIRCRAFT DIVISION

ANALYSIS HOT CYCLE MODEL 285 REPORT NO. 285-16 PAGE 5.4-8
 PREPARED BY C.R. SMITH
 CHECKED BY _____

5.4.2.3 BLADE FLEXURES - CONSTANT SECTION

IN THE INITIAL DESIGN, THE FLEXURES JOINING THE BLADE SEGMENTS WERE OF ELECTROFORMED NICKEL. HOWEVER DUE TO A PROCUREMENT PROBLEM WITH THE NICKEL PARTS, THE BASIC FLEXURE WAS CHANGED TO INCONEL "X" WHICH PROVED TO BE SUPERIOR FROM BOTH A FATIGUE AND TEMPERATURE STANDPOINT. THE INCONEL "X" PARTS WERE USED THROUGHOUT WITH THE EXCEPTION OF THE LAST THREE FLEXURES AT THE TIP, WHERE CYCLIC DEFLECTIONS ARE A MINIMUM. A COMPARISON OF PREDICTED AND MEASURED TEMPERATURES IS GIVEN BELOW. POST TEST INSPECTION SHOWED NO DAMAGE TO EITHER TYPE FLEXURE.

<u>FLEXURE</u>	<u>DESIGN TEMP.</u>	<u>MEASURED TEMP.</u>	
ELECTRO-FORM NICKEL	600°F	510°F	} (REF SECT. 5.3.1)
INCONEL "X"	600°F*	660°F	

*INCONEL "X" RETAINS ITS STRENGTH TO APPROX. 1000°F

5.4.2.4 ROTOR HUB & SHAFT

MEASURED TEMPERATURES OF SECTION 5.3.1 ARE BELOW PREDICTED TEMPERATURES FOR ALL STRUCTURAL COMPONENTS.

ANALYSIS HOT CYCLE
 PREPARED BY C.R. SMITH
 CHECKED BY _____

5.4.3 GIMBAL LUG STRESSES

THE HUB IS ATTACHED TO THE GIMBAL RING THRU LUGS THAT EXTEND DOWN FROM THE 285-0529 FITTING AND STRADDLE THE TWO BEARINGS. THE CRITICAL DESIGN LOAD WAS A SIDE LOAD WHICH PRODUCES BENDING IN THE LUGS. A COMPARISON OF DESIGN AND MEASURED LOADS AND STRESSES IS GIVEN BELOW.

LOADS

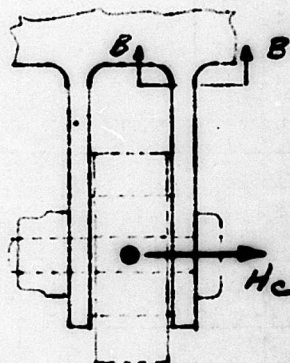
WEIGHTED FATIGUE (DESIGN):

$$H_c = \pm 1050 \text{ LBS.}$$

MEASURED (WHIRL TEST):

$$H_{c \text{ MAX.}} = \pm 3340 \text{ LBS.}$$

$$H_{c \text{ NORMAL}} = \pm 700 \text{ TO } \pm 1600 \text{ LBS.}$$



STRESSES (REF 5.4-1, PG. 5.3.2.12.3)

THE CRITICAL SECTION IN FATIGUE IS SECTION B-B AT THE RADIUS.

$$f = 4370 \pm 6580 \text{ PSI (WEIGHTED FATIGUE COND.)}$$

FOR MEASURED WHIRL TEST LOADS:

$$f_{\text{MAX.}} = \frac{3340}{1050} (\pm 6580) = \pm 21,000 \text{ PSI}$$

$$F_a = \pm 26000 \text{ PSI}$$

ALTHOUGH THIS CALCULATED CYCLIC STRESS IS ACCEPTABLE THERE ARE CERTAIN UNKNOWNNS INVOLVED SUCH AS THE LOAD DISTRIBUTION BETWEEN LUGS. IN VIEW OF THIS A MODIFICATION WAS MADE AT THE 35 HOUR INSPECTION TO INCREASE THE RIGIDITY AND STRENGTH OF THE LOAD PATH FOR TAKING SIDE LOADS. SET SCREWS WERE ADDED IN THE WALL OF THE HUB SURROUNDING THE GIMBAL TO BEAR DIRECTLY AGAINST THE LUG TO RING ATTACH BOLTS.

HUGHES TOOL COMPANY-AIRCRAFT DIVISION

ANALYSIS HOT CYCLE MODEL 285 REPORT NO 285-16 PAGE 5.4-10
PREPARED BY C.R. SMITH
CHECKED BY _____

GIMBAL LUG STRESSES (CONT'D.)

IN ADDITION FIBROID RUB STRIPS WERE
INSTALLED BETWEEN THE LUGS AND GIMBAL
RING TO LIMIT THE DEFLECTION.

FOR APPLICATION TO A FLIGHT ARTICLE
A MINOR DESIGN CHANGE TO STRENGTHEN
THE LUGS WOULD BE IN ORDER.

ANALYSIS _____

PREPARED BY _____

CHECKED BY _____

5.5 SOUND LEVEL MEASUREMENT

5.5.1 Test Noise Alleviation

During the early part of the whirl testing sound levels in the vicinity of the test site were relatively high. This was due to the fact that only about one third of the J57 exhaust flow was used to power the rotor, and the surplus flow was exhausted directly to the atmosphere. The noise associated with the surplus exhaust flow of the J57 proved bothersome and inconvenient to test site personnel, some of the neighbors of the test site, and particularly to Loyola University, which is located on a hill about 100 feet above the site and 800 feet distant. Because of the orientation of the test installation, the engine inlet was pointed almost directly at the University. The inlet noise is highly directional in nature, and thus in this position both the intake compressor whine and the exhaust roar were a source of irritation to Loyola University personnel.

In an effort to lower the sound levels to an acceptable range, sound suppressors were installed at both intake and exhaust ends of the J57 engine. These suppressors are shown on the frontispiece and on Figures 5.5-1 and 5.5-2. The intake suppressor was designed, built, and installed by General Acoustics Corporation, Los Angeles, California. The exhaust suppressor (Model 1195) was leased from Kittel Lacy, Inc., El Monte, California.

Overall sound level intensity measurements were taken on the crest of a hill above the test site and within 50 feet of the Loyola University cafeteria. These measurements were made with a General Radio 759B Sound Level Meter using the "c" scale only. Refer to Figure 5.5-3. Before installation of sound suppressors the sound intensity was 88 decibels and after suppressors were installed the sound intensity dropped to 76 decibels, considered an acceptable level for this location. This suppressed sound level is one sixteenth of the original unsuppressed sound level.

In addition, octave band sound pressure level measurements were made in St. Roberts Hall, which is the closest building, containing classrooms, to the Hot Cycle Rotor Test Site. These measurements were made with a General Radio type 1550-A Octave-band Sound Analyzer operating from the output of a type 759-B Sound Level Meter. Data obtained and representative curves are shown on Table 5.5-1 and Figure 5.5-4. The curves indicate that noise levels of the Hot Cycle Rotor plus suppressed engine noise fall almost directly on the lower curve of normal ambient classroom noise levels.

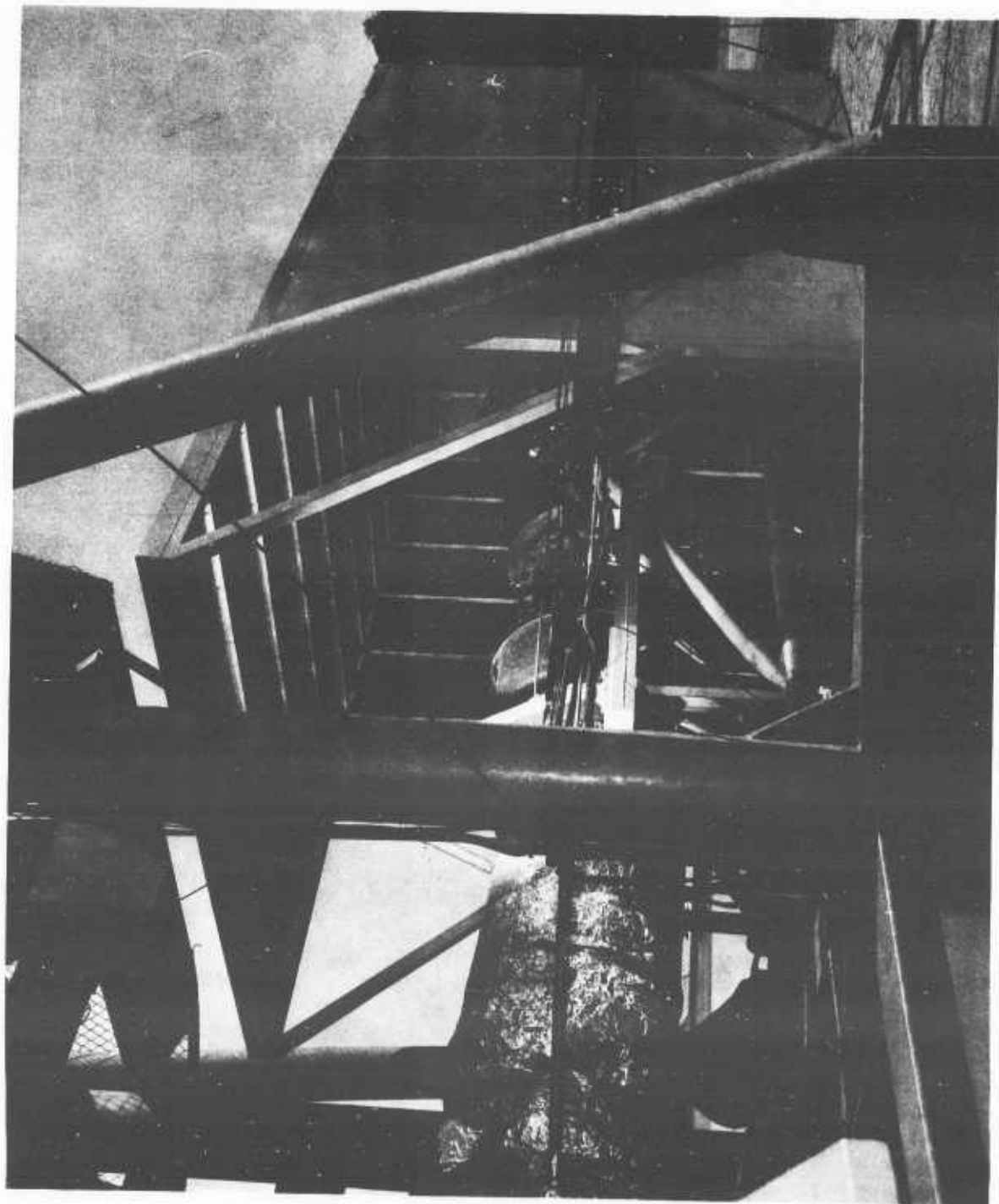


Figure 5.5-1 Engine Inlet Suppressor

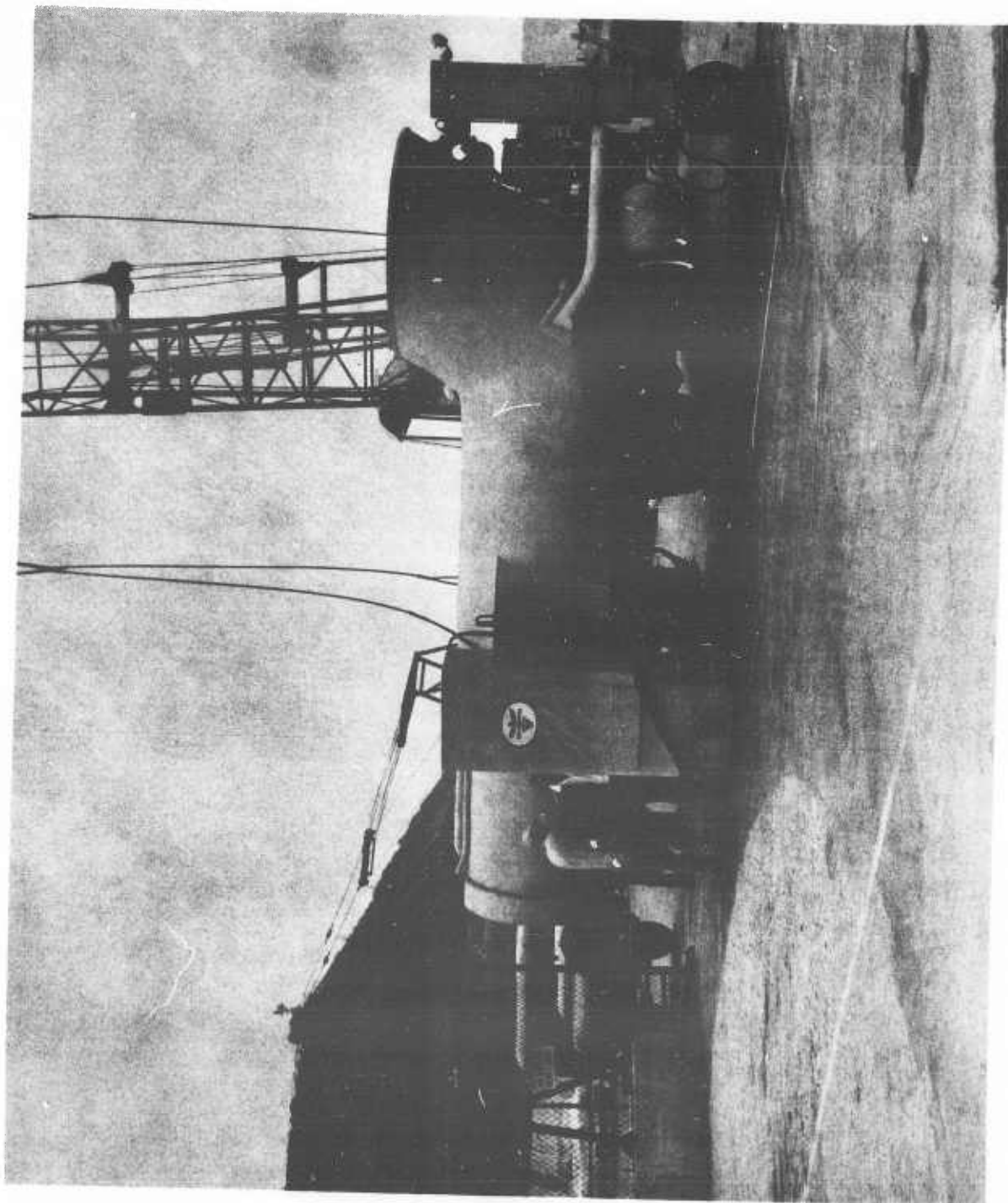


Figure 5. 5-2 Engine Surplus Flow Exhaust Suppressor

ANALYSIS

PREPARED BY

CHECKED BY

MODEL

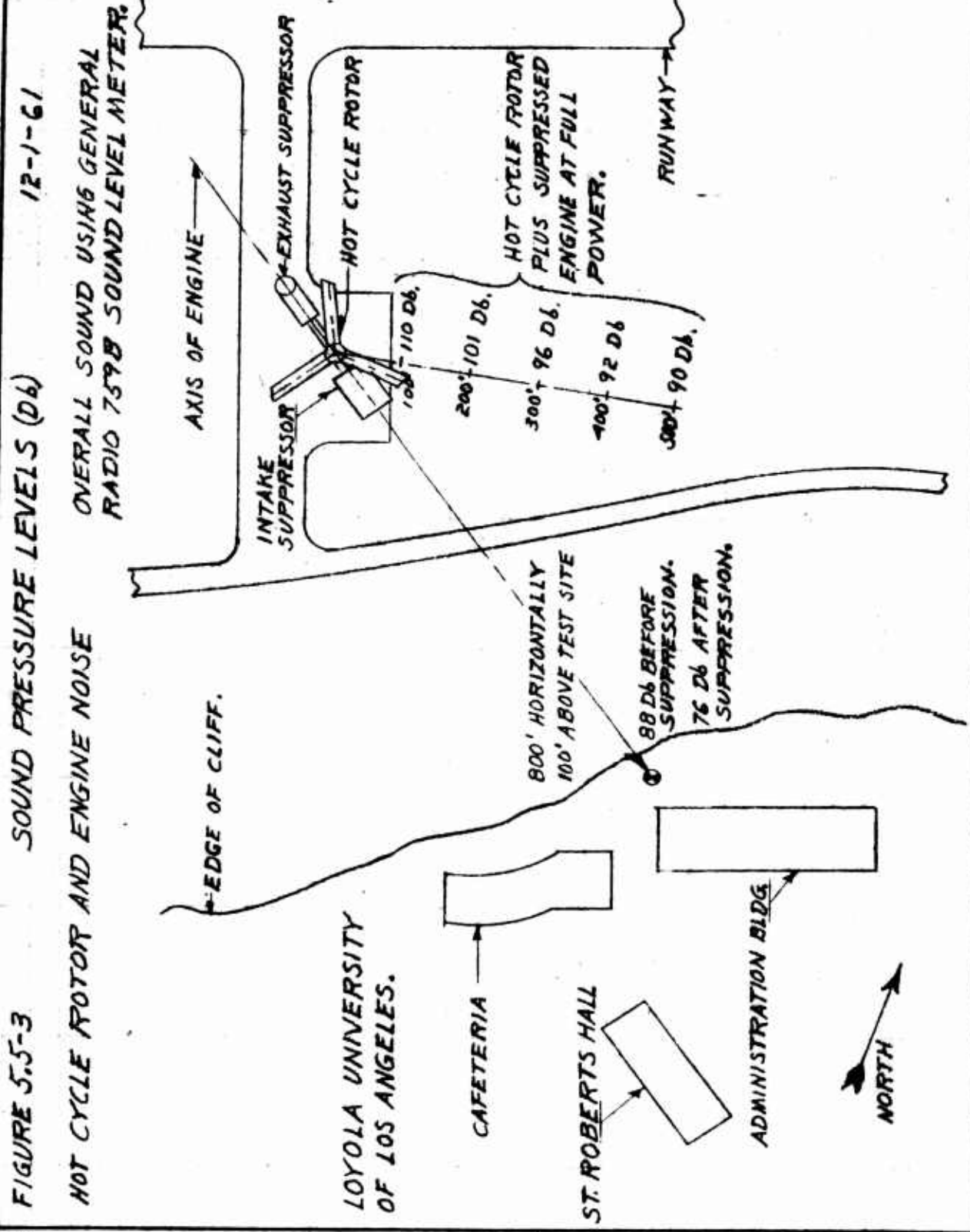


FIGURE 33-4
 SOUND PRESSURE LEVEL VS FREQUENCY
 OCTAVE BAND ANALYSIS, 2-27-62

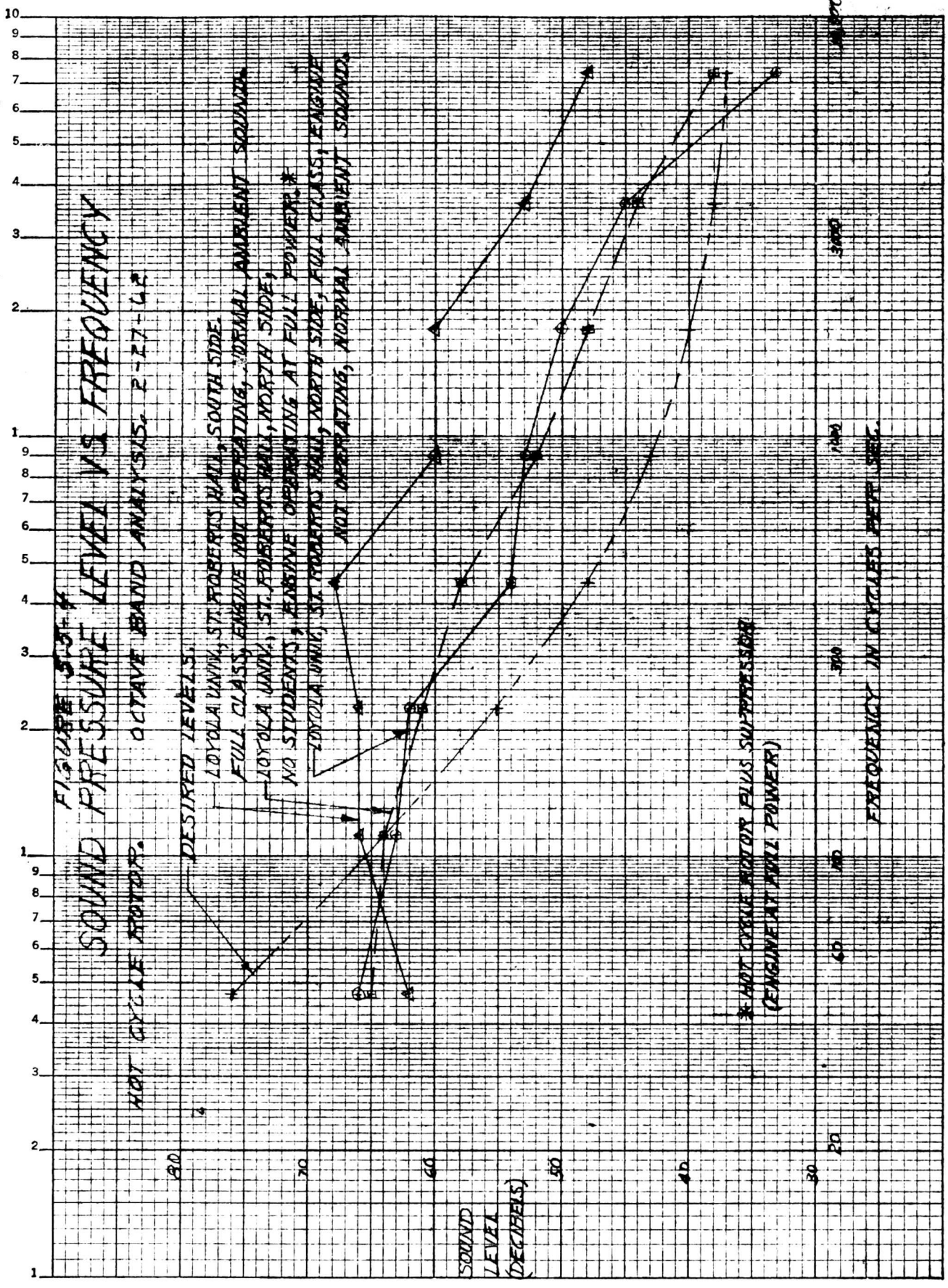
HOT CYCLE ROTOR.

DESIRED LEVELS.

LOYOLA UNIV, ST. ROBERTS HALL, SOUTH SIDE.
 FULL CLASS, ENGINE NOT OPERATING, NORMAL AMBIENT SOUND.
 LOYOLA UNIV, ST. ROBERTS HALL, NORTH SIDE,
 NO STUDENTS, ENGINE OPERATING AT FULL POWER.*
 LOYOLA UNIV, ST. ROBERTS HALL, NORTH SIDE, FULL CLASS, ENGINE
 NOT OPERATING, NORMAL AMBIENT SOUND.

* HOT CYCLE ROTOR PLUS SUPPRESSOR
 (ENGINE AT FULL POWER)

FREQUENCY IN CYCLES PER SEC.



ANALYSIS _____

PREPARED BY _____

CHECKED BY _____

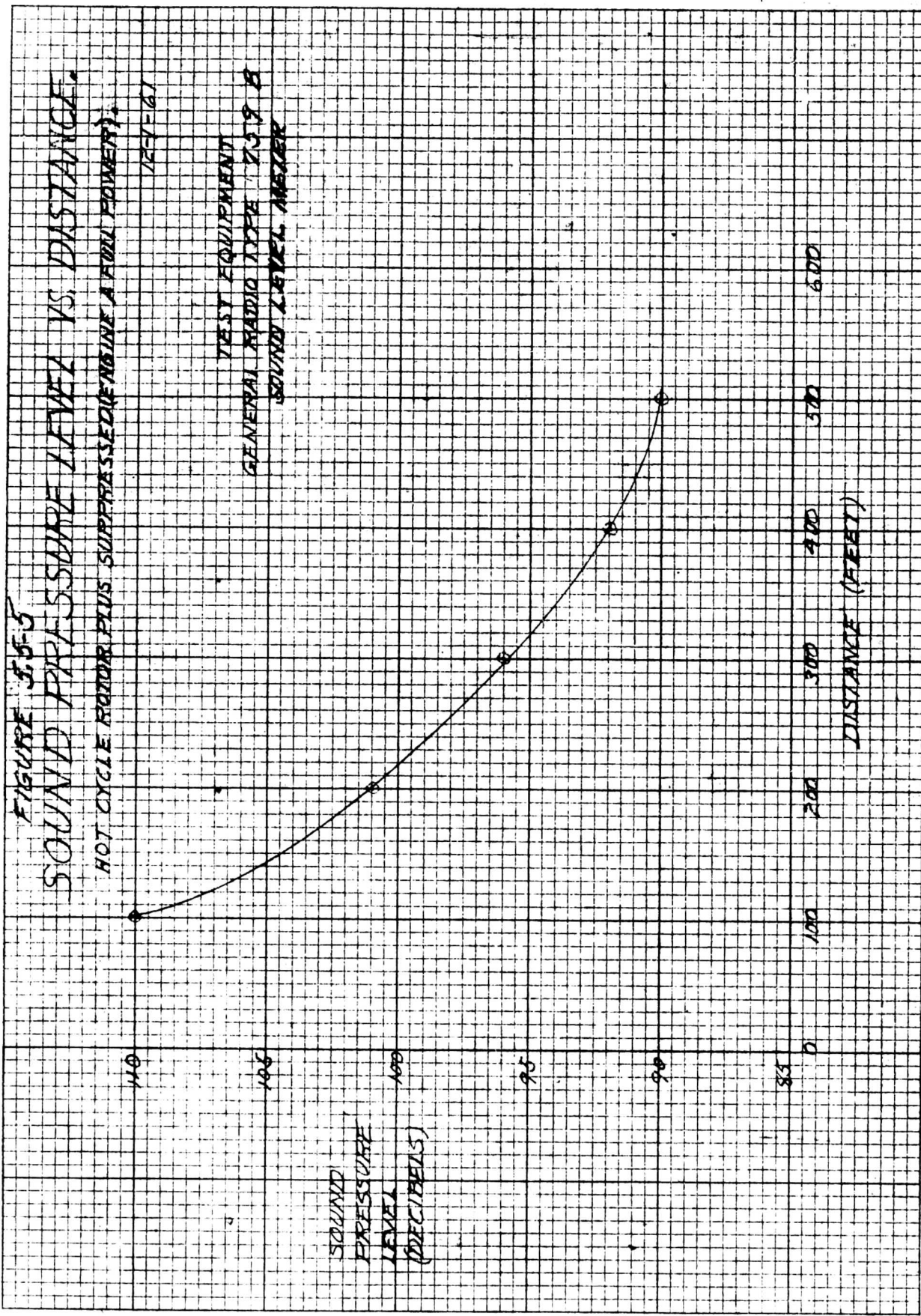
5. 5. 2 Prediction of Rotor Sound Level

After reducing the intake and exhaust noise levels of the J57 engine, overall sound pressure level measurements were made close to the test site so that a preliminary study of rotor blade tip exhaust sound levels could be made. Data obtained and a representative curve are shown on Figures 5. 5-3 and 5. 5-5.

Operation of the whirl test installation with the suppressor installed on the surplus flow exhaust, provides a good indication of the sound levels to be expected in an actual hot cycle helicopter with the same rotor. However, two differences between the whirl test installation and an actual helicopter should be noted.

1. The engine inlet contribution would be different in the case of an actual helicopter from that of the whirl test installation. Only one-third the air flow would be involved in the helicopter, but the inlet sound suppression would probably not be as effective as that used in the whirl testing. However, an examination of the data of Table III of Mr. Irving's excellent paper on this subject (Reference 5. 5-1), indicates a negligible contribution of inlet noise to the over-all sound level of typical turbine-powered helicopters. In each test reported, the lowest sound levels were actually recorded in front of the machines tested. Therefore, it can be concluded that differences in inlet configuration between the whirl test and an actual hot cycle helicopter should not contribute significantly to a difference in sound level between the two cases.

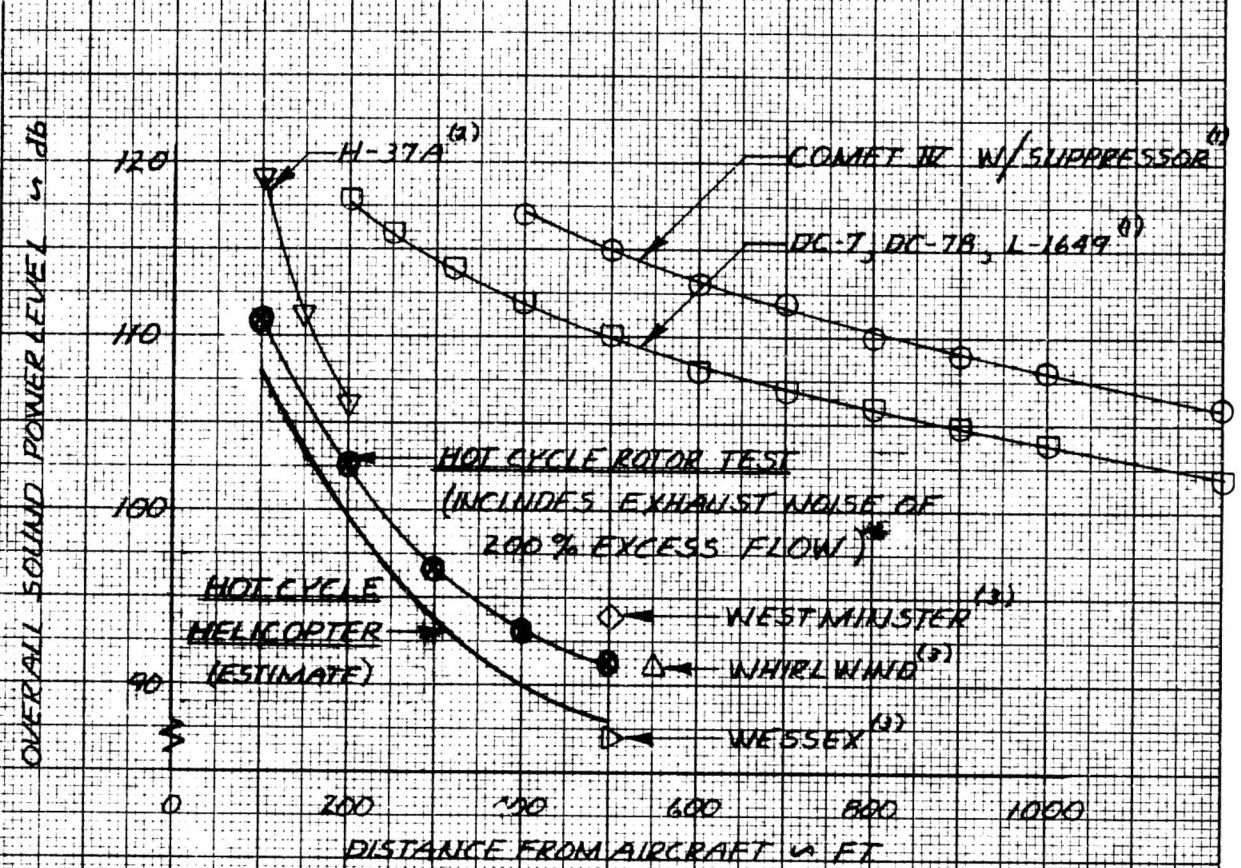
2. In an actual helicopter using the same rotor and two T64 engines, there would be no surplus exhaust flow. Thus, the sound level would be reduced by the amount contributed by the surplus flow of the J57 that is exhausted through the suppressor. Based on the observations of a number of persons with different affiliations and backgrounds, it has been estimated that somewhat more than one-half the sound output of the whirl test installation comes from the surplus exhaust. Accordingly, it has been conservatively estimated that an actual helicopter would have roughly one-half the sound power level, or three db less than measured during the whirl testing.



HUGHES TOOL COMPANY-AIRCRAFT DIVISION 285-16**REPORT NO. (62-16)****PAGE 5. 5-9****ANALYSIS** _____**MODEL** _____**PREPARED BY** _____**CHECKED BY** _____

Results of the measurements made during the whirl testing are re-plotted on Figure 5. 5-6 in the form of a comparison with other large helicopters and fixed-wing aircraft. The comparison is made for the take-off condition, and presents the over-all sound power level as a function of distance from the observer to the aircraft. It can be seen that the sound level of a hot cycle helicopter is much lower than a typical jet or piston airplane, 22 db lower than (or about 1/2 of 1 percent of) the sound power level of a DC-7. Significantly lower noise than recorded for the H-37A helicopter was also observed during the whirl testing. This measured result was verified by personal observations of individuals who observed the whirl testing and who were also experienced in H-37A operations.

FIGURE 5.5-6
NOISE COMPARISON
FOR
TAKE-OFF CONDITION



REFERENCES:

1. STUDIES OF THE NOISE CHARACTERISTICS OF THE COMET IV JET AIRLINER AND OF LARGE PROPELLER DRIVEN AIRLINERS BY BOLT, BERANEK AND NEWMAN FOR THE PORT OF NEW YORK AUTHORITY, OCTOBER 1958.
2. ARDC H-37A LIMITED STABILITY AND CONTROL EVALUATION, AFFTC-TR-60-15
3. HELICOPTER NOISE SUPPRESSION; H.B. IRVING, JOURNAL OF THE HELICOPTER ASSOCIATION OF GREAT BRITAIN, AUG 1959

TYPE	ENGINE(S)	HORSEPOWER
WESTMINSTER (S-56)	2 ELANDS	5000
WHIRLWIND (S-55)	GLIOME	1150
WESSEX (S-58)	GAZELLE	1450

* EXCESS FLOW FROM J-57 EXHAUSTED THRU SUPPRESSOR

100%
 FUELER & FERRIC CO.
 1010
 32

ANALYSIS _____

PREPARED BY _____

CHECKED BY _____

5.6 POST TEST INSPECTION

5.6.1 General

The hot cycle rotor was given an intensive major inspection three times during the whirl test program. These occurred at the end of eighteen, thirty-five and sixty cumulative hours of whirl testing. (Refer to Figures 5.6-1, 5.6-2, and 5.6-3.) The operating conditions experienced by the rotor system prior to each inspection are discussed in Section 4 of this present report.

For the purposes of the eighteen hour inspection, the rotor hub with blades attached was released from the support pylon and lifted down from the test tower. All fairings, trailing edge segments, tip cascades, cover plates and access panels were taken off. Blade root ducts were removed and the upper rotating duct was lowered out of the hub. All moving seals of the duct system and both bearings of the hub shaft were disassembled.

At the conclusion of the thirty-five hour whirl test period, the entire rotor was removed from the whirl tower to an indoor facility and torn down for inspection. Inasmuch as the inspection was in preparation for 25 hours of life-type testing, a very complete disassembly was undertaken. In addition to the parts taken off for the eighteen hour inspection all other major structural and mechanical components were removed and stripped of fittings, bearings, bushings, etc., and inspected by Magnaflux, Die Penetrant, visual or other methods, whichever was the most suitable in each case. All holes and edges of parts were carefully studied for the existence of such stress raisers as burrs and nicks.

At the conclusion of a total of 60 hours of whirl test, the entire rotor was again removed to an indoor facility. The major components were disassembled and given a thorough visual inspection.

None of the major inspections revealed any basic flaw in the hot cycle system. Of the few components replaced by new parts following inspection, not one was rejected for evidence of imminent structural failure. In general, replacements were made as conservative measures to ensure continued good mechanical performance, taking advantage of the disassembly and reassembly incidental to inspection rather than possibly incurring interruptions and delays of ensuing whirl tests. In a few instances, notably as applies to the hub duct inner seal, components were reinstalled after minor rework to improve their mechanical performance.

The discussions that follow are concerned with inspection findings of special interest. Materials problems are discussed at length in Reference 5.6. Unless stated otherwise, components were found to be in good condition and were kept in service throughout the entire 60 hours of whirl testing.

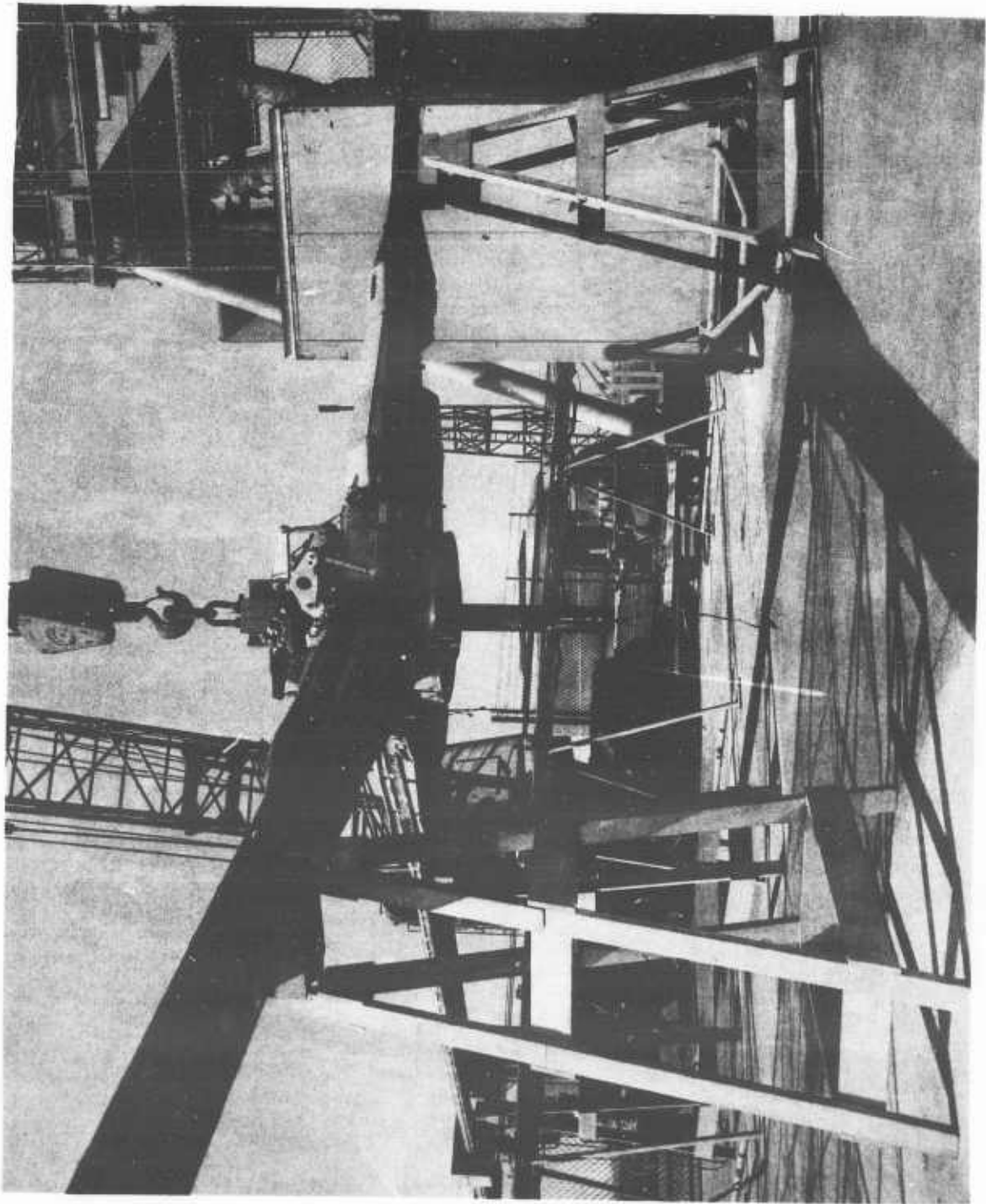


Figure 5.6-1 Rotor Removed from Tower for 18 Hour Inspection

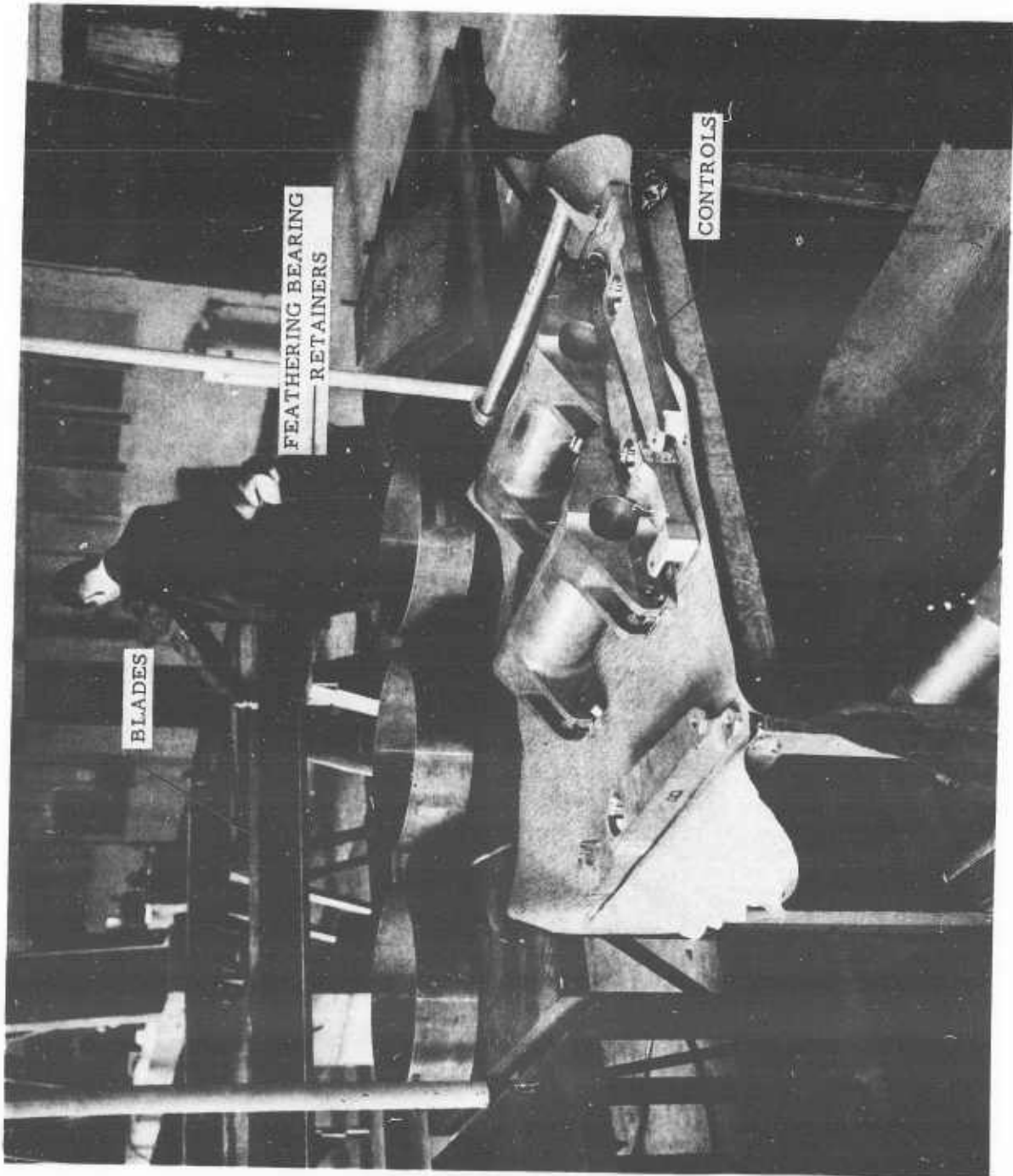


Figure 5. 6-2 Rotor Disassembled for 35 Hour Inspection

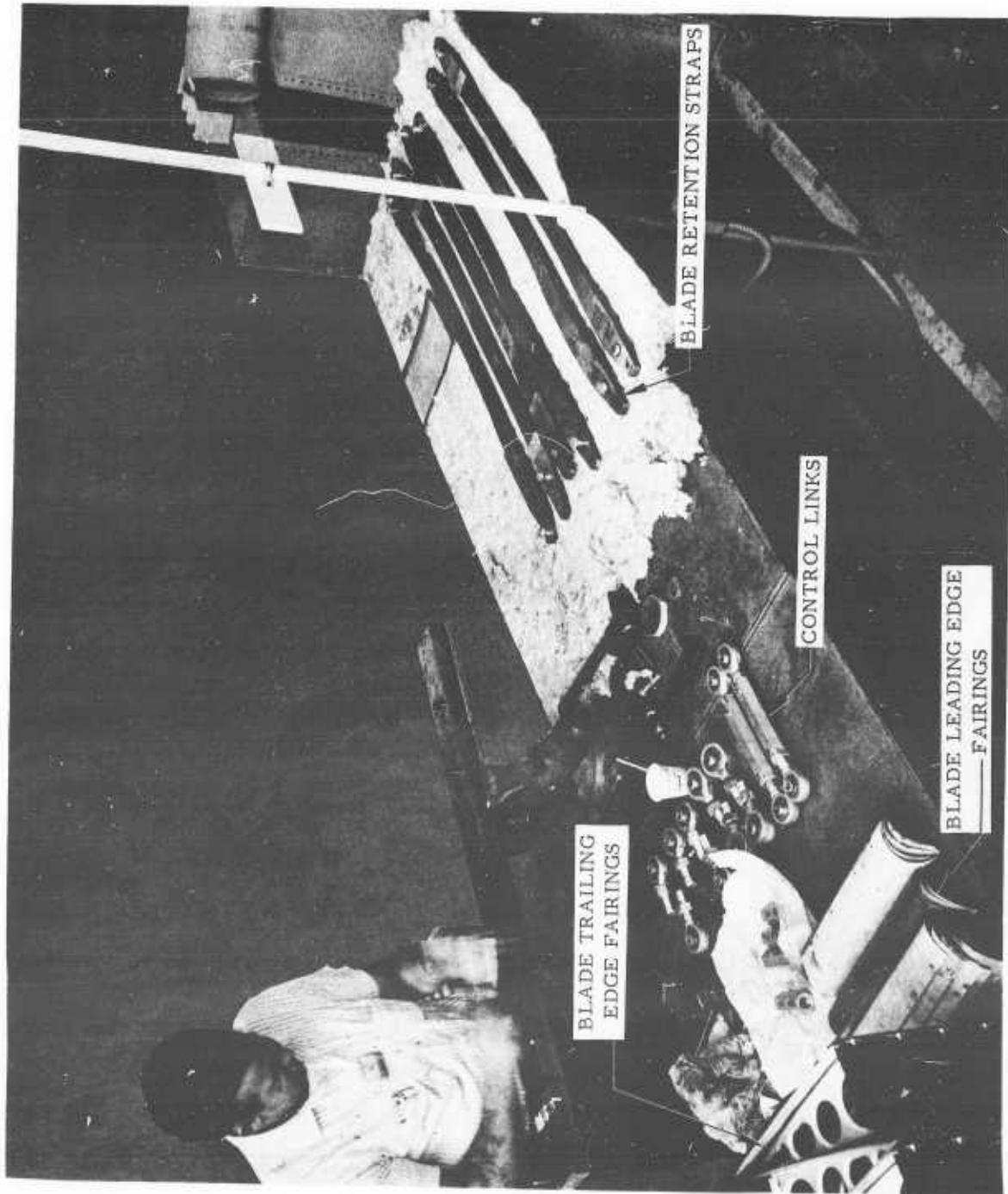


Figure 5.6-3 Rotor Disassembled for 35 Hour Inspection

ANALYSIS _____

PREPARED BY _____

CHECKED BY _____

5.6.2 Mechanical Components

5.6.2.1 Bearings

a. Thrust (Hub lower) Bearing Assembly

At eighteen hours this bearing, which reacts all lift loads, was found to be in good condition. However, circumferential marks (see Figure 5.6-4) on the black oxide surface of the hub shaft indicated the possibility of creep between the inner race and the shaft. Although there was no certainty that creep had occurred either during rotor operation or during assembly, the preload between the two Timken Bearings was reduced upon re-assembly and the clamping force across the inner races was considerably increased. In addition, a lubricant was added to the shaft in case there should be a tendency for the race to rotate on the shaft during subsequent testing.

At thirty-five hours, the thrust bearing was again found in good condition. Experience since the eighteen hour inspection had shown the reduction in bearing preload made at that time to be more than adequate. Therefore a housing shim was eliminated to produce an intermediate preload.

b. Hub Upper Bearing

This bearing takes only radial loads. All components of the bearing and oil retaining seals were found to be in excellent condition at all inspections. (Reference Figure 5.6-5)

c. Rotor Gimbal Bearings

These bearings were not accessible for direct inspection at eighteen hours; however, no roughness could be felt when the gimbal was rotated while loaded only by the weight of the shaft. At thirty-five hours, slight fretting was found in two SKF bearings which join the gimbal clevis and ring. All four SKF bearings were replaced. At 60 hours, all bearings revealed slight fretting.

d. Swash Plate Fafnir Bearings

These two ball bearings showed rust and some roughness at thirty-five hours. Although the condition was not serious, they were replaced. At 60 hours, they appeared in good condition.

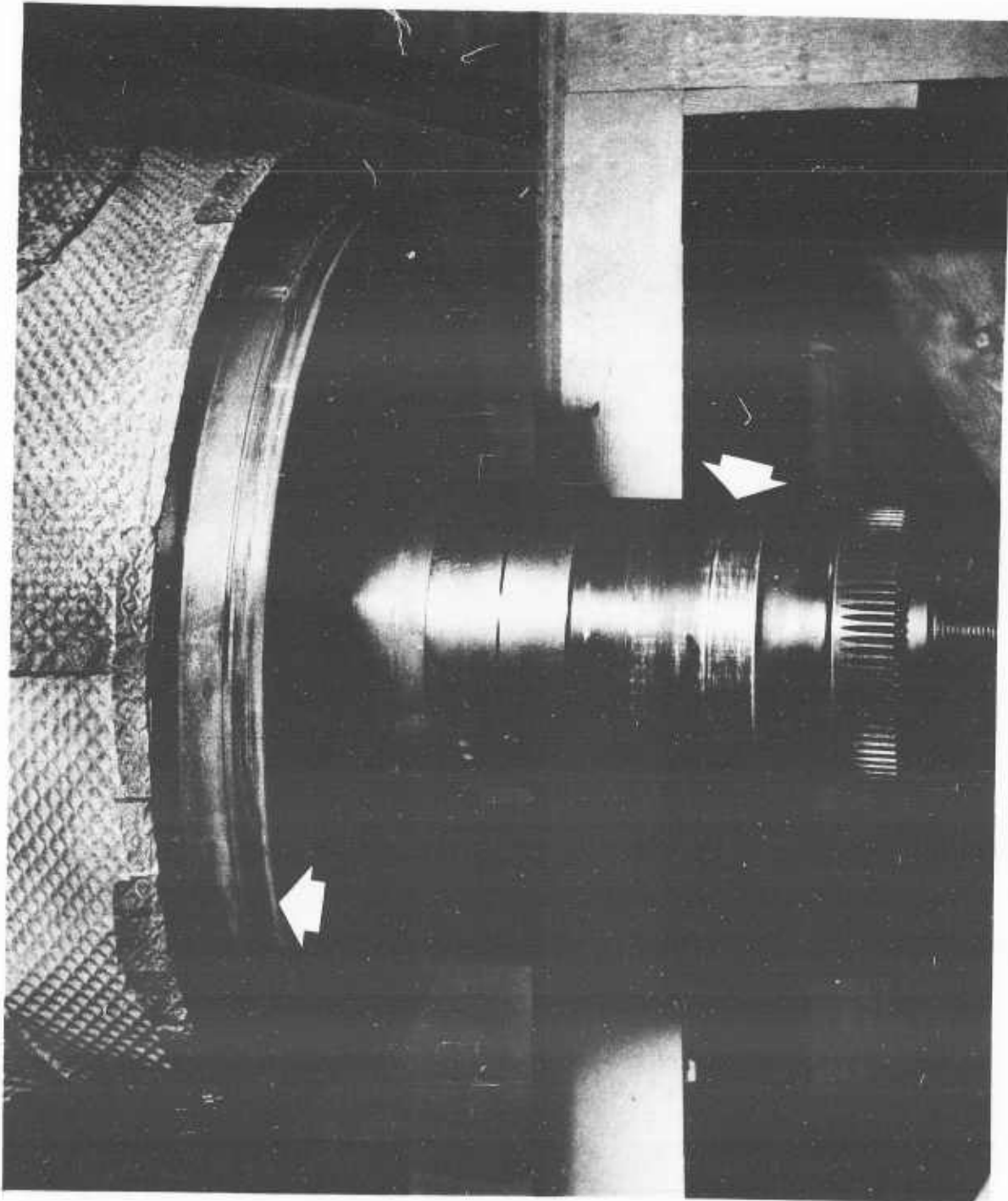


Figure 5. 6-4 Hub Lower Shaft and Duct Seal Outer Rotating Surface After 18 Hours.
Note lines on shaft at location of thrust bearing and corrosion
on lower edge of sealing surface.

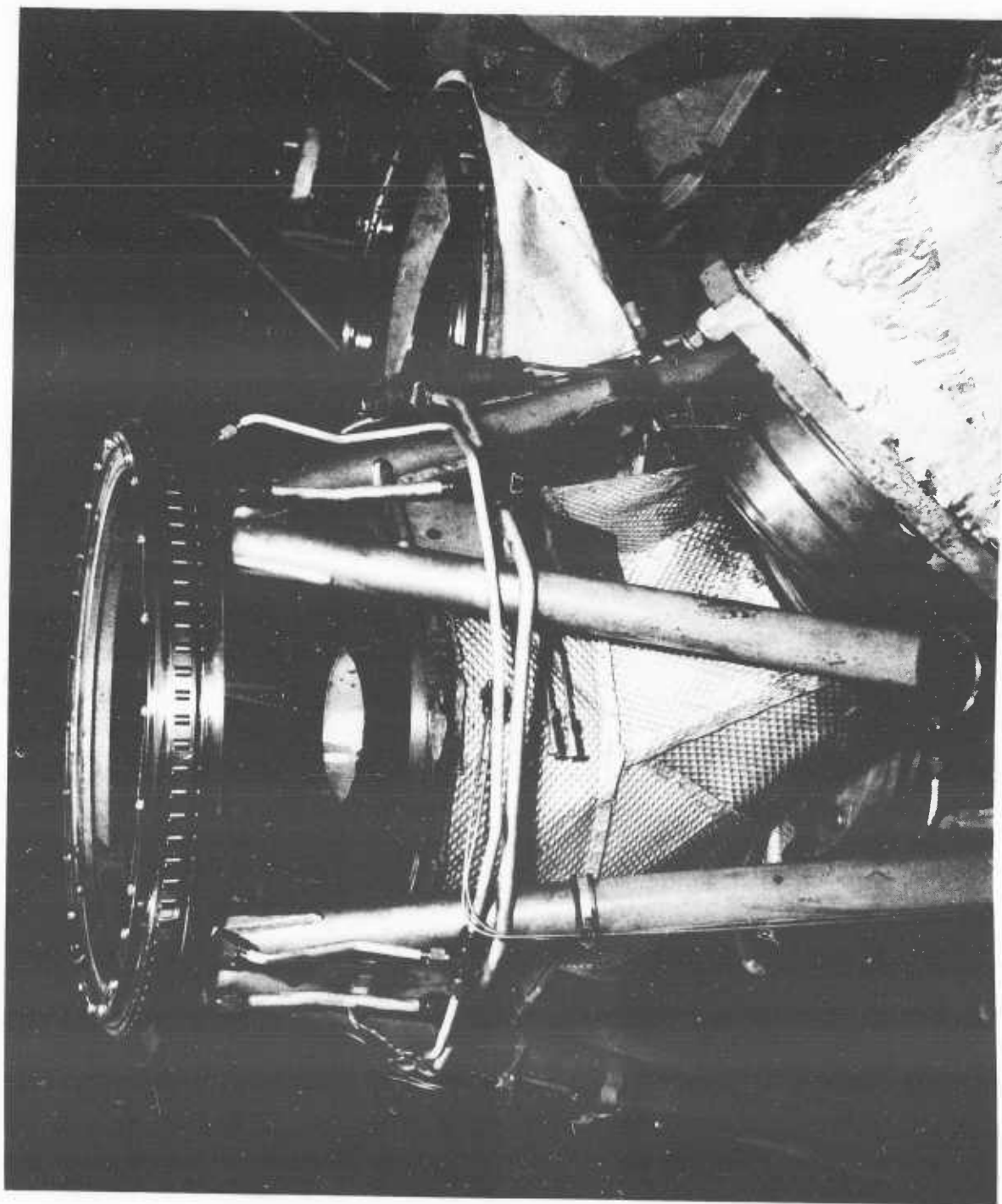


Figure 5.6-5 Hub Upper Radial Bearing and Seals Disassembled After 18 Hours.

ANALYSIS _____

PREPARED BY _____

CHECKED BY _____

e. Torque Tube Timken Bearing

At thirty-five hours a small amount of rust was found on one large Timken bearing in one of the three torque tubes. This particular bearing was replaced.

f. Rod End Bearings, Central Control Rods

At thirty-five hours all six shafer rod end bearings (in the three central control rods only) were replaced. This was done as a conservative measure because calculations indicated a relatively short service life under the design loads for the bearing in this particular location. On the other hand, although a destructive disassembly was not performed, the bearings showed no evidence of damage.

g. Feathering Bearing

This bearing consists of a chromium plated cast aluminum ball rotating within a Fabroid¹ faced ring. At eighteen hours the Fabroid surfaces were inspected by raising and lowering the blades through the maximum available clearance angles to expose the riding surfaces. These appeared to be in excellent condition with no evidence of significant wear.

At thirty-five hours the bearings were disassembled and the Fabroid wear surfaces found to be in generally good condition, as shown in Figure 5.6-6. Local areas of high contact pressure showed a general smearing of the teflon, which appears to have no effect on its load carrying ability or friction coefficient. Because two segments of one bearing had been scored in handling and two segments of another were locally unbonded, all segments of both these bearings were relined.

At eighteen hours the cast aluminum balls showed blisters of the chromium plate, apparently resulting from sub-surface corrosion. This phenomenon is discussed in detail in Reference 5.6-1. No action was taken at that time since the blisters were located outside of critical wear areas. At thirty-five hours one ball showed no blistering, one showed only a very small amount in a non-critical region, while the third had a considerable amount of blistering which approached a critical wear area. This third ball was replaced.

¹Fabroid is a teflon filament and fiberglass thread woven cloth manufactured by Microprecision Division of Micromatic Hone Company, Los Angeles 32, California

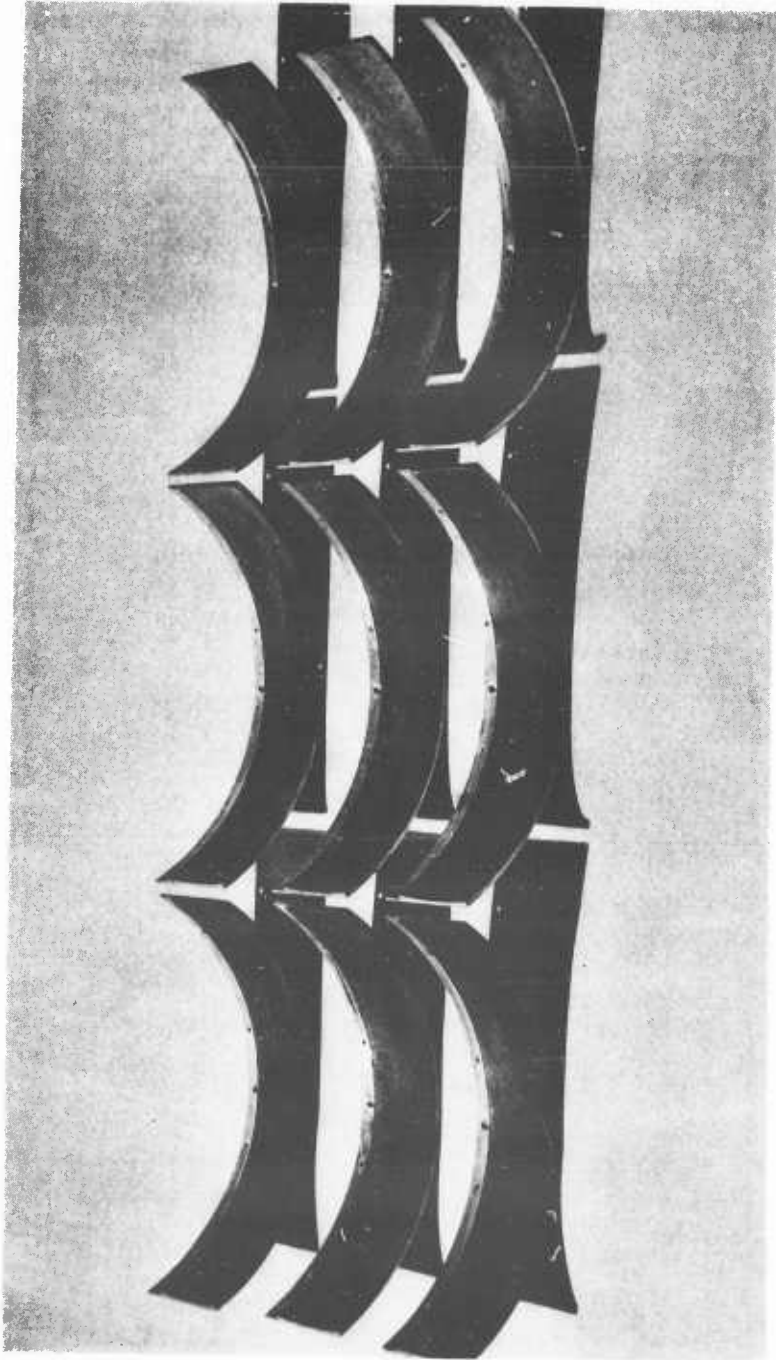


Figure 5. 6-6 Fabroid Flapping-Feathering Bearing, Showing Good Condition
After 35 Hours

ANALYSIS _____

PREPARED BY _____

CHECKED BY _____

5.6.2.2 Duct Seals

a. Hub Inner Seal (Figure 5.6-7)

This face-type seal prevents escape of gases at the inner surface of the hub stationary-to-rotating duct joint. Contact of the sealing faces is maintained by axial movement of a cylinder at the inner periphery of the stationary duct. At operating temperatures, differential expansion of this cylinder and the duct resulted in increased clearance between the two, and therefore the cylindrical portion of the seal could move freely. However, continued heating and cooling of the units produced slight warpage of the components which eliminated the small clearance originally incorporated into the parts. This interference in turn prevented axial movement and contact of the sealing faces at ambient temperatures, and thus the duct system could not be pressurized during the eighteen hour inspection. Action taken was to machine the surfaces to increase clearance.

Figure 5.6-8 shows what appears to be a slight subsurface corrosion beneath the aluminum oxide flame plate on the type 347 corrosion resistant steel base of the seal mating ring, first noted during the eighteen hour inspection. This corrosion did not become more extensive, and therefore no action was necessary.

The carbon portion of the Hub Inner Seal, after eighteen hours of test, appeared to have some local spots which were softer than the remaining material. This could be an indication of inconsistencies in the raw stock or in the impregnation, with a resultant deterioration of some of the material at the high temperatures encountered. The face of the carbon ring was surface ground to remove the soft spots.

At thirty-five hours, the inner seal showed essentially the same type of softening as had appeared at the 18 hour inspection period. Since it was believed that additional grinding would reduce the thickness of the riding element to an unacceptable dimension, a new part was installed. After 60 hours, this part was in excellent condition.

b. Hub Outer Seal (Figure 5.6-7)

This seal, which consists of two layers of carbon segments riding on a steel ring, apparently functioned with little leakage during

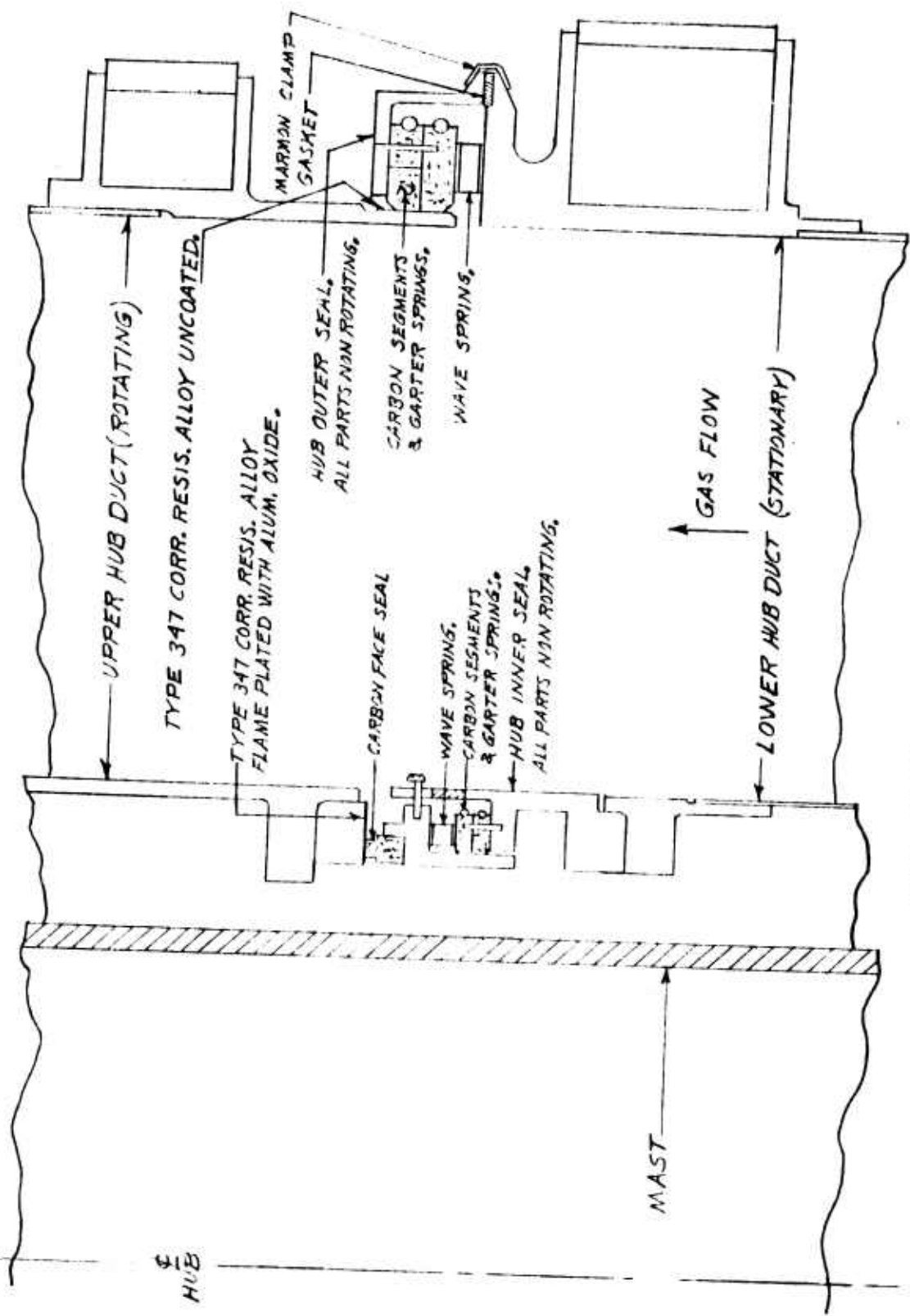


Figure 5.6-7 Hub Inner and Outer Seals



Figure 5.6-8 Hub Upper Duct and Seal Faces After 18 Hours.
Note apparent sub-surface corrosion
under aluminum oxide plating.

ANALYSIS _____

PREPARED BY _____

CHECKED BY _____

the whirl test. However, at eighteen hours the upper edge of the lower ring of carbon segments was found to be chipped evenly around the periphery (Shown in Figure 5.6-9) and both rings were replaced. Rather exhaustive investigation indicated the damage was probably done during preliminary calibration or trial assembly prior to any testing. Satisfactory performance under these conditions is evidence of the durability and practicality of the design.

At thirty-five (35) hours the seal carbon segments were in excellent condition and were retained. After sixty (60) hours, the upper ring of segments had an etched appearance, the cause of which has not yet been determined.

For ease of handling, the 24 small seal-seating coil springs were replaced by a single wave spring at the 35 hour inspection period.

The mating ring of this seal is fabricated of type 347 corrosion resistant steel. The surface actually in contact with the carbon segments was clean and smooth. However, the edge which was exposed to the hot gases and not wiped by continuous motion of the carbon had corroded severely, as shown in Figure 5.6-4. This corrosion was removed, but it is essential that on service craft more resistant materials or plating be used to prevent such corrosion.

c. Articulate Duct Inboard Seal

These seals, of carbon segments riding on type 347 corrosion resistant steel balls, were generally in good condition at all inspections. As noted above regarding the Hub Outer Seal Mating Ring, the metal balls showed definite corrosion in the area not generally wiped by the carbon. Material or a plating more resistant to corrosion will be required for longer seal life.

As noted for the hub inner seal, the carbon material used here indicated at the 18 hour period a very definite softening of some portions of the carbon segments with a resulting tendency for the edges to erode, as shown in Figure 5.6-10. Nevertheless, since these seals did not show signs of appreciable leakage, the whirl test was continued with these particular carbon segments.

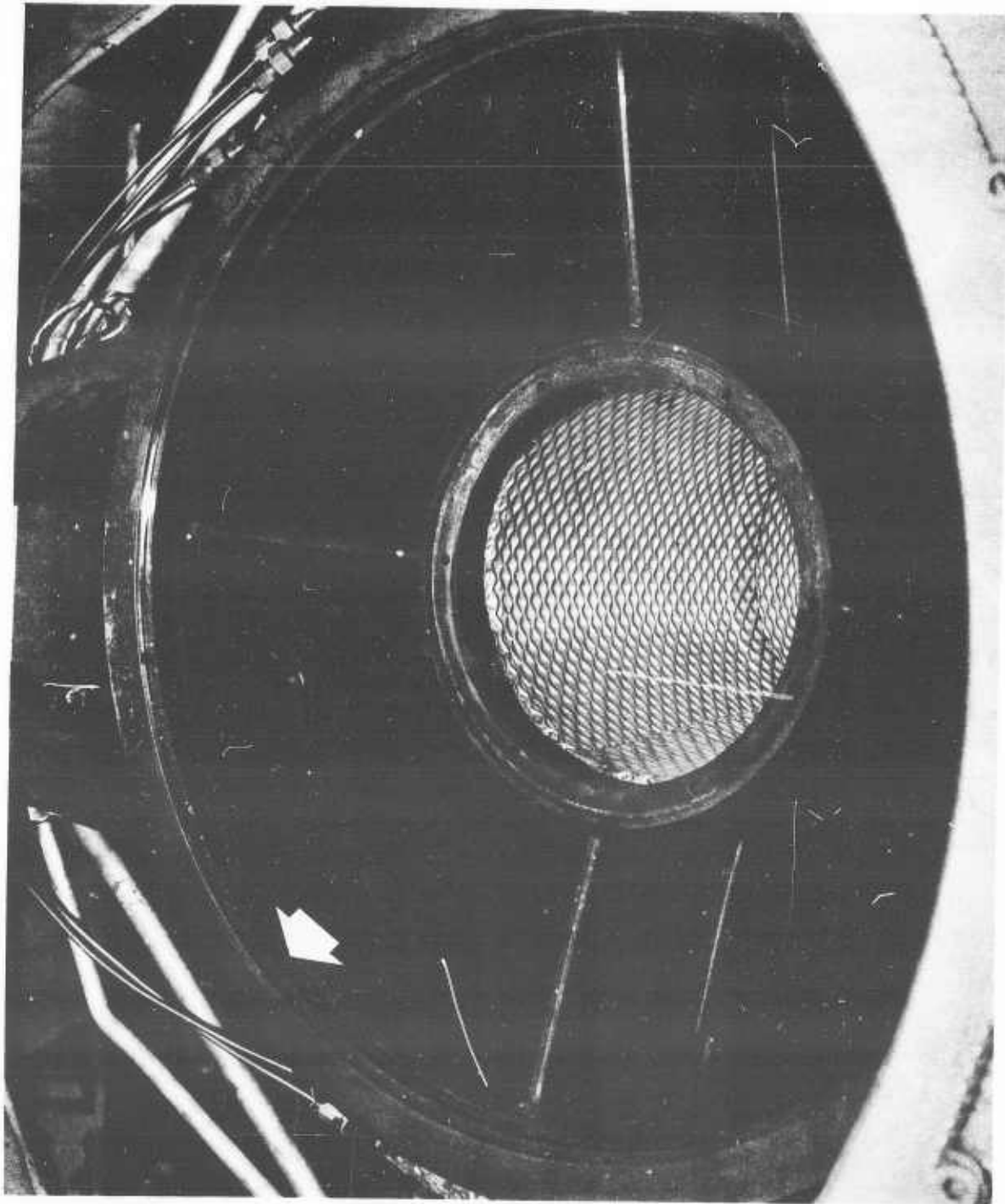


Figure 5.6-9 Hub Lower Duct with Outer Seal Segmented Rings in Position, After 18 Hours. Note uniform chipping (apparently from assembly and checkout operations) on upper edge of lower of two carbon rings.

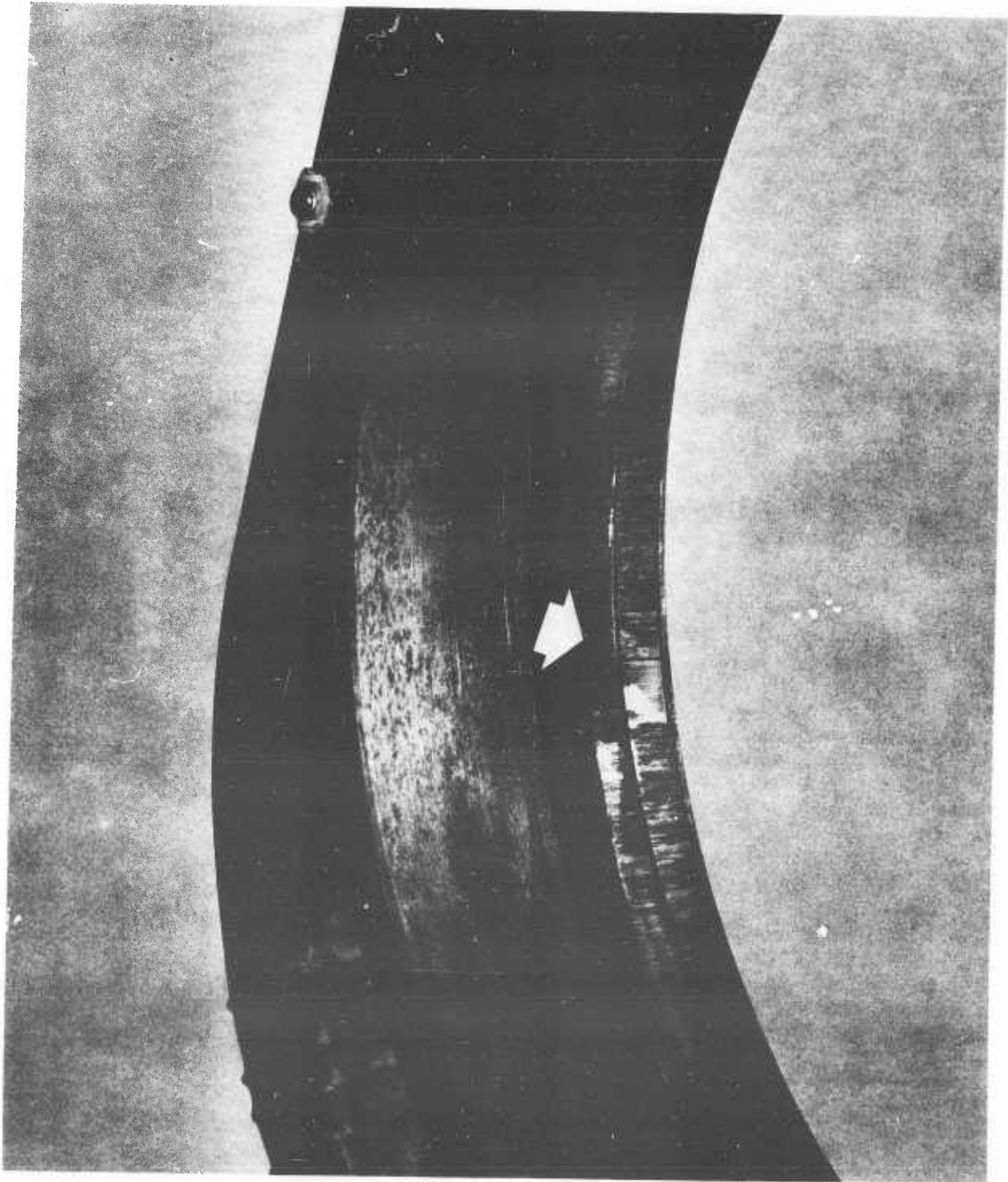


Figure 5. 6-10 Close-Up of Articulate Duct Inboard Seal Segmented Carbon Rings.
Note local softening of carbon and resulting erosion of edge.

ANALYSIS _____

PREPARED BY _____

CHECKED BY _____

At thirty-five hours their condition did not appear to have changed. Sealing performance had not deteriorated. It was decided, therefore, to continue the whirl tests with these same carbon segments. One set of carbon elements however, was inadvertently shattered in handling and was replaced by a new one. There was no significant change in any carbons at the end of sixty hours of test.

d. Articulate Duct Outboard Seal

This seal, discussed at length in Reference 5.6-2, consists of metal lips riding on a metal cylinder. The lips are fabricated of Rene' 41, while the cylinder is of type 347 corrosion resistant steel with tungsten carbide flame plate on the rubbing surface. Both surfaces were electrofilmed for lubrication.

At eighteen hours, wear on the lips of the three seals was moderate, but one of the lobes on one lip of one seal had a crack extending circumferentially 1/4 inch. As a conservative measure, a new set of lip rings was installed in all blades. At 35 hours, the metal lips of this seal again showed moderate wear, but there was no evidence of cracking. The lips were once more replaced by a new set.

The cylinders on which the lips rode were flame plated with tungsten carbide. Difficulty in maintaining roundness of the original cylinders during the fabrication process resulted in an uneven thickness of the tungsten carbide. As a result, it was believed the internal stresses due to differential thermal expansion were high. At thirty-five hours the tungsten carbide showed signs of spalling, possibly initiated by attachment of thermocouples or by other handling during the long check out periods on this particular seal, and aggravated by the thermal stresses. There was, therefore, a real possibility of extension of this spalling. In order to avoid an otherwise long delay of the whirl testing, all of the cylinders were replaced at thirty-five hours.

5.6.3 Structural Components

5.6.3.1 Hub Shaft-Spoke Assembly

Gold paint, because of its high heat reflectivity at temperatures in the 100 to 1000°F range, had been applied to the mast and upper hub support

ANALYSIS _____

PREPARED BY _____

CHECKED BY _____

spoke piece external surfaces over electroless nickel plate (See Reference 5.6-3 for a more extensive presentation.). At the eighteen hour inspection, the shaft exhibited a tendency to corrode severely, even though the spoke piece did not. Measured temperatures of the shaft and upper support, on the other hand, were well below critical values, and therefore it was decided a coating of less reflectivity could be used. For these reasons, the gold paint was removed and the surfaces coated with a high temperature aluminum paint having a substantially improved corrosion resistance.

At thirty-five hours the shaft-spoke assembly was separated for inspection, particularly in reference to the possibility of fretting and corrosion at the mating surfaces. A ring of corrosion pits was found at the outermost edges of the mating surfaces, in addition to sharp edges around the holes drilled and reamed on assembly for the retaining bolts. Both conditions were corrected, one by polishing off the corrosion area and the other by rounding off and polishing the edges of the holes. In order to facilitate separation at future inspection periods, interference fit between these two parts was reduced to zero. In addition, pitting of the lower part of the shaft due to presence of gold paint as described above, and all tool marks on the shaft were carefully polished away.

5.6.3.2 Hub Gimbal

Rotor horizontal forces, as measured in the gimbal clevises, were higher than originally estimated. Therefore, a reinforcement to the gimbal was installed at the eighteen hour inspection period to reduce the stresses resulting from these loads.

At thirty-five hours the trunnion shaft was found to have a flaw in the original hand forging from which the part was made. Although the original ultrasonic inspection and a final X-ray inspection failed to reveal this defect, it was found to penetrate from outer to inner wall. Fortunately this flaw was located in an area of reasonably low stress and therefore rework could be tolerated. In order to completely remove the flaw, a hole of approximately 1/4 inch diameter was drilled through, rounded at the edges and polished.

5.6.3.3 Swash Plate

It was noted at thirty-five hours that the stationary swash plate, which is aluminum alloy, had been brinnelled around the edges of some bolt holes. Bushings inserted in the holes left insufficient surface under the bolt head for bearing on the surface of the swash plate. The brinnelled areas were spot faced, and large diameter washers were added to increase bearing area.

ANALYSIS _____
 PREPARED BY _____
 CHECKED BY _____

5.6.3.4 Blade Spars

The spars were removed from the whirl test blades and given close scrutiny during the thirty-five hour inspection. Special attention was directed towards such potential stress raisers as burrs, sharp corners, scratches, nicks and tool marks. Upon reassembly, reinforcement plates, corresponding to that utilized on the Full Scale Fatigue Test specimen (Reference 5.6-4), were added to the rear spars at the bend point. At the end of 60 hours, careful inspection of the spar disclosed no evidence of damage.

ANALYSIS _____

MODEL _____

REPORT NO. (62-16) PAGE

PREPARED BY _____

CHECKED BY _____

SECTION 6REFERENCES

- 3.1-1 Sallows, S. E. and Plowe, O. I. ; "Hot Cycle Rotor System, Final Report, Detail Design of Rotor"; HTC-AD Report 285-12 (62-12), March 1962.
- 3.1-2 Doyle, J. T. ; "Hot Cycle Rotor System, Fabrication Effort"; HTC-AD Report 285-15 (62-15), March 1962.
- 3.1-3 Needham, J., Erle, L. and Nicholls, D. ; "Hot Cycle Rotor System, Structural Analysis"; HTC-AD Report 285-13 (62-13), March 1962.
- 3.3-1 Pratt and Whitney Aircraft; "Gas Turbine Installation Handbook, JT3 Turbojet Engines"; Volume 1, May 1956.
- 3.4-1 Pratt and Whitney Aircraft; "Specific Operation Instructions J57-P-19W; Turbojet Engine; Operation Instruction 138", July 1, 1957.
- 3.4-2 Jones, D. L. and Rabek, J. W. ; "Results of Static Test Program, Hot Cycle Rotor System, Gas Flows and Temperatures"; Hughes Tool Company, Aircraft Division Report 285-9-7 (61-79), February 1962.
- 4.1-1 Amer, K. B. ; "Hot Cycle Rotor System Anticipated Tests, Proposed Whirl Tower Program"; HTC-AD Report 285-8-3SR (62-23SR), Revised November 1961.
- 5.1-1 Jones, D. L. and Rabek, J. W. ; "Results of Static Test Program, Hot Cycle Rotor System, Gas Flows and Temperatures"; HTC-AD Report 285-9-7 (61-79), February 1962.
- 5.1-2 Hoerner, S. F. ; "Aerodynamic Drag"; Published by the Author.
- 5.1-3 Sullivan, R. J. ; "Hot Cycle Rotor System Final Report, Performance Calculation Method"; HTC-AD Report 285-20 (62-20), March 1962.

ANALYSIS _____

PREPARED BY _____

CHECKED BY _____

- 5.1-4 Keenan, J. H. and Kaye, J. ; "Gas Tables"; John Wiley and Sons, 1949.
- 5.1-5 Thompson, W. R. ; "Empirical Equations for Specific Heat", Aircraft Engineering, p. 251; August 1955.
- 5.1-6 Shapiro, Asher H. ; "The Dynamics and Thermodynamics of Compressible Fluid Flow." Volume I; The Ronald Press Company, New York 1953.
- 5.1-7 Henry, John R. ; "One-Dimensional, Compressible, Viscous Flow Relations Applicable to Flow in a Ducted Helicopter Blade"; NACA Technical Note TN3089 , December 1953.
- 5.1-8 Boswell, C. C. and Thurston, S. ; "Results of Component Test Program , Hot Cycle Rotor System, Test No. 4, Flow Distribution Studies of the Upper Static Duct"; HTC-AD Report No. 285-9-4, 30 August 1957.
- 5.1-9 Gessow, A. and Myers, G. ; "Aerodynamics of the Helicopter"; The Macmillan Company, New York, 1952.
- 5.1-10 Sullivan, R. J. ; "Hot Cycle Rotor System, Application Study", HTC-AD Report No. 285-6, February 1957.
- 5.2-1 LaForge, S. V. , "Hot Cycle Rotor System, Final Report, Rotor Dynamics"; HTC-AD Report No. 285-14 (62-14), March 1962.
- 5.3-1 E. E. Warner; "Hot Cycle Rotor System, Final Report, Thermal Analysis, Part I"; HTC-AD Report 285-10, June 1960.
- 5.3-2 HTC-AD Drawing 285-0937.
- 5.4-1 Needham, J. , Erle, L. and Nicholls, D. ; "Hot Cycle Rotor System, Structural Analysis"; HTC-AD Report No. 285-13 (62-13), March 1962.
- 5.5-1 Irving, H. B. ; "Helicopter Noise Suppression"; Journal of the Helicopter Association of Great Britain, August 1959.
- 5.6-1 French, J. C. ; "Hot Cycle Rotor System, Material and Processes"; HTC-AD Report No. 285-18 (62-18), March 1962.
- 5.6-2 Sallows, S. E. and Plowe, O. I. ; "Hot Cycle Rotor System, Final Report, Detail Design of Rotor"; HTC-AD Report No. 285-12 (62-12), March 1962.

ANALYSIS _____

MODEL _____

REPORT NO. _____

PREPARED BY _____

CHECKED BY _____

- 5.6-3 French, J. C. ; "Hot Cycle Rotor System, Materials and Processes"; HTC-AD Report No. 285-18 (62-18), March 1962.
- 5.6-4 Deveaux, G. ; "Results of Component Test Program, Hot Cycle Rotor System, Final Report"; HTC-AD Report No. 285-9-8 (62-8), March 1962.
- A.1-1 Needham, J., Erle, L. and Nicholls, D. ; "Hot Cycle Rotor System, Structural Analysis"; HTC-AD Report 285-13 (62-13), March 1962.
- A.3-1 MIL-HDBK-5; "Strength of Metal Aircraft Elements"; March 1959.

APPENDICES

- A. Whirl Tower Structural Analysis
- B. Test Log Sheets
- C. Method of Calculation; Area and Mass Weighted Parameters
- D. Thermodynamic Calculation Procedure; Non-Rotating Components
- E. Summary of Strain Gage and Thermocouple Locations
- F. Nomenclature & Computer Program Formats

APPENDIX A

WHIRL TOWER STRUCTURAL ANALYSIS

A. 1 INTRODUCTION

This section contains the structural analysis of the whirl tower used for testing the Hot Cycle Rotor System. The analysis includes both the tower structure and the duct system. Loads and pressures used are based on the design criteria given in HTC-AD Report 285-13 (Reference A. 1-1), Section 1. A sketch of the whirl tower installation is given in the figure on page 2 of this appendix.

HUGHES TOOL COMPANY-AIRCRAFT DIVISION

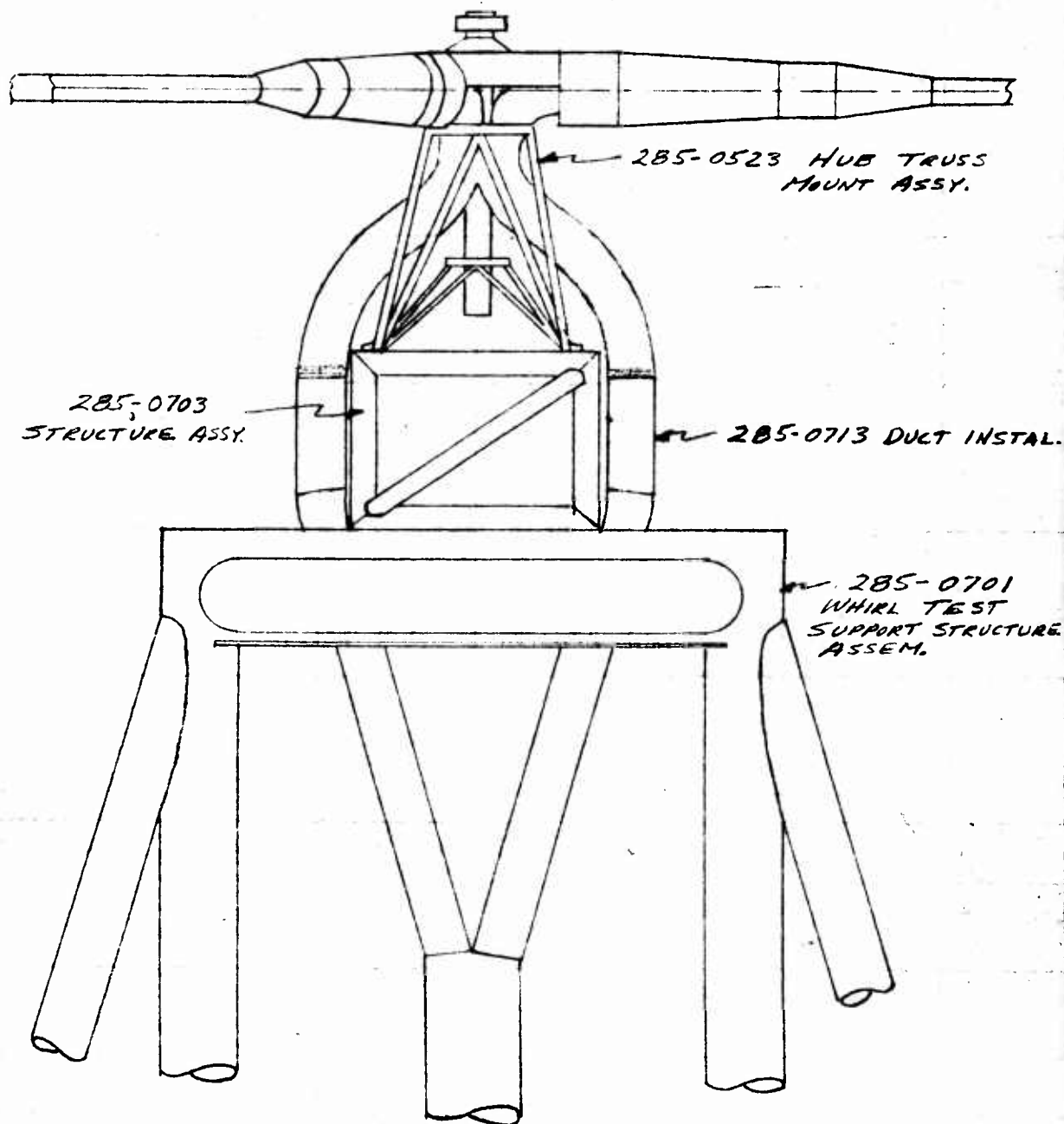
ANALYSIS HOT CYCLE
PREPARED BY G.R. SMITH
CHECKED BY _____

MODEL 285 REPORT NO. _____

PAGE A-2

WHIRL TOWER

WHIRL TOWER INSTALLATION REF DWGS. 285-0700
285-0720
285-0713
FIGURE A-1



ANALYSIS HOT CYCLE

MODEL

REPORT NO.

PAGE A.2-1

PREPARED BY C.R. SMITH

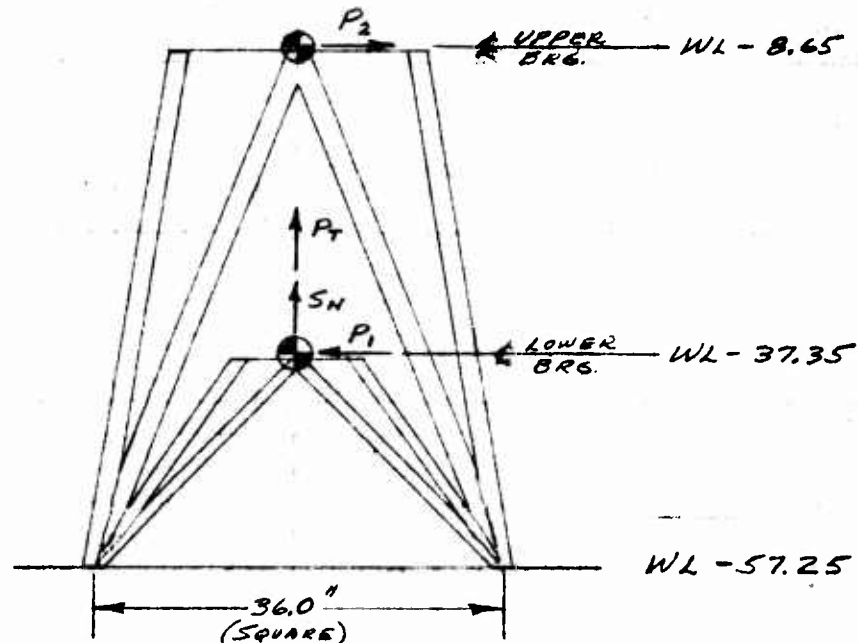
WHIRL TOWER STRUCTURE

CHECKED BY

A.2 WHIRL TOWER STRUCTURE

DESIGN LOADS

WHIRL TOWER DESIGN LOADS ARE TAKEN FROM ROTOR SYSTEM LOADS GIVEN IN SECTION 4, REF. A.1-1. LOADS USED ARE BASED ON THE MAX. FLIGHT MANEUVER CONDITION AND INCLUDE A LIMIT FACTOR OF $2\frac{1}{2}$. LOADS TRANSFERRED TO THE TOWER ARE FROM THE MAIN ROTOR SHAFT AT THE UPPER AND LOWER BEARING SUPPORTS.



LIMIT LOADS (REF. A.1-1, SECTION 4)

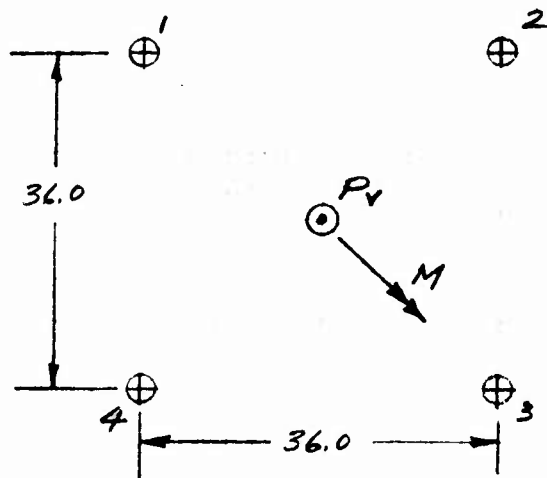
$S_N = 38,250$ LBS. = ROTOR LIFT VERTICAL COMPONENT

$P_T = 8,660$ LBS. = DUCT PRESSURE LOAD AT ROTATING SEAL

$P_2 = 9,770$ LBS. = SIDE LOAD FROM UPPER BRG. (-R_u)

$P_1 = *8,880$ LBS. = SIDE LOAD FROM LOWER BRG. (-R_l)

* INCLUDES ARBITRARY POWER TAKE-OFF LOAD. WITHOUT POWER TAKE-OFF REQUIREMENT $P_1 = 3,030$ LBS.

DESIGN LOADS (CONT'D.)
REACTIONS AT BASE OF MOUNTING TRUSS


$$P_v = 1.5 (38,250 + 8,660) = 1.5 (46,910) = 70,000 \text{ LBS. ULT.}$$

$$P_2 = 1.5 (9770) = 14,700 \text{ LBS. ULT.}$$

$$P_1 = 1.5 (3030) = 4545 \text{ LBS. ULT.}$$

$$M = 14,700 (57.25 - 8.65) - 4545 (57.25 - 37.35)$$

$$= 14,700 (48.6) - 4545 (19.9) = 624,000 \text{ IN. LBS.}$$

$$\text{DIAGONAL LENGTH} = \sqrt{2 (36.0)^2} = 51.0 \text{ IN.}$$

LOAD AT BOLT #4 IS:

$$P_T = \frac{70,000}{4} + \frac{624,000}{51} = 17,500 + 12,200 = \underline{\underline{29,700 \text{ LBS.}}}$$

HUGHES TOOL COMPANY-AIRCRAFT DIVISION

ANALYSIS HOT CYCLE ROTOR MODEL 285 REPORT NO. _____ PAGE A-2-3
 PREPARED BY C. KAYSING 4/14/60 WHIRL TOWER STRUCTURE
 CHECKED BY _____

MOUNTING TRUSS STRUCTURE

DWG. 285-0523

UPPER BANG SUPPORT SIDE LOAD:

$$P = 1.5 \times 9770 = 14700 \# \text{ U.L.T.}$$

LOWER SUPPORT:

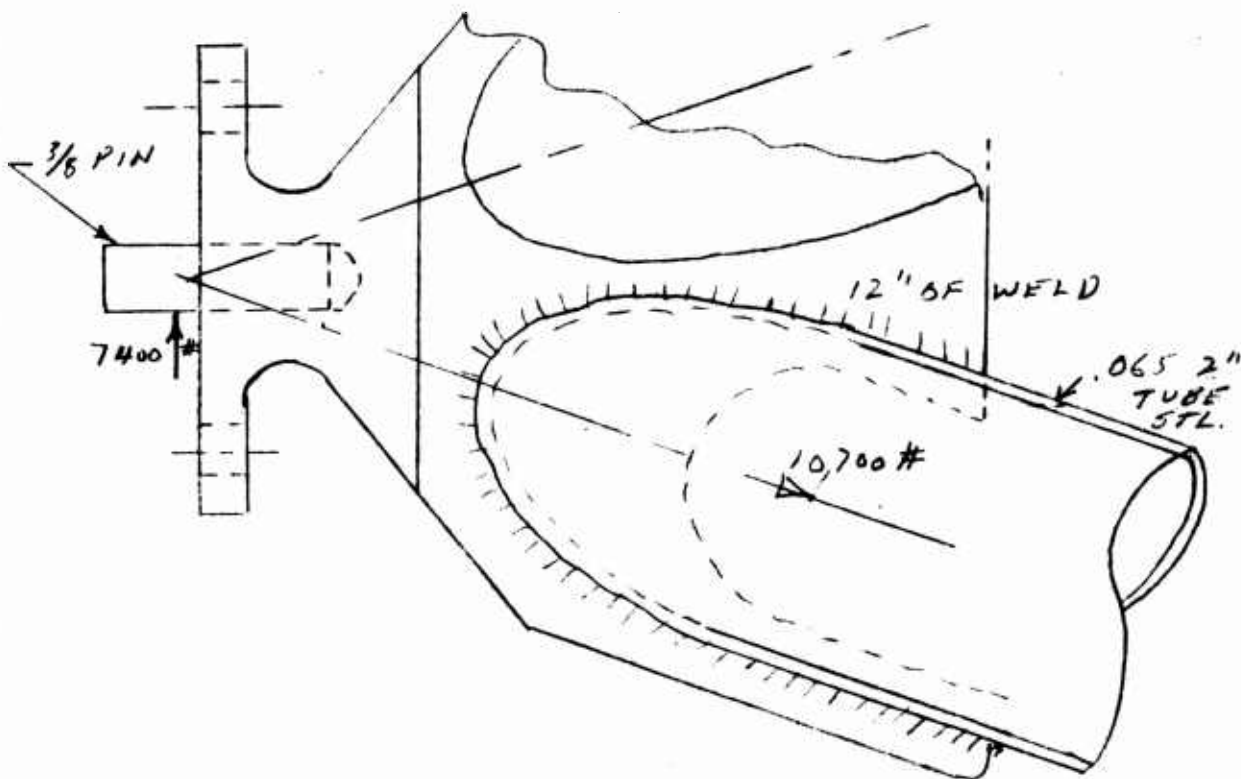
$$P_v = 1.5(38250 + 9660) = 70,000 \# \text{ U.L.T.}$$

$$P_{\text{SIDE}} = 1.5 \times 8880 = 13,300 \# \text{ U.L.T.}$$

$$= 1.5 \times 3030 = 4,545 \# \text{ U.L.T. (NEGLECTING P.T.O.)}$$

NOT USED ON
WHIRL TOWER)

UPPER SUPPORT STRUCTURE



285-0544-11 PIN

$$M.S. = \frac{10500}{7400} - 1 = \underline{\underline{.42}}$$

HUGHES TOOL COMPANY-AIRCRAFT DIVISION

ANALYSIS

HOT CYCLE ROTOR

MODEL

E85

REPORT NO.

PAGE

A.2-4

PREPARED BY

P. KAYSING

4/15/60

WHIRL TOWER STRUCTURE

CHECKED BY

MOUNTING TRUSS STRUCTURE (CONT)
#285-0523

UPPER SUPPORT STRUCTURE (CONT.)

ALLOWABLE WELD LOAD:

$$P_{ALLOW} = 12 \times .065 \times 45000 = 35000 \#$$

$$P = 10700 \#$$

$$M.S. = \frac{35000}{10700} - 1 = \underline{\underline{2.28}}$$

-11 TUBE AS COLUMN

$$D/t = \frac{2}{.065} = 31$$

$$l/p = \frac{51.8}{.685} = 75.5$$

$$A = .395 \text{ in}^2$$

$$F_{CD} = 42000 \text{ PSI}$$

$$P = 10700 \#$$

$$M.S. = \frac{42000 \times .395}{10700} - 1 = \underline{\underline{.55}}$$

HUGHES TOOL COMPANY-AIRCRAFT DIVISION

ANALYSIS HOT CYCLE ROTOR MODEL 285 REPORT NO. _____ PAGE A.2-5
 PREPARED BY C. KAYSING 4/15/60 WHEEL TOWER STRUCTURE
 CHECKED BY _____

MOUNTING TRUSS STRUCTURE (CONT)
DWG 285-0523

LOWER SUPPORT STRUCTURE

LOAD IN -9 TUBE DUE TO $P_V = 70,000 \#$

$$P_1 = \frac{70000}{8} \times \frac{28.4}{19.5} = \underline{12800 \#}$$

LOAD IN -9 TUBE DUE TO $P_{SIDE} = 13300 \#$

$$P_2 = \frac{13300}{4} \times \frac{28.4}{17.9} = \underline{5300 \#}$$

$$P_{MAX} = P_1 + P_2 = \underline{18100 \#} \text{ ULT.}$$

$$P_{ALLOW} (-9 \text{ TUBE}) = .32 \times 85000 = 27,200 \#$$

$$M.S. = \frac{27200}{18100} - 1 = \underline{\underline{.50}}$$

WELD ATTACHMENT TO DS44-5

$$P_{ALLOW} \approx 6 \times .093 \times 85000 \\ = 25600 \#$$

$$M.S. = \frac{25600}{18100} - 1 = \underline{\underline{.41}}$$

WELD ATTACHMENT TO DS44-3

10" OF WELD; OK BY COMPARISON

BOLT ATTACHMENT TO HOUSING DS24

BOLT IS $\frac{9}{16}$ HT 180000 PSI

$$M.S. = \frac{31000}{17500} - 1 = \underline{\underline{.77}}$$

BOLT ATTACHMENT TO BASE

BOLT IS $\frac{5}{8}$ HT 180000

$P_T = 29,700 \text{ LBS. ULT.}$

$$M.S. = \frac{39000}{29700} - 1 = \underline{\underline{.31}}$$

ANALYSIS HOT CYCLEMODEL 285

REPORT NO.

PAGE 2-6PREPARED BY C.R. SMITHWHIRL TOWER STRUCTURE

CHECKED BY _____

STRUCTURE ASSEMBLY 285-0703

THIS ASSEMBLY ACTS AS A SPACER AND SERVES TO TRANSFER LOADS FROM THE ROTOR MOUNTING TRUSS STRUCTURE (285-0523) AND THE MAIN TOWER STRUCTURE (285-0701). IN ADDITION IT PROVIDES THE SUPPORT FOR THE CONTROL SYSTEM ACTUATING CYLINDERS. THE ASSEMBLY IS A WELDED TRUSS STRUCTURE COMPOSED OF 5.0 INCH EXTRA STRONG STEEL PIPE AND IS SATISFACTORY BY COMPARISON TO THE 285-0523 MOUNTING TRUSS.

WHIRL TEST SUPPORT STRUCTURE 285-0701

THIS ASSEMBLY FORMS THE MAIN TOWER STRUCTURE FOR THE ROTOR SYSTEM. IT IS A WELDED ASSEMBLY COMPOSED OF LARGE STEEL TUBES, I-BEAMS AND GUSSET PLATES. THE BASE OF THE TOWER IS ATTACHED TO A 2 FOOT THICK REINFORCED CONCRETE PAD BY 68 1.0 IN. BOLTS. TOWER AND PAD ARE DESIGNED FOR RIGIDITY AND ARE NOT CRITICAL FOR ROTOR SYSTEM LOADS.

HUGHES TOOL COMPANY-AIRCRAFT DIVISION

ANALYSIS HOT CYCLE ROTOR
 PREPARED BY C. KAYSING, STR 60
 CHECKED BY _____

MODEL 285

REPORT NO.

PAGE A-2-7

WHIRL TOWER STRUCTURE

NATURAL FREQUENCY OF CONTROL TOWER

DWG 5.285-0701
 285-0700

$$\delta = \frac{\partial (\text{Strain Energy})}{\partial P} \quad (\text{Castigliano's 1st Theorem})$$

$l_1 = 259''$
 $l_2 = 280''$
 $l_3 = 107''$
 $A_1 = A_2 = 14.77''$
 $E = 29 \times 10^6$

$$\begin{aligned} \text{Str. Energy} &= \sum_0^{l_i} \int_0^{l_i} \frac{1}{2} \frac{P^2}{AE} dl \\ &= \int_0^{259} \frac{1}{2} \frac{(W_2 P)^2}{A_1 E} dl + \int_0^{280} \frac{1}{2} \frac{(W_3 P)^2}{A_2 E} dl \\ &= \left(\frac{259^3}{2 \times 10^7} + \frac{280^3}{2 \times 10^7} \right) \frac{P^2}{AE} \\ &= \frac{1720}{AE} P^2 = 3.12 \times 10^{-6} P^2 \quad (\text{IN } 285-0701) \end{aligned}$$

$$\delta = \frac{\partial (3.12 \times 10^{-6} P^2)}{\partial P} = 6.24 \times 10^{-6} P$$

$$P = 7000 \text{ LBS}$$

$$\delta = \underline{.0125''} \quad (285-0701)$$

DEFLECTION OF MOUNT ASSY. 285-0523

$A = .4''$
 $P = 900''$

$$\begin{aligned} \text{Str. Energy} &= 2 \int_0^{52} \frac{1}{2} \frac{(54.5 P)^2}{AE} dl \\ &= \frac{52^3 \times 4^2}{35.5^2 \times 1.4 \times 3 \times 10^7} \\ &= 9.3 \times 10^{-6} P^2 \end{aligned}$$

$$\delta = \frac{\partial (9.3 \times 10^{-6} P^2)}{\partial P} = 18.6 \times 10^{-6} P$$

$$\delta = 18.6 \times 10^{-6} \times 900 = \underline{.0167''}$$

HUGHES TOOL COMPANY-AIRCRAFT DIVISION

ANALYSIS HOT CYCLE ROTOR MODEL 285 REPORT NO. _____ PAGE A.2-8
 PREPARED BY C. KAYSING 5/19/60
 CHECKED BY _____

WHIRL TOWER STRUCTURE

NATURAL FREQUENCY OF TOWER (CONT'D)

$$\Sigma \delta = .0174 + .0157 = .0292''$$

$$f = 188 \delta^{-1/2} \text{ CPM}$$

$$= 188 \times .0292^{-1/2}$$

$$= \underline{\underline{1100 \text{ CPM}}}$$

HUGHES TOOL COMPANY-AIRCRAFT DIVISION

ANALYSIS HOT CYCLE MODEL 285 REPORT NO. PAGE A.3-1
 PREPARED BY C.R. SMITH
 CHECKED BY _____

WHIRL TEST
 DUCT INSTALLATION

DWG. 285-0713

A.3 WHIRL TEST DUCT INSTALLATION

THE DUCT SYSTEM SERVES TO TRANSFER THE HOT EXHAUST GASES FROM THE TURBO JET POWERPLANT TO THE ROTOR SYSTEM. THE SYSTEM IS COMPOSED OF VERTICAL DUCTING TO THE ROTOR AND HORIZONTAL DUCTING FOR OVERFLOW OF EXCESS GASES. BUTTERFLY VALVES ARE LOCATED IN BOTH THE VERTICAL AND HORIZONTAL PATHS TO ADJUST FOR OPERATING REQUIREMENTS. THE DUCT SYSTEM IS SUPPORTED FROM THE TOWER AND BELLOWES ARE PROVIDED TO ALLOW FOR DIFFERENTIAL EXPANSION.

DESIGN LOADS (REF. A.1-1, SECTION 4)

MAX. TEMPERATURES AND PRESSURES ARE:

$$t = \underline{1184}^{\circ}F \quad p = \underline{29.0} \text{ psig (LIMIT)}$$

FOLLOWING USED FOR DESIGN:

$$t = 1200^{\circ}F \quad p = 30 \text{ psig (LIMIT)}$$

$$= 60 \text{ psig (ULT.)}$$

MATERIAL PROPERTIES:

321 STAINLESS STEEL TEMP. = 1200°F

$F_{LY} = 18,000 \text{ PSI}$ — YIELD IS CRITICAL

$F_{TU} = 43,000 \text{ PSI}$

ANALYSIS HOT CYCLE

MODEL 285

REPORT NO.

PAGE A.3-2

PREPARED BY G.R. SMITH

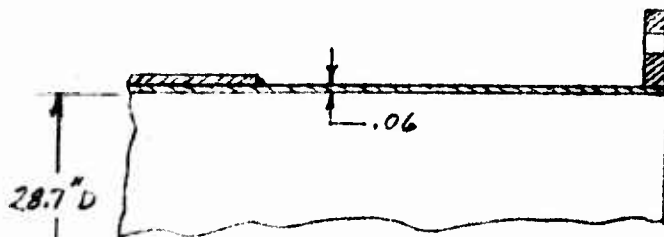
WHIRL TEST

CHECKED BY _____

DUCT INSTALLATION

ENGINE ADAPTER ASSEM.

DWG. 285-0726



MAT'L: 347 OR 321
STAINLESS STEEL

$p = 30$ PSIG LIMIT

HOOP TENSION:

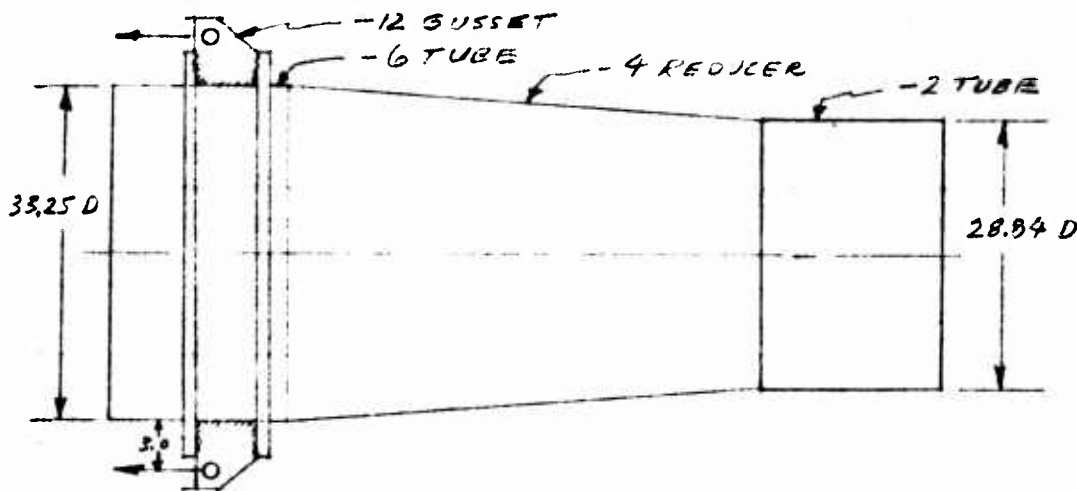
$$f_t = \frac{pD}{2t} = \frac{30(28.7)}{2(0.06)} = 7,180 \text{ PSI}$$

$F_{ty} = 18,000 \text{ PSI}$

$$M.S. = \frac{18,000}{7,180} - 1.0 = \underline{1.50}$$

ENGINE EXHAUST DUCT ASSEM.

DWG. 285-0727



MAT'L ALL PARTS 321 STAINLESS STEEL

LOADS: $p = 30$ PSIG LIMIT = 60 PSIG UAT.

- 6 TUBE

$$\text{HOOP TENSION } f_t = \frac{pD}{2t} = \frac{30(33.25)}{2(0.06)} = 8,300 \text{ PSI}$$

$F_{ty} = 18,000 \text{ PSI}$

$$M.S. = \frac{18,000}{8,300} - 1.0 = \underline{1.17}$$

HUGHES TOOL COMPANY-AIRCRAFT DIVISION

ANALYSIS HOT CYCLE MODEL 285 REPORT NO. PAGE A.3-3
 PREPARED BY C.R. SMITH WHIRL TEST
 CHECKED BY _____ DUCT INSTALLATION

ENGINE ADAPTER ASSEM. (CONT'D)

END LOAD ON ASSEMBLY IS:

$$P = \frac{\pi}{4} (33.25^2 - 28.84^2) 60 = 12,700 \text{ LBS. ULT.}$$

-12 GUSSET

BOLT ATTACH: 2 $\frac{3}{4}$ IN. AN BOLTS

$$\text{LOAD/BOLT} = \frac{12,700}{2} = 6,350 \text{ LBS.}$$

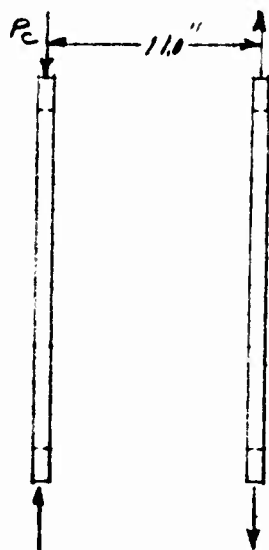
BOLTS OK BY INSPECTION

ATTACH -12 GUSSET TO TUBE:

WELD LENGTH = 10.5 IN. PER SIDE

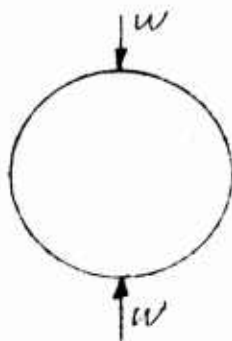
$$q_s = \frac{6,350}{2(10.5)} = 302 \text{ LBS./IN. } \quad \underline{\text{NOT CRITICAL}}$$

-10 RINGS 4130 STEEL PLATE - NORMALIZED



$$P_c = \frac{3.0(6350)}{11.0} = 1730 \text{ LBS. ULT.} \\ = 865 \text{ LBS. LIMIT}$$

RING MEDIAN DIA. = 36.0 IN.



$$M_{\text{MAX.}} = .3183 WR$$

(REF. A.3-1, TABLE VIII, CASE 1)

$$M = .3183(1730)18 = 9900 \text{ IN. LBS. (LIMIT)}$$

RING SECTION IS .50 x 2.00

$$f_b = \frac{9900(6)}{.5(2.0)^2} = 29,700 \text{ PSI LIMIT}$$

EST. TEMP. = 800 °F

$$F_{TU} = .75(95,000) = 71,000 \text{ PSI (REF. 32-3) } M.S. = \frac{71,000}{29,700} - 1.0 = \underline{1.40}$$

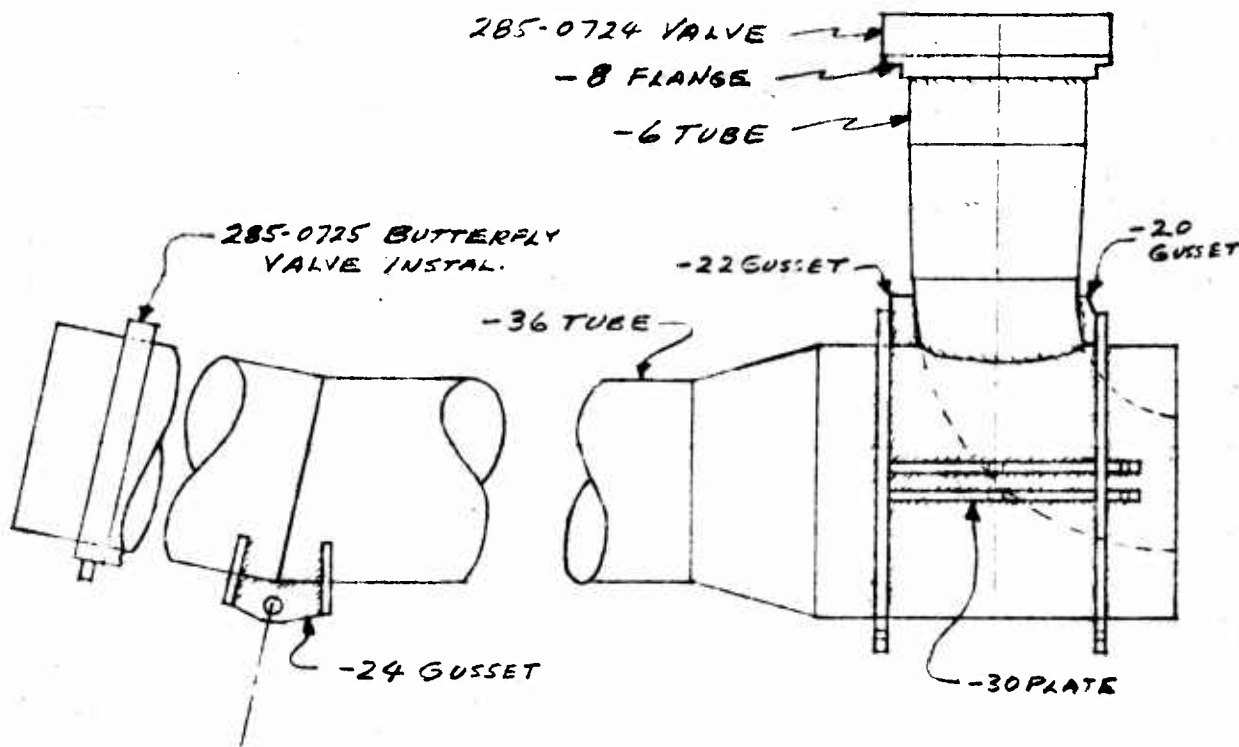
ANALYSIS HOT CYCLE
 PREPARED BY C.R. SMITH
 CHECKED BY _____

MODEL 285 REPORT NO. _____

PAGE A.3-4

WHIRL TEST
DUCT INSTALLATION

EXHAUST DIVERTER ASSEM. DWG. 285-072B



DISCUSSION

ADJUSTMENT OF THE 285-0725 VALVE IN THE OVERFLOW DUCT AND THE 285-0724 VALVE IN THE VERTICAL DUCT DETERMINES THE GAS FLOW. FOR DESIGN THE FOLLOWING LOAD CONDITIONS ARE CONSIDERED:

1. VALVE IN VERTICAL DUCT CLOSED ..

$$p = 30 \text{ PSIG LIMIT} = 60 \text{ PSIG ULT.}$$

$$t = 1200^\circ \text{F}$$

2. VALVE IN EXHAUST (HORIZONTAL) DUCT CLOSED

$$p = 30 \text{ PSIG LIMIT} = 60 \text{ PSIG ULT.}$$

$$t = 1200^\circ \text{F}$$

HUGHES TOOL COMPANY-AIRCRAFT DIVISION

ANALYSIS HOT CYCLE

MODEL 285

REPORT NO.

PAGE A-3-5

PREPARED BY C.R. SMITH

WHIRL TEST

CHECKED BY _____

DUCT INSTALLATION

EXHAUST DIVERTER ASSEM (CONT'D.)

ALL DUCTING IS LESS CRITICAL THAN THE 285-0727 DUCT ASSEMBLY BECAUSE OF MUCH GREATER WALL THICKNESS.

-20 & -22 GUSSETS

GUSSETS ARE ASSUMED TO TRANSFER THE TOTAL VERTICAL LOAD WHEN THE 285-0724 BUTTERFLY VALVE IS CLOSED.

$$A = \frac{\pi (18.0)^2}{4} = 255 \text{ IN.}^2 \quad (-2 \text{ ELBOW})$$

$$\text{END LOAD} = 255 (30) = 7650 \text{ LBS. LIMIT}$$

WELD OF GUSSETS TO -12 RINGS :

$$\text{WELD } A = 7.0 (1.0) = 7.0 \text{ IN.}^2$$

NOT CRITICAL

-30 PLATES

THESE PLATES, TWO PER SIDE, ATTACH TO THE MAIN TOWER STRUCTURE THRU TUBE TRUSSES AND SERVE TO TRANSFER END LOADS BUILT UP WHEN THE 285-0725 VALVE IS CLOSED.

END LOAD CONSERVATIVELY BASED ON 34" DIA. OF -32 TUBE

$$A = \frac{\pi (34)^2}{4} = 910 \text{ IN.}^2$$

$$P = 910 (60) = 54,500 \text{ LBS. U.L.T.}$$

WELD OF PLATES TO -32 TUBE NOT CRITICAL

FOR 2 1.0 INCH BOLTS IN DOUBLE SHEAR.

$$P_{ALLOW} = 27,489 (4) = 110,000 \text{ LBS.}$$

$$M.S. = \frac{110,000}{54,500} - 1.0 = \underline{\underline{1.02}}$$

ANALYSIS HOT CYCLE

MODEL 285

REPORT NO.

PAGE A.3-6

PREPARED BY C.R. SMITH

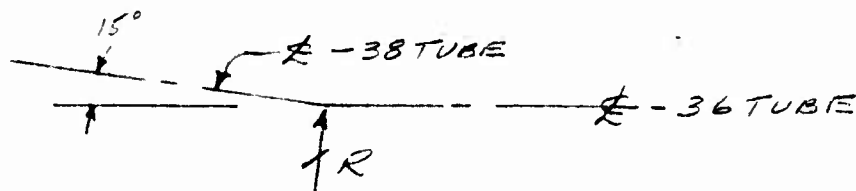
WHIRL TEST

CHECKED BY _____

DUCT INSTALLATION

EXHAUST DIVERTER ASSEM. (CONT'D)

ATTACH AT -24 GUSSET



$$\text{DUCT AREA} = \frac{\pi}{4} (26)^2 = 530 \text{ IN.}^2$$

$$P = 530 (60) = 32,000 \text{ LBS. ULT}$$

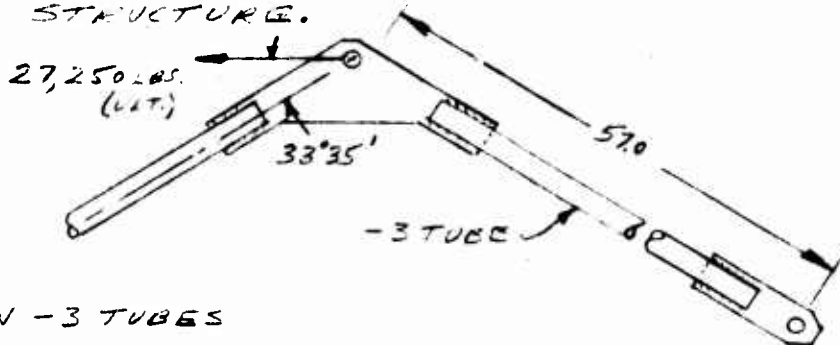
$$R = 32,000 (\sin 7.5^\circ)(2) = 8400 \text{ LBS ULT.}$$

GUSSET IS 1.0 IN. STEEL PLATE AND BOLT IS 1.0 IN. DIA.

OK BY INSPECTION

DIVERTER DUCT BRACE DWG. 285-0744

BRACE ATTACHES TO THE 285-0728-30 PLATES AND TRANSFERS THE END LOAD TO THE TOWER STRUCTURE.



LOAD IN -3 TUBES

$$P_c = P_t = \frac{27,250}{2 (\cos 33^\circ 35')} = 16,400 \text{ LBS.}$$

$$A = .799 \quad \rho = .62$$

$$\frac{L}{\rho} = \frac{57.0}{.62} = 92$$

$$f = \frac{16,400}{.799} = 20,500 \text{ PSI}$$

$$F_c = 26,000 \text{ PSI (REF. 3.2-3)}$$

$$M.S. = \frac{26,000}{20,500} - 1.0 = \underline{\underline{.27}}$$

HUGHES TOOL COMPANY-AIRCRAFT DIVISION

ANALYSIS HOT CYCLE

MODEL 285

REPORT NO.

PAGE A.3-7

PREPARED BY G.R. SMITH

WHIRL TEST

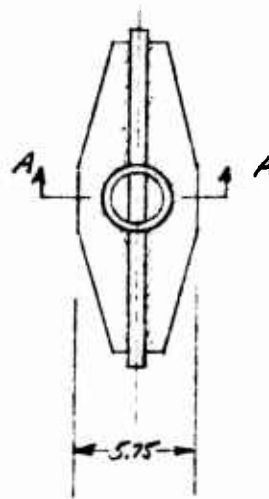
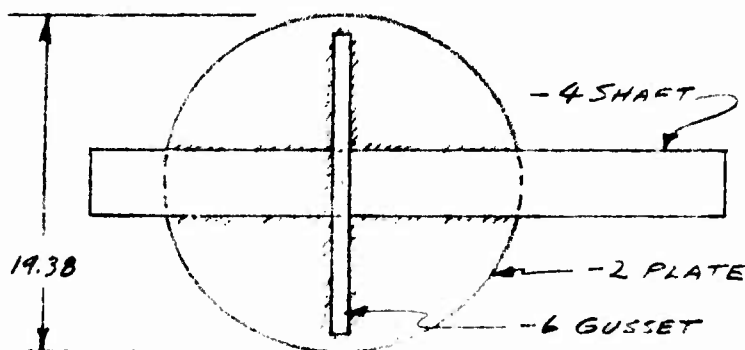
CHECKED BY _____

DUCT INSTALLATION

EXHAUST DIVERTER ASSEM. (CONT'D.)

ROTOR CONTROL BUTTERFLY ASSEM.

285-0724



MATL: 321 STAINLESS STEEL

-6 GUSSET $t = .75$ IN.

PRESSURE = 30 PSIG LIMIT

$$\text{AREA (SEMI-CIRCLE)} = \frac{\pi (9.7)^2}{2} = 148 \text{ IN.}^2$$

$$\text{LOAD} = 148 (30) = 4450 \text{ LBS.}$$

$$M_{A-A} = 4450 (.424) (9.7) = 18,300 \text{ IN. LBS. (LIMIT)}$$

$$f \approx \frac{18,300 (6)}{.75 (5.75)^2} = 4420 \text{ PSI}$$

M.S. HIGH

-4 SHAFT 4.0" O.D. x .25 WALL TUBE

$$M_{\text{MAX}} \approx 4450 (1.00 - .424) 10 = 25,600 \text{ IN. LBS. (LIMIT)}$$

$$I_{\text{SHAFT}} = 5.20 \text{ IN.}^4$$

$$f_b = \frac{25,600 (2.0)}{5.20} = 9900 \text{ PSI}$$

$$F_{TY} = 18,000 \text{ PSI}$$

$$M.S. = \frac{18,000}{9900} - 1.0 = \underline{\underline{.82}}$$

-2 PLATE NOT CRITICAL

ANALYSIS HOT CYCLE
 PREPARED BY C.R. SMITH
 CHECKED BY _____

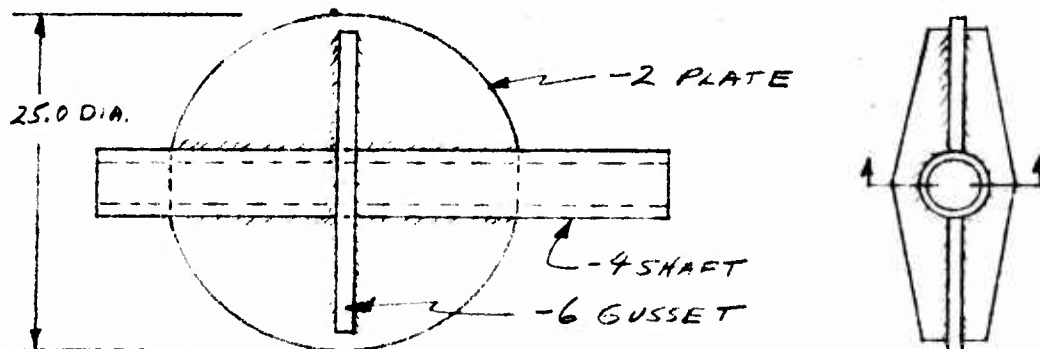
MODEL 285 REPORT NO. _____

PAGE A.3-8

WHIRL TEST
DUCT INSTALLATION

EXHAUST DIVERTER ASSEM. (CONT'D)

EXHAUST CONTROL BUTTERFLY ASSEM. 285-0725



MAT'L: 4130 STEEL - NORMALIZED

$$\left. \begin{aligned} \text{AT } t=1000^{\circ}\text{F} \quad F_{tU} &= .50(90,000) = 45,000 \text{ PSI} \\ F_{tY} &= .35(70,000) = 24,500 \text{ PSI} \end{aligned} \right\} \text{REF}$$

-6 GUSSET $t = 1.00 \text{ IN.}$ $p = 60 \text{ PSI/6 ULT.}$

$$\text{AREA (SEMI-CIRCLE)} = \frac{\pi}{2} (12.5)^2 = 245 \text{ IN.}^2$$

$$\text{LOAD} = 60(245) = 14,700 \text{ LBS. ULT.}$$

$$M_{A-A} = 14,700(.424)(12.5) = 78,000 \text{ IN. LBS.}$$

$$f_b = \frac{78,000(6)}{1.0(7.0)^2} = 9550 \text{ PSI}$$

M.S. = HIGH

-4 SHAFT 4.0 X .625 WALL

$$M_{MAX} = 14,700(1.0 - .424)(12.5) = 106,000 \text{ IN. LBS.}$$

$$I = 9.8 \text{ IN.}^4$$

$$f_b = \frac{106,000(2.0)}{9.8} = 21,600 \text{ PSI}$$

$$F_{tU} = 45,000 \text{ PSI}$$

$$M.S. = \frac{45,000}{21,600} - 1.0 = \underline{1.08}$$

HUGHES TOOL COMPANY-AIRCRAFT DIVISION

ANALYSIS HOT CYCLE
 PREPARED BY C.R. SMITH
 CHECKED BY _____

MODEL 285 REPORT NO. _____

PAGE A.3-9

WHIRL TEST
DUCT INSTALLATION

VERTICAL DUCT ASSEM.

285-0723

THE VERTICAL DUCT ASSEMBLY IS ATTACHED TO THE TOWER STRUCTURE AT POINTS "A" AND "B". BELLOWS AT THE ENDS OF THE -10 PIPE ALLOW FOR EXPANSION.

-10 PIPE

THIS CENTER DUCT IS SUPPORTED AT POINT "B" AND IS LOADED BY PRESSURE AND ITS OWN WEIGHT.

PIPE IS $12.5 \times \frac{3}{8}$ WALL APPROX. AND IS NOT CRITICAL FOR PRESSURE LOADS

$$AREA = \pi (12.5)(.375) = 14.7 \text{ IN.}^2/\text{IN.}$$

$$W = 14.7 (.29)(160) = 680 \text{ LBS.}$$

ATTACH AT "B" - 2 1.0 INCH BOLTS - NOT CRITICAL

BELLOWS (STAINLESS STEEL)

BELLOWS MAX. DIA. = 15.8 IN.
 THICKNESS = .062

HOOP TENSION:

$$p = 30 \text{ PSIG. LIMIT}$$

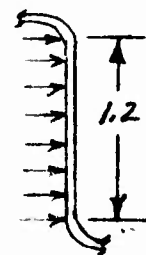
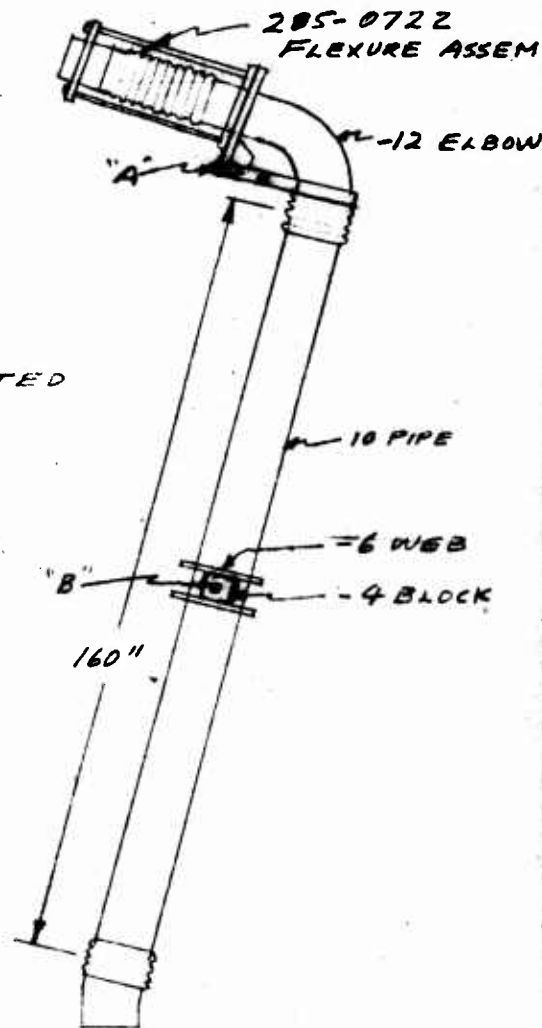
$$f_t = \frac{30 (15.8)}{2 (.062)} = 3820 \text{ PSI}$$

BENDING OF FLATS:

$$M_{MAX} = \frac{wl^2}{12} = \frac{30 (1.2)^2}{12} = 3.6 \text{ IN. LB. LIMIT}$$

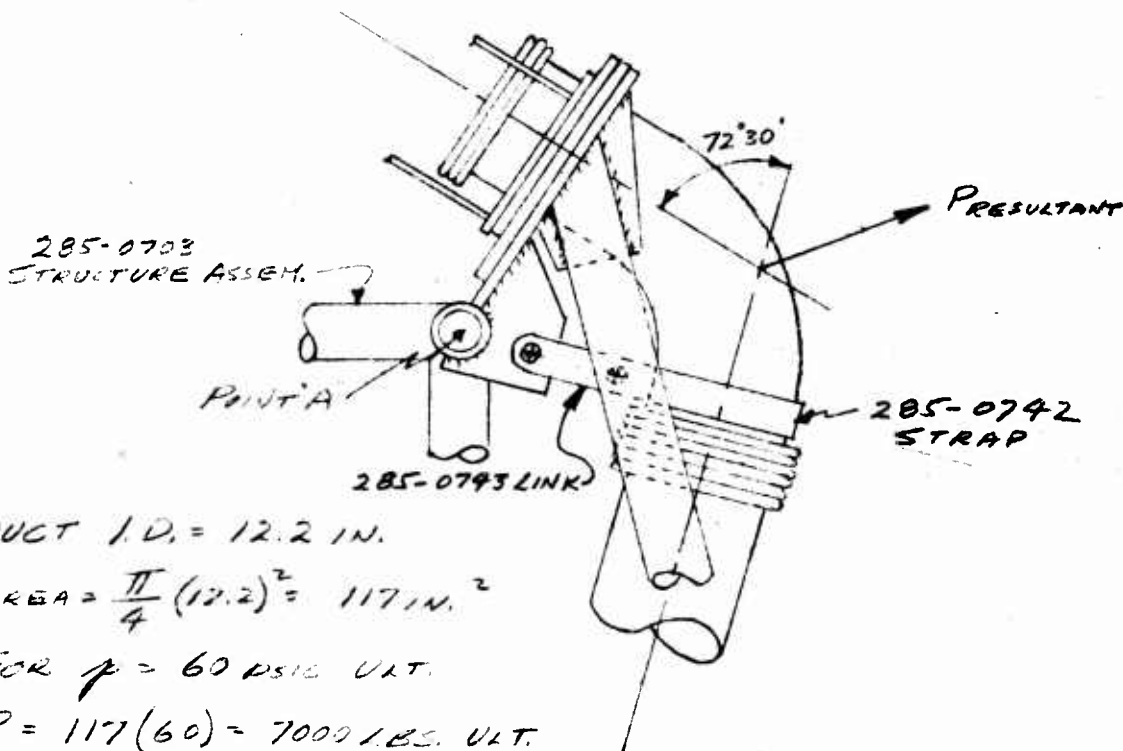
$$f_b = \frac{3.6 (6)}{(.062)^2} = 5600 \text{ PSI}$$

M.S. HIGH



VERTICAL DUCT ASSEM.

ATTACH AT POINT "A"



DUCT I.D. = 12.2 IN.

AREA = $\frac{\pi}{4} (12.2)^2 = 117 \text{ IN.}^2$

FOR $p = 60 \text{ PSIG ULT.}$

$P = 117(60) = 7000 \text{ LBS. ULT.}$

$P_{RES.} = 7000(2)(\cos 53.75^\circ) = 10,100 \text{ LBS.}$

285-0742 STRAP (COMM. STEEL)

$P_T = 11,500 \text{ LBS. ULT. (BY GRAPHICAL ANAL.)}$

$A_{SIDE} = .50(1.50) = .75 \text{ IN.}^2$

$f_t = \frac{11,500}{.75} = 15,400 \text{ PSI}$

ATTACH BOLTS ARE 1.0 DIA. AND NOT CRITICAL

ASSUME $F_{TU}(\text{STRAP}) = 50\% F_{T0}(\text{ROOM T}) = 27,500 \text{ PSI}$

$M.S. = \frac{27,500}{15,400} - 1.0 = \underline{\underline{.78}}$

285-0743 LINK - LESS CRITICAL THAN STRAP.

ANALYSIS HOT CYCLE

MODEL 285

REPORT NO.

PAGE A.3-11

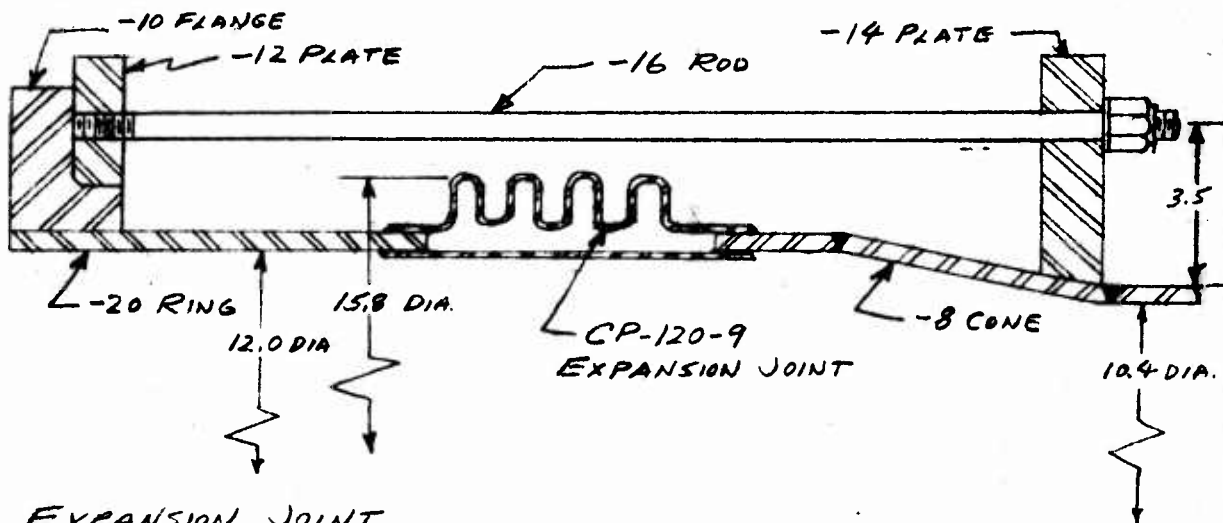
PREPARED BY C.R. SMITH

WHIRL TEST
DUCT INSTALLATION

CHECKED BY

VERTICAL DUCT ASSEM. (CONT'D)

285-0722 FLEXURE ASSEM.



EXPANSION JOINT

SATISFACTORY BY COMPARISON TO 285-0723 BELLOWS
CHECKED ON PREVIOUS PAGE.

-16 RODS

$$A = \frac{\pi}{4} (15.8^2 - 10.4^2) = 142 \text{ IN.}^2, \quad f = 60 \text{ PSI ULT.}$$

$$P = 142 (60) = 8500 \text{ LBS. ULT.}$$

LOAD IS TAKEN BY 3 -16 RODS ($\frac{1}{2}$ " DIA.)

- OK BY INSPECTION

ATTACH -12 PLATE TO -10 FLANGE

$$\text{WELD SHEAR AREA} \approx 3.0 (.25) = .75 \text{ IN.}^2$$

$$\text{LOAD/PLATE} = \frac{8500}{3.0} = 2830 \text{ LBS. ULT.}$$

$$f = \frac{2830}{.75} = 3800 \text{ PSI}$$

M.S. = HIGH

HUGHES TOOL COMPANY-AIRCRAFT DIVISION

ANALYSIS _____ MODEL _____ REPORT NO. _____ PAGE B. 1
PREPARED BY _____
CHECKED BY _____

APPENDIX B TEST LOG SHEETS

B. 1 INTRODUCTION

Included herein are the 44 engine log sheets bearing the signatures of USAF witnesses; a summary of the whirl operation following the 35 hour tear-down inspection; and turbine discharge temperature as a function of time as plotted by a continuous recorder for the most severe transient runs. The latter plots are read with time beginning at the bottom of the page. The space between each horizontal line corresponds to 15 seconds. Each transient is identified by number and date so that corresponding engine data can be read from the engine log sheets.

WHIRL TEST - J57-PW-19W
ENGINE DATA SHEET.

CALIBRATION										CHECK OUT									
DATE	RUN NO.	T ₀ OF	P ₀ IN/IN ²	N ₁ %	N ₂ %	P _{T₁} PSIG	T _{T₁} °C	W _F LBS/HR	P _{oil} PSIG	T _{oil} °C	TIME	TOTAL TIME	REMARKS						
5-17-61	1	-	-	≈10	≈25	-	-	-	-	-	11:00	1	MOTORED 4 TIMES FOR 20, 10, 10, 30 SEC. TO DISPERSE INITIAL START TO FAMILIARIZE STARTER RUN 60Y30 UNDERLOAD						
	2	-	-	35	61	1.0	260	960	46	30	11:04		STARTER RUN 60Y30 UNDERLOAD						
	3			56	75	2.5	260	1500	48	38	11:07		RETURN TO IDLE						
	4			79	85.8	8.0	355	3050	48	44	11:12								
	5			89	90.2	12.7	423	4900	50	44	11:15								
	6				96						11:18		NO DATA TAKEN						
	7				IDLE						11:21	21	SHUT DOWN NORMAL						
5-18-61	1	64	29.97	34.2	60	1.0	255	940	45	36	10:52		30 SEC ON STARTER						
	2	63	"	46	70.5	1.8	240	1190	45.5	42	10:56		NORMAL START						
	3	63	"	53.4	75.5	2.7	262	1450	45.8	43	10:59								
	4	63	29.98	65.4	80.9	4.5	302	2080	46	45	11:02								
	5				IDLE						11:07		ELECTRICAL FIRE ON VALVE						
	6	63	"	77.2	85.2	7.7	345	2990	47	44	11:09		MOTOR - RETURN TO IDLE						
	7				IDLE						11:12		CHECKED FOR ENGINE FIRE						
	8	62	"	88.2	90	12.5	411	4800	47.5	43	11:15		WAS ONLY OIL BREATHER						
	9	62	"	92	92	14.8	450	5400	47.5	42	11:17								
	10				IDLE						11:18		RETURN TO IDLE						

Cum. TOTAL TIME 1:15

7 STARTS

WITNESSED
BY
USA F

RAN OUT OF THROTTLE
@ 92% N₂ - WILL ADJUST LINKAGE

NORMAL SHUT DOWN

WHIRL TEST - J57-PW-19W
ENGINE DATA SHEET

CALIBRATION

DATE	RUN No.	T ₀ OF	P ₀ %	N ₁ %	N ₂ %	P _T %	T _T °C	W ₁ %	P _{oil} %	T _{oil} %	TIME	TOTAL TIME	REMARKS
5-18-61	11	66	29.98	34.5	60.2	1.1	260	925	45	36	1311 1316		NORMAL START
	12	64	"	91.9	92	14.5	452	5500	47.5	41	1314 1324		
	13	64	"	95.5	94.1	17.6	492	6300	47.9	41	1321 1326		MAX. THROTTLE - WILL CONTINUE AT LOWER POWER
	14	64	"	98.2	95.7	19.8	525	7000	48	41	1324 1330		
	15	64	"	95.2	93.9	17.2	485	6250	48	41	1330 1334		
	16	64	"	88.8	90	12.2	408	4650	47	43	1334 1337		NOTICED N ₁ FLUCTUATION OF I.O.3%
	17	64	"	76.5	85.1	7.4	342	2930	46.5	46	1337 1342		
	18	64	"	63.4	80.1	4.2	295	1920	46	46	1342 1346		
	19	63	"	52.7	75.3	2.7	248	1420	46	46	1346 1350		ATTEMPT TO FIX THROTTLE
	20										1350 1410	59	-NORMAL SHUT DOWN
	21										1410 1605		NORMAL START
	22	62	29.95	88.3	90.1	12.5	419	4850	47.5	42	1610 1615		
	23	62	"	99	96.2	20	540	7250	48	40	1615 1618		
	24	62	"	100.3	97	21.2	558	7800	48	41	1618 1621		EMIL POWER
	25	62	"	98.5	96	19.5	531	7000	48	42	1621 1624		
	26										1624 1630	25	NORMAL SHUT DOWN
													WITH 55° D ₁ & 5° A ₁ WITH 3/4" B ₁ & 1/4" B ₂

CUM TOTAL TIME 2:49

9 STARTS

89-218

WHIRL TEST - J57-PW-19W
ENGINE DATA SHEET

CHECK OUT WITH DUCT
AND B.P. VALUE

DATE	RUN NO.	T ₀ °F	P ₀ IN/HG	N ₁ %	N ₂ %	P _T PSI	T _T °C	W _T KG/HR	P _{oil} PSI	T _{oil} °C	TIME	TOTAL TIME	REMARKS
5-23-61	1	66	29.95								1337		ABORTED STARTS (2) NO TAGH.
	2	65	29.95		80M/DLE						1336		ABNORMAL START WITH 80% N ₂ - THROTTLE MUST BE ADJUSTED
	3	65	29.95	64	80.4	4.1	302	1990	46	43	1336		
	4	65	"	83.8	90.2	12.4	448	4900	47.5	46	1444		
	5	66	"	96.2	97	21.2	587	7350	48	44	1449		
	6	66	"	82.8	90	12	440	4450	47.5	48	1452		ADJUSTED B.P. VALUE
	7	66	"	80.8	90	12.85	461	4450	47	46	1455		" " " "
	8	66	"	78.2	90	13.7	489	4450	47.5	48	1503		" " " "
	9	66	"	83.8	90	12.1	440	4500	47	46	1505		" " " "
	10				DLE						1505	38	RELEASED DUCT & ATTAINED STD. IDLE NORMAL SHUTDOWN USING EMERGENCY THROTTLE CUT-OFF.
5-24-61	1	66	29.95		104.8		NORMAL				1000		NORMAL START
	2	66	"	52.2	75	2.2	261	1400	46	44	1009		
	3	67	"	64.5	80.4	4.0	296	1960	46.2	45.5	1006		
	4	67	"	88.7	90	12	410	4700	47.5	45	1020		
	5	67	"	95.6	94.1	17	490	6250	48	45	1032		
	6	66	"	100.4	92.1	20.75	558	7600	48.3	44	1036	36	

CUM. TOTAL TIME 4:05

12 STARTS

[Handwritten signature]

B.2-4

WHIRL TEST - J57-PW-19W
ENGINE DATA SHEET

BLADE ROTATION
@ IDLE

CHECK OUT WITH
DUCT & B.P. VALVE

DATE	RUN No.	T ₀ °F	P ₀ IN. Hg	N ₁ %	N ₂ %	P _T PSI	T _T °F	W _E LB/HR	P _{oil} PSI	T _{oil} °F	TIME	TOTAL TIME	REMARKS
5-24	7	67	29.95	94.7	93.8	16.1	480	6000	48	45	1036		
6-1	8	67	24.96	96.1	94.7	17.5	500	6400	48	45	1041		NORMAL CONT - WILL CLOSE B.P. VALVE TO
	9	67	"	91.3	94.8	18.2	539	6300	48	45	1051		DETERMINE EFFECT @ THIS THROTTLE SETTING HOLDING N ₁ CONSTANT
	10	67	"	89	94.9	19	563	6300	48	45	1051		
	11	67	"	84.5	94.9	18.9	590	6150	48	45	1058		OPENED THROTTLE TO GET MIL. PT. AND MAX. TR
	12	67	"	87.1	96.4	21.7	626	7000	48	45	1102		
	13	71	"	95	94.2	17.1	494	6200	48	45	1105		NRP - ON LINE
	14	71	"	"	IDLE						1109		WILL SIMULATE VALVE FAILURE BY OPENING VALVE QUICKLY @ 90% N ₁
	15	71	"	"	90.1						1113		SLOW ENGINE REACTION EASILY CONTROLLED -
	16	71	"	"	IDLE						1118	42	NORMAL SHUTDOWN NORMAL START - PILOT @ CONTROLS
6-5	1			35.8	60.7	1.0	221	890	45.5	30	1123		PILOT FAMILIARIZATION
	2			VARIOUS	RUDDER SETTINGS						1136		OPENED B.F. VALVE ± 30 RPM ROTOR CLOSED B.F. VALVE
	3			36	61	.95	210	870	46	44	1142		NORMAL SHUTDOWN
	4			IDLE							1147	32	
6-9	1	66	29.94	35.5	60.6	1.0	228	840	45.5	32	1053		NORMAL START WIND ESE 6 MPH
	2	66	"	35.1	60.3	0.9	212	840	46	43	1077		OPENED VALVE (B.F.) OPER. BY ROTOR CONTROLS CLOSED VALVE (B.F.)
	3				IDLE						1101	33	NORMAL SHUTDOWN

CUM. TOTAL TIME 5:52 - 15 STARTS

WIND ESE 6 MPH
WIND 30 RPM ROTOR

WHIRL TEST - J57-PW-19W
 ENGINE DATA SHEET

DATE	RUN NO.	T ₀	P IN. Hg	N ₁ %	N ₂ %	P PSI	T ₁ °F	W _e LBS	P OIL PSI	T _{oil} °C	TIME	REMARKS
6-9-61		64	29.67									
	1	"	"	35.4	60.6	1.0	240	890	505	33	0413	ABORT START - MISMIXER OF STALL - UNORDER
				ROTOR	ROF	ROF	37.5 RPM				0453	THROTTLE CLOSED NORMAL START
				"	FLAT P	38 RPM					0507	OPENED 3.5 WIND 5.10 RPM
					FULL P	37 RPM					0558	
					20 P						1000	
					20 P	Full L.					1001	
				"	"	"	29 RPM	Full F.			1002	
				"	"	"	28 RPM	BEAR			1003	
				"	"	"	L.	F. BEAR			1004	
				NEUTRAL							1005	
				GEN. FULL DOWN							1006	
											1007	
											1008	
											1009	
											1010	
											1011	
											1012	
											1013	
											1014	
											1015	
											1016	
	2	64	29.67								0516	AT 60 RPM ROTOR

GUM TOTAL TIME 6:14

17 STARTS

1005
 1006
 1007
 1008
 1009
 1010
 1011
 1012
 1013
 1014
 1015
 1016
 1017
 1018
 1019
 1020
 1021
 1022
 1023
 1024
 1025
 1026
 1027
 1028
 1029
 1030
 1031
 1032
 1033
 1034
 1035
 1036
 1037
 1038
 1039
 1040
 1041
 1042
 1043
 1044
 1045
 1046
 1047
 1048
 1049
 1050

8.2-6

WHIRL TEST - J57-PW-19W
ENGINE DATA SHEET

Date	Run No.	T _P °F	P _o %	N ₁ %	N ₂ %	P _{Tn} PSI	T _{Tn} °C	W _e %	P _{oil} PSI	T _{oil} °F	TIME	REMARKS
6-	3	64	29.89	45	90	1.5	250	1070	46	46	1010	76 RPM
	4	64	"	51	94.5	2.3	273	1340	46	48	1023	58 RPM
				IDLE							1032	VALVE SHUT NORMAL SHUT DOWN
											1037	14
											1038	
											1039	
											1040	
											1041	
											1042	
											1043	
											1044	
											1045	
											1046	
											1047	
											1048	
											1049	
											1050	
											1051	
											1052	
											1053	
											1054	
											1055	
											1056	
											1057	
											1058	
											1059	
											1060	

Handwritten notes:
 1. 10:15
 2. 10:20
 3. 10:25
 4. 10:30
 5. 10:35
 6. 10:40
 7. 10:45
 8. 10:50
 9. 10:55
 10. 11:00

CUM TOTAL TIME 6:28 17 STARTS

B.2-7

WHIRL TEST - J57-PW-19W
ENGINE DATA SHEET

TETHER TEST

DATE	RUN NO.	T ₀	P ₀	N ₁	N ₂	P _{T₉}	T _{T₉}	W _g	P _{oil}	T _{oil}	TIME	REMARKS	
7-5-61	1	72		34	60	95	208	900	45.5	39	1:05	NORMAL START CHECKED VALVE VALVE OPEN	
	1			ATTEMPTED TO GET 6000 RPM									
				MINIMUM TEST 3200 RPM									
				DURING TEST									
7-6-61				IDLE									
				IDLE									
				IDLE									
7-6-61	1			66.5	83.1	6.8	295	2500	46.5	48	1:05	N. WATER INJECTION	
	2			90.1	86	9.4	340	3000	45	50	1:07	" "	
	3			93.5	88	11.0	368	3800	47	50	1:08	DOOR TO REELOW	
	4			95	88.8	11.9	382	4100	47	51	1:09	WATER INJECTION	
	4'			"	"	11.6	398	"	"	"	1:09	" "	
	4''										1:09	" "	
				IDLE									
				IDLE									
				IDLE									
	4			71	86	8.8	330	2900	47	50	1:07	WATER TO BEY APPROX. 10000	
	7			98	91.6	14.7	440	490	47	50	1:08	WATER TO BEY APPROX. 10000	
				IDLE									

Cum. Total Time 8:41 20 STARTS

NCD

Handwritten signature and initials

WHIRL TEST - J57-PW-19W
ENGINE DATA SHEET

DATE	RUN NO.	T ₀	P ₀	N ₁ %	N ₂ %	P ₀ PSI	T ₀ °F	W ₀ LBS	P ₀ PSI	T ₀ °C	TIME	REMARKS
7-7-61				100%							1:33	NORMAL START SIB O-2 WITH WIND
	1			90	84.2	2.5	350	2700	47	49	4:30	VALUE DOWN
	2			71	86	9.3	390	3000	47	50	4:33	
	3			95	88.5	11.5	400	3000	47	50	4:35	
	4			76	89	12	450	4080	47	50	4:37	
	5			88	90.2	13	470	4600	47	50	4:38	
	6	75		80	91.5	14.5	490	4500	47	50	4:39	
	7			81.2	93.5	16.7	540	5500	48	50	4:40	
	8			100	96.9	19	578	7000	48	50	4:41	
	9			84	96	19.7	573	6300	48	53	4:42	
	10			83.2	95.8	19.9	573	6200	48	54	4:43	NCD
					100%						1:33	NCD
7-10-61		76	29.85	100%							3:00	NORMAL START
	15			71.2	96	18.2	433	6800	48	49	3:29	
	16			98.5	94.5	16	400	6000	48	50	3:35	
					100%						3:44	NCD
					100%						3:46	NCD
					100%						4:35	NORMAL START
					100%						4:37	
	15			92.5	96.5	20.2	490	7000	48.4	47	4:40	
											4:49	

CON. TOTAL TIME 11:06 23 STARTS

Handwritten notes:
 11:06
 23 STARTS
 NCD
 38
 NORMAL START

B.2-10

WHIRL TEST - J57-PW-19W
ENGINE DATA SHEET

DATE	RUN NO.	T ₀	P ₀	N ₁	N ₂	P _{T₉}	T _{T₉}	W _f	P _{oil}	T _{oil}	TIME	REMARKS
8-1 -61	10:				10L6						10:59	NORMAL START ALL READINGS IN ORDER
											11:04	
	1		2972	100.6	97	19.2	1030	730	48	50	11:19	MIL POWER ~ AT 11:12 SUDDENLY IN W N ₂ & N ₁ WITH DROP IN P ₀ FAN BELT SUPPRESSOR WAS LATER FOUND TO HAVE FAILED @ 11:20 NORMAL SHUTDOWN
		TAKING		SOUND	LEVEL	READINGS	ON				11:20	
		.		HILL.							11:24	
					10L6						11:26	NORMAL START
8-28 -61	1				10L6						11:30	ROTOR BEARING TEMP. TO HIGH. DUST TEMP @ 620°F
	2				MIL	POWER					11:33	
	3					10L6					11:37	BEARING TEMP. TO HIGH
	4				MIL	POWER					11:38	
	5					10L6					11:39	
	6				MIL	POWER					11:43	BEARING TO HOT
	7					10L6					11:45	
	8					10L6					1:50	NORMAL COAST DOWN
	9				MIL						2:20	NORMAL START
	10				10L6						2:22	BEARING TO HOT
											2:24	
											2:29	M.C.D.
											2:29	<i>Handwritten signature</i>

TOTAL TIME 13:51 27 STARTS

WHIRL TEST - J57-PW-19W
ENGINE DATA SHEET

1
2
3
4

DATE	RUN No.	T ₀	P ₀	N ₁	N ₂	P _{Tn}	T _{Tn}	W _e	P _{OIL}	T _{OIL}	TIME	REMARKS
5-25-61					IDLE						9:17	NORMAL START
	1			97.1	97	20.4	571	2300	48	43	9:21	MIL POWER FOR SOUND TEST
	2			96.8	97	20.5	575	2100	48	44	9:31	
					IDLE						9:45	NCD
5-28-61					IDLE						9:50	NORMAL START
	1			97	97	20	571	2200	48	46	10:05	SOUND RUN
					IDLE						10:20	REMOVE EX. SUPPRESSOR
					IDLE						10:30	NCD
					IDLE						10:35	NORMAL START
					IDLE						10:45	NOZ. REMOVED
	2			99.9	96.6	18.8	525	2000	48	48	10:55	
					IDLE						11:05	
	3			94.8	96.7	20	568	1800	48	50	11:15	
					IDLE						11:25	NCD
					IDLE						11:35	NORMAL START
5-27-61					IDLE						11:45	VALVE OILED
	1	63		277.5	57.3	77.7	3.3	264	46	49	11:55	118 ROTOR RPM
					IDLE						12:05	NCD
					IDLE						12:15	NORMAL START
5-20-61					IDLE						12:30	NORMAL START
					IDLE						12:40	NOZ. REMOVED
	1	69		57.4	99.9	3.4	268	1500	46	45	12:50	127 RPM ROTOR
	2	72		289.8	63.7	80.3	4.1	303	46	46	12:55	140 RPM
	3			64	82.7	4.9	308	2100	46	47	1:00	158 RPM

16:36

32 STARTS

Handwritten notes:
1. 10:30
2. 10:35
3. 10:45
4. 10:55
5. 11:05
6. 11:15
7. 11:25
8. 11:35
9. 11:45
10. 11:55
11. 12:05
12. 12:15
13. 12:30
14. 12:40
15. 12:50
16. 12:55
17. 1:00

1:34

B.2-12

WHIRL TEST - J57-PW-19W
ENGINE DATA SHEET

DATE	Run No.	T ₀	P ₀	N ₁	N ₂	P _{T₁}	T _{T₁}	W _e	P _{oil}	T _{oil}	TIME	REMARKS
	4			92.5	83.9	10.71 5.9	316	2420	47	47	10:57 10:59	170 RPM
	5			94.3	84.5	11.61 6.3	322	2580	47	47	10:58 10:59	179 RPM
	6			98	85.8	12.0 6.3	323	2940	47	47	10:58 11:00	193 RPM
	7			99	86.3	9.5	332	2900	47	47	11:00 11:01	197
						10LE					11:01	NCD
9-1-61						10LE					10:05	NORMAL START V.O. 9:57
				VARIABLES		P5	TO 200 RPM				10:17	10:17 VALVE SHUT
						10LE					10:17	
	1			91.7	86.2	7.4	330	2920	47	46	10:58 11:00	10:38 V.O. 7 MPH WIND START OUT @ 150 RPM
	2			83.2	81.9	8.2	340	3100	47	46	11:01 11:02	210 RPM
	3			80.1	88	8.5	350	3680	47	46	11:30 11:31	218 RPM
	4			85.2	88.3	9.6	354	3900	47	47	11:31 11:35	230 RPM
	5			87	87.2	10.5	370	4100	47	45	11:34 11:39	240 RPM
						10LE					11:40	NCD
9-6-61						10LE					11:58	NORMAL START 9:32 VALVE OPEN 100 RPM
	1			80.5	87.4	7.6	350	2980	47	55	11:58 12:01	168 ROTOR RPM 6.0 COLLECT.
	2			83.5	88.5	8.5	358	3000	47	52	12:01 12:02	179 RPM NCD 19:59 52

19:59

34 STARTS

1:01

20

1:25

WHIRL TEST - J57-PW-19W
ENGINE DATA SHEET

DATE	RUN No.	T ₀	P ₀	N ₁	N ₂	P _{T₀}	T _{T₀}	W _c	P _{oil}	T _{oil}	TIME	REMARKS
9-25-61	6			98.6	95.6	18.2	515	6000	48	43	11:17	210 RPM
	7			98.8	95.7	18.2	516	6000	48	43	11:28	218 RPM
											11:39	NCD
9-26-61											11:53	23
	1			95.3	95.4	18.5	528	6600	48	43	9:08	NORMAL START TRAINING I.S.M. NRP - 172.5 RPM
	2			93.6	95.7	18.5	545	6400	48	43	9:14	7° COLL 171 RPM
	3			95.0	95.8	18.6	540	6600	48	44	9:18	220 RPM SUPPRESSOR FAILED
											9:24	41
9-26-61	4			88.5	94.8	18.1	561	6200	48	43	10:38	7° COLL 230 RPM NCD
											10:48	28
											11:02	NORMAL START STARTER RUN 1 MIN. NCD
	5			87	94.2	18	554	6000	48	43	12:08	230 RPM
	6			87	94.2	18	552	6050	48	43	12:20	8° COLL 240 RPM 4" HIGH
	7			88.5	94.8	18.1	552	6100	48	43	12:30	170 RPM WIND STEADY 13 SW
	8			88.5	94.8	18.3	554	6100	48	43	12:32	180 RPM
	9			88.4	94.8	18.3	556	6100	48	43	12:40	190 RPM
	10			88.2	94.8	18.5	562	6200	48	43	12:44	200 RPM

25:46

38

WITNESSED
BY
USAF

20

49

119

B-2-15

WHIRL TEST - J57-PW-19W
ENGINE DATA SHEET

DATE	RUN NO.	T ₀	P ₀	N ₁	N ₂	P _{T₉}	T _{T₉}	W _g	P _{OLL}	T _{oil}	TIME	REMARKS
9-16	11			88.8	94.8	18.5	558	6200	48	42	12:38 12:44	210 RPM 8° COLL.
				10L8							12:49	NCD 10:18hrs ROTOR
9-27											12:58	
	1			87.1	94.2	17.9	550	6000	48	42	9:25	NORMAL START
	2			86.8	94.2	17.9	550	6000	48	42	9:29	210 RPM
	3			86.2	94.2	17.9	550	6000	48	42	9:33	220 RPM
	4			93.2	95.8	19	555	6600	48	42	9:36	230 RPM
	5			87.4	94.8	18.05	600	6100	48	42	9:38	236 RPM
	6			87.0	94.8	18.1	576	6000	49	42	9:56	9° COLL
	7			88.0	94.8	18.1	566	6000	48	43	10:00	170 RPM
	8			88.7	94.8	18.1	556	6100	48	43	10:01	180
	9			88.5	94.8	18.1	561	6100	48	43	10:02	190
	10			88.5	94.8	18.1	585	6100	48	43	10:03	200
	11			85.6	95.2	19.6	595	6300	48	43	10:04	210 RPM
	12			84.9	95.2	19.6	600	6300	48	43	10:05	220
	13			88.7	94.9	18.0	555	6000	48	44	10:06	230°
	14			88.0	94.5	18.0	560	6000	48	44	10:08	9°
	15			89.0	95.1	18.1	560	6100	48	44	11:05	8°

27:56 39

WITNESSED
[Signature]

82-10

WHIRL TEST - J57-PW-19W
ENGINE DATA SHEET

DATE	RUN No.	T ₀	P ₀	N ₁	N ₂	P _{th}	T _{th}	W _g	P _{OLL}	T _{oil}	TIME	REMARKS
9-29-61	16			88.5	95.5	18.0	56.2	6150	48	44	11:38	10° COLL 200 RPM
	17			90.3	95.1	18.0	55.4	6100	48	44	11:48	210 RPM
						IDLE					11:53	NCD
						IDLE					11:59	NORMAL START
	18			86	96.5	21	630	6800	48	44	12:07	1018.27 235 RPM 90° COLL 190° W/O 210 RPM Powder Rg 103° COLL
	19			88.5	94.7	17.5	55.0	6000	48	44	12:17	210 RPM
	20			92.4	96.9	20.5	600	7000	48	44	12:28	100° COLL 220 RPM 243 RPM 1309 HRS
	21			96.5	96.2	19.5	55.5	6800	48	44	12:43	8° COLL 243
	22			90	96	19.6	58.5	6600	48	44	12:56	8° 13:42
						IDLE					13:01	NCD
9-28-61						IDLE					13:07	START
	1			86.2	95.8	19.5	61.0	6400	48	44	13:16	V.O. 9:01 242 8.5° COLL
	2			81.5	95.8	19.9	64.2	6300	48	44	13:34	242 RPM 8.5° COLL
						IDLE					13:56	
						IDLE					14:00	V.O. 10:25
9-29-61	1			82.8	96.2	20.2	64.5	6400	48	45	14:09	8.5° COLL 240 RPM
						IDLE					14:24	
	2			82.7	96.2	20.5	65.5	6600	48	45	14:31	WITNESSED BY 14:31

30:09 41

WITNESSED BY
14:31

105

2:10

8425-18

WHIRL TEST - J57-PW-19W
 ENGINE DATA SHEET

DATE	RUN No.	T ₀	P ₀	N ₁	N ₂	P ₁ T ₁	T ₁	W ₁	P _{oil}	T _{oil}	TIME	REMARKS
8-29-61	3			81.8	96.1	21.0	658	6500	48	46	2:08 2:17	B.S. Cold 240 RPM
	4			80.8	96	20.9	660	6600	48	46	2:25 2:37	B.S. Cold 240 RPM
10-2-61											13:29 13:44	NCD TOTAL ROTOR 18:10
											13:44 13:59	NORMAL-START NO. 1617
											16:16	
											16:30	
	1			80	96	21.8	650	6600	48	44	16:32	B.S. Cold 240 RPM
											16:44	NCD
											16:49	KC 1645- 1658
10-20-61				35	60.9	1.2					11:58	START
				96.4	97.1	19.75	600	7200	48	45	12:03	FAMILIARIZATION RUN
											12:25	OPERATED DUMP VALVE
											12:34	NORMAL
											12:34	WITNESSED
												USAF QC

32:56

44

18:38

8-2-10

WHIRL TEST - J57-PW-19W
 ENGINE DATA SHEET

DATE	RUN NO.	T ₀	P ₀	N ₁	N ₂	P _{T₁}	T _{T₁}	W _g	P _{oil}	T _{oil}	TIME	REMARKS
10/27	65	3000	37.8 T.D.E.	60.5	1.6	260	930	45.5	30	1101	11:19	START FAMILIARIZATION RUN WITH REACKS INSTALLED VALVE OPEN - BUTTERFLY 10.5 RPM - 40°C oil
	"	"	65	80	3.0	285	1720	46	50	1101		
			IDLE							1181		
	2	"	82.5	87	7.0	340	3000	47	48	1134	11:34	T _{T₁} FLUCTUATED 150°C DURING IDLE
	3	"	84.5	87.8	7.7	350	3400	47	48	1153	11:53	8-VALVE OPEN - 6°C oil
	4	"	88	89	9.1	370	4000	47	46	1155	11:55	181 rpm - 6°C oil
	5	"	88	90	10.7	405	4400	47	46	1201	12:01	200 rpm - 6°C oil
	6	"	92.3	92.5	13.5	455	5200	47	45	1210	12:10	219 rpm - 6°C oil
			IDLE							1215		243 rpm - 6°C oil
10/27	66	2994	70.75% N ₂ -30.5% O ₂ -1.0% H ₂ O	60.2	1.0	260	940	45	37	1228	12:28	OBSERVED CLATTER FROM STARTER
	7		88.5	90	10.4	480	4200	47	46	1188	11:58	START
	8		94.5	93.2	14.4	470	5800	48	45	1116	11:16	240 rpm - 4°C oil
	9		96	95.5	17.0	540	6500	48	45.5	1120	11:20	239 rpm - 6°C oil
	10		87.5	96.5	20.4	630	6700	48	45	1132	11:32	242 rpm - 9°C oil
	11		80.3	96.2	20.6	670	6400	48	44	1134	11:34	240 rpm - 9°C oil
	12		95	96.5	20	585	6900	48	45	1111	11:11	240 rpm - 9°C oil
	13		94.8	94	15.5	490	5700	48	45	1116	11:16	220 rpm 8.5°C oil

35:12

313
46
10:59 F

20:20

WHIRL TEST - J57-PW-19W
ENGINE DATA SHEET

02-19

DATE	Run No.	T ₀	P ₀	N ₁	N ₂	P _{T_h}	T _{T_h}	W _g	P _{oil}	T _{oil}	TIME	REMARKS
10/27	14			91	92	12.6	445	5000	47	46	451	200 rpm, 8.5 coll
	15			86.8	89.8	10.2	400	4400	47	46	455	180 rpm, 8.5 coll
												NO. 1 - SHUT DOWN
10/30		62	29.89	35.5	61	1.2	235	870	44	48	855	STACK VALVE OPEN - 0.5 C
				74	83.7	5.0	320	2650	46	48	901	
	16	67		86.8	88.8	9.2	380	3800	47	46	919	170 rpm - 2° COLL BIG WIND - 1-2° N/NW 170 rpm - 8.5 COLL
	17			88.5	90.0	10.2	400	4200	47	45	925	18.5 rpm - 8.5° COLL
	18			88.5	90.6	10.2	398	4200	47	45	934	170 rpm - 9° COLL
	19			90	90.5	10.8	410	4400	47	45	937	180 rpm - 9° COLL
	20			92	92.5	13.5	460	5100	48	45	941	200 rpm - 9° COLL
	21			96	94.5	16.5	510	6000	48	44	948	220 rpm - 9° COLL
	22			94.2	96.7	20.3	605	6900	48	42	955	240 rpm - 9° COLL 100% WIND - 3 mph - NNE 170 rpm - 10° COLL
	23			90	91	14	420	4500	47	46	1002	231 rpm - 10° COLL
	24			81	96.2	20.7	670	6300	48	43	1011	STACK VALVE CLOSED
				35	61	1.4	240	850	45	51	1029	
												SHUT DOWN
												NORMAL

30:52 47
1800 rpm 8.0 F
21:49

WHIRL TEST - J57-PW-19W
ENGINE DATA SHEET

B-2-20

DATE	RUN NO.	T ₀	P ₀	N ₁	N ₂	P _{T_η}	T _{T_η}	W _η	P _{oil}	T _{oil}	TIME	REMARKS
10/30												
	69	2983		34	60.2	.9	250	890	45	41	1338	1342 - 8 VALVE CREU
	25			71	83.2	4.9	320	2320	46	47	1344	WIND - 14 MPH - NNE
	26			84.3	88.5	8.6	370	3500	47	50	1354	170 rpm, 2° coil
												Down to 30 at end of data read
	27			97.2	97.1	20.0	590	7000	48	44	1409	241 rpm, 2° coil
	28			80	88.4	8.6	395	3200	47	50	1416	240 rpm, 9° coil
	29			97.3	97.1	20.4	600	7100	48	45	1419	240 rpm, 2° coil
	30			81.2	96.4	20.3	665	6300	48	45	1424	240 rpm, 9° coil
	31			97	96.4	18.9	570	6700	48	45	1433	231 rpm, 10° coil
	32			92	93.8	15.0	510	5400	48	45	1441	220 rpm, 10° coil
	33			87	91	12.0	445	4300	48	45	1447	200 rpm, 10° coil
	34	69		85.5	90	11.0	425	4200	48	45	1450	180 rpm, 10° coil
												WIND - 15 MPH - NNE
	35			81.4	88.5	8.6	390	3400	47	49	1456	170 rpm, 8° coil
	36			84.1	89.9	9.6	415	3900	47	49	1508	180 rpm, 8° coil
	37			88.2	91.1	11.9	445	4200	47	49	1514	200 rpm, 8° coil
	38			92.1	93.2	14.4	490	5300	47	45	1518	220 rpm, 8° coil
	39			97	96	18.0	545	6500	47	46	1524	240 rpm, 8° coil
				34	60.8	1.4	235	850	47	46	1534	Noema - Shut Down 1:51

38.5V 49

2340

WHIRL TEST - J57-PW-19W
ENGINE DATA SHEET

8-2-21

DATE	RUN No.	T ₀	P ₀	N ₁	N ₂	P _{Tn}	T _{Tn}	W _g	P _{OIL}	T _{OIL}	TIME	REMARKS
10/30		67	29.82	34	IDLE 60	1.3	250	920	START	44	1607	1608 - B VALVE OPEN
	40			79	87	7.5	370	2970	47	49	1613	220 rpm - 2° coll
	41			82.5	88.8	8.7	400	3600	47	49	1621	WIND - 4 mph - N
	42			87.5	90.9	11.8	435	4500	47	46	1625	220 rpm - 4° coll
	43			91.5	93.1	14.3	490	5200	47	45	1628	WIND - 2 mph - N
	44			97.7	96.6	19.0	570	6900	48	45	1638	220 rpm - 8° coll
	45			94.8	97.1	20.6	610	7000	48	45	1643	WIND - 0
	46			92.8	96.0	18.3	580	6300	48	46	1648	220 rpm - 10.5° coll
	47			95	97.2	20.6	610	7000	48	44	1650	220 rpm - 8° coll
				67	83	4.8	340	2010	48	50	1657	240 rpm - 9° coll
									IDLE		1659	WIND - 0
											1708	170 rpm - 20° coll
											1708	EMPTY SEC
											1713	240 rpm - 2° coll
											1715	1 mph - 2° coll
											1718	240 rpm - 9° coll
											1719	1 mph
											1720	NORMAL SHUT DOWN
											1726	WIND E - 4 mph
10/31		58	30.00	36	IDLE 61.2	1.3	230	920	48		8:34	START 2.5 MIN
											8:35	B VALVE OPEN 8:28
											8:33	170 rpm, 2° coll
											8:41	NORMAL SHUT DOWN

40:28 51

[Signature]

24:51

108

9.2-22

WHIRL TEST - J57-PW-19W
ENGINE DATA SHEET

DATE	RUN No.	T ₀	P ₀	N ₁	N ₂	P _{Tn}	T _{Tn}	W _f	P _{oil}	T _{oil}	TIME	REMARKS
10/31												
		63	30.00	34.2	60.1	1.5	26.5	920	45	39	1008	ABOVE OPEN 1009 RYALVE HO SEC 0.05 SPARKER START WAS SLOW
											1013	WIND - 0 mph
											1015	170rpm - 2° COLL
	48			98	97	20.5	580	7200	48	44	1017	240rpm - 2° COLL
											1031	170rpm - 2° COLL
											1034	240rpm - 2° COLL
											1037	WIND 1 mph - N
	49			94.5	97	21	610	7100	48	40	1044	240rpm - 2° COLL
											1048	170rpm - 2° COLL
											1053	240rpm - 2° COLL
											1108	240rpm - 2° COLL
											1108.5	240rpm - 2° COLL
											1111.5	240rpm - 2° COLL
											1123	240rpm - 2° COLL
											1125	240rpm - 2° COLL
											1139	B VALVE CLOSED 1132
				97.2	97	21	605	7200	48	45	1139	
											1139	
				35	61	1.0	250	780	45	45	1139	

W. J. Johnson
W. J. Johnson

4153 53

2677

B.2-23

 WHIRL TEST - J57-PW-19W
 ENGINE DATA SHEET

DATE	RUN NO.	T ₀	P ₀	N ₁	N ₂	P _{T_h}	T _{T_h}	W _f	P _{oil}	T _{oil}	TIME	REMARKS
11/16		61	29.95	36	61.5	1	230	1000	46	18	1033 1059	START WIND - 5MPH - S
									46	44	1047	1700rpm - 2° coil HYDRAULIC PUMP MOTOR FAILURE
											1055	IDLE
											1110	SHUT NORMAL SHUT DOWN
11/16		62	29.90	35.5	104E 61	1.1	240	900	45	32	1248 1205	START WIND - 2MPH - SW
											1258	170rpm - 2° coil
											1258	240rpm - 2° coil
	50			98	97	20	580	7000	48	42	1257	240rpm - 9° coil
											1053	104E
											929	SHUT NO. 2 MILS SLUT DOWN
11/16		75	30.0	34.5	104E 60.5	1.0	270	900	45	30	936	START RYLIVE OPEN 9:30 WIND - NWE - 2MPH
				75	85.1	5.8	370	2770	47	45	943	170rpm - 4° coil
				87.2	91	10.5	440	4300	47	50	958	240rpm - 4° coil WIND - D
	1	78	95.2	97.3	19.6		602	6900	48	46	1003	240rpm - 7.6° coil 170rpm - 4° coil
											1005	104E
											1010	SHUT NORMAL SHUT DOWN
												USAF Q

43-27' 56 27-41'

B-2-24

WHIRL TEST - J57-PW-19W
ENGINE DATA SHEET

DATE	RUN NO.	T ₀	P ₀	N ₁	N ₂	P _{T₃}	T _{T₃}	W ₄	P _{oil}	T _{oil}	TIME	REMARKS
11/9/61	78	29.96	54	60	1.5	290	900	45	45	45	1:43	START WIND SW - 2 RYALVE OPEN 1121
				79.5	88.2	8.2	400	3100	47	52	1:53	WIND SW - 3 170 rpm - 4°C coil
	2			97	97.3	19	590	6900	48	50	1:54	WIND SW - 2 200 rpm - 4°C coil
											1:28	200 rpm - 7.6°C oil
											1:28	IDLE
											1:28	STOP NORMA - SHUT DOWN
11/9/61	75	29.96	54	60.4	1.3	280	900	45	45	45	2:09	WIND SW - 4 RYALVE OPEN - 210
											2:15	170 rpm - 4°C oil
											2:18	WIND SW - 3 200 rpm - 4°C coil
											2:23	WIND 5 - 2 - FUEL FLOW MARK 240 rpm - 9°C coil FLOW MARK
	3			97.5	97.2	19	580	6900	48	50	2:28	FUEL FLOW STEADY
											2:34	STOP Normal Shut Down

WIND SW - 2
RYALVE OPEN 1121
WIND SW - 3
170 rpm - 4°C coil
WIND SW - 2
200 rpm - 4°C coil

44-141 58 28-181

ENGINE TIME STARTS BLADE TIME

9-2-25

WHIRL TEST - J57-PW-19W
ENGINE DATA SHEET

DATE	RUN NO.	T ₀	P ₀	N ₁	N ₂	P _{T₁}	T _{T₁}	W _f	P _{oil}	T _{oil}	TIME	REMARKS	
12/1/61	64	3001	35	60.5	1.1	285	890	45	32	1:25	START	STARTER SLUGGISH 5000C START - 12 SEC VALVE OPEN 5MPH - NRK	
										1:28			
				53.5	97	4.6	355	1820	46	45	1:35		170 RPM - 20°C oil EAK - 7MPH 192 RPM 8°C oil
	66	2077	77.8	89	11.6	470	4100	47	47	1:41			
				87.8	96.5	20.2	630	6600	48	41	1:47		
	4			96.3	97	20.4	595	7100	48	48	1:49		238 RPM 8.7°C oil 5MPH - E 230 RPM 8.5°C oil
	5			79.5	96	20.8	670	6300	48	44	1:59		234 RPM - 8.5°C oil 5MPH - E 235 RPM - 8.5°C oil 5MPH - KRK
	6			79	96	21.1	682	6400	48	44	2:01		170 RPM - 4°C oil 5MPH - KRK 4MPH - ESK 240 RPM - 4°C oil
										2:05			240 RPM - 8.5°C oil 236 VALVE CLOSED
										2:30			
										2:39			
										2:59			
12/9/61	61	3015	36	61.4	1.2	240	960	45	17	11:07	START	SLOW START - T ₂ 490°C 10MPH - W VALVE OPEN 11:10	
										11:08			
										11:10			
										11:34			12 mph - W
	7			91.5	96.9	20.7	610	6900	48	40	11:34		218 RPM - 10°C oil
										11:35			
	8			79.2	96	21.1	670	6500	48	41	11:38		221 RPM - 10°C oil 170 RPM - 4°C oil

WITNESSED BY
12/1/61

15"

WHIRL TEST - J57-PW-19W
ENGINE DATA SHEET

B2-27

DATE	RUN NO.	AMBIENT TEMP. - °F	AMBIENT PRESS. in Hg.	LOW COMPRESSOR % SPEED	HIGH COMPRESSOR % SPEED	TURBINE DISCHARG PRESS. - PSIG	TURBINE DISCHARG TEMP. - °C	FUEL FLOW RATE - Lb/Hr	OIL PRESSURE PSIG	OIL TEMP. °C	WIND VELOCITY MPH	WIND DIRECTION	ROTOR rpm	COLLECTIVE PITCH	TIME	STARTS	REMARKS	
12/16/61	60	To	Po 29.82	N1 36	N2 61	Pt7 1.3	Tt7 240	wf 920	Po1 46	To1 18	Vwind 4	SE	-	-	1:43	START	500°C START IDLE - VALVE OPEN - 1:48	
															1:52		1700rpm - 2:01	
															1:58		RED LIGHT OUT - SARK CHECK IDLE DEFECTOR INDIKATOR VALVE CLOSED - 1:57 VALVE ADD PARTED VALVE OPEN - 2:13	
															2:15		1700rpm - 2:00 COLL	
															2:18		YELLOW LIGHT OUT VALVE CLOSED 2:19 VALVE OPEN 2:30	
															2:31		1700rpm - 2:00 COLL VALVE CLOSED - 2:36 IDLE	
															2:39	STOP		
															10:45	START	500°C START - VALVE IDLE 10:46	
12/16/61	56	30.05	35.5	60.8	1.3	240	910	45	28	5	SW				10:51			
															10:57			
															11:03			
															11:07			
															11:10			
															11:12			
															11:16			
															11:20			
															11:25			
19	20																	CONDENSER TO IDLE 10 SEC

WHIRL TEST - J57-PW-19W
ENGINE DATA SHEET

B.2-31

DATE	RUN NO.	AMBIENT TEMP. - °F	AMBIENT PRESS. in Hg.	LOW COMPRESSOR % SPEED	HIGH COMPRESSOR % SPEED	TURBINE DISCHARGE PRESS. - PSIG	TURBINE DISCHARGE TEMP. - °C	FUEL FLOW RATE - Lb/Hr	OIL PRESSURE PSIG	OIL TEMP. °C	WIND VELOCITY MPH	WIND DIRECTION	ROTOR rpm	COLLECTIVE PITCH	TIME	START'S	REMARKS
3/4/2	1			35	60.5	1.4	275	910	45	44	5	SW	60	4	11:25		B VALVE OPEN
	2			"	"	"	"	"	"	"	"	"	58	"	11:28		" 3/4
	3			34.9	60.5	"	280	"	"	"	"	"	43	"	11:32		" 1/2
	4			34.4	60	1.6	312	"	"	"	5	SSW	13	"	11:34		" 1/4
	5			35	60.5	1.45	270	910	"	"	5	S	60	"	11:37		B VALVE OPEN
	6			"	"	"	"	"	"	"	"	SW	58	"	11:41		" 3/4
	7			34.5	60.5	"	283	"	"	"	1	S	43	"	11:45		" 1/2
	8			34.2	60	1.6	305	"	"	"	5	SW	13	"	11:49		" 1/4
				74	84.8	0.5	325	2720	46	44	5	SW	170	"	11:57		B VALVE OPEN
				99.5	76.8	21	580	7500	44	45	12	SW	240	8	12:27		B VALVE CLOSED 12:33
				99.5	95.8	21.1	670	6600	"	40	14	"	240	8	12:30		B VALVE CLOSED 12:33
															12:36	STOP	NORMAL SHUT DOWN

Withstand
4/16/63
B.2-31

67

WHIRL TEST - J57-PW-19W
ENGINE DATA SHEET

B.2-32

DATE	RUN NO.	AMBIENT TEMP. - OF	AMBIENT PRESS. in Hg.	LOW COMPRESSOR SPEED	HIGH COMPRESSOR SPEED	TURBINE DISCHARG. PRESS. - PSIG	TURBINE DISCHARG. TEMP. - °C	FUEL FLOW RATE - Lb/Hr	OIL PRESSURE PSIG	OIL TEMP. °C	WIND VELOCITY MPH	WIND DIRECTION	ROTOR rpm	COLLECTIVE PITCH	TIME	STARTS	REMARKS	
7/26/62	59	30.06	36	61.5	1.2	225	980	45	20	16	SW	-	-	1:54	START	35 SEC ON STARTER 510°C START		
																	1:59 - 13 VALVE OPEN	
	9		78	86	6.4	335	2900	48	46	16	SW	170	4	2:05			2:35 - 50 L/R Fwd, Aff Cyclic	
	10			95.2	94	16	490	6000	48	40	22	SW	240	5.75	2:40		50 LEFT CYCLIC 2:48 - 50 L/R Fwd, Aff Cyclic 50 LEFT CYCLIC	
	11			96.9	95	16.7	510	6250	48	41	16	SW	240	6.5	2:52		50 LEFT CYCLIC 2:56 - 50 L/R Fwd, Aff Cyclic 3:06 - 50 L/R Fwd, Aff Cyclic	
	12			98.2	95.7	18	530	6700	48	41	18	SW	240	6.7	3:02		50 LEFT CYCLIC 3:06 - 50 L/R Fwd, Aff Cyclic	
	13			99	95.7	17.5	525	6800	48	41	16	SW	240	6.5	3:22		IDLE 50 LEFT CYCLIC 3:28 - 50 L/R Fwd, Aff Cyclic 50 LEFT CYCLIC	
	14			98	97	19.8	565	7200	49	41	19	SW	240	7.5	3:32		3:37 - 50 L/R Fwd, Aff Cyclic 50 CYCLIC	
	15			98.2	97.1	20.4	580	7200	48	41	11	SW	240	8.0	3:44		50 CYCLIC	
	16			98.0	96	21.0	670	6400	48	41	16	SW	240	8.0	3:47		50 CYCLIC	
	17			98	97	20.1	585	7200	49	41	16	SW	240	7.5	3:48		3:56 - 13 VALVE CLOSED FLUID BEGINS UP IN MANIFOLD NORMAL SHUT DOWN 3:58 SEC START 3:20°C START 13 VALVE OPEN - 3:27 13 VALVE CLOSED - 3:29 8 VALVE OPEN - 3:39 50 LEFT CYCLIC	
	18			94	96.9	20.8	600	7100	49	41	16	SW	240	7.5	4:00		START	

69

WHIRL TEST - J57-PW-19W
ENGINE DATA SHEET

B-2-33

DATE	RUN NO.	AMBIENT TEMP. - °F	AMBIENT PRESS. in Hg.	LOW COMPRESSOR % SPEED	HIGH COMPRESSOR % SPEED	TURBINE DISCHARG PRESS. - PSIG	TURBINE DISCHARG. TEMP. - °C	FUEL FLOW RATE - Lb/Hr	OIL PRESSURE PSIG	OIL TEMP. °C	WIND VELOCITY MPH	WIND DIRECTION	ROTOR rpm	COLLECTIVE PITCH	TIME	STARTS	REMARKS
2/19/62	19	59	30.05	94	96.9	20.6	595	7100	48	40	15	SW	240	7.5	4:04		50 L/R, 40 L, Fuel cyclic 50 LEFT CYCLIC
	20			94	96.9	20.9	600	7100	48	41	15	WSW	240	8.0	4:13		"
	21			82.7	90.8	11.2	440	4200	48	41	14	SW	240	3.5	4:19		40 LEFT CYCLIC
	22														4:26		IDLE
	23			36	61.2	1.5	240	900	48	41	14	SW	70	4.0	4:32		8 VALVE OPEN - 20 LEFT CYCLIC
	24			36	61.2	1.5	238	900	48	41	18	WSW	66	4.0	4:34		3/4 OPEN
	25			35.9	61	1.6	242	920	47	41	18	SW	51	4.0	4:37		1/2 OPEN
				35.5	60.8	2.0	270	1000	47	45	18	SW	20	4.0	4:38		1/4 OPEN
															4:43		8 VALVE CLOSED - 4:45
															5:00		STOP
2/19/62		65	30.03	36	61.5	1.2	235	910	45	18	10	SW	IDLE		10:27		40 SEC START
				72	84.6	1.4	330	2630	45	43	10	SW	170	4.0	10:39		8 VALVE OPEN 10:51
	26			96	97	20.4	590	7100	48	40	10	WSW	240	7.5	10:48		11:07 - 50 L/R, Fuel, 40 L, Fuel cyclic
	27			99.5	96.8	20	610	6700	48	40	10	SW	231	8.25	11:00		11:14 - REPAIR 11:21 REPAIR
													IDLE		11:24		8 VALVE CLOSED
															11:24		11:24
															11:29		STOP NORMAL SHUT DOWN

70

WHIRL TEST - J57-PW-19W
ENGINE DATA SHEET

B.2-35

DATE	RUN NO.	AMBIENT TEMP. - °F	AMBIENT PRESS. in Hg.	LOW COMPRESSOR 1/2 SPEED	HIGH COMPRESSOR 1/2 SPEED	TURBINE DISCHARGE PRESS. - PSIG	TURBINE DISCHARGE TEMP. - °C	FUEL FLOW RATE - Lb/Hr	OIL PRESSURE PSIG	OIL TEMP. °C	WIND VELOCITY MPH	WIND DIRECTION	ROTOR rpm	COLLECTIVE PITCH	TIME	STARTS	REMARKS
3/4/62	28	58	29.00	36	61	1	-	980	45	22	8	S	240	6	10:39	START	T ₇ not recording
	29	"	"	95	94.8	15.5	940	6200	47	41	10	SW	240	6	11:12		R VALVE OPEN 10:57 ITEM 7 - KUBUIS 11:17 - 50° LEFT CYCLIC
	30	"	"	96.5	95.5	16.6	540	6600	48	41	13	SW	240	7	11:17		50° LEFT CYCLIC
	31	"	"	97.5	96.2	17.5	555	7000	48	41	10	SW	240	7	11:22		"
	32	"	"	95.2	96.8	19.8	590	7100	48	40	12	SW	240	7.6	11:33		11:36 50° L, R, FA CYCLIC
	33	"	"	95.2	96.8	19.8	590	7100	48	40	7	SW	240	7.5	11:40		0° CYCLIC
	34	"	"	77.8	87.5	7.6	378	3200	47	44	13	SW	222	2	11:44		50° LEFT CYCLIC
	35	"	"	77.8	78	7.5	370	3100	46	44	7	SW	220	2	11:50		55° CCW TO FULL PWR 55° CCW TO TOLG - 50° L CYCLIC 11:58 - 50° L, R, FA CYCLIC 50° L CYCLIC SAME AS ABOVE
	36	"	"	90.8	96.5	19.8	610	6800	48	41	13	SW	240	7.6	12:14		50° L, R, FA CYCLIC 50° L CYCLIC 12:22 50° L, R, FA CYCLIC 50° L CYCLIC VALVE CLOSED 12:30 0° CYCLIC
				45	71	2	250	1100	45	50	10	W	160	2	12:27		VALVE CLOSED 12:30 0° CYCLIC
															12:38	STOP	WORKING

64 hr 31 min 73 42 hr 49 min

Added to next table

12:38 STOP WORKING

WHIRL TEST - J57-PW-19W
ENGINE DATA SHEET

8-2-36

DATE	RUN NO.	AMBIENT TEMP. - OF	AMBIENT PRESS. in Hg.	LOW COMPRESSOR % SPEED	HIGH COMPRESSOR % SPEED	TURBINE DISCHARG. PRESS. - PSIG	TURBINE DISCHARG. TEMP. - °C	FUEL FLOW RATE - Lb/Hr	OIL PRESSURE PSIG	OIL TEMP. °C	WIND VELOCITY MPH	WIND DIRECTION	ROTOR rpm	COLLECTIVE PITCH	TIME	STARTS	REMARKS
8/2/36	55	29.8	29.88				Idle								1:25	START	500°C START
				35	60.8	1.2	215	890	45	43	10	W	62	2	1:32		500°C START
				85	77	6.2	330	2880	49	40	10	SW	170	4	1:38		10% CYCLIC
	37	"	"	79	96	19.4	670	6500	48	41	8	W	240	7.6	1:40		50% R.A.F. CYCLIC - 1:55
															2:06		RET TO START - 2:07
															2:12	STOP	NORMAL SHUT DOWN
															4:11	START	8 VALVE OPEN 4:13
				55	29.8	36	61.5	1.5	230	900	45	38	8	NE			
															4:20		50% R CYCLIC
															4:32		50% R.L.F.A
															4:40		50% R.L.F.A CYCLIC
															4:50		50% R.L.F.A CYCLIC
															5:00		50% R CYCLIC
															5:10		50% R.L.F.A CYCLIC - 5:03
															5:11		50% R CYCLIC - 5:09
															5:11		8 VALVE - CLOSED 5:18
															5:24		50% R CYCLIC
															5:24		50% R CYCLIC

W. J. Johnson
8/2/36

*Note - Leak found in 89 line

WHIRL TEST - J57-PW-19W
ENGINE DATA SHEET

B-2-37

DATE	RUN NO.	AMBIENT TEMP. ° OF	AMBIENT PRESS. in Hg.	LOW COMPRESSOR % SPEED	HIGH COMPRESSOR % SPEED	TURBINE DISCHARG PRESS. - PSIG	TURBINE DISCHARGE TEMP. - °C	FUEL FLOW RATE - Lb/Hr	OIL PRESSURE PSIG	OIL TEMP. °C	WIND VELOCITY MPH	WIND DIRECTION	ROTOR rpm	COLLECTIVE PITCH	TIME	STARTS	REMARKS
4/21/62	48	55	29.95	36	61.5	1.2	230	710	46	16	7	NE	IDLE	4	9:53	START	BY VALVE - 9:48 - OPEN 5000 RPM 30° CYCLIC
	49	"	"	72	86	8.2	370	2950	48	44	12	SW	220	2	11:30		5 sec to max Pwr 5 sec to idle
	46	"	"	90	96.7	20.1	610	6700	48	40	8	SW	230	8	11:31		10° L CYCLIC - 11:35
	45	"	"	91	94.2	16.8	525	6000	48	40	4	E	240	6	11:13		5° R CYCLIC
	44	"	"	99.7	96.5	20.9	610	6900	48	38	5	NE	240	7.5	10:42		50° R LFA - 10:48
	43	"	"	96	96.2	20	570	7000	48	38	5	E	240	7	10:17		50° R LFA - 10:32
	42	"	"	97.2	96.6	20.4	590	7200	46	38	10	NE	240	7.3	10:11		5° R CYCLIC
													170	4	10:07		5° R CYCLIC
													IDLE	4	9:59		8 VALVE - 10:02 CLOSED 10:06 OPEN
																	50° R CYCLIC
																	50° R LFA - 10:22
																	50° R LFA - 10:41
																	50° R CYCLIC 10:53
																	50° R LFA - 11:02
																	50° R LFA - 11:17
																	50° R CYCLIC
																	50° R LFA - 11:26
																	50° R CYCLIC
																	0° CYCLIC - 11:35
																	10° L CYCLIC
																	5 sec to max Pwr 5 sec to idle
																	"
																	"
																	5° L CYCLIC
																	50° R LFA - 12:00
																	12:05
																	12:11
																	12:11
																	12:17
																	12:18 STOP
																	NORMAL

Engine 68-58 76 Starts
R18 de 46-53

11200 6000 30

with
4/21/62

Transient from Run 47 Settings

WHIRL TEST - J57-PW-19W
ENGINE DATA SHEET

B. 2-38

DATE	RUN NO.	AMBIENT TEMP. - OF	AMBIENT PRESS. in Hg.	LOW COMPRESSOR % SPEED	HIGH COMPRESSOR % SPEED	TURBINE DISCHARGE PRESS. - PSIG	TURBINE DISCHARGE TEMP. - °C	FUEL FLOW RATE - Lb/Hr	OIL PRESSURE PSIG	OIL TEMP. °C	WIND VELOCITY MPH	WIND DIRECTION	ROTOR rpm	COLLECTIVE PITCH	TIME	STARTS	REMARKS
4/21/62	55	29.9	36	61.5	1.3	230	900	45	30	16	SW	IDLE	7.5	2:00	START	500°C Start B VALVE OPEN - 2:05	
	49	"	"	98.5	97	20	570	7200	48	42	17	SW	240	7.5	2:15		10% CYCLIC
	50	"	"	81	94	16.7	570	5500	48	42	16	SW	240	6	2:28		10% CYCLIC
	51	"	"	90	95.3	18.2	570	6300	48	42	16	SW	240	6.5	2:45		10% CYCLIC
	52	"	"	88	92.5	20	620	6700	48	42	16	SW	240	7.5	3:00		10% CYCLIC
	53	"	"	79.2	96	21	670	6400	48	42	18	SW	240	8	3:10		10% CYCLIC
	54	"	"	91.5	94.2	16.7	520	6000	48	42	18	SW	240	6	3:25		10% CYCLIC 3:30 SOL REFA CYCLIC 3:30 SOL CYCLIC-1 3:50 20% CYCLIC
	55	"	"	87.8	96.4	20.5	600	6800	48	42	19	SW	240	7.5	3:32		10% CYCLIC
							320	2600	46	42	22	SW	100	2	4:00		4:15 20% CYCLIC
									48	42	15	SW	230	8	4:28		50% CYCLIC 4:30
									48	42	15	SW	240	6	4:54		50% CYCLIC
									48	42	15	SW	230	8	5:02		50% CYCLIC 5:18
													100	2	5:12		50% CYCLIC 5:18
															5:18		IDLE
															5:23	STOP	NOISE STOPPING

72hrs 2min ENGINE
5045 01-18-02E

77 STARTS

WHIRL TEST - J57-PW-19W
ENGINE DATA SHEET

B-2-41

DATE	RUN NO.	AMBIENT TEMP. - OF	AMBIENT PRESS. in Hg.	LOW COMPRESSOR SPEED	HIGH COMPRESSOR SPEED	TURBINE DISCHARG PRESS. - PSIG	TURBINE DISCHARG. TEMP. - °C	FUEL FLOW RATE - Lb/Hr	OIL PRESSURE PSIG	OIL TEMP. °C	WIND VELOCITY MPH	WIND DIRECTION	ROTOR rpm	COLLECTIVE PITCH	TIME	STARTS	REMARKS
12/21/59	7			70	83	5.2	300	2220	46	46	7	SW	170	2	11:54		0° CYCLIC
	8			75	87.8	6.3	330	2660	46	46	7	SW	170	4	11:55		0° CYCLIC
	9			80.5	87	8	350	3100	46	46	7	S	200	4	11:59		"
	10			84	88.5	9.2	375	3900	47	42	5	SW	220	4	12:05		"
	11			86	89.5	10	395	4200	47	42	7	SW	240	4	12:07		"
	12			79	86.8	7.8	350	3000	47	42	5	S	200	4	12:11		"
	13			73	84	6	320	2800	46	44	8	SW	170	4	12:16		"
							610						240	8.5	12:17		VALVE CLOSED 12:21
	14			77	85.3	7	335	2910	46	44	10	SW	170	6	12:28		VALVE OPEN 12:25 0.5° CYCLIC
	15			84.6	88.4	9.5	370	3910	47	42	10	SW	200	6	12:31		"
	16			87.8	89.9	11	400	4400	47	42	10	SW	220	6	12:38		"
	17			92	92.1	14	445	5200	47	41	8	WSW	240	6	12:39		"
	18			81.5	90	11	400	4300	47	41	16	SW	220	6	12:43		"
	19			77.5	86	7	340	2920	47	42	15	SW	170	6	12:48		"
	20			87.8	88.4	9.3	375	4000	47	42	18	SW	170	8	12:55		80° CYCLIC
	21			89.9	91	10	420	4800	47	42	16	SW	200	8	12:59		"

B. 3
OPERATION SUMMARY OF HOT CYCLE AFTER
35 HOUR INSPECTION

DATE	T ₁ T ₂ T ₃	rpm	Coll. Pitch	Cyclic Pitch	Time Min.	Coll. Rotor Time	Coll. Engine Time	Starts	Page			
2-5-62					2	—	2	66	30			
	464	40	4		5	5	7					
	608	175	4		5	10	12					
	1105	240	8		5	15	17					
	1240	240	8		4	19	21					
					2	21	23					
					3	—	26					
	2-6-62	460				14	—			40	67	
			170	4		3	24			43		
			170	4		7	31			50		
		240	4		5	36	55					
1112		240	8		5	41	60					
					1	42	61					
					14	—	75					
					5	47	80					
527		60	4		3	50	83	31				
527		58	4		4	54	87					
536	43	4		2	56	89						
590	13	4		3	59	92						
518	60	4		4	63	96						
518	58	4		4	67	100						
590	43	4		4	71	104						
585	13	4		8	79	112						
615	170	4		30	109	142						
1076	240	8		3	112	145						
1240	240	8		1	113	146	68	32				
				2	115	148						
				3	—	151						
2-12-62	437				5	—			156			
	437				6	121			162			
	635	170	4		20	141			182			
	850	240	5	5	15	156			197			
	914	240	5.25	5	12	168			209			
	950	240	6.5	5	10	178			219			
	986	240	6.7	5	7	185			226			
					13	198	239					
	975	240	6.5	5	10	208	249					

OPERATION SUMMARY OF HOT CYCLE AFTER
35 HOUR INSPECTION

DATE	T _{T7} °F	rpm	Coll. Pitch	Cyclic Pitch	Time Min.	Coll. Rotor Time	Coll. Engine Time	Starts	Page
6-13-62	1050	240	7.5	5	12	220	261	69	32
	1076	240	8	5	3	223	264		
	1240	240	8	5	2	225	266		
					7	232	273		
					4	—	277		
	470				13	—	290		
	470				2	234	292		
	470				10	—	302		
	1085	240	7.5	5	9	243	311		
	1112	240	7.5	5	12	255	323		
	1112	240	7.5	5	4	259	327		
	1104	240	7.5	5	9	268	336		
	1112	240	8	5	3	271	339		
	1110	240	8	5	3	274	342		
	824	240	3.5	4	7	281	349		
					6	287	355		
	464	70	4		2	289	357		
	460	66	4		3	292	360		
	470	51	4		1	293	361		
	518	20	4		5	298	366		
					2	300	368		
					5	—	373		
	455				4	—	377		
	455				8	308	385		
	662	170	4		9	317	394		
	1094	240	7.5	5	4	331	408		
	1130	231	8.25	5	22	353	430		
				5	—	435			
							71	34	
ABORTED START							72		
482					5	—	440		
482					6	359	446		
482	170	4		4	363	450			
644	220	4		5	368	455			
734	220	2	5	3	371	458			
				5	—	463			

OPERATION SUMMARY OF HOT CYCLE AFTER
55 HOUR INSPECTION

DATE	T ₁₇ °F	rpm	Cell. Pitch	Cyclic Pitch	Time Min.	Cell. Rotor Time	Cell. Engine Time	Starts	Page	
2-20-62					18	371	501	73	35	
		900	240	6	4	375	505			
		900	240	6		386	516			
		940	240	6	5	391	521			
		1004	240	7	5	396	526			
		1030	240	7	5	407	537			
		1094	240	7.6	5	414	544			
		1094	240	7.5	0	418	548			
		715	222	2	5	430	560			
		698	220	2	0.5	448	578			
		1130	240	7.6	5	461	591			
						3	464			594
						3	464			597
	2-20-62					7	—			604
		419	62	2	6	470	610			
		626	170	4	1	472	612			
		1240	240	7.6	5	26	498	638		
						1	499	639		
						5	—	644		
						2	—	646		
		446			0	508	655			
		1112	240	7.5	5	13	521	668		
		1094	240	7.3	5	10	531	678		
		1130	230	8	5	6	537	684		
		932	230	6	5	8	545	692		
		1140	230	8	5	12	557	704		
		473	100	2	0	7	564	711		
2-21-62					2	—	713	76	37	
		446			1	—	714			
					5	569	719			
			170	4	5	6	575			725
						3	578			728
						4	—			732
						1	579			733
			170	4	5	4	583			737
		1094	240	7.3	5	6	589			743
		1058	240	7	5	25	614			768
		1130	240	7.5	5	24	638			792
		1130	230	8	5	7	645			799
		977	244	6		10	655			809
		1130	240	7	5	8	663			817

OPERATION SUMMARY OF HOT CYCLE AFTER
35 HOUR INSPECTION

DATE	T _{T7} °F	rpm	Coll. Pitch	Cyclic Pitch	Time Min.	Coll. Rotor Time	Coll. Engine Time	Starts	Page			
2-27-62	437				1	1100	1274	80				
					6	—	1280					
					1	—	1281					
					1	1101	1282					
			617	184	4	.5	13			1114	1295	
			860	240	6	.5	4			1118	1299	
			1103	240	8.5	.5	6			1124	1305	
							2			1126	1307	
							1			—	1308	
							1			—	1309	81
							2			1128	1311	
							1			—	1312	82
			464	63	2		6			1134	1318	
			576	170	2		7			1141	1325	
			635	200	2		5			1146	1330	
			671	220	2		2			1148	1332	
			716	240	2		7			1155	1339	
			667	220	2		5			1160	1344	
			572	170	2		3			1162	1347	41
			626	170	4		4			1167	1351	
			662	200	4		4			1171	1355	
			707	220	4		4			1175	1359	
			743	240	4		4			1179	1363	
			662	200	4		5			1184	1368	
			608	170	4		1			1185	1369	
			1130	240	8.5		1			1186	1370	
							3			1189	1373	
							4			—	1377	
							3			1192	1380	
			635	170	6	.5	3			1195	1383	
			698	200	6	.5	4			1199	1387	
			752	220	6	.5	4			1203	1391	
			833	240	6	.5	4			1207	1395	
			752	220	6	.5	5			1212	1400	
			644	170	6	.5	7			1219	1407	
			707	170	8	2	4			1223	1411	
			788	200	8	2	5			1228	1416	42
			878	220	8	2	6			1234	1422	
			1004	240	8		8			1242	1430	
			842	200	8		5			1247	1435	

B: 4-1

B. 4

°C 0 200 400 600 800 1000 Chr. Al. Couples

12/11/61
Run #10
~ 850C Transient
TT7

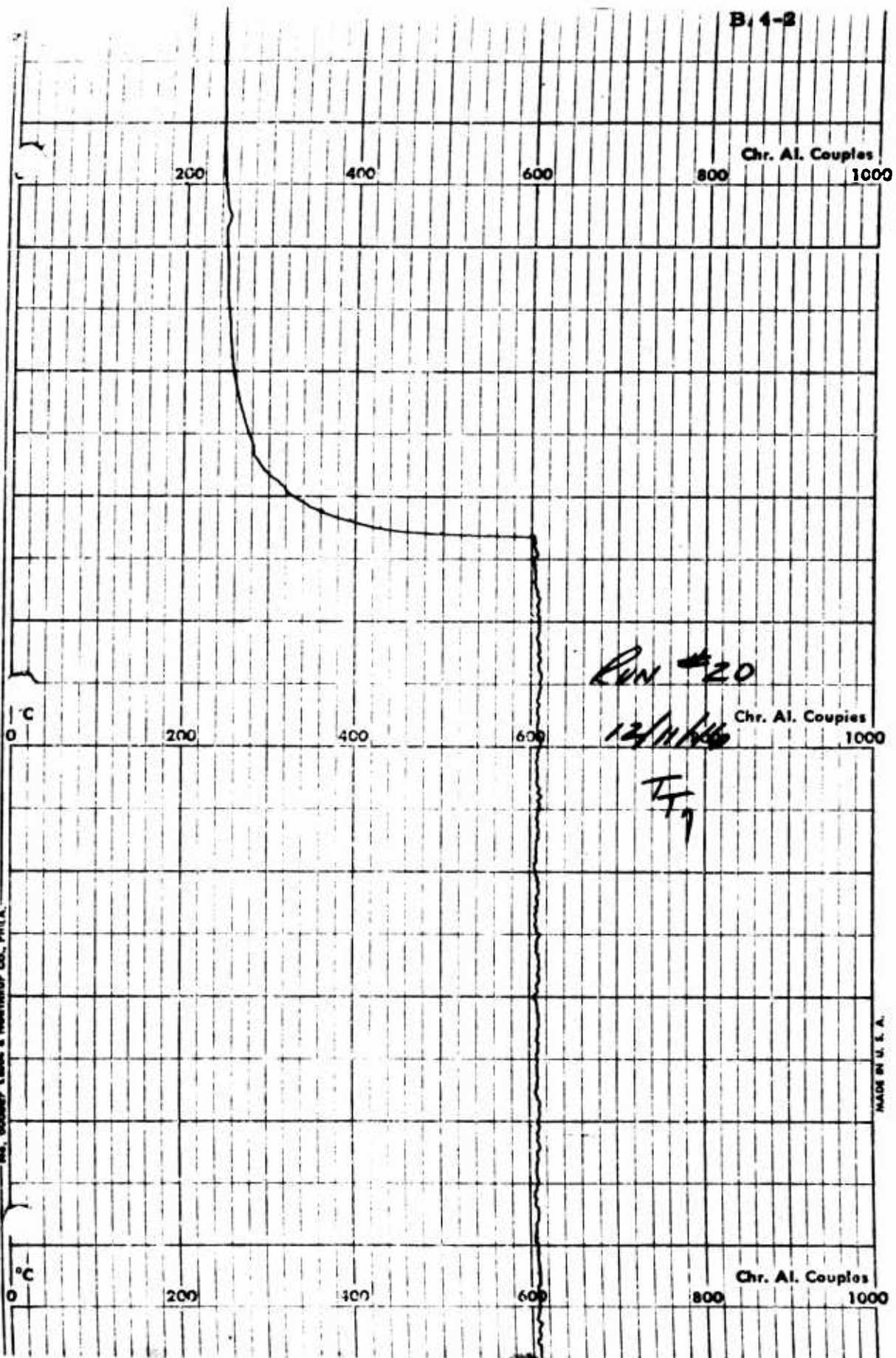
Transient

No. 600077 LEEDS & NORPLUP CO. PHILA.

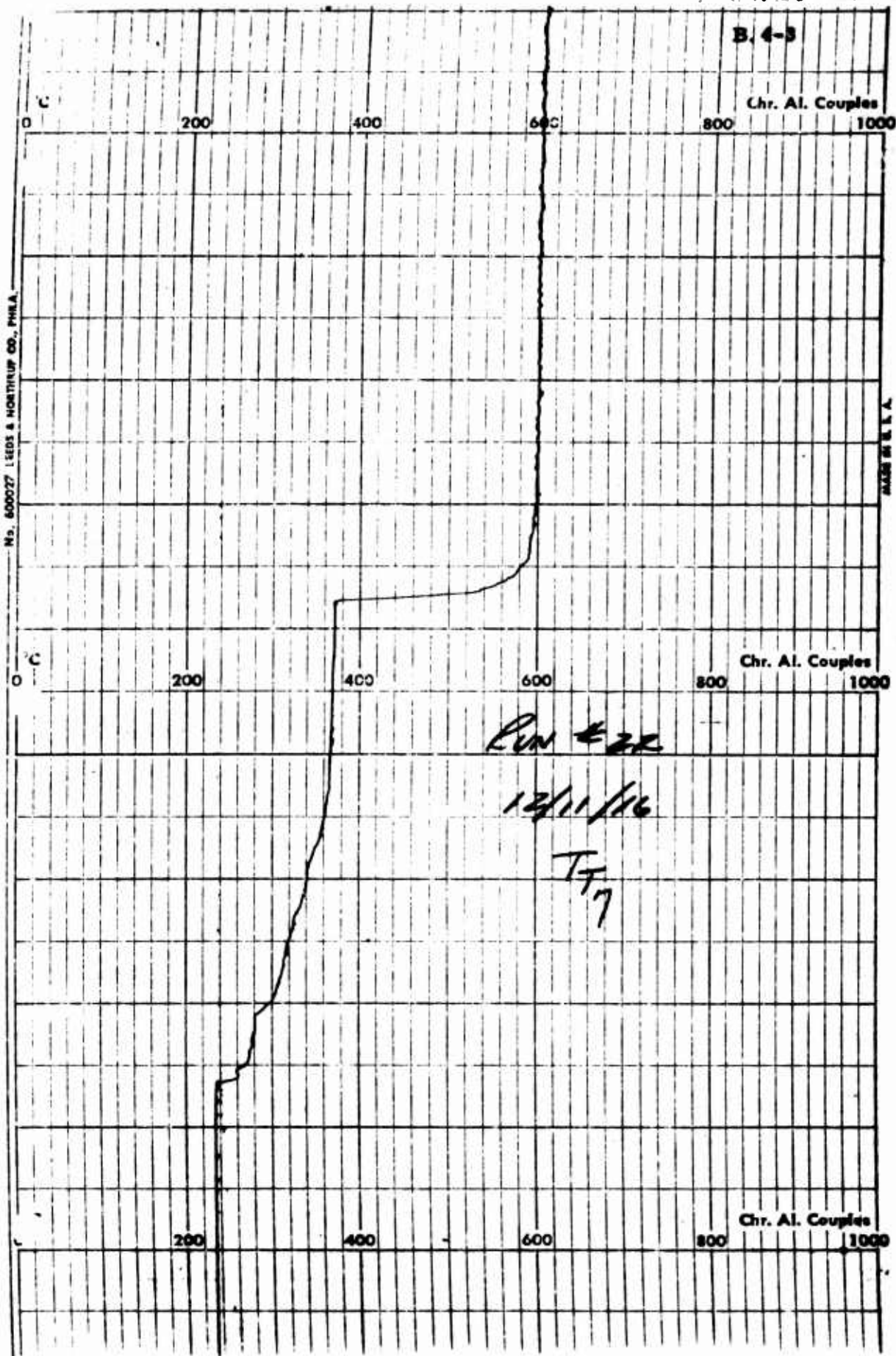
MADE IN U.S.A.

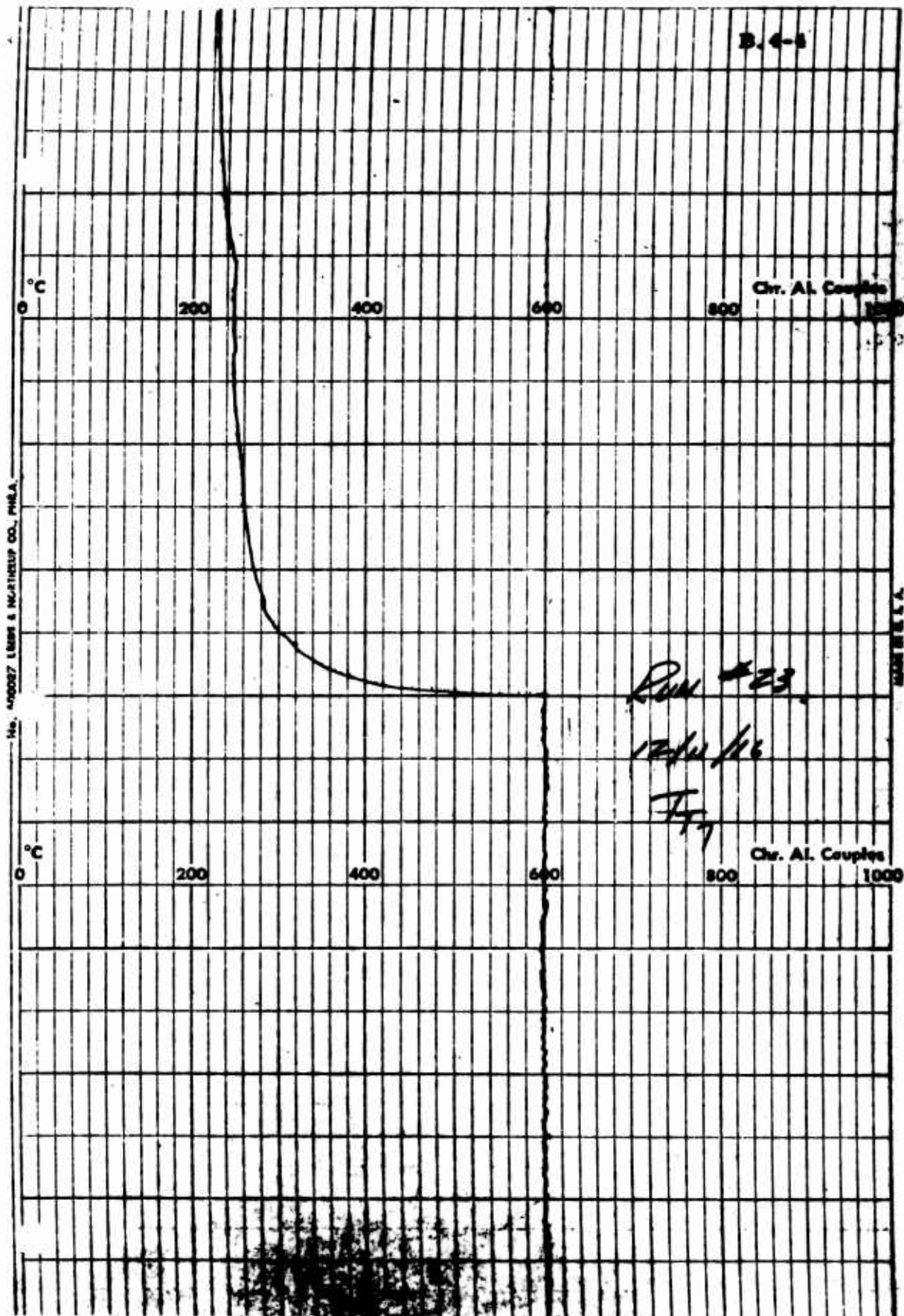
°C 0 200 400 600 800 1000 Chr. Al. Couples

B. 4-3

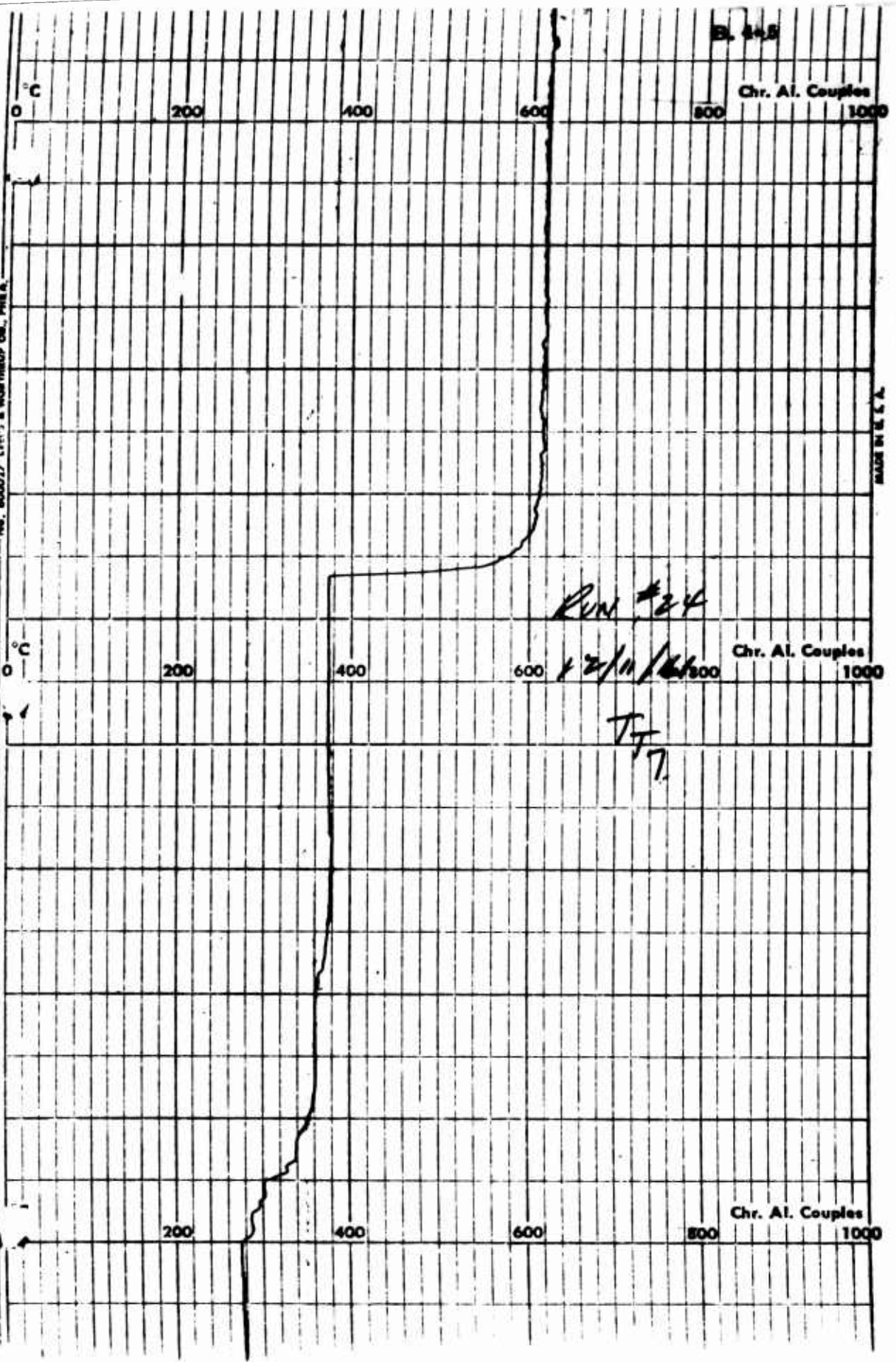


No. 800027 LEEDS & NORTHUP CO., PHILA.



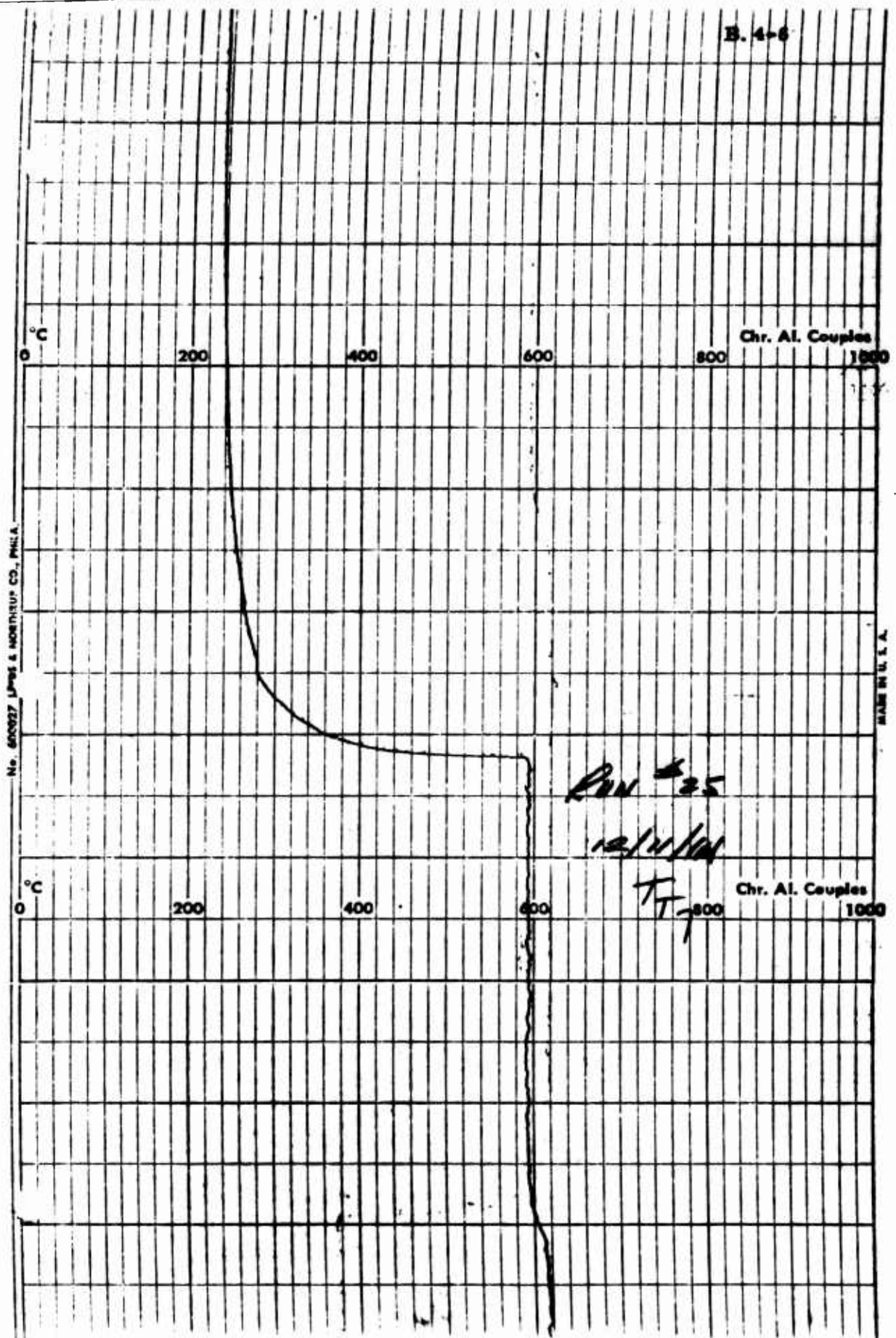


No. 600017 LEFC'S & HOUGHTON CO., PHIA.



MADE IN U.S.A.

B. 4-6



No. 60027 LIPS & MORTIMER CO., PHILA.

MADE IN U.S.A.

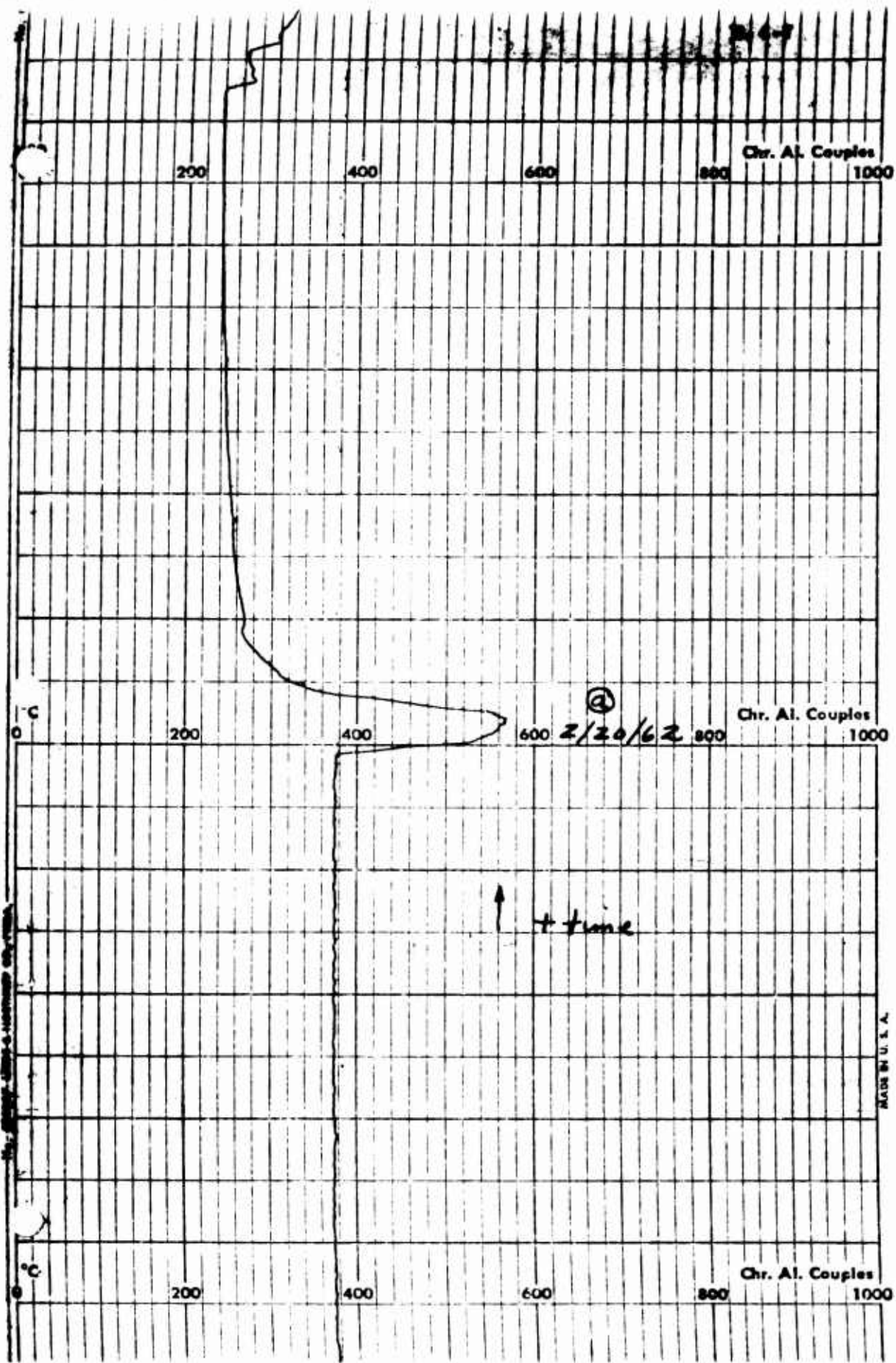
RUN # 25

12/14/64

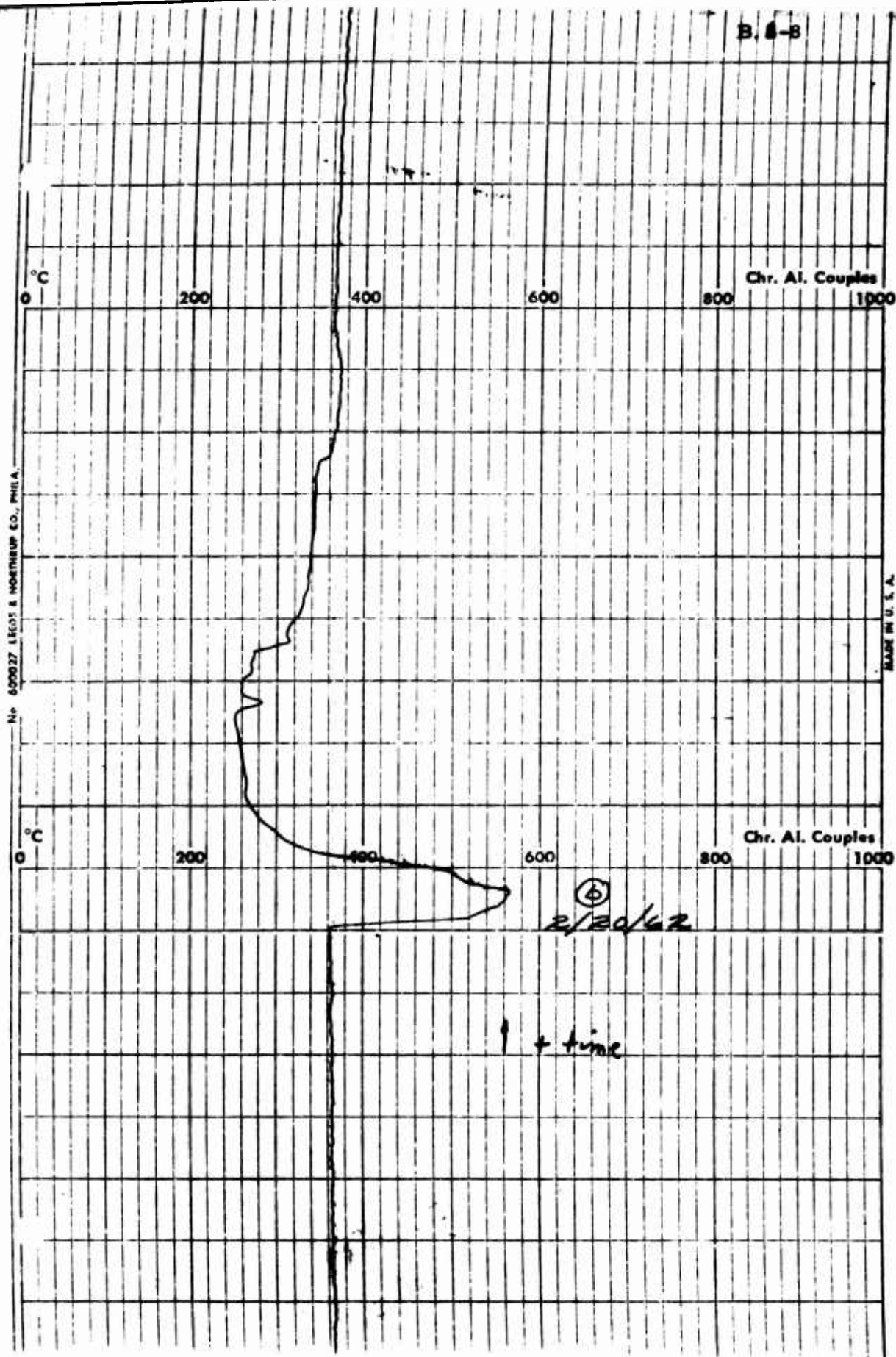
TT-800

Chr. Al. Couples

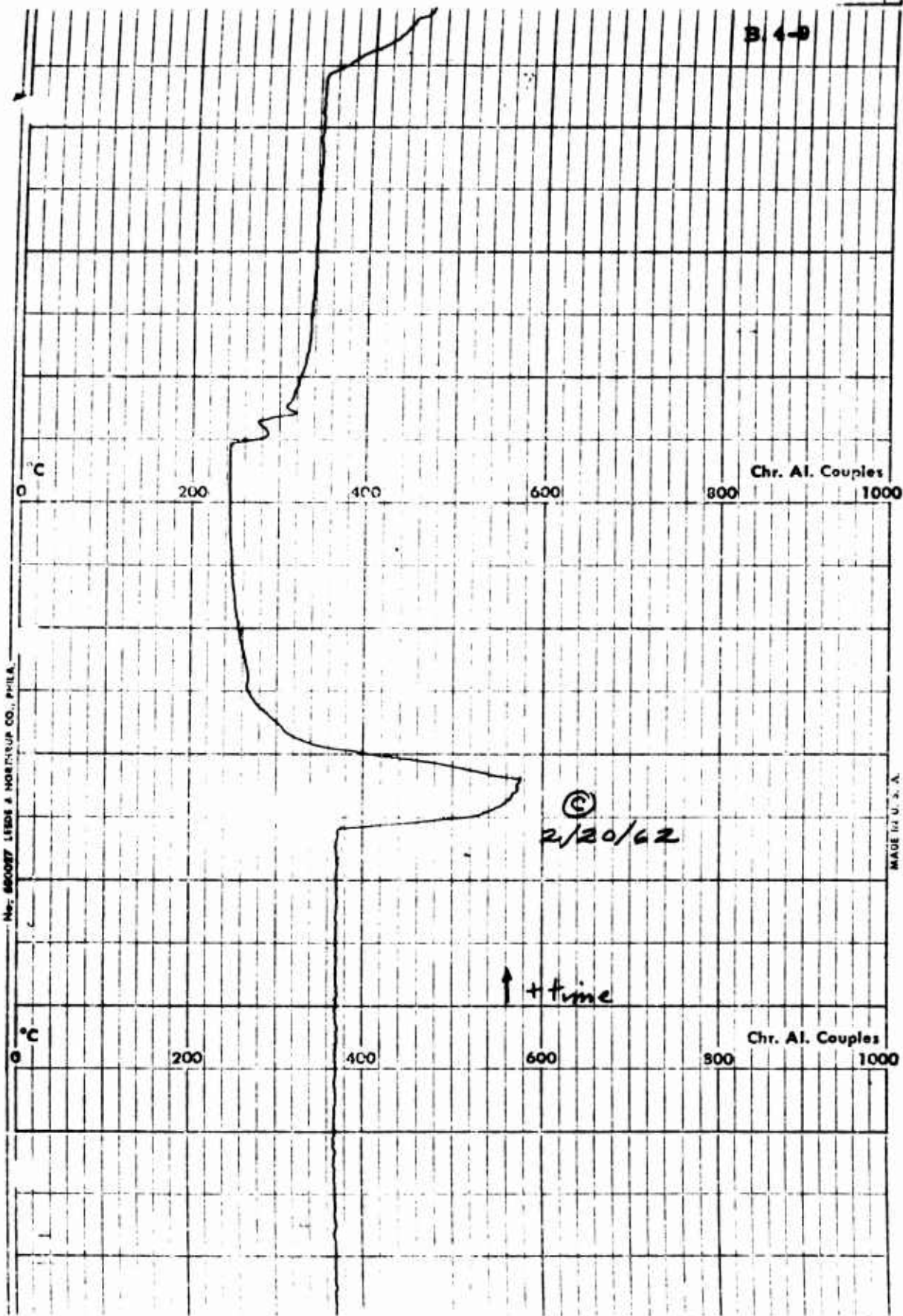
1000



B. 4-8



B. 4-9

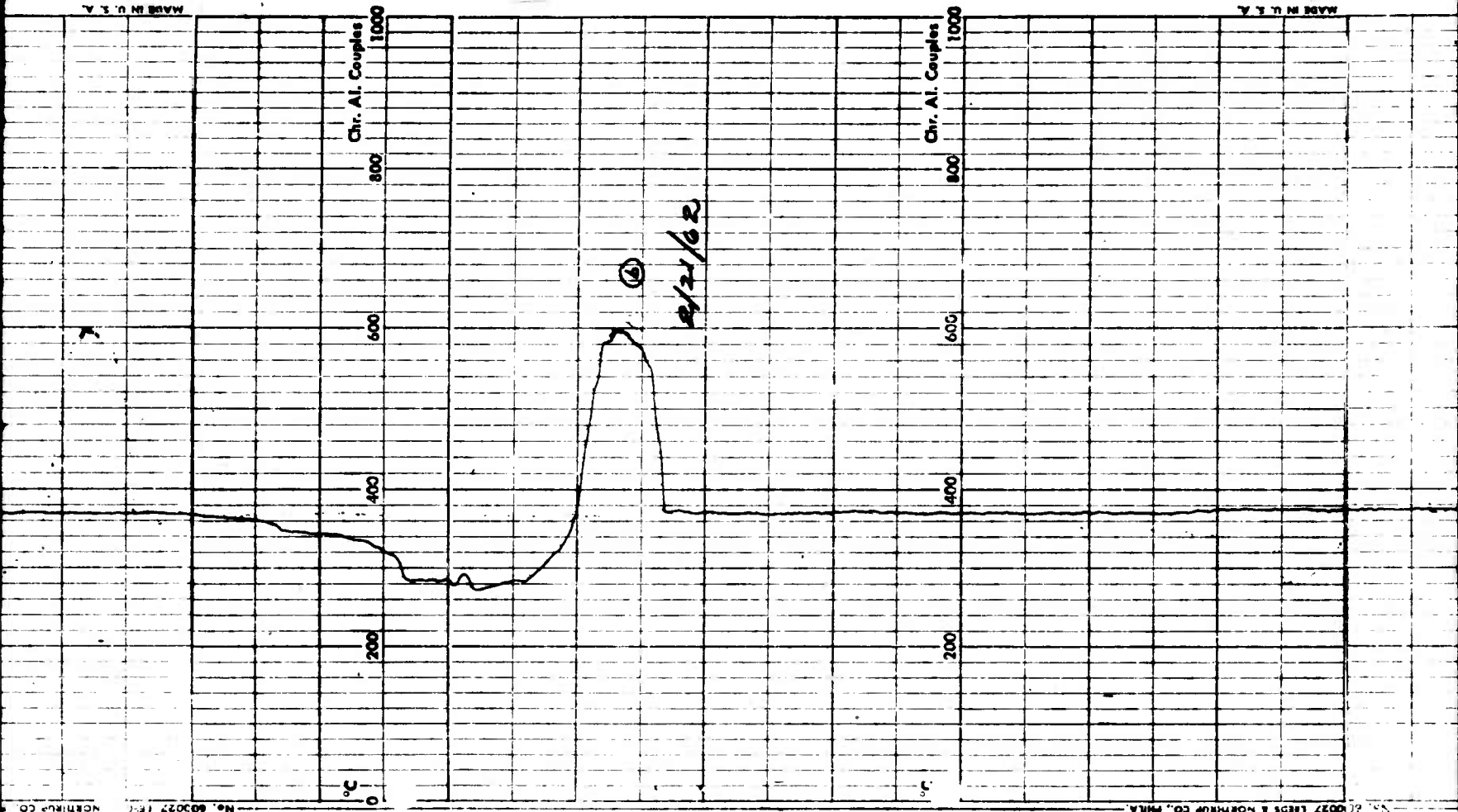


Mr. SCOTT LEBES & HORTON CO., PHILA.

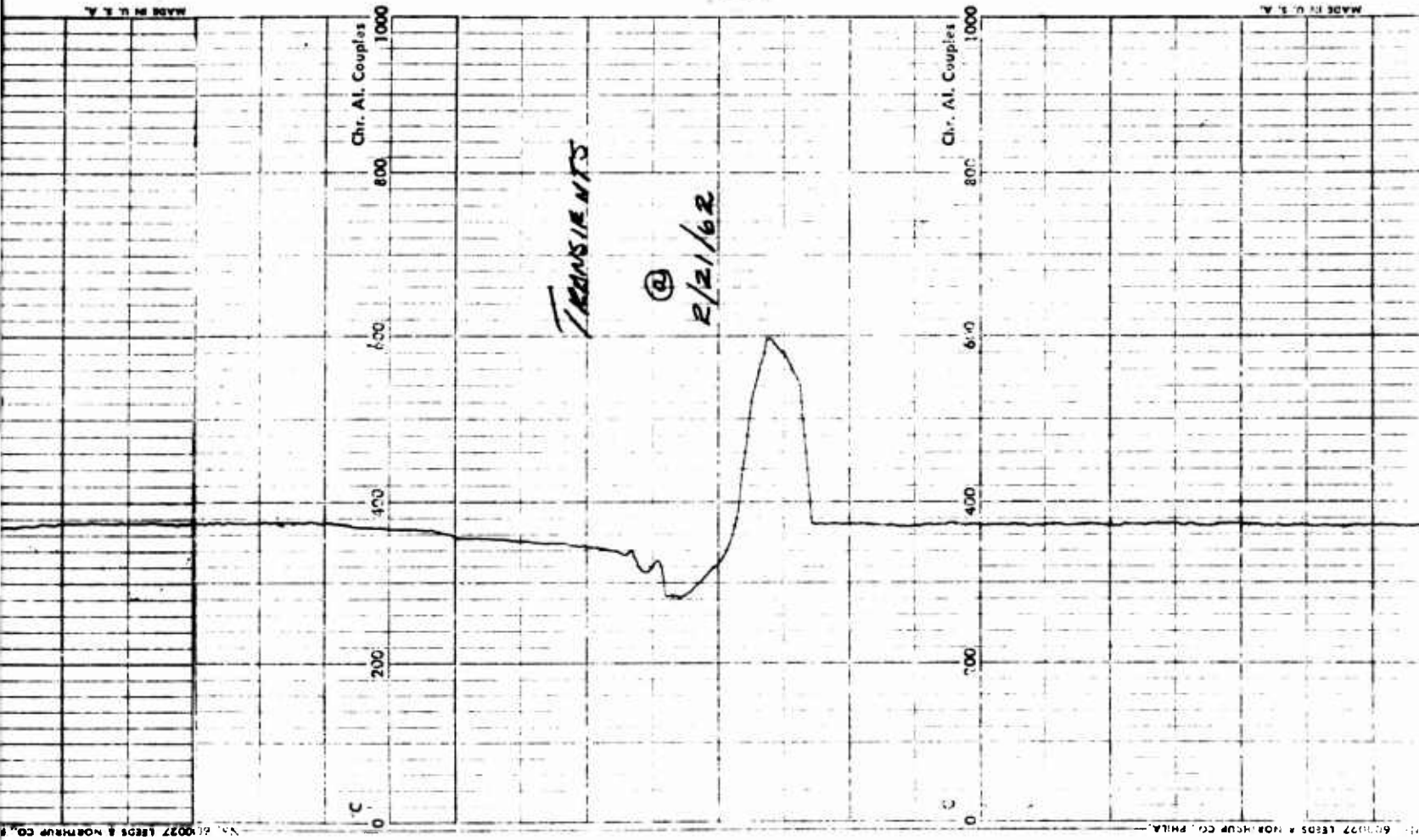
1

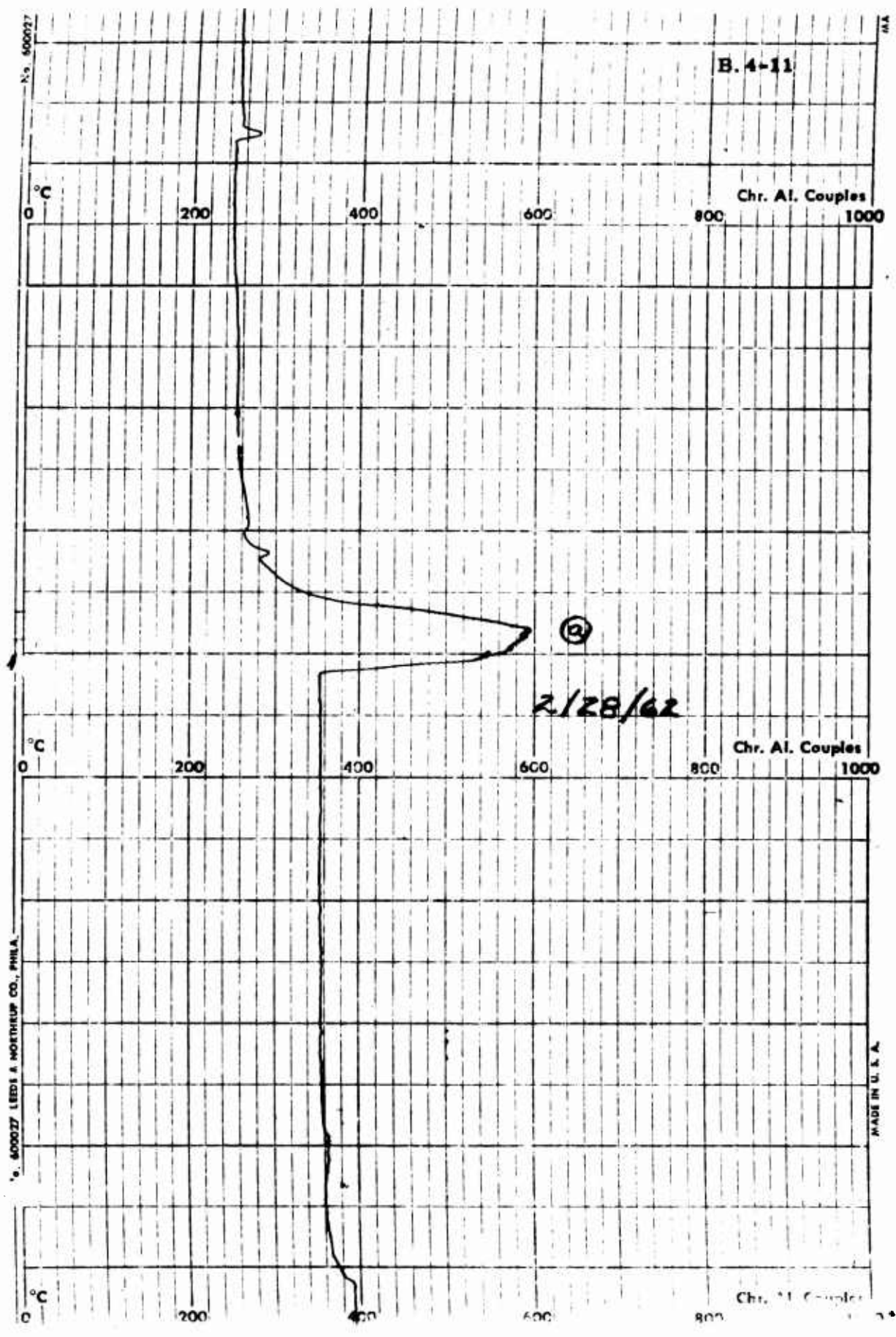


2



3

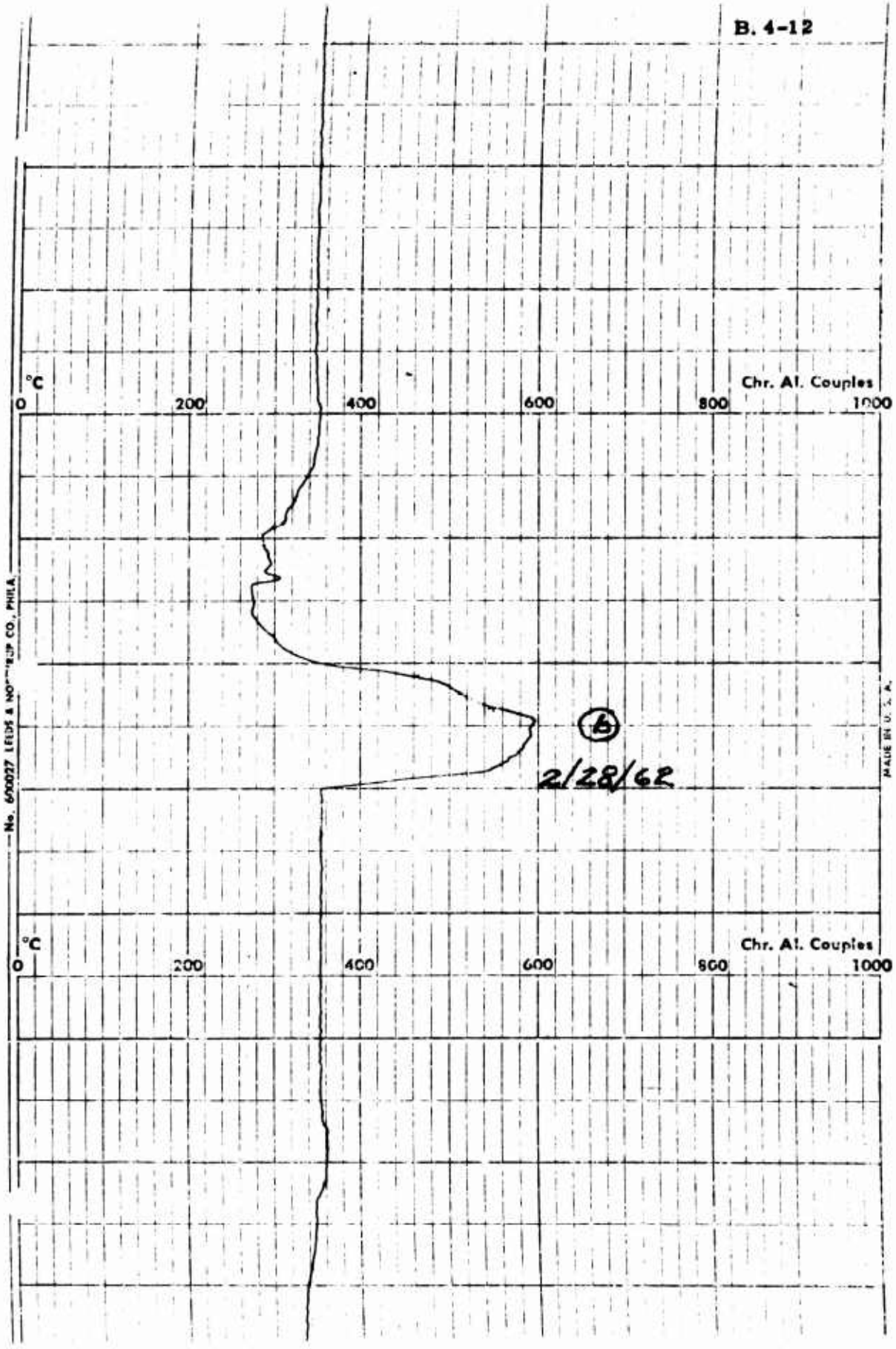




No. 400027 LEEDI & NORTHEUP CO., PHILA.

MADE IN U. S. A.

B. 4-12



No. 600027 1" x 1" NICHROME CO. PHIL.

°C

200

400

600

800

1000

Chr. Al. Couples

B. 4-13

MADE IN U. S. A.

°C

200

400

600

800

1000

Chr. Al. Couples

2/28/62

60-377 LTED. & NICHROME CO., PHILA.

MADE IN U. S. A.

B. 4-14

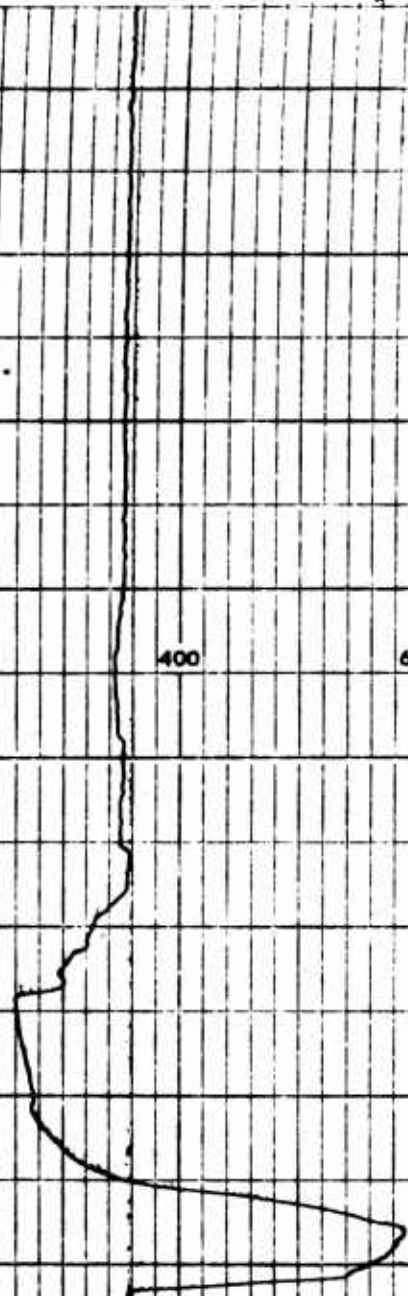
No. 600027 LIBBE & HORTSMAN PHILA.

LIBBE & HORTSMAN

0 °C 200 400 600 800 1000 Chr. Al. Couples

0 °C 200 400 600 800 1000 Chr. Al. Couples

HORTSMAN CO., PHILA.



(D)
2/28/62

B. 4-15

RENEW CHART

°C

0

200

400

600

800

1000

Chr. Al. Couplet

No. 670037 LEIDE & HORTHEUP CO. "U.S.A."

MADE IN U.S.A.

RENEW CHART

(E)

2/28/62

°C

0

200

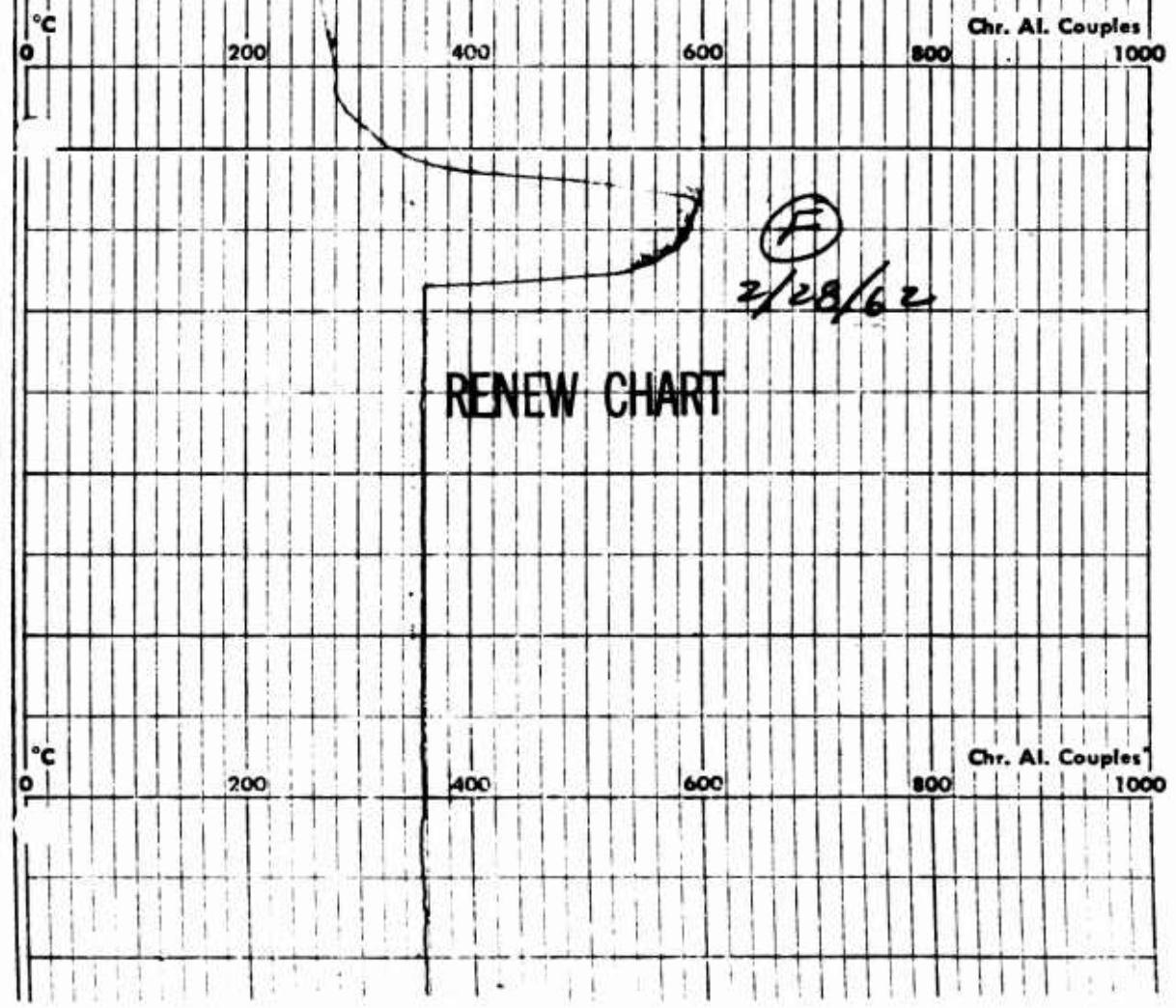
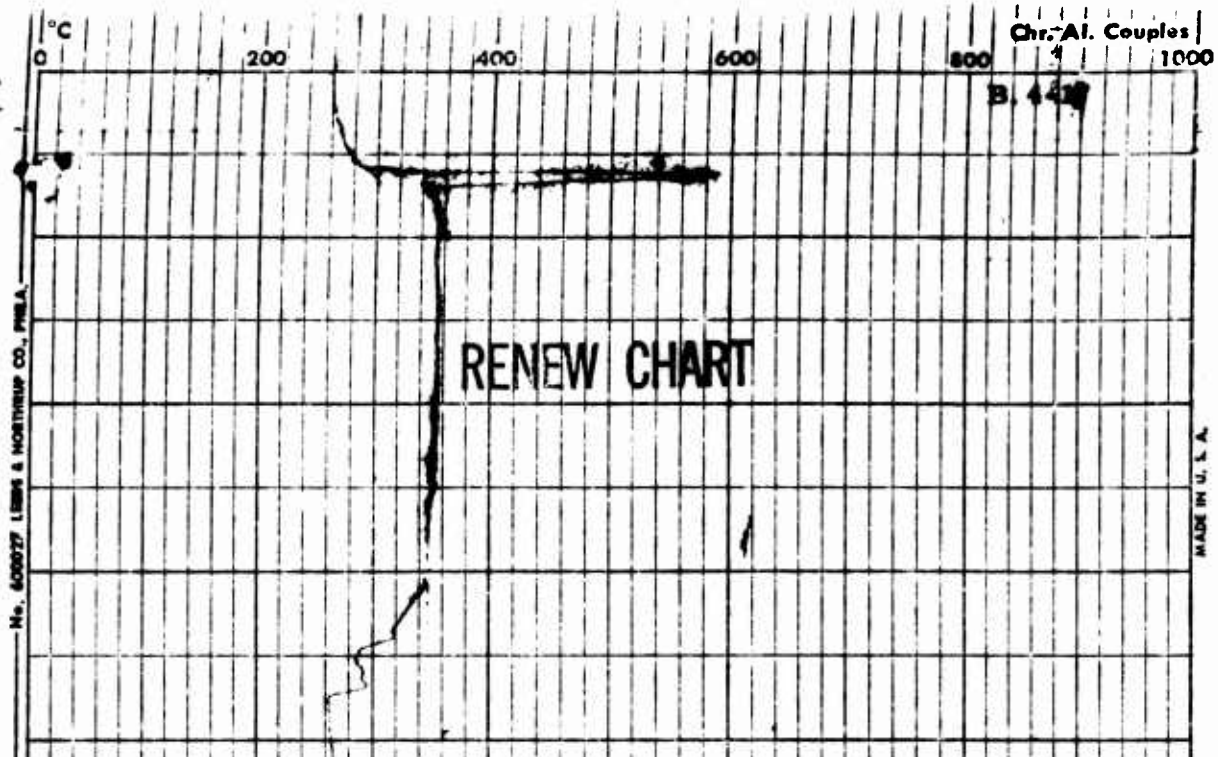
400

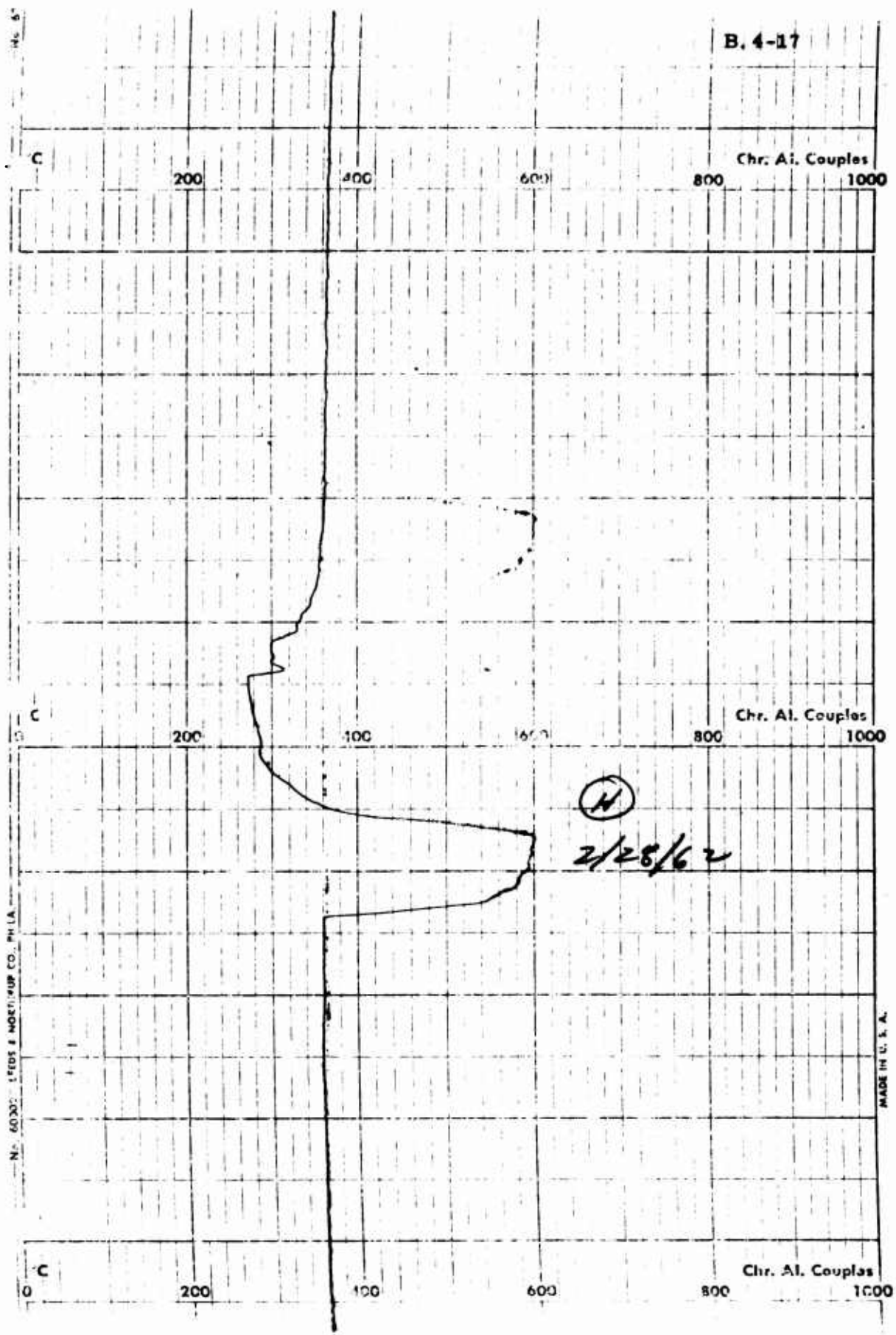
600

800

1000

Chr. Al. Couplet





B. 4-17

Chr. Al. Couples

200

400

600

800

1000

C

C

200

400

600

800

1000

Chr. Al. Couples

(H)

2/28/62

No. 60300 SEEDS & INSTRUM CO., PHILA.

MADE IN U. S. A.

C

200

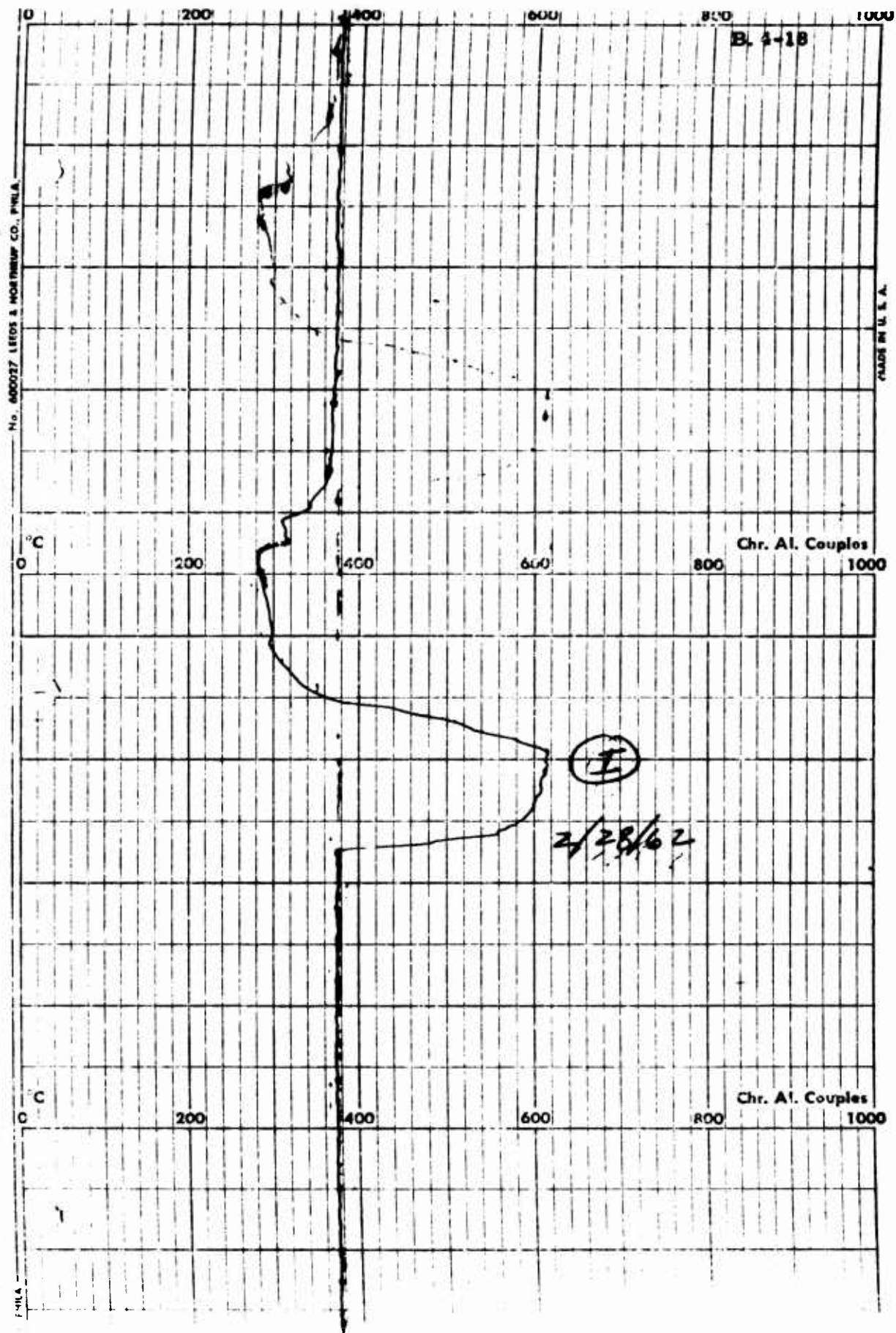
400

600

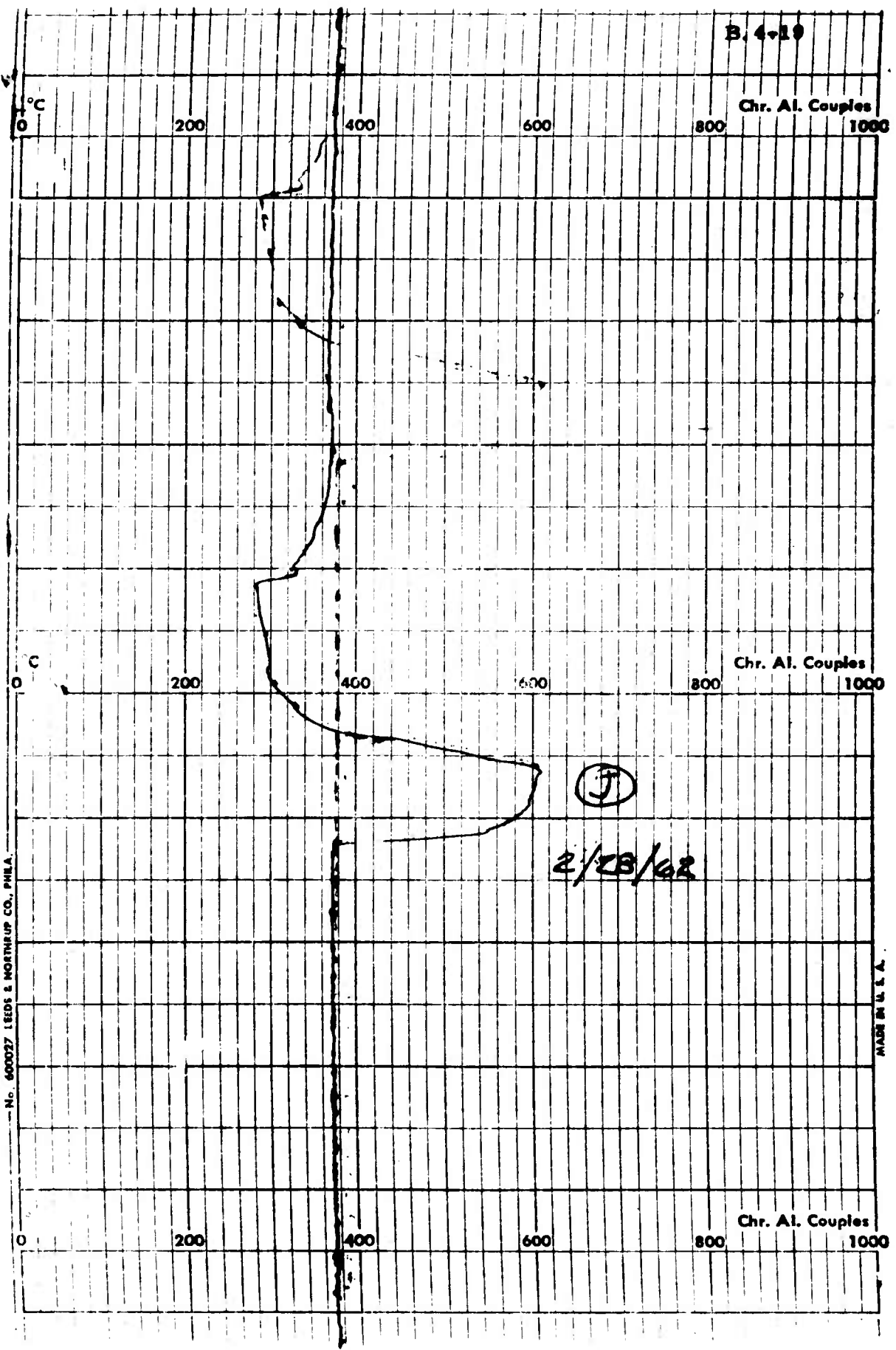
800

1000

Chr. Al. Couples



B. 4-19



No. 60027 LEEDS & NORTHUP CO., PHILA.

MADE IN U.S.A.

Chr. Al. Couples

Chr. Al. Couples

Chr. Al. Couples

°C

°C

B. 4-20

Chr. Al. Couples
1000

200

400

600

800

500
400
300
200
100
0

MADE IN U. S. A.

Chr. Al. Couples
1000

200

400

600

800

C

0

(K)

2/28/62

Chr. Al. Couples
1000

200

400

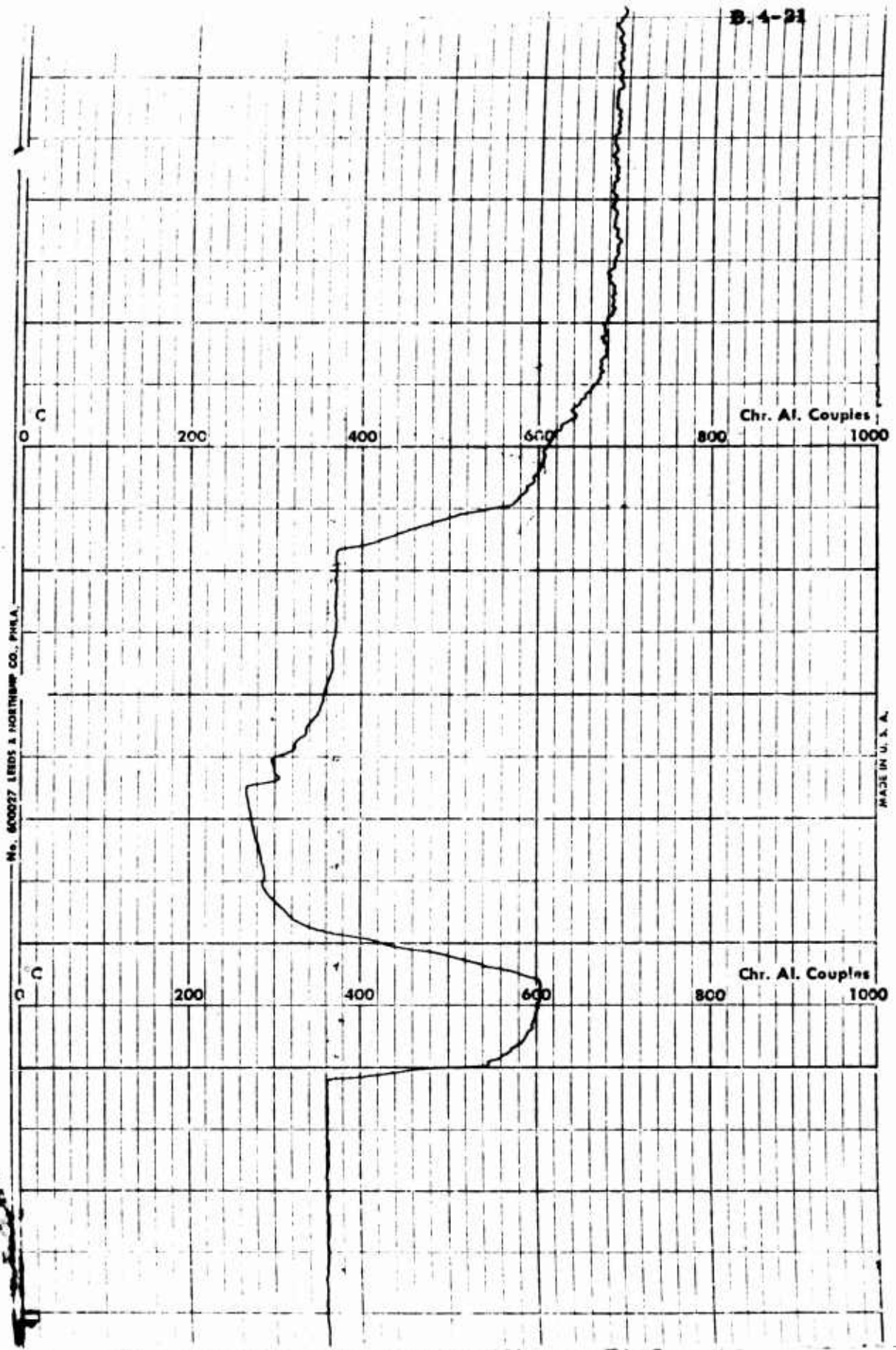
600

800

C

0

B. 4-21



APPENDIX C

METHOD OF CALCULATION; AREA AND MASS WEIGHTED PARAMETERS

C.1 AREA WEIGHTED VELOCITY

It is assumed that the velocity profile is a body of revolution determined graphically in a nondimensional form $(\frac{v}{v_c}) = f(\frac{r}{r_p})$ where v_c designates the velocity measured in the center of pipe, and r_p is the inside radius of the pipe. From the definition of the area weighted velocity,

$$v_{\text{area weighted}} = \frac{v_c}{A_{p0}} \int_0^{A_p} \left(\frac{v}{v_c}\right) dA = \frac{v_c}{r_p^2} \int_0^{r_p} \left(\frac{v}{v_c}\right) 2\pi r dr$$

or in a nondimensional form

$$v_{a.w} = \frac{v_c}{\pi} \int_0^{r_p} \left(\frac{v}{v_c}\right) 2\pi \left(\frac{r}{r_p}\right) d\left(\frac{r}{r_p}\right) = 2v_c \int_0^1 \left(\frac{v}{v_c}\right) \left(\frac{r}{r_p}\right) d\left(\frac{r}{r_p}\right) \quad (1)$$

the integral $\int_0^1 \left(\frac{v}{v_c}\right) \left(\frac{r}{r_p}\right) d\left(\frac{r}{r_p}\right)$ is found by measuring the area

under the curve $\left(\frac{v}{v_c}\right) = f\left(\frac{r}{r_p}\right)$ shown on Figures 5.1-8 and 5.1-9.

C. 2 MASS WEIGHTED TOTAL PRESSURE \overline{P}_T . (1)

By definition, the mass weighted total pressure is $\overline{P}_T = \frac{1}{W} \int_0^r \rho P_t dW$.

At $M = 0.3$, an equation for incompressible flow can be used with fair accuracy. This simplification leads to conservative solution.

$$P_T = P + \rho \frac{v^2}{2g} \tag{2}$$

Also, the weight flow is

$$W = \int_0^{r_p} \rho v (2 \pi r) dr. \tag{3}$$

Substituting (2) and (3) into (1)

$$\overline{P}_T \approx P + \frac{\rho \int_0^{r_p} v^3 r dr}{\int_0^{r_p} \rho v r dr}.$$

Expressed in nondimensional form, where $q_c = \frac{\rho v_c^2}{2g}$

$$\overline{P}_T = P + q_c \frac{\int_0^1 \left(\frac{v}{v_c}\right)^3 \left(\frac{r}{r_p}\right) d\left(\frac{r}{r_p}\right)}{\int_0^1 \left(\frac{v}{v_c}\right) \left(\frac{r}{r_p}\right) d\left(\frac{r}{r_p}\right)} \tag{4}$$

Both integrals in the above equation can be solved graphically as shown on Figures 5.1-8 and 5.1-9.

ANALYSIS _____

PREPARED BY _____

CHECKED BY _____

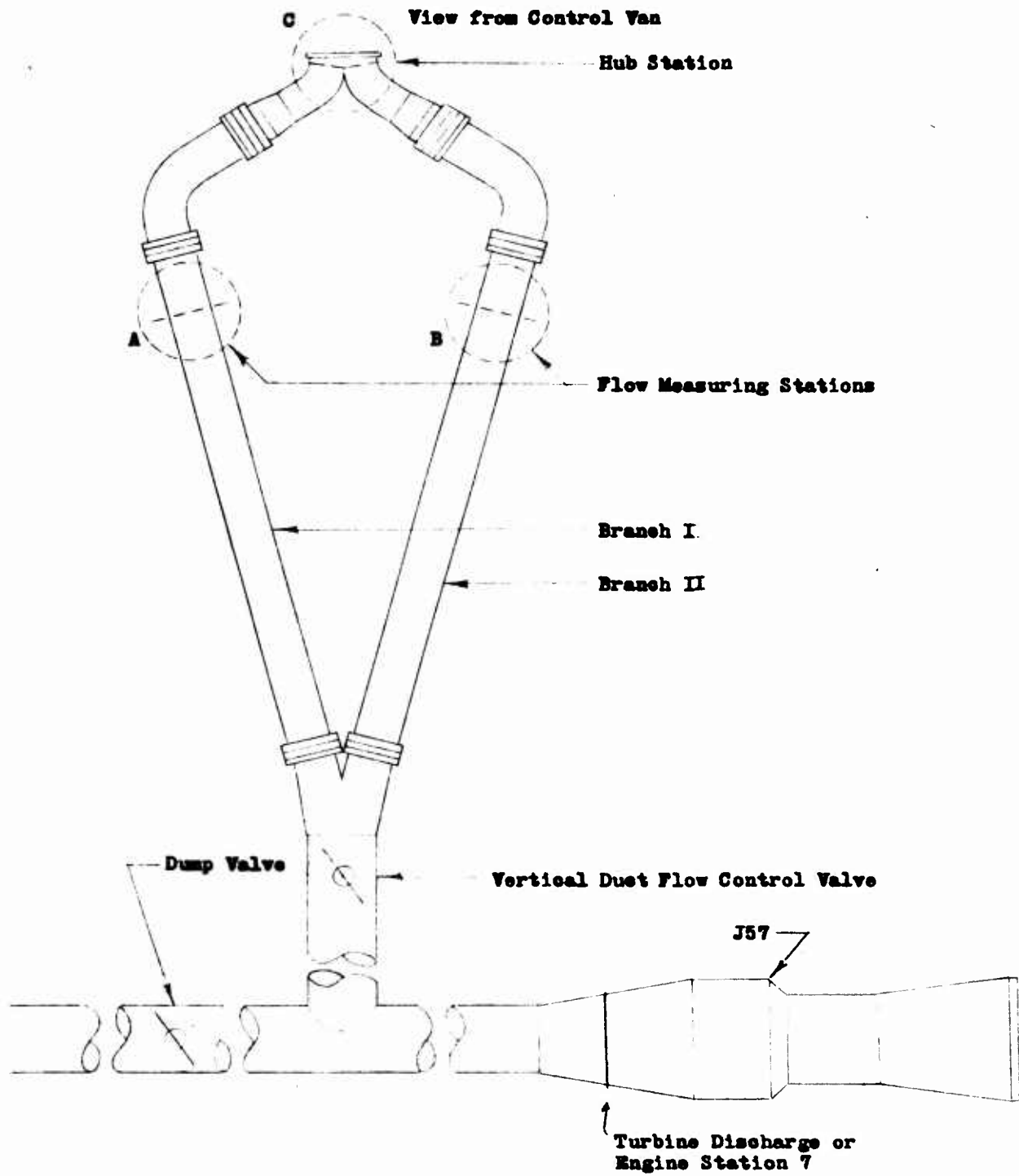
APPENDIX D

THERMODYNAMIC CALCULATION PROCEDURE; NON-ROTATING
 COMPONENTS

The various pressure and temperature measuring stations are shown in Figure D-1. Details of the various rakes are given by Figure D-2. The basic equations used in conjunction with these instrumentation locations are given in Reference 3.4-2 and the computer equation flow scheme is presented herein (see Appendix F for nomenclature).

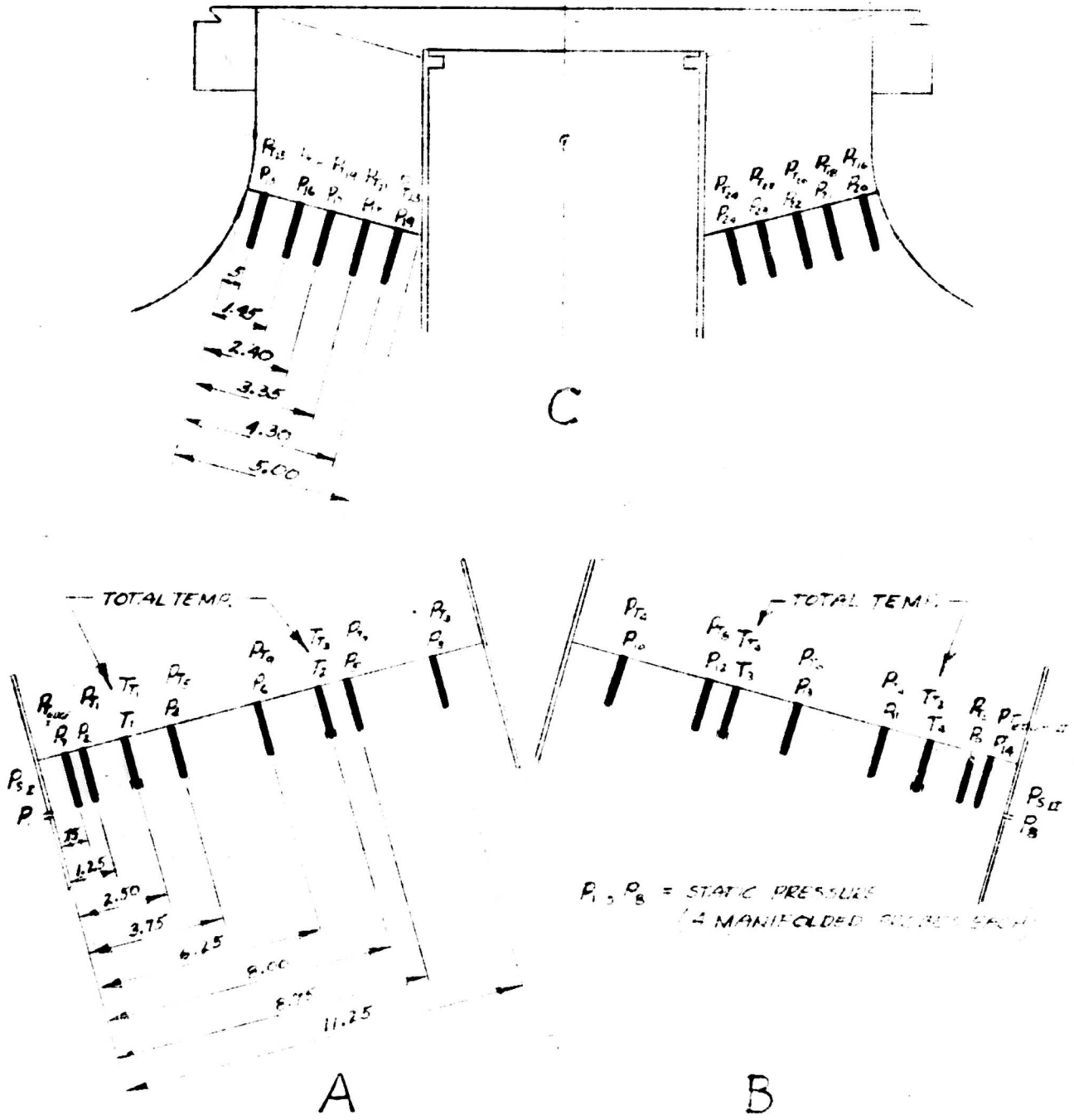
Due to the length of this calculation, the flow scheme follows steps e, a, b, c, d, f, g, h, i, j, k, l, m, n. Step "e" is misplaced as it was initially intended as part of an iterative procedure to determine the effect of water injection on δ and R which required the output of Steps "a" through "f" based on initially assumed values of δ and R. Since virtually all running was done without water injection, the iterative procedure is unnecessary when the output of Step "e" (no water injection) is used as input for Steps "a", "b", etc. The hub area weighted total pressure values of Steps "h" and "i" are used only for reference since the distortion of the velocity profile at that station does not permit accurate area weighted pressure values with the instrumentation provided. These values do provide a useful reference, however, and together with the results of Reference 3.4-2 help in determining the loss coefficients C_I' and C_{II}' .

FIGURE D-1

VERTICAL DUCTS SHOWING LOCATION OF FLOW
MEASURING AND HUB STATIONS

IDENTIFICATION OF PROBE LOCATIONS AT FLOW MEASURING AND HUB STATIONS

1. ALL PROBES ARE TOTAL PRESSURE EXCEPT AS NOTED
2. UPPER SYMBOLS USED IN ANALYSIS, CORRESPONDING LOWER SYMBOLS APPEAR IN READOUT.



Step a). Flow Rate - Branch I

Input: δ, R , from Step "e."

$$g = 32.17 \text{ ft/sec}^2$$

$$T_1 (^\circ\text{F}), T_2 (^\circ\text{F}), P_{\text{res}} (\text{in-Hg}), P_1 (\text{in-TBE}), P_6 (\text{in-TBE})$$

Calculation:

$$1. T_{fsI} = \frac{T_1 + T_2}{2} + 460; \text{ } ^\circ\text{R}$$

$$2. P_{\text{ref}} = P_{\text{res}} (70.721); \text{ psfa}$$

$$3. P_{fsI} = P_1 (15.365) + \textcircled{2}; \text{ psfa}$$

$$4. P_{fsI_{\text{max}}} = P_6 (15.365) + \textcircled{2}; \text{ psfa}$$

$$5. M_{fsI_{\text{max}}} = \sqrt{\frac{2}{\delta - 1} \left[\left(\frac{\textcircled{4}}{\textcircled{3}} \right)^{\frac{\delta - 1}{\gamma}} - 1 \right]}; \text{ dimensionless}$$

$$6. T_{fsI_{\text{max}}} = \frac{\textcircled{1}}{1 + \frac{\delta - 1}{2} \textcircled{5}}; \text{ } ^\circ\text{R}$$

$$7. a_{fsI_{\text{max}}} = \sqrt{\gamma g R \textcircled{6}}; \text{ ft/sec}$$

$$8. V_{fsI_{\text{max}}} = \textcircled{7} \textcircled{5}; \text{ ft/sec}$$

$$9. \rho_{fsI_{\text{max}}} = \frac{\textcircled{3}}{R \textcircled{6}}; \text{ #/ft}^3$$

$$10. \mu_{fsI_{\text{max}}} = \left[1.937348 + 1.786448 \times 10^{-2} \times \textcircled{1} - 4.170257 \times 10^{-6} \times \textcircled{1}^2 \right. \\ \left. + 5.805605 \times 10^{-10} \times \textcircled{1}^3 - 2.156955 \times 10^{-14} \times \textcircled{1}^4 \right] \\ \times [4.32 \times 10^{-3}]; \text{ #/in} \cdot \text{ft}$$

$$11. Re_{FSI_{max}} = \frac{(9)(8)(1.021)(3.6 \times 10^3)}{(10)}; \text{ dimensionless}$$

$$12. v_{FSI_{avg}} = Z_1 \times (8); \text{ ft/sec}$$

$$13. M_{FSI_{avg}} = \frac{(12)(5)}{(8)}; \text{ dimensionless}$$

$$14. T_{FSI_{avg}} = \frac{(1)}{1 + \frac{v-1}{2} (13)^2}; \text{ } ^\circ K$$

$$15. R_{FSI_{avg}} = \frac{(3)}{R(14)}; \text{ #/ft}^3$$

$$16. a_{FSI_{avg}} = \sqrt{gK(14)}; \text{ ft/sec}$$

$$17. (v_{FSI_{avg}})_{corrected} = (16)(13); \text{ ft/sec}$$

$$18. w_{FSI} = (15)(17)(0.818); \text{ #/sec}$$

Step 6). Flow Rate - Branch II

Input: v, R from Step "e"

$$g = 32.17 \text{ ft/sec}^2$$

$$T_3(^{\circ}F), T_4(^{\circ}F), P_3(\text{in-Hg}), P_4(\text{in-Hg})$$

Calculation:

$$19. T_{FSI_{II}} = \frac{T_3 + T_4 + 460}{2}; \text{ } ^\circ K$$

$$20. P_{FSI_{max}} = P_3(15.365) + (2); \text{ psfa}$$

$$21. P_{f_{sII} \max} = P_{15} (15.365) + 2 ; \text{ psfa}$$

$$22. M_{f_{sII} \max} = \sqrt{\frac{2}{\gamma-1} \left[\left(\frac{21}{20} \right)^{\frac{\gamma-1}{\gamma}} - 1 \right]} ; \text{ dimensionless}$$

$$23. T_{f_{sII} \max} = \frac{19}{1 + \frac{\gamma-1}{2} (22)^2} ; \text{ } ^\circ\text{R}$$

$$24. a_{f_{sII} \max} = \sqrt{\gamma g R (23)} ; \text{ ft/sec}$$

$$25. v_{f_{sII} \max} = (24) (22) ; \text{ ft/sec}$$

$$26. P_{f_{sII} \max} = \frac{(20)}{R (23)} ; \text{ } \#/\text{ft}^3$$

$$27. \rho_{f_{sII} \max} = \text{Eq. 10 with } \textcircled{1} \text{ replaced by } \textcircled{19} \text{ therein}$$

$$28. K_{e_{f_{sII} \max}} = \frac{(20) (25) (1.021) (3.6 \times 10^3)}{(27)} ; \text{ dimensionless}$$

$$29. v_{f_{sII} \text{ avg}} = F_2 \times (25) ; \text{ ft/sec}$$

$$30. M_{f_{sII} \text{ avg}} = \frac{(29) (22)}{(25)} ; \text{ dimensionless}$$

$$31. T_{f_{sII} \text{ avg}} = \frac{19}{1 + \frac{\gamma-1}{2} (30)^2} ; \text{ } ^\circ\text{R}$$

32. } Not Used

33. }

$$34. P_{f_{sII} \text{ avg}} = \frac{29}{R (31)} ; \text{ } \#/\text{ft}^3$$

$$35. a_{fs_{avg}} = \sqrt{rgK(37)}; \text{ ft/sec}$$

$$36. (U_{fs_{II}})_{avg} \text{ corrected} = (35)(30); \text{ ft/sec}$$

$$37. w_{fs_{II}} = (32)(36)(0.818); \text{ ft/sec}$$

$$38. w_{TOT} = (18) + (37); \text{ ft/sec}$$

Step c). Velocity Profile - Branch I

Input: P_2 (in-TBE), P_3 (in-TBE), P_4 (in-TBE), P_5 (in-TBE),
 P_6 (in-TBE), P_7 (in-TBE)

Calculation:

$$39. P_{T_{I1}} = P_2(15.365) + (2); \text{ psfa}$$

$$40. P_{T_{I2}} = P_3(15.365) + (2); \text{ psfa}$$

$$41. P_{T_{I3}} = P_4(15.365) + (2); \text{ psfa}$$

$$42. P_{T_{I4}} = P_5(15.365) + (2); \text{ psfa}$$

$$43. P_{T_{I5}} = P_6(15.365) + (2); \text{ psfa}$$

$$44. P_{T_{I6}} = P_7(15.365) + (2); \text{ psfa}$$

$$45. M_1 = \sqrt{\frac{2}{\gamma-1} \left[\left(\frac{30}{3} \right)^{\frac{\gamma-1}{\gamma}} - 1 \right]}; \text{ dimensionless}$$

$$46. M_{2I} = \sqrt{\frac{2}{\gamma-1} \left[\left(\frac{40}{3} \right)^{\frac{\gamma-1}{\gamma}} - 1 \right]}; \text{ dimensionless}$$

$$47. M_{5I} = \frac{40}{3} \text{ etc} \quad "$$

$$48. M_{7I} = \frac{42}{3} \quad "$$

$$49. M_{9I} = \frac{42}{3} \quad "$$

$$50. M_{E1} = \frac{44}{3} \quad "$$

$$51. \left(\frac{U_1}{U_{max}} \right)_I = \frac{45}{49} \quad "$$

$$52. \left(\frac{U_3}{U_{max}} \right)_I = \frac{46}{49} \quad "$$

$$53. \left(\frac{U_5}{U_{max}} \right)_I = \frac{47}{49} \quad "$$

$$54. \left(\frac{U_7}{U_{max}} \right)_I = \frac{48}{49} \quad "$$

$$55. \left(\frac{U_9}{U_{max}} \right)_I = \frac{49}{49} \quad "$$

$$56. \left(\frac{U_{E1}}{U_{max}} \right)_I = \frac{50}{49} \quad "$$

Step d). Velocity Profile - Branch II

Input: P_9 (in-TISE), P_{10} (in-TISE), P_{11} (in-TISE), P_{12} (in-TISE),
 P_{13} (in-TISE); T_{12} (in-TISE)

$$57. P_{T_2} = P_9 (15.365) + \textcircled{2}; \text{ psfa}$$

$$58. P_{T_4} = P_{10} (15.365) + \textcircled{2}; \text{ psfa}$$

$$59. P_{T_6} = P_{11} (15.365) + \textcircled{2}; \text{ psfa}$$

$$60. P_{T_8} = P_{12} (15.365) + \textcircled{2}; \text{ psfa}$$

$$61. P_{T_{10}} = P_{13} (15.365) + \textcircled{2}; \text{ psfa}$$

$$62. P_{T_{12}} = P_{14} (15.365) + \textcircled{2}; \text{ psfa}$$

$$63. M_{T_2} = \sqrt{\frac{2}{8-1} \left[\left(\frac{\textcircled{57}}{\textcircled{20}} \right)^{T-1} - 1 \right]}; \text{ dimensionless}$$

$$64. M_{T_4} = \frac{\textcircled{58}}{\textcircled{20}} \text{ etc}$$

$$65. M_{T_6} = \frac{\textcircled{59}}{\textcircled{20}}$$

$$66. M_{T_8} = \frac{\textcircled{60}}{\textcircled{20}}$$

$$66.a. M_{T_{10}} = \frac{\textcircled{61}}{\textcircled{20}}$$

$$67. M_{T_{12}} = \frac{\textcircled{62}}{\textcircled{20}}$$

$$68. \left(\frac{V_2}{V_{max}} \right)_{II} = \frac{\textcircled{63}}{\textcircled{64}}$$

$$69. \left(\frac{U_4}{U_{\max}} \right)_{II} = \frac{64}{662} ; \text{ dimensionless}$$

$$70. \left(\frac{U_6}{U_{\max}} \right)_{II} = \frac{65}{662} \quad "$$

$$71. \left(\frac{U_8}{U_{\max}} \right)_{II} = \frac{66}{662} \quad "$$

$$72. \left(\frac{U_{10}}{U_{\max}} \right)_{II} = \frac{662}{662} \quad "$$

$$73. \left(\frac{U_{EII}}{U_{\max}} \right)_{II} = \frac{67}{662} \quad "$$

Step e). Engine Parameters

Input: w_f (#/sec); T_{T_2} ($^{\circ}K$), T_{T_7} ($^{\circ}K$)

$$74. \text{ for } 500^{\circ}K < T_{T_2} \leq 1000^{\circ}K$$

$$h_{T_2} = 120.42 + (0.2477)(T_{T_2} - 500); \text{ Btu/\#}$$

$$75. \text{ (a) for } 500^{\circ}K < T_{T_7} \leq 1000^{\circ}K$$

$$h_{T_7} = 120.42 + (0.2477)(T_{T_7} - 500); \text{ Btu/\#}$$

$$\text{(b) for } 1000^{\circ}K < T_{T_7} \leq 1500^{\circ}K$$

$$h_{T_7} = 244.25 + (0.2627)(T_{T_7} - 1000); \text{ Btu/\#}$$

$$\text{(c) for } 1500^{\circ}K < T_{T_7} \leq 2250^{\circ}K$$

$$h_{T_7} = 375.62 + (0.2819)(T_{T_7} - 1500); \text{ Btu/\#}$$

$$76. w_7 = \frac{(17,664 - 75)}{(75 - 11)} w_f ; \text{ \# / sec}$$

$$77. \frac{w_f}{w_a} = \frac{w_f}{(76) - w_f}; \text{ dimensionless}$$

$$78. \% \text{ Air} = \frac{0.0677 \times 100}{(77)}; \%$$

$$79. R = [0.0095 (77) + 53.34]; \text{ ft}^2/\text{OR}$$

$$80. \text{ (a) for } 360^\circ\text{R} < T_{T_7} \leq 990^\circ\text{R}$$

$$c_p = (0.2430 - 0.08 (77)) - (0.00343 - 0.115 (77)) \left(\frac{5 T_{T_7}}{900} \right) + (0.0008 - 0.008 (77)) \left(\frac{5 T_{T_7}}{900} \right)^2; \text{ Btu}/\#^\circ\text{R}$$

$$\text{ (b) for } 990^\circ\text{R} < T_{T_7} \leq 1530^\circ\text{R}$$

$$c_p = (0.2170 + 0.157 (77)) + (0.0057 + 0.0267 (77)) \left(\frac{5 T_{T_7}}{900} \right); \text{ Btu}/\#^\circ\text{R}$$

$$\text{ (c) for } 1530^\circ\text{R} < T_{T_7} \leq 6300^\circ\text{R}$$

$$c_p = (0.3340 + 0.0 (77)) - \left\{ \frac{0.834 + 7.6 (77) + 10 (77)^2}{\frac{5 T_{T_7}}{900} + 3.65 + 20 (77)} \right\}; \text{ Btu}/\#^\circ\text{R}$$

$$81. \text{ for } T_{T_7} < 2700^\circ\text{R}$$

$$c_v = c_p - 0.06855$$

$$82. \gamma = \frac{(80)}{(81)}$$

Step f). Flow Measuring Station Mass Weighted Mean Total Pressure; Branch I

Input: All values are taken from previous steps

Calculation:

$$83. \bar{P}_{T_{fs1}} = \textcircled{3} \left\{ 1 + X_1 \left[1 + \frac{1}{2(\textcircled{82}-1)} \left(\frac{\textcircled{1}}{\textcircled{6}} - 1 \right) \right] \frac{\textcircled{8}^2}{32.17 \textcircled{79} \textcircled{6}} \right\}, \text{psfa}$$

Step g). Flow Measuring Station Mass Weighted Mean Total Pressure; Branch II

Input: All values are taken from prior steps

Calculation:

$$84. \bar{P}_{T_{fs2}} = \textcircled{20} \left\{ 1 + X_2 \left[1 + \frac{1}{2(\textcircled{82}-1)} \left(\frac{\textcircled{19}}{\textcircled{25}} - 1 \right) \right] \frac{\textcircled{29}^2}{32.17 \textcircled{79} \textcircled{23}} \right\}, \text{psfa}$$

Step h). Hub Station Area Weighted Total Pressure; Branch I

Input: P_{15} (in-TSE), P_{16} (in-TSE), P_{17} (in-TSE), P_{18} (in-TSE)
 P_{19} (in-TSE)

Calculation:

$$85. P_{T_{15}} = P_{15} (15.365) + \textcircled{2}, \text{psfa}$$

$$86. P_{T_{17}} = P_{16} (15.365) + \textcircled{2}, \text{psfa}$$

$$87. P_{T_{19}} = P_{17} (15.365) + \textcircled{2}, \text{psfa}$$

$$88. P_{T_{21}} = P_{18} (15.365) + \textcircled{2} ; \text{psfa}$$

$$89. P_{T_{23}} = P_{19} (15.365) + \textcircled{2} ; \text{psfa}$$

$$90. \left(P_{T_{\text{hub I}}} \right)_{aw} = 0.298 \textcircled{85} + 0.192 \textcircled{86} + 0.169 \textcircled{87} \\ + 0.146 \textcircled{88} + 0.195 \textcircled{89} ; \text{psfa}$$

Step c) Hub Station Area Weighted Total Pressure; Branch II

Input: P_{20} (in-TBE), P_{21} (in-TBE), P_{22} (in-TBE), P_{23} (in-TBE),
 P_{24} (in-TBE), P_{T_7} (in-Hg)

Calculation:

$$91. P_{T_{16}} = P_{20} (15.365) + \textcircled{2} ; \text{psfa}$$

$$92. P_{T_{18}} = P_{21} (15.365) + \textcircled{2} ; \text{psfa}$$

$$93. P_{T_{20}} = P_{22} (15.365) + \textcircled{2} ; \text{psfa}$$

$$94. P_{T_{22}} = P_{23} (15.365) + \textcircled{2} ; \text{psfa}$$

$$95. P_{T_{24}} = P_{24} (15.365) + \textcircled{2} ; \text{psfa}$$

$$96. \left(P_{T_{\text{hub II}}} \right)_{aw} = 0.298 \textcircled{91} + 0.192 \textcircled{92} + 0.169 \textcircled{93} \\ + 0.146 \textcircled{94} + 0.195 \textcircled{95} ; \text{psfa}$$

$$97. \left(P_{T_{\text{hub}}} \right)_{aw} = \frac{\textcircled{90} + \textcircled{96}}{2} ; \text{psfa}$$

$$98. P_{T_1} = P_{T_1} (70.721) ; \text{psfa}$$

$$98a. C_I = \frac{\bar{P}_{T_{fsI}} - (P_{T_{hubI}})_{aw}}{P_{T_1}} = \frac{(83) - (90)}{(98)} ; \text{dimensionless}$$

$$98b. C_{II} = \frac{\bar{P}_{T_{fsII}} - (P_{T_{hubII}})_{aw}}{P_{T_1}} = \frac{(81) - (96)}{(98)} ; \text{dimensionless}$$

Step j) Hub Station Total Pressure; Mass Weighted;
Calculated; Branch I.

Input: C_I' , assumed value based on prior run values
of C_I above plus results of full scale mock up test

Calculation:

$$99. \bar{P}_{T_{hubI}} = (83) - C_I' (98) ; \text{psfa}$$

Step k). Hub Station Total Pressure; Mass Weighted;
Calculated; Branch II.

Input: C_{II}' , assumed value based on prior run values
of C_{II} above plus results of full scale mock up test

Calculation:

$$100. \bar{P}_{T_{hubII}} = (81) - C_{II}' (98) ; \text{psfa}$$

Step l) Hub Station Parameters for Input to Polytropic
Compressant Subroutine

Input: δ_1, δ_2

Calculations:

$$100a. \bar{P}_{hub} = \frac{99 + 100}{2}; \text{ psfa}$$

$$100b. \bar{T}_{hub} = \frac{0 + 19}{2}; \text{ } ^\circ R$$

100c. Not Used

$$100d. T_{TIP} = 1000 - 5; \text{ } ^\circ R$$

Step m). Total Pressure Loss Parameters; Branch I

Input: All values are taken from previous steps

Calculations:

$$101. \frac{P_{T7} - \bar{P}_{F5I}}{P_{T7}} = \frac{98 - 83}{98}; \text{ dimensionless}$$

$$101a. \frac{\bar{P}_{F5I} - \bar{P}_{hubI}}{P_{T7}} = \frac{83 - 99}{98}; \text{ dimensionless}$$

$$102. \frac{P_{T7} - \bar{P}_{hubII}}{P_{T7}} = \frac{98 - 99}{98}; \text{ dimensionless}$$

Step n). Total Pressure Loss Parameters; Branch II

Input: All input are taken from previous steps

Calculations:

$$103. \frac{P_{T7} - \bar{P}_{F5II}}{P_{T7}} = \frac{98 - 84}{98}; \text{ dimensionless}$$

$$103a. \frac{\bar{P}_{T_{3II}} - \bar{P}_{T_{hubII}}}{P_{T1}} = \frac{84 - 100}{98}; \text{ dimensionless}$$

$$104. \frac{P_{T1} - \bar{P}_{T_{hubII}}}{P_{T1}} = \frac{98 - 100}{98}; \text{ dimensionless}$$

ANALYSIS _____

PREPARED BY _____

CHECKED BY _____

APPENDIX E

SUMMARY

OF

STRAIN GAGE AND THERMOCOUPLE LOCATIONS

E. 1 INTRODUCTION

Table E. 2-1 following lists all strain gage locations, and the type of gage and the data desired at each location. Table E. 2-2 is a compilation of the thermocouple locations.

TABLE E.2-1

TABULATION OF STRAIN GAGE INSTALLATIONS

Bridge Name	Bridge Number	Gage Type	No. of Gages	Bridge Type	Wiring Configuration	Gage Location		Station
						Part Name	Part No.	
Pitch Arm	1	ABD-13	4	Bending	Normal	Feathering Arm	285-0140	23.00
Flapwise Bending	4	ABD-13	8	Bending	Parallel	Front Spar	285-0170	62.50
Flapwise Bending	5	ABD-13	8	Bending	Parallel	Aft Spar	285-0170	62.50
Flapwise Bending	6	ABD-13	8	Bending	Parallel	Front Spar	285-0170	73.40
Flapwise Bending	7	ABD-13	8	Bending	Parallel	Aft Spar	285-0170	73.40
Flapwise Bending	8	ABD-13	8	Bending	Parallel	Front Spar	285-0170	53.50
Flapwise Bending	9	ABD-13	8	Bending	Parallel	Aft Spar	285-0170	53.50
Flapwise Bending	10	ABD-13	8	Bending	Parallel	Front Spar	285-0170	78.30
Chordwise Bending	11	ABD-13	4	Tension	Normal	Front Spar	285-0170	83.50
Flapwise Bending	12	ABD-13	8	Bending	Parallel	Aft Spar	285-0170	78.30
Chordwise Bending	13	ABD-13	4	Tension	Normal	Aft Spar	285-0170	103.00*

*Moved from Station 83.5 after addition of aft spar doubler

TABLE E.2-1 (Continued)

Bridge Name	Bridge Number	Gage Type	No. of Gages	Bridge Type	Wiring Configuration	Gage Location Part Name	Part No.	Station
Flapwise Bending	17	ABD-13	8	Bending	Parallel	Aft Spar	285-0170	138.30
Flapwise Bending	23	ABD-13	8	Bending	Parallel	Aft Spar	285-0170	164.50
Flapwise Bending	24	ABD-13	8	Bending	Parallel	Front Spar	285-0170	206.00
Flapwise Bending	25	C6-142-350B	8	Bending	Parallel	Aft Spar	285-0170	206.00
Flapwise Bending	29	C6-142-350B	8	Bending	Parallel	Aft Spar	285-0170	270.00
Thrust	30	ABD-13	8	Tension	Parallel	Shaft Assembly	285-0534	W. L. -1.4
Thrust	30X	ABD-13	8	Tension	Parallel	Shaft Assembly	285-0534	W. L. -1.4
In-plane Bending	31	ABD-13	8	Bending	Parallel	Shaft Assembly	285-0534	W. L. -1.4
90° to In-plane Bending	32	ABD-13	8	Bending	Parallel	Shaft Assembly	285-0534	W. L. -1.4
Hub Gimbal	33	ABD-13	4	Bending	Normal	Hub Gimbal Beam	285-0529	W. L. +4.25
Hub Gimbal	34	ABD-13	4	Bending	Normal	Hub Gimbal Beam	285-0529	W. L. +4.25
Blade Torsion	36	ABD-13	4	Shear	Normal	Blade Structure	285-0166	Top. Skin 38.0

TABLE E.2-1 (Continued)

Bridge Name	Bridge Number	Gage Type	No of Gages	Bridge Type	Wiring Configuration	Gage Location Part Name	Part.No.	Station
Blade Torsion	37	ABD-13	4	Shear	Normal	Blade Structure	285-0166	Bottom Skin 38.00
Blade Torsion	38	ABD-13	4	Shear	Normal	Blade Structure	285-0138	Top Skin 82.00
Blade Torsion	39	ABD-13	4	Shear	Normal	Blade Structure	285-0138	Bottom Skin 82.00
Horizontal Shear	40	ABD-13	4	Shear	Normal	Blade Structure	285-0127	23.50
Vertical Shear	41	ABD-13	4	Shear	Normal	Blade Structure	285-0127	23.50
Swashplate Drag Link		ABD-13	4	Tension	Normal	Swash Plate Drag Link	285-0332	Shown on 285-0300 W.L. -57.2
Flapping Angle Pickup		ABD-13	4	Bending	Normal	Flapping Angle Pickup	285-0947	Hub 19.00
Strap Wind-up Pickup		ABD-13	4	Bending	Normal	Feathering Angle Pickup	285-0948	Hub 19.00
Hub Tilt Pickup		ABD-13	4	Bending	Normal	Hub Tilt Pickup	285-0956	Hub 6.00
Blue Blade Duct Torsion		ABD-13	8	Bending	Parallel	Duct Gimbal Ring Gages Installed per 285-0995	285-0178	Shaft Assy. 19.00

TABLE E.2-1 (Continued)

Bridge Name	Bridge Number	Gage Type	No. of Gages	Bridge Type	Wiring Configuration	Gage Location Part Name	Part No.	Station
2.		ABD-13	8	Bending	Parallel	Duct Gimbal Ring Installed per 285-0955	285-0178	Shaft Assy. 19.00
Red Blade Duct Torsion 1.		ABD-13	8	Bending	Parallel	Duct Gimbal Ring Gages Installed per 285-0955		Shaft Assy. 19.00
2.		ABD-13	8	Bending	Parallel	Duct Gimbal Ring Gages Installed per 285-0955		Shaft Assy. 19.00
Yellow Blade Duct Torsion 1.		ABD-13	8	Bending	Parallel	Duct Gimbal Ring Gages Installed per 285-0955		Shaft Assy. 19.00
2.		ABD-13	8	Bending	Parallel	Duct Gimbal Ring Gages Installed per 285-0955		Shaft Assy. 19.00
For and Aft Horizontal Force Pickup		ABD-13	4	Tension	Normal	Upper Truss	285- 0523-1	W. L. -43.00
Lateral Horizontal Force Pickup		ABD-13	4	Tension	Normal	Upper Truss	285- 0523-1	W. L. -43.00
Pylon Thrust A		ABD-13	4	Tension	Normal*	Lower Truss	285- 0523-3	W. L. -52.00

*All eight tubes of the lower truss were strain gaged and diametrically opposed tubes were wired in parallel at the plug to cancel side loads. The configuration of these gages are A and E, B and F, C and G, and D and H.

TABLE E.2-1 (Continued)

Bridge Name	Bridge Number	Gage Type	No. of Gages	Bridge Type	Wiring Configuration	Part Name	Gage Location	Part No.	Station
Pylon Thrust	B	ABD-13	4	Tension	Normal	Lower Truss		285-0 0523-3	W.L. -52.00
"	C	"	"	"	"	"	"	"	"
"	D	"	"	"	"	"	"	"	"
"	E	"	"	"	"	"	"	"	"
"	F	"	"	"	"	"	"	"	"
"	G	"	"	"	"	"	"	"	"
"	H	"	"	"	"	"	"	"	"
Control Force	1	AB-19	4	Tension	Normal	Rod End		285- 0326-3	W.L. -57.00
Control Force	2	AB-19	4	Tension	Normal	Rod End		285- 0326-3	W.L. -57.00
Control Force	3	AB-19	4	Tension	Normal	Rod End		285- 0326-3	W.L. -57.00

TABLE E. 2-2

THERMOCOUPLE SUMMARY

General Location	Thermocouple Identification	Number Thermocouples Involved	Blade Station or HUB W. L.	Blade	Specific Location
1. Coupling	BC-2, #1 thru 4	4	103.5	Blue	Coupling No. 2, Dwg. 285-1002
	BC-4, #1 thru 4	4	128.5	Blue	Coupling No. 4, Dwg. 285-1002
	BC-6, #1 thru 4	4	153.5	Blue	Coupling No. 6, Dwg. 285-1002
	BC-8, #1 thru 4	4	178.5	Blue	Coupling No. 8, Dwg. 285-1002
	BC-10, #1 thru 4	4	203.5	Blue	Coupling No. 10, Dwg. 285-1002
	BC-12, #1 thru 4	4	228.5	Blue	Coupling No. 12, Dwg. 285-1002
	BC-14, #1 thru 4	4	253.5	Blue	Coupling No. 14, Dwg. 285-1002
	BC-16, #1 thru 4	4	278.5	Blue	Coupling No. 16, Dwg. 285-1002
	BC-18, #1 thru 4	4	303.5	Blue	Coupling No. 18, Dwg. 285-1002
	RC-2, #1 thru 4	4	103.5	Red	Coupling No. 2, Dwg. 285-1002
	RC-18, #1 thru 4	4	303.5	Red	Coupling No. 18, Dwg. 285-1002
	YC-2, #1 thru 4	4	103.5	Yellow	Coupling No. 2, Dwg. 285-1002
	YC-18, #1 thru 4	4	303.5	Yellow	Coupling No. 18, Dwg. 285-1002
	2. Mast	#1	1	WL-34	-----
#2		1	WL-13	-----	Mast Structure, Dwg. 285-0937

TABLE E.2-2 (Continued)

THERMOCOUPLE SUMMARY

General Location	Thermocouple Identification	Number Thermocouples Involved	Blade Station or HUB W. L.	Blade	Specific Location
2. Mast	#3	1	WL-8	-----	Mast Structure, Dwg. 285-0937
	#4	1	WL-1.0	-----	Mast Structure, Dwg. 285-0937
	#5	1	WL-6.5	-----	Spoke, Inboard Section, Dwg. 285-0937
	#6	1	WL-6.5	-----	Spoke, Station 7.0 (half-way out), Dwg. 285-0937
	#7	1	WL-6.5	-----	Spoke Station 14.0 (at tip), Dwg. 285-0937
	#8	1	WL-2.5	-----	Outer Skirt of Gimbal fitting, Dwg. 285-0937
3. Misc.	BBJ-1	1	21.88	Blue	Inner Surface ball joint, at top, Dwg. 285-0949
	BHD-1	1	15.50	Blue	Outer Surface of inboard articulated Duct seal housing at top, Dwg. 285-0951
4. Ribs	H-1	1	-----	-----	Hub cooling air near spoke
	BR-1	1	33.25	Blue	Inner surface closest to duct at top, Rib at Station 33.25, Dwg. 285-0949
	BR-2	1	63.0	Blue	Inner surface closest to duct at top, Rib at Station 63.0, Dwg. 285-0950

TABLE E. 2-2 (Continued)

THERMOCOUPLE SUMMARY

General Location	Thermocouple Identification	Number Thermocouples Involved	Blade Station or HUB W. L.	Blade	Specific Location
4. Ribs	BR-3	1	73.0	Blue	Inner surface closest to duct at top, Rib at Station 73.0, Dwg. 285-0950
5. Segments	BS-1, #1 thru 6	6	10B	Blue	On Rib No. 9, Segment No. 1, Dwg. 285-1002
	BS-1, #1 thru 10	4	97	Blue	Ribs, outer surface of skin, Segment No. 1, Dwg. 285-1002
	BS-1, #11 thru 14	4	97	Blue	Between ducts on Rib No. 5, Segment No. 1, Dwg. 285-1002
	BS-18, #1 thru 6 and No. 11	7	321	Blue	Segment No. 18, Rib No. 5, Dwg. 285-1002
	BS-18, #7 thru 10	4	321	Blue	Segment No. 18, outer skin, Rib No. 5, Dwg. 285-1002
6. Spars	BFS-1	1	83.1	Blue	Front spar, Neutral Axis
	BFS-2	1	135.38	Blue	Front spar, Neutral Axis
	BFS-3	1	206	Blue	Front spar, Neutral Axis
	BRS-1	1	83.3	Blue	Rear spar, Neutral Axis
	BRS-2	1	135.38	Blue	Rear spar, Neutral Axis
	BRS-3	1	206	Blue	Rear spar, Neutral Axis

TABLE E.2-2 (Continued)

THERMOCOUPLE SUMMARY

General Location	Thermocouple Identification	Number Thermocouples Involved	Blade Station or HUB W. L.	Blade	Specific Location
6. Spars	C13	1	206	Blue	Front spar, top
	C14	1	206	Blue	Front spar, bottom
	C15	1	78.3	Blue	Front spar, top
	C16	1	78.3	Blue	Front spar, bottom
	C17	1	270	Blue	Aft spar, top
	C18	1	270	Blue	Aft spar, bottom
	C19	1	206	Blue	Aft spar, top
	C20	1	206	Blue	Aft spar, bottom
	C21	1	135.3	Blue	Aft spar, top
	C22	1	135.3	Blue	Aft spar, bottom
	C23	1	78.3	Blue	Aft spar, top
	C24	1	78.3	Blue	Aft spar, bottom
7. Cooling Ducts	BCD-1	1	330	Blue	Probe, front spar cooling duct
	BCD-2	1	321	Blue	Probe, rear spar cooling duct
	BCD-5	1	78	Blue	Probe, main duct cooling space outboard of Station 73 near exit hole in upper skin

TABLE E.2-2 (Continued)

THERMOCOUPLE SUMMARY

General Location	Thermocouple Identification	Number Thermocouples Involved	Blade Station or HUB W. L.	Blade	Specific Location
7. Cooling Ducts	Cooling Air	1	57	Blue	Probe, main duct cooling space near exit hole in bottom skin
	RCDF	1	325	Red	Probe, front spar cooling duct
	RCDR	1	325	Red	Probe, rear spar cooling duct
	Cooling Air	1	78	Red	Probe, main duct cooling space near exit hole in upper skin
	Cooling Air	1	57	Red	Probe, main duct cooling space near exit hole in lower skin
	YCDF	1	325	Yellow	Probe, front spar cooling duct
8. Primary Ducts	YCDR	1	325	Yellow	Probe, Aft spar cooling duct
	Cooling Air	1	78	Yellow	Probe, main duct cooling space near exit hole in upper skin
	Cooling Air	1	57	Yellow	Probe, main duct cooling space, near exit hole in lower skin
	C1	1	325	Blue	Probe, centered in aft duct 1" upstream of rotor tip nozzle cascade
	C2	1	325	Blue	Probe, centered in forward duct 1" upstream of rotor tip nozzle cascade

TABLE E. 2-2 (Continued)

THERMOCOUPLE SUMMARY

General Location	Thermocouple Identification	Number Thermocouples Involved	Blade Station or HUB W. L.	Blade	Specific Location
9. Seal Gimbal Ring	Gimbal Ring	1	19	Blue	Duct Gimbal ring, Dwg. 285-0178
	Gimbal Ring	1	19	Red	Duct Gimbal ring, Dwg. 285-0178
	Gimbal Ring	1	19	Yellow	Duct Gimbal ring, Dwg. 285-0178

ANALYSIS

MODEL

REPORT NO.

(62-16) PAGE

PREPARED BY

CHECKED BY

APPENDIX FNOMENCLATURE
AND
COMPUTER PROGRAM FORMATSF.1 INTRODUCTION

This section provides the nomenclature, input and output format, and computer program listing for the thermodynamics and aerodynamics of the hot cycle system. This information is included in this appendix for convenience and is introduced and discussed further in Section 5.1.5 and Appendix D.

ANALYSIS

PREPARED BY

CHECKED BY

F. 2 Nomenclature

Analysis	Fortran Program	Definition
a	A	Velocity of sound; Slope of lift curve in radians
A	BAD	Total duct cross-section area - square feet
A _D		Duct cross-section area per blade - square feet
A _N	ANT	Total nozzle area at blade tips - square feet
b	B	Number of blades
B		Tip loss factor (assumed = 0.97)
c	C	Blade chord - inches
c _p	CP	Specific heat at constant pressure - BTU/pound-°F
c _v	CV	Specific heat at constant volume - BTU/pound-°F
C	CORR	Profile power increase
C _I		Calculated hub pressure loss coefficient based on hub area - weighted total pressure, Branch I
C _{II}		Calculated hub pressure loss coefficient based on hub area - weighted total pressure, Branch II
C _I '	C1	Estimated turning pressure loss coefficient through hub, Branch I
C _{II} '	C2	Estimated turning pressure loss coefficient through hub, Branch II
C _i	C1	Power correction factor for blade twist
C _f		Nozzle thrust coefficient
C _p	CA	Nozzle power coefficient = $\frac{RHP \times 550}{\rho \pi R^2 V_t^3}$

ANALYSIS _____

MODEL _____

REPORT NO. _____

PREPARED BY _____

CHECKED BY _____

Analysis	Fortran Program	Definition
C_T	CT	Rotor thrust coefficient = $\frac{T}{\rho \pi R^2 V_t^2}$
C_{V_e}, C_{V_f}	CF	Nozzle velocity coefficient
C_w		Nozzle flow coefficient
dr		Increment of blade length - feet
D		Duct hydraulic diameter - $\frac{4 \times A_D}{\text{wetted perimeter}}$
E		Number of gas generators
f	F	Duct friction coefficient
g		Acceleration due to gravity - 32.2 feet/seconds ²
GN1 } GN2 } GN3 }	GN1 } GN2 } GN3 }	$\frac{T_g}{T} = GN1 + GN2 \left(\frac{C_T}{\delta} \right) + GN3 \left(\frac{C_T}{\delta} \right)^2$
h_{T_2}		Compressor inlet total enthalpy
h_{T_7}		Turbine discharge total enthalpy
J		Mechanical equivalent of heat - 778 feet-pound/BTU
M	AM	Mach number
n		Blade station index number for 100 step computation, n = 0, 1, 2, 3, 99.
N_1		Low pressure compressor rpm
N_2		Low pressure compressor rpm
P_{amb}	PAMB	Ambient pressure - in Hg

ANALYSIS

PREPARED BY

CHECKED BY

Analysis	Fortran Program	Definition
P_o		Ambient pressure - pound/feet ²
P_t	PT	Gas total pressure - pound/feet ² (absolute)
P_{T7}		Turbine discharge total pressure
P_{T_c} or P_c	PT or P	Total and static pressures described by Figure D-2, P ₁₋₂₄ readout
r		Gas total pressure ratio, P_{T/P_o}
r_3/r_2	R3R2	Static duct pressure ratio
R		Gas constant
R	RAD	Blade radius, feet
Re		Reynolds number
t/c	TCR	Blade thickness ratio
T	T	Rotor thrust - pounds
T_{amb}	TAMB	Ambient Temperature
T_{t1-4}		Total temperatures described by Figure D-2, T ₁₋₂₄ readout
T_T	TT	Gas total temperature - °R
T_{T7}	TT7	Turbine discharge total temperature
T_g/T	TGTi	Ground effect parameter = $\frac{T \text{ in ground effect}}{T \text{ out of ground effect}}$
U	U	Duct utilization = $\frac{\text{duct area}}{\text{blade cross - section area}}$
v	V	Velocity
V_j	Vj	Jet velocity at blade tip - foot/second

ANALYSIS

MODEL

REPORT NO.

PREPARED BY

CHECKED BY

Analysis	Fortran Program	Definition
V_T	VT	Blade tip speed - feet/second
W		Flow rate
W_7		Turbine discharge flow rate
W_f	WF	Fuel flow rate
W	WG	Total gas flow, pound/second = EXW_g
W_g	WG	Gas flow per engine, pound/second
X_1	X1	<u>Mass weighted total pressure</u> , flow measuring Sta. I max. total pressure
X_2	X2	<u>Mass weighted total pressure</u> , flow measuring Sta. II max. total pressure
Z_1	Z1	<u>Area weighted velocity</u> , Branch I max. velocity
Z_2	Z2	<u>Area weighted velocity</u> , Branch II max. velocity
γ	GAMMA	Ratio of specific heats - c_p/c_v
δ	DEL	Temperature droop of gas at blade tip below temperature of gas or blade root
δ_i		Coefficients of NASA drag polar
μ	MU	Absolute viscosity
ρ	RHO	Density
σ		Blade solidity ratio
ω		Rotor angular velocity - radius/second
SUPERSCRIPTS		
—		Mass weighted value
SUBSCRIPTS		
0		Ambient air away from engine
1		Face of gas generator

ANALYSIS _____

PREPARED BY _____

CHECKED BY _____

Analysis	Fortran Program	Definition
2		Hub measuring station
3		Blade root
4		Blade tip and nozzle inlet
5		Nozzle exit
I		Branch I
II		Branch II
aw		Area weighted value
e		Position at edge of flow station rake
f_s		Flow measuring station
hub		Hub station below rotating seal
max		Maximum value at center of duct
ref		Reference value
res		Reservoir value
tot		Total or summation
T		Total or stagnation

FIGURE F. 3-1 INPUT FORMAT
 HUGHES TOOL COMPANY-AIRCRAFT DIVISION 285-16

MODEL REPORT NO (62-16) PAGE F. 3-1

ANALYSIS

PREPARED BY

CHECKED BY

HOT CYCLE HELICOPTER -
 WHIRL TEST DATA
 INPUT TO COMPUTER PROGRAM

DATE	2/28/62	
RUN NO.	35	
1	Z ₁	.935
2	Z ₂	.927
3	X ₁	.442
4	X ₂	.440
5	C ₁	.01
6	C ₂	.01
7	P _{amb}	30.17
8	RPM	240
9	W _f	6500
10	T _{T2}	54
11	P _{T7}	71.37
12	T _{T1}	1143
13	T _{T2}	1143
14	T _{T3}	1142
15	T _{T4}	1137
16	P _{Tres}	68.61
17	T _{T7}	665
18	P ₁	-20.90
19	P ₂	- 4.70
20	P ₃	- 7.80
21	P ₄	- 3.60
22	P ₅	- 5.70
23	P ₆	- 4.30
24	P ₇	- 6.15
25	P ₈	-25.50
26	P ₉	-11.10
27	P ₁₀	-11.40
28	P ₁₁	- 9.30
29	P ₁₂	- 8.70
30	P ₁₃	- 8.60
31	P ₁₄	-12.50
32	P ₁₅	- 5.90
33	P ₁₆	- 6.40
34	P ₁₇	- 7.70
35	P ₁₈	-10.10
36	P ₁₉	-13.60
37	P ₂₀	-11.10
38	P ₂₁	-13.90
39	P ₂₂	-17.00
40	P ₂₃	-11.20
41	P ₂₄	-11.80
42	RAD	27.5
43	C	31.5
44	B	3.

HUGHES TOOL COMPANY-AIRCRAFT DIVISION 285-16

MODEL

REPORT NO

(62-16) PAGE F. 3-2

ANALYSIS

PREPARED BY

CHECKED BY

HOT CYCLE HELICOPTER -
WHIRL TEST DATA
INPUT TO COMPUTER PROGRAM

DATE									
	RUN NO.	35							
45	TOR	.18							
46	EAD	1.117							
47	RSR2	.98							
48	F	1.004							
49	OF	.955							
50	ANT	.7375							
51	QW1	1.21							
52	QW2	-3.0							
53	QW3	17.5							
54	CORR	1.0							

FIGURE F.3-3 PRINTOUT

XEQ

1

ENTRY POINTS TO SUBROUTINES REQUESTED FROM LIBRARY,

(FPI) (TSHM) (RTN) (STHM) (FIL) SORTI EXP(

EXECUTION TIME 1659

RAD = 27.5 CHORD = 31.5 NO. BLADES = 3. T/C = 0.18 TOTAL DUCT AREA = 1.14
 E = 0.00400 CF = 0.95500 TOTAL NOZZLE AREA = 0.73750
 TG/TI = 1.2100 + -3.0000 X CT/S + 12.5000 X CT/S X CT/S, Z1 = 0.9350 Z2
 KI = 0.4420 X2 = 0.4400 PROFILE CORR. = 1.0000
 TEST = 35 C1 = 0.01000 C2 = 0.01000
 PAMB = 30.17 RPM = 240. DEL = 0. WF LB/HR = 6500. TAMB F = 54.
 FLOW ST. TEMP F = 1143. 1143. 1142. 1137. PRES = 68.61
 FROM ST. PRESS = -20.90 -4.70 -7.80 -3.60 -5.70 -4.30 -6.15 -25.80 -11.10
 -8.60 -12.50 -5.90 -6.40 -7.70 -10.10 -13.60 -11.10 -13.90 -17.00 -11.20 -11.8
 RT7 = 665.

MF = 0.10202E 03 WF/WA = 0.18017E-01 O/O AIR = 0.37574E 03 RM
 QR = 0.27748E-00 CV = 0.20893E-00 GAMMA = 0.13281E 01

FLOW MEASURING STATION

BRANCH	1	2	BRANCH	1
TT	0.16030E 04	0.15995E 04	PMAX	0.4531
PTMAX	0.47861E 04	0.47200E 04	MMAX	0.2881
TMAX	0.15815E 04	0.15773E 04	AMAX	0.1898
VMAX	0.54704E 03	0.55539E 03	RHOMAX	0.5371
MUMAX	0.95087E-01	0.94958E-01	REMAX	0.1135
VAVG	0.51148E 03	0.51484E 03	MAVG	0.2694
TAVG	0.15841E 04	0.15804E 04	RHOAVG	0.5362
AAVG	0.19000E 04	0.18978E 04	(VAVG)CORR	0.5119
W	0.22454E 02	0.22305E 02		

TOTAL GAS FLOW = 0.44759E 02

FLOW MEASURING STAT. MASS WEIGHTED MEAN TOTAL PRESSURE

BRANCH 1 = 0.47565E 04 BRANCH 2 = 0.46888E 04

HUB STATION TOTAL TEMP = 0.16012E 04

VELOCITY PROFILE FLOW MEASURING STATION

VELOCITY PROFILE BRANCH 1

PT1 = 0.47800E 04 PT3 = 0.47323E 04 PT5 = 0.47969E 04 PT7 =
 PT9 = 0.47861E 04 PTE = 0.47577E 04 M1 = 0.28473E-00 M3 =
 M5 = 0.29404E-00 M7 = 0.27597E-00 M9 = 0.28815E-00 ME =
 V1/VMAX = 0.98812E 00 V3/VMAX = 0.89026E 00 V5/VMAX = 0.16204E 01
 V7/VMAX = 0.95772E 00 V9/VMAX = 0.10000E 01 VE/VMAX = 0.98370E 00

VELOCITY PROFILE BRANCH 2

PT2 = 0.46816E 04 PT4 = 0.46770E 04 PT6 = 0.47093E 04 PT8 =
 PT10 = 0.47200E 04 PTE = 0.46601E 04 M2 = 0.27082E-00 M4 =
 M6 = 0.28693E-00 M8 = 0.29209E-00 M10 = 0.29294E-00 ME =
 V2/VMAX = 0.92451E 00 V4/VMAX = 0.91500E 00 V6/VMAX = 0.97950E 00
 V8/VMAX = 0.92710E 00 V10/VMAX = 0.10000E 01 VE/VMAX = 0.81919E 00

HUB STATION AREA WEIGHTED TOTAL PRESSURE BRANCH 1 = 0.47229E 04

PT15 = 0.47615E 04 PT17 = 0.47538E 04 PT19 = 0.47339E 04 PT21 =

HUB STATION AREA WEIGHTED TOTAL PRESSURE BRANCH 2 = 0.46557E 04

PT16 = 0.46816E 04 PT18 = 0.46386E 04 PT20 = 0.45910E 04 PT22 =

HUB STATION TOTAL PRESSURE, MASS WEIGHTED, CALCULATED

BRANCH 1 = 0.47060E 04 BRANCH 2 = 0.46383E 04 AVERAGE = 0.46722E

C1 = 0.00666 C2 = 0.00658 101 = 0.05763 101A = 0.01000 102 = 0.06763
 103 = 0.07103 103A = 0.01000 104 = 0.08103

DESIGN M3 = 0.4245 PRESS RATIO = 0.95765 R4 = 2.05507 CT/SOLID = 0.080780

ROTOR THRUST = 20192. DISC LOADING = 8.5033 R2 = 2.1890

CP = 0.57326E-03 CPO = 0.12907E-03 CT = 0.69932E-02

Copyright © 1980 by McDonnell Douglas Aircraft Company, Inc.

2

ED FROM LIBRARY,

(SIHM)

(FIL)

SORT1

EXP(3)

BLADES = 3. T/C = 0.18 TOTAL DUCT AREA = 1.14166 R3/R2 = 0.980

AL NOZZLE AREA = 0.73750

/S + 12.5000 X CT/S X CT/S, Z1 = 0.9350 Z2 = 0.9270

LE CORR. = 1.0000

C2 = 0.01000

= 0. WF LB/HR = 6500. TAMB F = 54. PT7 = 71.37

1142. 1137. PRES = 68.61

7.80 -3.60 -5.70 -4.30 -6.15 -25.80 -11.10 -11.40 -9.30 -8.70

-10.10 -13.60 -11.10 -13.90 -17.00 -11.20 -11.80

0.18017E-01 O/O AIR = 0.37576E 03 RN = 0.53340E 02

20893E-00 GAMMA = 0.13281E 01

2	BRANCH	1	2
0.15995E 04	PMAX	0.45310E 04	0.44604E 04
0.47200E 04	MMAX	0.28815E-00	0.29294E-00
0.15773E 04	AMAX	0.18984E 04	0.18959E 04
0.55539E 03	RHOMAX	0.53714E-01	0.53015E-01
0.94958E-01	REMAX	0.11358E 07	0.11397E 07
0.51484E 03	MAVG	0.26942E-00	0.27155E-00
0.15804E 04	RHOAVG	0.53623E-01	0.52912E-01
0.18978E 04	(VAVG)CORR	0.51191E 03	0.51535E 03
0.22305E 02			

PE 02

ED MEAN TOTAL PRESSURE

BRANCH 2 = 0.46888E 04

012E 04

STATION

0.47323E 04	PT5 =	0.47969E 04	PT7 =	0.47646E 04
0.47577E 04	M1 =	0.28473E-00	M3 =	0.25653E-00
0.27597E-00	M9 =	0.28815E-00	ME =	0.27193E-00
K =	0.89026E 00	V5/VMAX =	0.10204E 01	
K =	0.10000E 01	VE/VMAX =	0.90370E 00	

0.46770E 04	PT6 =	0.47093E 04	PT8 =	0.47185E 04
0.46601E 04	M2 =	0.27082E-00	M4 =	0.26804E-00
0.29209E-00	M10 =	0.29294E-00	ME =	0.25755E-00
K =	0.91500E 00	V6/VMAX =	0.97950E 00	
K =	0.10000E 01	VE/VMAX =	0.87919E 00	

PRESSURE BRANCH 1 =	0.47229E 04			
0.47538E 04	PT19 =	0.47339E 04	PT21 =	0.46970E 04
PRESSURE BRANCH 2 =	0.46557E 04			
0.46386E 04	PT20 =	0.45910E 04	PT22 =	0.46801E 04
			PT23 =	0.4643
			PT24 =	0.4670

WEIGHTED, CALCULATED

BRANCH 2 = 0.46383E 04 AVERAGE = 0.46722E 04

101 = 0.05763 101A = 0.01000 102 = 0.06763

104 = 0.08103

= 0.95765 R4 = 2.05507 CT/SOLID = 0.080780 RHP = 1972.

LOADING = 8.5033 R2 = 2.1898

0.12907E-03 CT = 0.69932E-02

```

C   HOT CYCLE TEST DATA REDUCTION
    READINPUTTAPE3,100,RAD,C,B,TCR,BAD,R3R2,F,CF,ANT
    READINPUTTAPE3,101,GN1,GN2,GN3,Z1,Z2,X1,X2,CORR
    WRITEOUTPUTTAPE2,102,RAD,C,B,TCR,BAD,R3R2,F,CF,ANT,GN1,GN2,GN3,Z1,
1  1Z2,X1,X2,CORR
    READINPUTTAPE3,103,PAMB,RPM,DEL1,WF,TT2,PT7,T1,T2,T3,T4,PRES,TT7
    READINPUTTAPE3,104,P1,P2,P3,P4,P5,P6,P7,P8,P9,P10,P11,P12
    READINPUTTAPE3,104,P13,P14,P15,P16,P17,P18,P19,P20,P21,P22,P23,P24
    READINPUTTAPE3,106,TEST,C11,C21
    WRITEOUTPUTTAPE2,107,TEST,C11,C21
    WRITEOUTPUTTAPE2,105,PAMB,RPM,DEL1,WF,TT2,PT7,T1,T2,T3,T4,PRES,P1,
1  1P2,P3,P4,P5,P6,P7,P8,P9,P10,P11,P12,P13,P14,P15,P16,P17,P18,P19,P2
20,P21,P22,P23,P24,TT7
    VT=(RPM*6.28*RAD)/60.
    DR=(17.32*PAMB)/(TT2+460.)
    P=70.721*PAMB
    CALL ENPR(WF,TT2,TT7,R,GAMMA,CP)
    CALL FLRAT(GAMMA,R,T1,T2,PRES,P1,P6,T3,T4,P8,P13,Z1,Z2,X1,X2,WTOT,
1  1PREF,P1M,P2M,PT1B,PT2B,TTHUB)
    CALL VELPR(P2,P3,P4,P5,P6,P7,PREF,P1M,P2M,GAMMA,P9,P10,P11,P12,P13
1  1,P14)
    CALL EXTRA(PREF,P15,P16,P17,P18,P19,P20,P21,P22,P23,P24,PT7,PT1B,P
1  1T2B,PTHB,C11,C21)
    CALL POWER(RAD,C,B,VT,GAMMA,TCR,BAD,DR,WTOT,TTHUB,PTHB,R3R2,F,CP,C
1  1F,P,ANT,DEL1,GN1,GN2,GN3,CORR)
    WRITEOUTPUTTAPE2,110
    GOTO1
100  FORMAT(2F5.1,F2.0,6F7.5)
101  FORMAT(8F7.4)
102  FORMAT( 9H   RAD =F5.1,10H   CHORD =F5.1,15H   NO. BLADES =F2.0,8
1  1H   T/C =F4.2,20H   TOTAL DUCT AREA =F8.5,10H   R3/R2 =F6.3/7H
2  2F =F8.5,7H   CF =F8.5,22H   TOTAL NOZZLE AREA =F8.5/11H   TG/TT =
3  3F8.4,4H   + F8.4,9H X CT/S +F8.4,23H X CT/S X CT/S,   Z1 =F7.4,7H
4  4   Z2 =F7.4/7H   X1 =F7.4,7H   X2 =F7.4,18H   PROFILE CORR. =F7.4)
103  FORMAT(F6.2,2F5.0,F6.0,F5.0,F6.2,4F5.0,F6.2,F5.0)
104  FORMAT(12F6.2)
105  FORMAT(10H   PAMB =F7.2,8H   RPM =F5.0,7H   DEL =F5.0,13H   WF LB/
1  1HR =F7.0,11H   TAMB F =F6.0,8H   PT7 =F7.5/20H   FLOW ST. TEMP F =
2  24F7.0,9H   PRES =F7.2/19H   FLOW ST. PRESS =12F7.2/12F7.2/8H   TT7
3  3 =F7.0)
110  FORMAT(1H1)
106  FORMAT(15,2F8.5)
107  FORMAT(10H   TEST =15,8H   C1 =F9.5,8H   C2 =F9.5)
111  FORMAT(8F9.0)
112  FORMAT(8H   RPM =F6.0,9H   PAMB =F6.2,9H   TAMB =F4.0,7H   WG =F6.
1  12,9H   THUB =6.0,9H   PHUB =F7.0,7H   CP =F6.4,10H   GAMMA =F7.3)
110  FORMAT(1H /1H /1H /)

```

```

SUBROUTINE ENPR(WF1,TT21,TT71,R,GAMMA,CP)
WF=WF1/3600.
TT2=TT21+460.
TT7=1.8*(TT71+17.8)+460.
HT2=120.42+.2477*(TT2-500.)
IF(TT7-1000.)1,1,2
1 HT7=120.42+.2477*(TT7-500.)
GOTO5
2 IF(TT7-1500.)3,3,4
3 HT7=244.25+.2627*(TT7-1000.)
GOTO5
4 HT7=375.62+.2819*(TT7-1500.)
5 W7=((17664.-HT7)*WF)/(HT7-HT2)
WFWA=WF/(W7-WF)
PAIR=6.77/WFWA
R=.0095*WFWA+53.34
TT7C=TT7/180.
IF(TT7-990.)6,6,7
6 CP=(.243-.08*WFWA)-(.00343-.115*WFWA)*TT7C+(.0008-.008*WFWA)*TT7C*
TT7C
GOTO10
7 IF(TT7-1530.)8,8,9
8 CP=(.217-.157*WFWA)+(.0057+.0267*WFWA)*TT7C
GOTO10
9 CP=(.334+.9*WFWA)-((.834+7.6*WFWA+10.*WFWA*WFWA)/(TT7C+3.65+20.*WF
1WA))
10 CV=CP-.06855
GAMMA=CP/CV
WRITEOUTPUTTAPE2,100,W7,WFWA,PAIR,R,CP,CV,GAMMA
100 FORMAT(8H WF =E15.5,11H WFWA =E15.5,13H O/O AIR =E15.5,8
1H RN =E15.5/8H CP =E15.5,8H CV =E15.5,11H GAMMA =E15.5
2)
RETURN

```

```

SUBROUTINE FLRAT(GAMMA,R,T1,T2,PRES,P1,P6,T3,T4,P8,P13,Z1,Z2,X1,X2
1,WTOT,PREF,P1M,P2M,PT1B,PT2B,TTHUB)
A=1.937348
B=1.780448 E-02
C=-4.170257 E-06
D=5.805605 E-10
E=-2.156955 E-14
F=4.32 E-03
TT1=(T1+T2)/2.+460.
PREF=PRES*70.721
P1M=P1*15.365+PREF
PT1M=P6*15.365+PREF
CO1=(GAMMA-1.)/GAMMA
CO2=(GAMMA-1.)/2.
AM1M2=(1./CO2)*((PT1M/P1M)**CO1-1.)
AM1M=SQRT1F(AM1M2)
T1M=TT1/(1.+CO2*AM1M*AM1M)
A1M2=GAMMA*32.17*R*T1M
A1M=SQRT1F(A1M2)
V1M=A1M*AM1M
RH1M=P1M/(R*T1M)
AMU1M=(A+B*TT1+C*(TT1**2)+D*(TT1**3)+E*(TT1**4))*F
RE1M=(RH1M*V1M*1.021*3600.)/AMU1M
V1A=Z1*V1M
AM1A=(V1A*AM1M)/V1M
T1A=TT1/(1.+CO2*AM1A*AM1A)
RH1A=P1M/(R*T1A)
A1A2=GAMMA*32.17*R*T1A
A1A=SQRT1F(A1A2)
V1AC=A1A*AM1A
W1=RH1A*V1AC*.818
TT2=(T3+T4)/2.+460.
P2M=P8*15.365+PREF
PT2M=P13*15.365+PREF
AM2M2=(1./CO2)*((PT2M/P2M)**CO1-1.)
AM2M=SQRT1F(AM2M2)
T2M=TT2/(1.+CO2*AM2M*AM2M)
A2M2=GAMMA*32.17*R*T2M
A2M=SQRT1F(A2M2)
V2M=A2M*AM2M
RH2M=P2M/(R*T2M)
AMU2M=(A+B*TT2+C*(TT2**2)+D*(TT2**3)+E*(TT2**4))*F
RE2M=(RH2M*V2M*1.021*3600.)/AMU2M
V2A=Z2*V2M
AM2A=(V2A*AM2M)/V2M
T2A=TT2/(1.+CO2*AM2A*AM2A)
RH2A=P2M/(R*T2A)
A2A2=GAMMA*32.17*R*T2A
A2A=SQRT1F(A2A2)
V2AC=A2A*AM2A
W2=RH2A*V2AC*.818
WTOT=W1+W2
WRITEOUTPUTTAPE2,100
WRITEOUTPUTTAPE2,101,TT1,TT2,P1M,P2M,PT1M,PT2M,AM1M,AM2M,T1M,T2M,A
11M,A2M,V1M,V2M,RH1M,RH2M,AMU1M,AMU2M,RE1M,RE2M,V1A,V2A,AM1A,AM2A,T
21A,T2A,RH1A,RH2A,A1A,A2A,V1AC,V2AC,W1,W2,WTOT
100  FORMAT(26H      FLOW MEASURING STATION/97H      BRANCH      1
1      2      BRANCH      1
2      2)
CO3=1./(2.*(GAMMA-1.))

```



```

CO4=(V1M*V1M)/(32.17*R*T1M)
PT1B=P1M*(1.+X1*(1.+CO3*(TT1/T1M-1.))*CO4)
CO5=(V2M*V2M)/(32.17*R*T2M)
PT2B=P2M*(1.+X2*(1.+CO3*(TT2/T2M-1.))*CO5)
WRITEOUTPUTTAPE2,102,PT1B,PT2B
TTHUB=(TT1+TT2)/2.
WRITEOUTPUTTAPE2,103,TTHUB
103 FORMAT(28H      HUB STATION TOTAL TEMP =E15.5)
102 FORMAT(58H      FLOW MEASURING STAT. MASS WEIGHTED MEAD TOTAL PRESSU
1RE/14H      BRANCH 1 =E16.5,14H      BRANCH 2 =E16.5)
101 FORMAT(18H      TT          2E16.5,22H          PMAX          2E16.5
1/18H      PTMAX          2E16.5,22H          MMAX          2E16.5/18H
2          TMAX          2E16.5,22H          AMAX          2E16.5/18H
3VMAX      2E16.5,22H          RHOMAX          2E16.5/18H          MUMAX
4          2E16.5,22H          REMAX          2E16.5/18H          VAVG          2E
516.5,22H          MAVG          2E16.5/18H          TAVG          2E16.5,2
62H          RHOAVG          2E16.5/18H          AAVG          2E16.5,22H
7          (VAVG)CORR 2E15.5/18H          W          2E16.5/25H          TO
8TAL GAS FLOW =E16.5)
RETURN

```

SUBROUTINE VELPR(P2,P3,P4,P5,P6,P7,PREF,P1M,P2M,GAMMA,P9,P10,P11,P12,P13,P14)

```

PT11=P2*15.365+PREF
PT31=P3*15.365+PREF
PT51=P4*15.365+PREF
PT71=P5*15.365+PREF
PT91=P6*15.365+PREF
PTE1=P7*15.365+PREF
G1=2./(GAMMA-1.)
G2=(GAMMA-1.)/GAMMA
AM112=G1*((PT11/P1M)**G2-1.)
AM312=G1*((PT31/P1M)**G2-1.)
AM11=SQRT1F(AM112)
AM31=SQRT1F(AM312)
AM512=G1*((PT51/P1M)**G2-1.)
AM712=G1*((PT71/P1M)**G2-1.)
AM912=G1*((PT91/P1M)**G2-1.)
AME12=G1*((PTE1/P1M)**G2-1.)
AM51=SQRT1F(AM512)
AM71=SQRT1F(AM712)
AM91=SQRT1F(AM912)
AME1=SQRT1F(AME12)
V1VM1=AM11/AM91
V3VM1=AM31/AM91
V5VM1=AM51/AM91
V7VM1=AM71/AM91
V9VM1=1.
VE1VM1=AME1/AM91
PT22=P9*15.365+PREF
PT42=P10*15.365+PREF
PT62=P11*15.365+PREF
PT82=P12*15.365+PREF
PT102=P13*15.365+PREF
PTE2=P14*15.365+PREF
AM222=G1*((PT22/P2M)**G2-1.)
AM22=SQRT1F(AM222)
AM422=G1*((PT42/P2M)**G2-1.)
AM622=G1*((PT62/P2M)**G2-1.)
AM822=G1*((PT82/P2M)**G2-1.)
AM1022=G1*((PT102/P2M)**G2-1.)
AME22=G1*((PTE2/P2M)**G2-1.)
AM42=SQRT1F(AM422)
AM62=SQRT1F(AM622)
AM82=SQRT1F(AM822)
AM102=SQRT1F(AM1022)
AME2=SQRT1F(AME22)
V2VM2=AM22/AM102
V4VM2=AM42/AM102
V6VM2=AM62/AM102
V8VM2=AM82/AM102
V10VM2=1.
VE2VM2=AME2/AM102
WRITEOUTPUTTAPE2,100,PT11,PT31,PT51,PT71,PT91,PTE1,AM11,AM31,AM51,
1AM71,AM91,AME1,V1VM1,V3VM1,V5VM1,V7VM1,V9VM1,VE1VM1
WRITEOUTPUTTAPE2,101,PT22,PT42,PT62,PT82,PT102,PTE2,AM22,AM42,AM62,
1,AM82,AM102,AME2,V2VM2,V4VM2,V6VM2,V8VM2,V10VM2,VE2VM2
100 FORMAT(29H VELOCITY PROFILE BRANCH 1/9H PT1 =E15.5,9H PT3
1 =E15.5,9H PT5 =E15.5,9H PT7 =E15.5/9H PT9 =E15.5,9H
2PTE =E15.5,9H M1 =E15.5,9H M3 =E15.5/9H M5 =E15.5,9H

```

```
3 M7 =E15.5,9H M9 =E15.5,9H ME =E15.5/12H V1/VMAX =E15.
45,12H V3/VMAX =E15.5,12H V5/VMAX =E15.5/12H V7/VMAX =E15.5,1
52H V9/VMAX =E15.5,12H VE/VMAX =E15.5)
101 FORMAT(29H VELOCITY PROFILE BRANCH 2/9H PT2 =E15.5,9H PT4
1 =E15.5,9H PT6 =E15.5,9H PT8 =E15.5/9H PT10 =E15.5,9H P
2TE =E15.5,9H M2 =E15.5,9H M4 =E15.5/9H M6 =E15.5,9H
3 M8 =E15.5,9H M10 =E15.5,9H ME =E15.5/12H V2/VMAX =E15.5
4,12H V4/VMAX =E15.5,12H V6/VMAX =E15.5/12H V8/VMAX =E15.5,12
5H V10/VMAX =E15.5,12H VE/VMAX =E15.5)
102 FORMAT(43H VELOCITY PROFILE FLOW MEASURING STATION)
RETURN
```

```

SUBROUTINE EXTRA(PREF,P15,P16,P17,P18,P19,P20,P21,P22,P23,P24,PT7,
1PT18,PT28,PTHB,C11,C21)
PT15=P15*15.365+PREF
PT17=P16*15.365+PREF
PT19=P17*15.365+PREF
PT21=P18*15.365+PREF
PT23=P19*15.365+PREF
PTH1AW=.298*PT15+.192*PT17+.169*PT19+.146*PT21+.195*PT23
WRITEOUTTAPE2,100,PTH1AW,PT15,PT17,PT19,PT21,PT23
PT16=P20*15.365+PREF
PT18=P21*15.365+PREF
PT20=P22*15.365+PREF
PT22=P23*15.365+PREF
PT24=P24*15.365+PREF
PTH2AW=.298*PT16+.192*PT18+.169*PT20+.146*PT22+.195*PT24
WRITEOUTTAPE2,101,PTH2AW,PT16,PT18,PT20,PT22,PT24
PTHAW=(PTH1AW+PTH2AW)/2.
PT7A=PT7*70.721
C1=(PT18-PTH1AW)/PT7A
C2=(PT28-PTH2AW)/PT7A
PTH1B=PT18-C11*PT7A
PTH2B=PT28-C21*PT7A
PTHB=(PTH1B+PTH2B)/2.
PLF1=(PT7A-PT18)/PT7A
PLFH1=(PT18-PTH1B)/PT7A
PLH1=(PT7A-PTH1B)/PT7A
PLF2=(PT7A-PT28)/PT7A
PLFH2=(PT28-PTH2B)/PT7A
PLH2=(PT7A-PTH2B)/PT7A
WRITEOUTTAPE2,102,PTH1B,PTH2B,PTHB
WRITEOUTTAPE2,103,C1,C2,PLF1,PLFH1,PLH1,PLF2,PLFH2,PLH2
103 FORMAT(7H C1 =F9.5,7H C2 =F9.5,8H 101 =F9.5,9H 101A =F9.5,
18H 102 =F9.5/8H 103 =F9.5,9H 103A =F9.5,8H 104 =F9.5)
100 FORMAT(55H HUB STATION AREA WEIGHTED TOTAL PRESSURE BRANCH 1 =E
115.5/10H PT15 =E15.5,10H PT17 =E15.5,10H PT19 =E15.5,10H
2 PT21 =E15.5,10H PT23 =E15.5)
101 FORMAT(55H HUB STATION AREA WEIGHTED TOTAL PRESSURE BRANCH 2 =E
115.5/10H PT16 =E15.5,10H PT18 =E15.5,10H PT20 =E15.5,10H
2 PT22 =E15.5,10H PT24 =E15.5)
102 FORMAT(57H HUB STATION TOTAL PRESSURE, MASS WEIGHTED, CALCULATE
1D/14H BRANCH 1 =E15.5,14H BRANCH 2 =E15.5,13H AVERAGE =E1
25.5)
RETURN

```

```

SUBROUTINE POWER(RAD,C,B,VT,GAMMA,TCR,BAD,DR,WG,TTHUB,PTHB,R3R2,F,
1CP,CV,P,ANT,DEL1,GN1,GN2,GN3,CORR)
R2=PTHB/P
TT=TTHUB-DEL1
SOLID=(B*C)/(37.68*RAD)
UR=(BAD*144.)/(B*TCR*C*.68)
WAR=WG/BAD
WTAP=(WAR*SQRT1F(TTHUB))/(P*R2*R3R2)
GA1=(GAMMA-1.)/2.
GA2=(GAMMA+1.)/(2.*(GAMMA-1.))
ROOT=SQRT1F(.603*GAMMA)
AM3T=.35
1 AM3=(WTAP*(1.+GA1*AM3T*AM3T)**GA2)/ROOT
IF(ABS(AM3-AM3T)-.0009)3,3,2
2 AM3T=AM3
GOTO1
3 AM3D=AM3
FGLDR=((1.1*SQRT1F(1.34*TCR*TCR+UR*UR)+TCR)*F*B*.5723)/(UR*TCR*SOL
1ID)
DO4I=1,100
CON=I-1
DM=(.01*FGLDR*AM3*AM3*AM3*(1.+GA1*AM3*AM3))/(1.-AM3*AM3)-((VT*VT*.
10001)*(2.*CON+1.)*AM3*(1.+GA1*AM3*AM3)**2.)/(3438.96*TT*(1.-AM3*AM
23))
4 AM3=AM3+DM
PR=((AM3D/AM3)*((1.+GA1*AM3*AM3)/(1.+GA1*AM3D*AM3D))**GA2)
R4=R2*R3R2*PR
XX1=(GAMMA-1.)/GAMMA
AET4=CP*(1.-(1./R4)**XX1)
VJ=224.*CV*SQRT1F(AET4*TT)
RHPWG=((VJ-VT)*VT)/17710.
RHP=RHPWG*WG
CPA=(RHP*550.)/(0.002378*DR*3.14*RAD*RAD*VT*VT*VT)
BT=.97
CTT=(CPA*BT*1.414141)**.66667
9 CTST=CTT/SOLID
TGTI=GN1+GN2*CTST+GN3*CTST*CTST
CTOGT=CTT*TGTI
C1=1.02+.15*CTST*TGTI
CPO=(.00127238*SOLID-(.00294031*CTOGT)/(BT*BT)+(.05701598*CTOGT*CT
1OGT)/(SOLID*BT*BT))*CORR
CPI=CPA/C1-CPO
CT=(CPI*BT*1.414141)**.66667
IF(ABS(CT-CTT)-.000005)10,10,13
3 CTT=CT
GOTO9
10 CTS=CT/SOLID
TGTI=GN1+GN2*CTS+GN3*CTS*CTS
CTSG=CTS*TGTI
TR=CTSG*VT*VT*RAD*RAD*.0074707*DR*SOLID
DL=TR/(3.14*RAD*RAD)
WRITEOUTPUTTAPE2,100,AM3D,PR,R4,CTSG,RHP,TR,DL,R2
WRITEOUTPUTTAPE2,101,CPA,CPO,CT
01 FORMAT(8H CP =E15.5,9H CPO =E15.5,8H CT =E15.5)
00 FORMAT(15H DESIGN M3 =F7.4,16H PRESS RATIO =F8.5,7H R4 =F8.
15,13H CT/SOLID =F9.6,8H RHP =F8.0/18H ROTOR THRUST =F10.0,1
28H DISC LOADING =F9.4,8H R2 =F9.4)
RETURN

```

UNCLASSIFIED

UNCLASSIFIED